University of Southampton

Faculty of Medicine

Human Development and Health

Characterising Bi-atrial Mechanisms of Atrial Fibrillation Using High Density Non-contact Mapping

by

Michael TB Pope

ORCID ID https://orcid.org/0000-0002-4166-3746

Thesis for the degree of Doctor of Philosophy

January 2023

University of Southampton

Abstract

Faculty of Medicine
Human Development and Health
Doctor of Philosophy

Characterising Bi-atrial Mechanisms of Atrial Fibrillation Using High Density Non-contact Mapping

by
Michael TB Pope

A universal description of mechanisms of AF activation remains elusive. This thesis seeks to apply emerging techniques of global non-contact mapping to further understand mechanisms of AF activation and identify patient specific phenotypes.

Methods were developed to allow quantification of complex patterns of activation and apply signal processing tools including dominant frequency and phase analysis to characterise AF properties.

These methods were applied to analyse the impact of adenosine during AF, which is known to alter atrial electrophysiological properties. A significant shortening of atrial fibrillation cycle length, alongside an increase in dominant frequency was associated with a promotion of rotational patterns of activation throughout the left atrium.

Extended and repeated recordings were analysed to identify both the optimal time period required for mapping and the spatial consistency of complex activation. Localised irregular activation patterns characterised by wavefront pivoting, partial rotation and splitting were highly spatially stable and coincided with areas of increasing conduction heterogeneity during short coupled atrial pacing.

A technique using mean phase coherence was developed to allow analysis of interatrial propagation during simultaneous bi-atrial mapping of AF. Properties of atrial activation were identified to reveal predictors of AF termination with targeted ablation. Differences in the balance of interatrial activation could be observed between patients with changes in right atrial activation properties reflecting more arrhythmia complexity, refractory to acute termination with ablation.

A novel method was developed to attempt to further characterise individual AF phenotypes based on whole chamber patterns of AF activation. The concept of recurrence was used to calculate both whole chamber and localised measures of organisation which was shown to correlate closely with both clinical AF phenotype and predict acute AF termination with ablation.

Finally, clinical outcomes of a cohort of patients treated with a charge density guided ablation strategy are presented.

In conclusion, novel insights into the bi-atrial properties of AF activation identified with charge density non-contact mapping are presented alongside a novel technique to quantify whole chamber organisation during AF, which aims to identify AF phenotypes and predicts acute AF termination with ablation.

Table of Contents

Table of Tables

Table of Figures

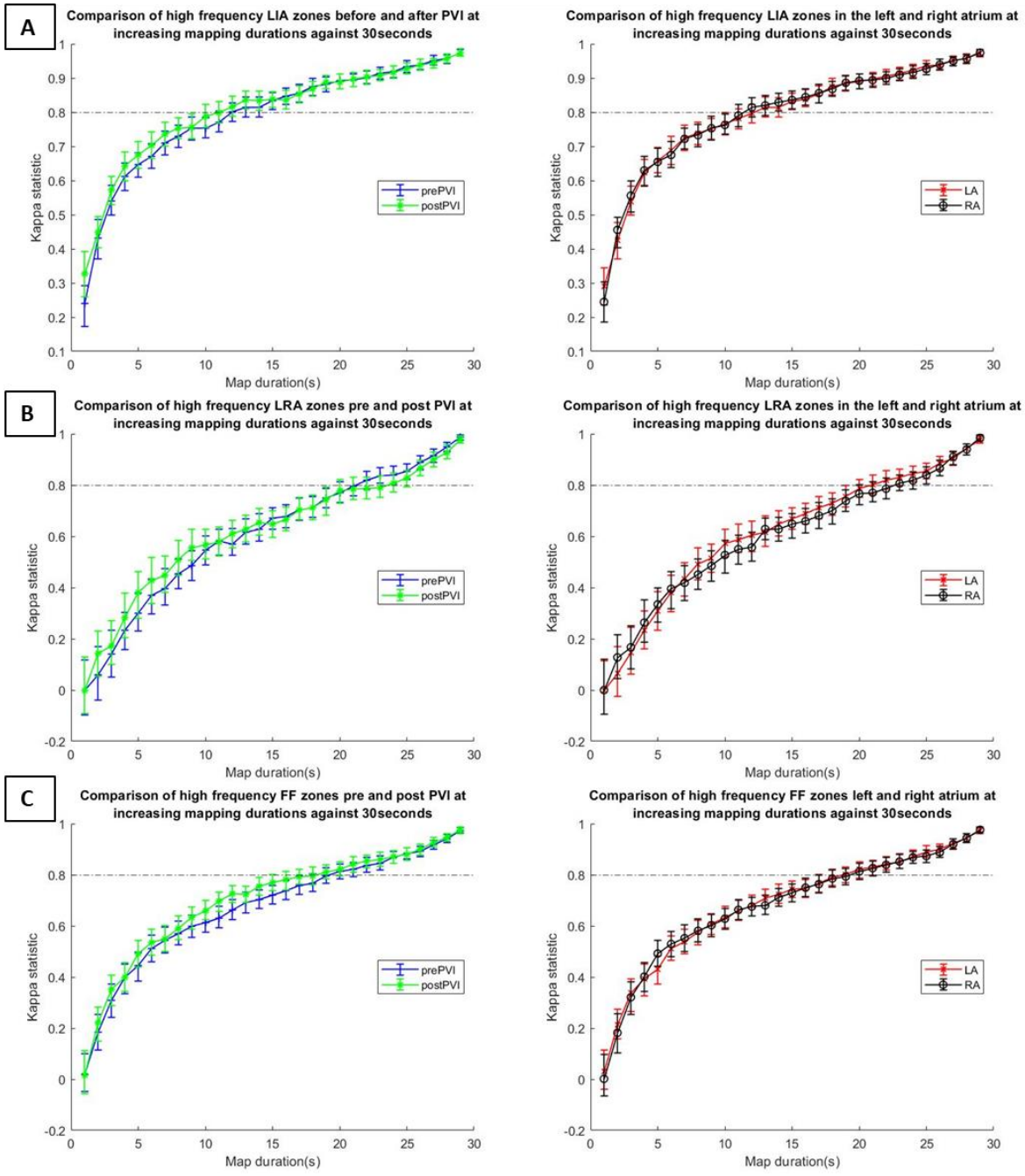

Research Thesis: Declaration of Authorship

Print name: Michael Timothy Bryan Pope

Title of thesis: Characterising Bi-atrial Mechanisms of Atrial Fibrillation Using High Density Non-contact Mapping

I declare that this thesis and the work presented in it are my own and has been generated by me as the result of my own original research.

I confirm that:

1. This work was done wholly or mainly while in candidature for a research degree at this University;
2. Where any part of this thesis has previously been submitted for a degree or any other qualification at this University or any other institution, this has been clearly stated;
3. Where I have consulted the published work of others, this is always clearly attributed;
4. Where I have quoted from the work of others, the source is always given. With the exception of such quotations, this thesis is entirely my own work;
5. I have acknowledged all main sources of help;
6. Where the thesis is based on work done by myself jointly with others, I have made clear exactly what was done by others and what I have contributed myself;
7. Parts of this work have been published or presented as outlined in the following section

Signature: .....Date: .....

Presentations and publications arising from this work

Publications:

Chapter 1:

Pope MTB, Betts TR. Global Substrate Mapping and Targeted Ablation with Novel Gold-tip Catheter in De Novo Persistent AF. Arrhythm Electrophysiol Rev 2022;1: e06 10.15420/aer.2021.64

Chapter 3:

Pope MTB, Kuklik P, Briosa e Gala A, Leo M, Mahmoudi M, Paisey J, et al. Impact of Adenosine on Wavefront Propagation in Persistent Atrial Fibrillation: Insights From Global Noncontact Charge Density Mapping of the Left Atrium. J Am Heart Assoc. 2022;11(11):e021166

Chapter 4:

Pope MTB, Kuklik P, Briosa e Gala A, Leo M, Mahmoudi M, Paisey J, Betts TR. Spatial and temporal variability of rotational, focal, and irregular activity: Practical implications for mapping of atrial fibrillation. J Cardiovasc Electrophysiol. 2021;32:2393-2403

Chapter 5:

Pope MTB, Kuklik P, Banerjee A, Briosa e Gala A, Leo M, Paisey J, Mahmoudi M, Betts TR. Insights into Bi-Atrial Mechanisms during Atrial Fibrillation (manuscript in preparation)

Chapter 6:

Pope MTB, Kuklik P, Banerjee A, Briosa e Gala A, Leo M, Paisey J, Mahmoudi M, Betts TR. Recurrence Matrix Mapping – Novel Approach to Characterising Atrial Fibrillation Phenotype (manuscript in preparation)

Presentations and abstracts:

Chapter 3:

Pope MTB, Kuklik P, Mahmoudi M, Paisey J, Betts TR. Impact of Adenosine on Mechanisms of Wavefront Propagation in Persistent Atrial Fibrillation. Abstract presentation, Heart Rhythm Congress, Birmingham, 2019

Pope MTB, Kuklik P, Briosa e Gala A, Mahmoudi M, Paisey J, Betts TR. Impact of Adenosine on Mechanisms of Propagation in Persistent Atrial Fibrillation. Abstract presentation, HRS, 2020

Chapter 4:

Pope MTB, Kuklik P, Briosa e Gala A, Mahmoudi M, Paisey J, Betts T. Spatial Stability of Complex Propagation Patterns in Atrial Fibrillation. Abstract presentation at AF

symposium 2020. AFS-28. Journal of Cardiovascular Electrophysiology. March 2020, 31(3). https://doi.org/10.1111/jce.14375

Pope MTB, Bates MG, Gouda S, James S, Shepherd E, Murray S, Thornley AR, Betts TR. Spatiotemporal stability of non-pulmonary vein propagation patterns in persistent atrial fibrillation identified through novel dipole-density non-contact mapping before and after pulmonary vein isolation. Abstract presentation at HRC, Birmingham, 2018. EP Europace, Volume 20, Issue suppl_4, October 2018, Pages iv38–iv39, https://doi.org/10.1093/europace/euy205.028

Chapter 5:

Pope MTB, Kuklik P, Briosa e Gala A, Mahmoudi M, Paisey J, Betts TR. Revealing channels of interatrial communication during atrial fibrillation. Abstract presentation at EHRA 2020 (virtual)

Pope MTB, Kuklik P, Banerjee A, Briosa e Gala A, Leo M, Mahmoudi M, Paisey J, Betts TR. Insights into Electrophysiological Mechanisms of Atrial Fibrillation Propagation using Simultaneous Bi-Atrial Mapping. Abstract presentation at EHRA 2021 (virtual).

Chapter 6:

Pope MTB, Kuklik P, Briosa e Gala A, Leo M, Paisey J, Mahmoudi M, Betts TR. Application of Recurrence Plot Analysis to Characterise Whole Chamber Propagation of Atrial Fibrillation. Abstract presentation at EHRA 2021 (virtual)

Pope MTB, Kuklik P, Banerjee A, Briosa e Gala A, Leo M, Paisey J, Mahmoudi M, Betts TR. Recurrence Matrix Mapping – Novel Approach to Characterising Atrial Fibrillation Phenotype. Abstract presentation at HRC 2021 (virtual), finalist in Young Investigator Award

Acknowledgements

This work would not have been possible without the help and support of many. Particular thanks go to my main supervisor Prof Tim Betts, particularly for his patience both in setting up the studies involved with this project and particularly for carrying out the often long mapping and ablation procedures required to gather the data. In addition, I would like to thank all the staff in the cardiac catheter laboratories including radiographers, anaesthetic staff, physiologists and nurses for their incredible patience and help with all the procedures performed. The length of some of the bi-atrial mapping procedures often lead to a collective groan at my appearance for a procedure list but the support and help of all staff involved never faltered and I'm immensely grateful. I would also like to thank my additional supervisors, Prof Michael Mahmoudi and Dr John Paisey for their help and advice throughout.

I collaborated on much of the work performed in this study with Pawel Kuklik who helped enormously with the designing and troubleshooting of custom coded programmes to execute the analyses required. We spent countless hours discussing and developing the methods applied and I am incredibly grateful for his help and advice as well as his expertise in developing custom designed analytical programmes. My thanks and recognition must also go to Abhi Bannerjee who provided valuable statistical advice and guidance and was always patient despite no doubt many a foolish question and misunderstanding of statistics!

Sincere thanks also go to all of the patients who kindly agreed to take part in the research studies. It should go without saying that none of this would be possible without the generous help of patients in supporting research, for which I am deeply grateful and appreciative.

My thanks also go to two further members of the John Radcliffe research team – Milena and Andre. They were subjected to brainstorming sessions and provided a sympathetic ear to any frustrations experienced whilst often providing practical and helpful advice. Thank you! The team from Acutus Medical also provided significant assistance and support, particularly in loaning the second AcQMap console required for simultaneous bi-atrial mapping and developing a custom programme to facilitate this approach. There are too many to name everyone but I would like to particularly thank Richard Chambers, Stephen Brown, Nathan Angel and Derrick Chou.

Lastly, but by no means least, I would like to thank my wonderful wife, Gems. She has served as a solid sounding board without complaint and provided incredible support

throughout as well as giving birth to our first child. I could not have achieved a fraction of this without her.

Abbreviations

AF – Atrial fibrillation

AFCL – Atrial fibrillation cycle length

CHI – Conduction heterogeneity index

DCCV – Direct current cardioversion

DF – Dominant frequency

EAVM – Electroanatomic voltage mapping

FF – Focal firing

LA – Left atrium

LGE – Late gadolinium enhancement

LIA – Local irregular activation

LRA – Localised rotational activation

MAT – Median activation time

MRI – Magnetic resonance imaging

MPC – Mean phase coherence

pAF – Paroxysmal atrial fibrillation

persAF – Persistent atrial fibrillation

PV – Pulmonary vein

PVI – Pulmonary vein isolation

RA – Right atrium

RI – Recurrence index

SDE – Symbolic dynamic entropy

SR – Sinus rhythm

1 Background and Literature Review

1.1 Atrial Fibrillation – the clinical problem

Atrial fibrillation (AF) is the most common sustained cardiac arrhythmia, and in the context of an ageing population, prevalence is increasing.(1, 2) In a UK study of adults ≥35 years of age in primary care between 2000 and 2016, prevalence of AF rose from 2.0% to 3.3%, with the greatest increase observed in those aged ≥85 years. In this age group, AF was observed in 22.1% of men and 16.5% of women.(1) This mirrors data from the United States where forecasts suggest that >5.6 million adults will have atrial fibrillation by 2050.(3) Furthermore, although prevalence rates vary worldwide, a pattern of increasing AF burden is seen in both "developed" and "developing" nations as well as both "Western" and "non-Western" societies.(2, 4) Importantly, the consequences of AF and the resultant socioeconomic burden incurred from this condition relate to both symptoms associated with the disease itself as well as associated morbidity resulting in hospitalisation and significant healthcare costs.(5) Increases in AF prevalence have been mirrored by increases in hospitalisation and accompanied by growing economic impact.(6-9)

The increased risk of embolic stroke associated with AF is well recognised.(10) However, the impact of the condition extends well beyond this and is highlighted by studies exploring the reasons for hospitalisation in this patient group. The ROCKET-AF trial was a worldwide study comparing the efficacy of Rivaroxaban versus warfarin for stroke prevention in non-valvular AF.(11) In a post hoc analysis of the >14 thousand patients randomised, 14% of patients experienced at least one hospitalisation during the 2 years of follow up with the broad reasons for admission split almost equally between cardiovascular and non-cardiovascular causes.(12) Furthermore, AF itself was the cause for admission in only 4% of cases, with the largest single cardiovascular cause being congestive heart failure (in 14%).(12) In addition, epidemiological studies have revealed a significant association with increased mortality even when accounting for the presence of a wide range of comorbidities.(13, 14) Causes of death in this population are most commonly cardiovascular, with stroke often cited as one of the leading single causes.(14-16) However, particularly in the UK, rates of initiation of effective thromboprophylaxis have significantly improved(1) whilst direct oral anticoagulants have been shown to result in lower rates of cardiovascular death, major bleeding and intracranial haemorrhage when compared to warfarin.(17-19) In this context, the predominant causes of death in this population may be shifting away from stroke and intracranial bleeding towards heart failure and sudden cardiac death.(16, 20, 21)

However, none of this data considers the impact on symptoms and quality of life. The majority of patients with AF will notice some symptomatic impact, and in one registry study of >10 thousand patients 16.5% had either severe or disabling symptoms.(22) In addition, more debilitating symptoms and worse quality of life were both associated with higher rates of hospitalisation.(22)

1.2 Approach to AF therapies

In this context, management of AF involves treatment of the arrythmia itself as well as targeting complications and associated co-morbidity. The most important of these is deciding between a strategy of heart rate control versus “rhythm control” (aiming to maintain sinus rhythm) as well as initiation of anticoagulation for prevention of stroke and systemic thromboembolism.(23, 24) The AFFIRM trial was a pivotal study comparing strategies of rate versus rhythm control in a mixed cohort of patients with recurrent (both paroxysmal and persistent) AF, which showed no difference in the primary end point of all cause mortality.(25) However, it must be remembered in its appropriate context. The study was published in 2002, prior to the widespread use of catheter ablation for rhythm control and was therefore a trial of pharmacological management (excluding a small number who underwent atrioventricular node ablation as part of a rate control strategy) in a population with an average age of 70 years. All patients in the rhythm control arm took either amiodarone or sotalol at some point during the study with a higher rate of Torsade de pointes, bradycardia and cardiac arrest seen in this group.(25) Furthermore, in contrast with current practice, a number of patients in the rhythm control arm discontinued anticoagulation and suffered an ischaemic stroke as a consequence.(25) Similar results were observed in patients with persistent AF, but with the same limitations.(26) Since then, catheter ablation has emerged and become a widely adopted strategy for rhythm control.(27, 28)

Recently, the EAST-AFNET 4 study provided an updated analysis along similar lines to that provided by the AFFIRM trial using modern medical therapy and invasive treatment strategies with a focus on evaluating an early rhythm control strategy compared to rate control, and alongside guideline directed management of associated cardiovascular conditions including antithrombotic therapy for stroke prevention.(29) The trial was stopped early for efficacy, driven mainly by reduction in cardiovascular death and stroke in patients assigned to rhythm control. Importantly, this was not a trial of catheter ablation specifically, with only 19.4% of patients in the rhythm control group undergoing ablation over the two years of the study, and 8% underwent ablation as the initial management strategy.(29)

Furthermore, additional evidence from randomised controlled studies has demonstrated significant improvements in left ventricular ejection fraction, quality of life and hospitalisations (primarily in patients with heart failure).(30-33) Although the recently published CABANA trial failed to show a statistically significant benefit of catheter ablation in its primary outcome of a composite of mortality, disabling stroke, serious bleeding or cardiac arrest, it did demonstrate the safety of this approach(34) and additional analyses suggested a significant improvement in quality of life in line with previous smaller studies.(35-37) Although catheter ablation has been shown to be superior to anti-arrhythmic drug therapy at maintaining sinus rhythm, the benefit obtained with a broader rhythm control strategy in EAST-AFNET 4 perhaps explains why CABANA failed to demonstrate improvement in its primary outcome (using the prespecified intention to treat analysis).(38-42) However, a recent meta-analysis of all published randomised studies and including CABANA, which contributed 2204 of the 4464 included, highlighted a significant reduction in cardiovascular hospitalisation associated with catheter ablation (HR 0.56, CI 0.39 – 0.81, p=0.002).(43)

The aims of catheter ablation can therefore be considered to 1. Improve symptoms and quality of life 2. Reduce risk of recurrent hospitalisation and possibly stroke and 3. Improve left ventricular ejection fraction and survival in patients with heart failure and reduced ejection fraction.

Since the discovery in the late 1990s of rapidly firing ectopic foci from the pulmonary veins (PV) initiating and maintaining AF, and the observation that ablation of these ectopic foci could abolish the arrhythmia, the mainstay of catheter ablation has consisted of wide antral circumferential ablation to achieve pulmonary vein isolation.(44) However, understanding of AF mechanisms beyond the role of PV ectopy remains limited. In addition, significant technical challenges exist in the development of tools for accurate AF activation mapping. As novel technologies emerge to meet these challenges, they may provide further insights into AF mechanisms that can inform our approach to catheter ablation with the aim of improving clinical outcomes.

1.3 Understanding AF Mechanisms

Mackenzie first identified evidence of atrial fibrillation (then referred to as auricular fibrillation) through analysis of jugular venous pressure waveforms, primarily in patients with mitral stenosis. Following collaboration with Thomas Lewis, who applied the newly developed tools of electrocardiography using Einthoven's string galvanometer, the first electrocardiograms of atrial fibrillation were obtained.(45) Over the early period of research following these initial observations, competing theories to explain mechanisms of

fibrillatory propagation developed in parallel. Although further refinement of these theories has occurred with incremental developments in our understanding and the emergence of new experimental data, there are still significant gaps in our knowledge.

1.3.1 Re-entry and Multiwavelet theory

Mayer provided the first experimental evidence of re-entry in studies conducted using a ring of excitable tissue excised from the contractile bell of the rhyzostomous Scyphomedusa (jellyfish) *Cassiopea xamachana,* and rings of muscle cut from the ventricles of turtles.(46) In these experiments, he showed that the application of appropriate stimuli could induce wavefront propagation that then perpetuated around the ring independent of the initial stimuli.(46) This gained particular interest following the description of atrial fibrillation by Lewis soon after.

Mines initially observed what he termed “reciprocating rhythms” in “auricle-ventricle” preparations of animals including frogs and the electric ray.(47) He observed that after application of rhythmic stimuli at an appropriate rate, followed by cessation of this stimulus was followed by continued contraction of each chamber in turn that could be terminated by the delivery of an appropriately timed stimulus to either chamber. He hypothesised the existence of multiple A-V connections between chambers that demonstrated different rates of recovery following excitation. This allowed the occurrence of an extra-systole in the ventricle following the stimulus that occurred after conduction down one connection to spread back up to the auricle via the connection with the quicker recovery period. At this point, the alternative A-V connection would have re-gained excitability and allow transmission back to the ventricle.(47) This hypothesis was further tested in excised ring preparations of the tortoise heart resulting in coining of the phrase “circulating excitation”.(47) Mines proposed the existence of multiple closed circuits in the mammalian heart brought about by numerous connections between layers of cells that would support “circulating excitation” and explain the activation observed during fibrillation.(47)

Garrey independently made similar observations using rings of muscle cut from the ventricles of large water turtles.(48) In the same paper he made the observation that fibrillation is much more easily initiated and maintained in large compared to small volumes of heart muscle. Furthermore, dividing fibrillatory tissue into sections resulted in continuation of fibrillation within each section above a certain volume, leading to the suggestion of the requirement for a critical mass of tissue to maintain fibrillation, which likely resulted from the existence of closed circuits of waves within the myocardium.(48)

Lewis subsequently extended and incorporated this experimental evidence in attempting to provide a description of the mechanisms of both atrial flutter and atrial fibrillation having observed a close relationship between the two as well as the ability to convert flutter into fibrillation with the administration of digitalis.(49) He paid particular attention to the importance of refractory periods, especially the concept of relative refractoriness in providing the physiological circumstances for re-entry. In describing the processes involved in atrial flutter he coined the term “circus movement” to describe the nature of the pattern of re-entry seen over a relatively large circuit, as shown in figure 1.1A and 1.1B.(50) Shortening of refractoriness allowed the same re-entry mechanism to exist over far smaller wavelengths during fibrillation but as a result of varying refractoriness, the path of re-entry is non-uniform with islands of refractory tissue acting as barriers resulting in variation of the path of both the re-entry wavefront and the waves emanating from this originating circuit as illustrated in figure 1.1B and 1.1C.

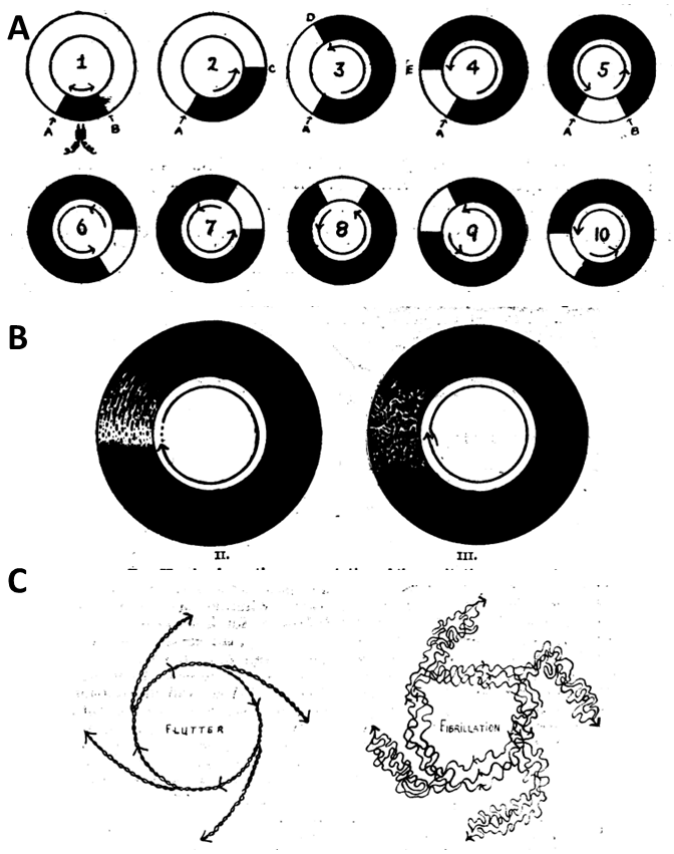

Figure 1.1 Mechanisms of re-entry in atrial flutter and fibrillation. In A, a stimulus results in activation that meets a region of conduction block resulting in unidirectional conduction around a circular path with recovery of excitation at its tail allowing for continuation of circus re-entry. In B, the leading edge of a re-entry wavefront in flutter (on the left) meets more uniformly excitable tissue resulting in a smooth wavefront of propagation, whilst during fibrillation (on the right), the leading edge of the wavefront meets more heterogeneously refractory and excitable tissue resulting in barriers to conduction. This is further illustrated in C with organised outward activation to surrounding tissue during flutter (on the left) in contrast to coarse and disorganised activation seen during fibrillation (on the right). Adapted from Lewis(49, 50).

The conclusions of Sir Thomas Lewis based around re-entry became widely accepted as the leading explanation for the mechanism of atrial fibrillation until further experimentation conducted in the late 1950s. Moe however was unconvinced that circus re-entry over such a short wavelength with a refractory period shorter than the rest of the atrium would be stable enough to maintain fibrillation over years as clinically observed. He felt the same was true of the alternative theory of a high frequency ectopic focus.(51) He was the first to make the distinction between mechanisms that may initiate arrhythmia, such as rapid external stimuli by electrodes, spontaneous ectopic beats, or circus re-entry around an anatomic obstacle such as in atrial flutter, and those responsible for sustaining the arrhythmia. High frequency stimuli were delivered to the right atrial appendage of dog hearts with and without vagal stimulation. Although high frequency stimulation was able to provoke AF, this only sustained following termination of the stimulus during vagal stimulation. In order to exclude the possibility of an ectopic focus at the site of stimulation brought about by the external stimulus and persisting after its removal, a clamp was applied across the appendage during sustained fibrillation. This resulted in termination within the appendage but maintenance of fibrillation within the body of the atrium thus providing evidence separating the initiating and sustaining arrhythmia mechanisms.(51)

In discussing the implications of these results, Moe postulated the existence of “randomly wondering wavelets” responsible for continuous fibrillatory activation. Spatial variation in refractoriness results in varying degrees of excitability of tissue in response to repeated stimulation. As multiple stimuli are delivered, the temporal dispersion of refractoriness and thus excitability increase, resulting in disorganised impulse propagation and fractionation of wavefronts around islands of refractory tissue resulting in multiple “daughter wavelets” that propagate dependent on the excitability and refractoriness of surrounding tissue resulting in a self-sustaining state independent of the initial stimuli.(51) This model becomes more stable in the context of large numbers of daughter wavelets, larger tissue mass (therefore able to accommodate more wavefronts), shorter refractoriness, and slower conduction velocities. The opposite conditions are more likely to result in fusion of wavefronts resulting in resumption of sinus rhythm. This description formed the basis for the multiple wavelet hypothesis.(51)

This hypothesis led to the development of early mathematical modelling of atrial fibrillation based around knowledge of heterogeneity in refractoriness, conduction velocity and the response to increase rate as well as vagal stimulation. Results of these mathematical simulations supported the multiple wavelet hypothesis and suggested the existence of a possible minimal number of wavefront needed for sustained arrhythmia, termed a “fibrillation number”.(52)

An important component of the multiwavelet theory of re-entry was the lack of requirement of an anatomic boundary. Allessie performed key experiments using microelectrode recordings on the endocardial surface of isolated rabbit hearts during application of single extra-stimuli at varying coupling intervals. In these experiments, single extrastimuli resulted in sustained vortices of re-entry in the absence of anatomical boundaries and resulting in tachycardia.(53) This, in combination with further studies provided the basis for the concept of the leading circle theory of functional re-entry with a vortex around a centre of in-excitable tissue maintained by continued, repetitive bombardment by centripetal wavefronts as shown in figure 1.2A and in contrast with the Mines concept described above. These centripetal wavefronts are blocked within the centre of the circuit, where fibres remain refractory following activation from a previous centripetal wavefront within half a revolution of the circuit, preventing “short-circuiting” and providing a functional obstacle around which to turn.(54)

Subsequent developments in the field of computational biology and observations of chemical reactions resulted in evolution in the concept of re-entry in the form of rotors brought about further by theoretical studies conducted initially in the USSR and subsequently in the US.(55, 56) Technological advances in the form of development of potentiometric dyes and charge coupled device imaging technology allowed Davidenko to conduct early high resolution mapping studies in isolated ventricular muscle preparations of sheep and dogs in which he showed the first evidence of spiral wave re-entry in the heart.(57)

Interest in spiral wave re-entry gathered significant momentum in subsequent decades and this concept has gone on to eclipse the leading circle theory of Allessie. An important weakness of the leading circle description is that the mechanism of continued centripetal activation of the core would result in fixing of the re-entry mechanism in space. Whilst both concepts are based around functional re-entry, the spiral wave theory is based around a curved wavefront of activation that meets its tail at the centre/pivot point where the tissue is not refractory, termed the phase singularity as shown in figure 1.2B. The key feature of this core is the increased curvature of the wavefront towards this point with slowing of conduction that reaches a critical point preventing invasion. Importantly, tissue at the core of spiral wave re-entry is unexcited, but excitable, allowing for meandering of the rotating wave.(58) The concept of spiral wave re-entry has since become the focus of a large volume of subsequent work as discussed further below.

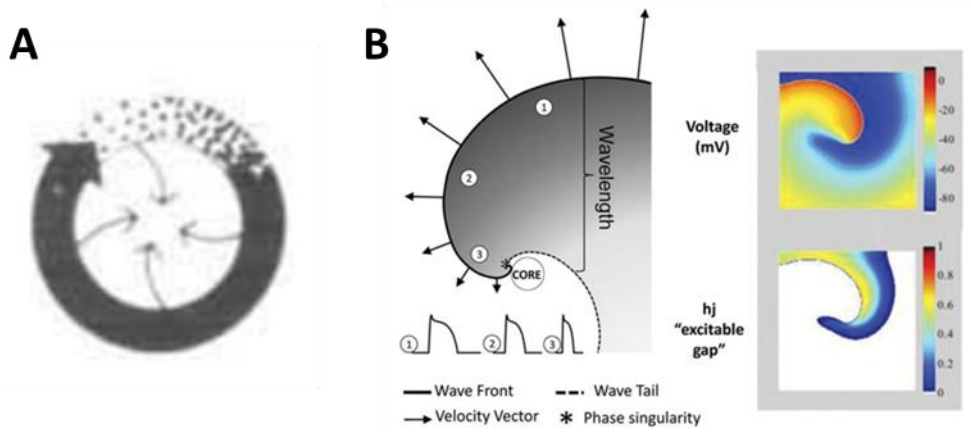

Figure 1.2 Leading circle and spiral wave theories of re-entry.Leading circle re-entry (A) lacks a fully excitable gap as shown by the dotted area ahead of the leading wavefront (arrow) with the core continually invaded by centripetal wavefronts. Spiral wave re-entry (B) involves a convex wavefront with increasing curvature towards the core characterised by reducing conduction velocities (shown by shortening of arrow length), shortening of action potential duration and shortening of wavelength (gap between wave front and wave tail). Adapted from Allessie(54) and Pandit et al.(58)

1.3.2 Double Layer Hypothesis

An important observation of the spiral wave theory is the 3-dimensional nature of the mechanism in contrast with the 2-dimensional studies hitherto performed. It may seem obvious to state that the atrial myocardium is a 3-dimensional structure, but it was only with more recent advances in technology that studies of the 3-dimensional nature of fibrillatory activation could be undertaken. High density mapping studies on Langendorff-perfused sheep hearts conducted by Gray et al drew attention to the importance of the complex 3-dimensional atrial structure and its importance in AF activation.(59) Using optical mapping studies they demonstrated patterns of incomplete re-entry on the epicardial surface, which they proposed was the result of transmural conduction maintaining the re-entry circuit. In addition, they identified sites of centrifugal activation that they proposed were sites of breakthrough conduction, although they did not provide direct evidence of this.(59)

High density mapping studies performed in patients undergoing cardiac surgery provided further support to this theory with the observation of focal areas of epicardial activation with centrifugal spread of excitation.(60) However, again, direct proof of mechanism was not provided. The presence of specific unipolar electrogram timing and morphology criteria were used to support the epicardial breakthrough hypothesis, including a close relationship with atrial fibrillation cycle length (AFCL), a lack of prematurity in terms of timing relative to the expected activation determined by average local AFCL, and the presence of a unipolar r wave.(60) However, these factors would not necessarily exclude an automatic focus mechanisms, particularly if it was

irregular/unstable and given challenges of interpreting what are often fractionated unipolar electrogram signals. Although more direct proof of this concept had been shown in animal models using simultaneous endocardial and epicardial contact mapping, only later was this evidence obtained using similar techniques in humans.(61, 62)

1.3.3 Hierarchical theory

The convincing evidence for re-entry mechanisms proposed by Mines and Lewis, through to Moe, Allessie and subsequent description of spiral waves largely drowned out competing theories proposing the existence of focal sources, in large part due to the distinction by Moe between AF sustaining processes and the original initiating mechanism. Interest in the role of ectopic foci was reinvigorated with the experiments of Scherf et al in which the application of aconitine (a voltage gated sodium channel activator) to the epicardial surface of the right atrial appendage of dog hearts induced atrial fibrillation.(63) However, it was not until the pivotal work of Haissaguerre et al. that convincing evidence of the role of ectopic foci arising from the pulmonary veins in initiating paroxysms of AF was presented, alongside demonstration of the effectiveness of eliminating these foci through the use of radiofrequency ablation.(44)

Nonetheless, this purely dealt with arrhythmia initiation, with significant controversy around sustaining mechanisms remaining. Competing theories centre around the ideas of anarchical mechanisms exhibiting chaos and random activation aligned more to multiwavelet activation, versus hierarchical mechanisms in which one or more sources are responsible for the generation of high frequency wavefronts thereby “driving” fibrillation. One difficulty with discussion of this field is the terminology used where the description of focal sources often has mechanistic implications suggestive of automatic firing of a single cell, or group of cells, with centrifugal activation, akin to automatic focal atrial tachycardia. However, localised re-entry mechanisms have also been proposed as being responsible for observed “focal” mechanisms. As such, better terminology is perhaps “localised sources”, which is mechanistically agnostic but implies a key role in giving rise to downstream atrial activation and thus may represent a site responsible for AF maintenance.

Spiral wave re-entry has been proposed as a mechanism responsible for localised high frequency rotors originating as a result of wave-break brought about by interaction of a wavefront with regions of anatomical or functional block, which may arise as a result of appropriately timed extrastimuli. The resultant re-entry creates high frequency sources that give rise to wave fragmentation in the context of the heterogeneous atrial substrate

into which the emanating waves propagate, resulting in the disorder observed in fibrillation.(64)

Early evidence for high frequency localised sources came from optical mapping studies in animal models of induced AF.(65, 66) However, although these studies suggested high frequency localised sources, the presence of rotors was inferred rather than demonstrably identified. The possibility of high frequency localised sources concentrated in the posterior left atrium has been strongly proposed and has led to concerted efforts to identify these mechanisms in human AF. (67)

1.4 Structural and Functional Substrate

As has been outlined thus far, although the role of the pulmonary veins in AF initiation has been firmly established, AF requires both a trigger and a vulnerable atrial substrate in order to become sustained. Precisely what the mechanisms are that represent this vulnerable substrate are poorly understood.

1.4.1 Structural substrate

Pulmonary veins

Haissaguerre's seminal work focussed attention on the sleeves of cardiomyocytes extending from the left atrium into the pulmonary veins and led to further work exploring their arrhythmogenesis. Canine studies have revealed cellular electrophysiological properties resulting in enhanced spontaneous focal activity including shortened action potential duration and higher resting membrane potentials as a result of reduced inward rectifier potassium current density.(68) In addition, local re-entry is also thought to play an important role.(69) Strands of myocytes are arranged in discrete bundles with little electrical connection to surrounding tissue and abrupt changes in fibre orientation.(70, 71) This results in conduction slowing, particularly at excitation frequencies approaching refractoriness, potentiating re-entry around the pulmonary vein-left atrial (PV-LA) junction.(70) In addition adenosine has been shown to increase dominant frequencies at the PV-LA junction, suggestive of local re-entrant mechanisms.(72) These complex electrophysiological properties at the PV-LA junction provide further evidence in support of the critical role of the PVs in AF.

Recognition of the importance of the PV-LA junction led to a progression in catheter ablation approaches from focal PV ablation to ostial segmental ablation and subsequently to wide area circumferential ablation incorporating part of the posterior LA wall and the complex PV-LA junction.(73, 74) Randomised controlled trials and meta-analyses have since demonstrated increased efficacy of this approach, which is also thought to result in lower risk of pulmonary vein stenosis.(73, 75, 76) In patients with

paroxysmal AF, outcomes are good. At 12 months, success rates approach 65%, increasing to 80% following repeat procedures.(77, 78) However, the observation of late recurrences with long term follow up despite pulmonary vein isolation and the significantly lower success rates in patients with persistent arrhythmia highlight the importance of additional non-pulmonary vein mechanisms in AF initiation and maintenance.(77-81)

Atrial fibrosis and scar

Electroanatomic voltage mapping (EAVM) is widely used to measure bipolar electrogram signal amplitude in order to characterise the atrial anatomic substrate with low voltage amplitude serving as a surrogate for fibrosis.(82) The presence of regions with low amplitude predict worse outcomes following catheter ablation.(82-84) However, a number of factors can impact the amplitude of the signal recorded, ranging from technological factors such as electrode size, interelectrode distance and electrode tissue contact, to electrophysiological factors such as rhythm (impacting wavefront direction) and cycle length.(85-88)

Myocardial fibrosis can be termed reparative or reactive. Whilst reparative fibrosis occurs as a result of cardiomyocyte death, typically following infarction, resulting in replacement with fibrotic scar tissue, reactive fibrosis is characterised by interstitial collagen deposition without replacement of cardiomyocytes.(89) The distribution of fibrosis may be described as compact, diffuse, patchy, or interstitial, with important potential implications for arrhythmogenesis.(90) The development of fibrosis has been associated with both re-entry and automaticity. The former is primarily thought to result from myocardial fibre disarray resulting in conduction delay and anisotropy resulting in both anatomic and functional re-entry, whilst the latter may arise by direct cell-cell signalling between myofibroblasts and myocardial cells triggering spontaneous depolarisation.(89) Paracrine effects may also result in conduction slowing and dispersion of refractoriness.(91) These mechanisms are summarised in figure 1.3.

The earliest study directly assessing the impact of atrial fibrosis on outcome of catheter ablation defined scar as an absence of electrograms or voltage of <0.05mV in sinus rhythm using a 4mm tip bipolar catheter but before the advent of contact force analysis.(83) Only 6% (42 patients) of 700 patients undergoing first time PVI fulfilled these criteria, and they had significantly higher rates of AF recurrence.(83) However, the most appropriate ranges for voltage correlating with either healthy or fibrotic atria are difficult to define and no doubt there is no clear cut-off between healthy and fibrotic areas. It seems likely that there is a spectrum of fibrosis represented by a similar spectrum in electrogram amplitude, and potentially other electrophysiological properties. Lin et al performed

detailed EAVM in 13 patients with left sided accessory pathways. In this group, 95% of bipolar voltages were >0.38mV, which therefore set a cut-off for fibrotic regions of 0.4mV.(92) However, transitional zones with voltage 0.3-1.3mV were identified in which electrograms revealed a high degree of fractionation suggesting localised conduction abnormalities.(92) A further study conducted EAVM in 6 control patients to determine the lower limit of normal voltage, which was set as the limit of the upper 95% value for each atrial segment and found to be 1.1mV.(93) Detailed EAVM was then undertaken in a cohort of 100 patients undergoing PVI who did not have any regions of voltage <0.5mV (using a bipolar ablation catheter without contact force sensing).(93) The presence of regions with voltage <1.1mV (classified as mildly abnormal low voltage areas – maLVA) and abnormal electrograms was an independent predictor of AF recurrence.(93) maLVA were present in 43% of the cohort and 44% of electrograms in maLVA were abnormal compared to 4.4% of electrograms in regions of normal voltage (>1.1mV).(93)

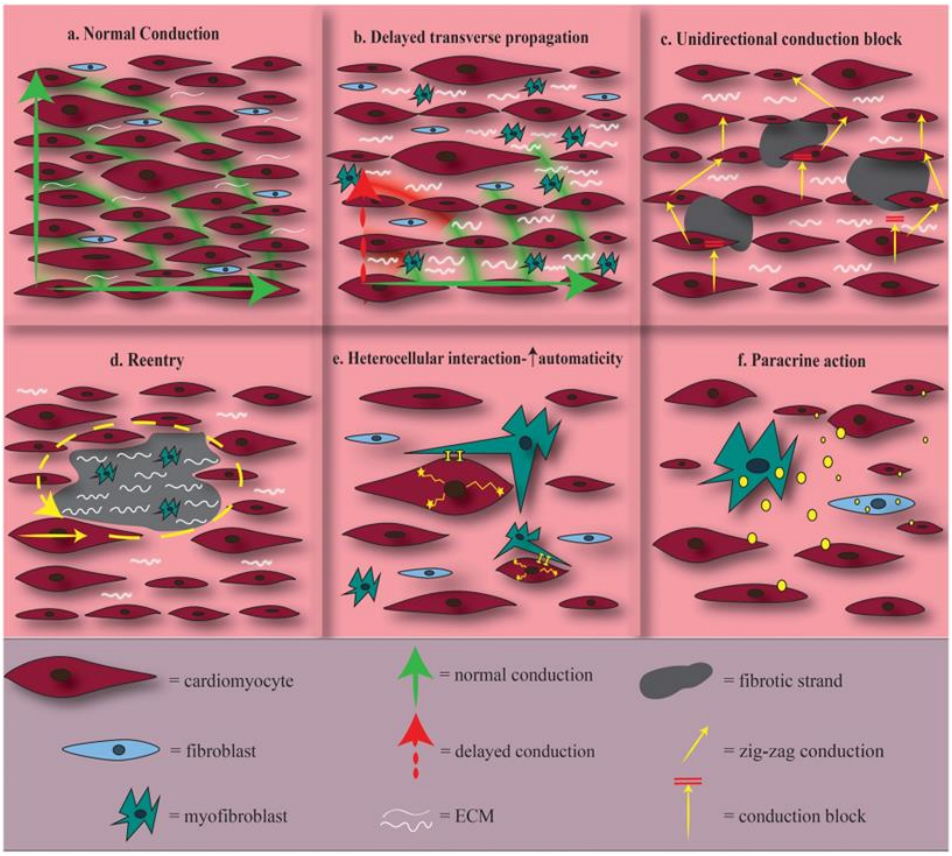

Figure 1.3 Arrhythmogenic impact of fibrosis. Organised myofiber orientation is key to normal conduction (a), whilst interstitial fibrosis may result in delayed transverse propagation (b) and unidirectional conduction block (c) with slow conduction resulting in functional re-entry. Localised deposition may result in anatomic re-entry (d) with local effects resulting in increased automaticity (e) and paracrine effects (f) influencing more distant conduction properties. Reproduced from Xintarakou et al.(89)

These findings have led to an interest in the role of low voltage regions in AF maintenance and the potential for ablation of these areas to improve outcomes. Rolf et al conducted detailed EAVM in a cohort of patients undergoing first time ablation for either paroxysmal or persistent atrial fibrillation.(84) Bipolar voltage mapping was performed following cardioversion and PVI using decapolar circular mapping catheters and confirmation using the ablation catheter (although without contact force guidance). Healthy tissue was defined as a bipolar peak to peak amplitude of >0.5mV. All patients with areas of low voltage then underwent additional ablation aiming to homogenize confined areas with linear lesions added when deemed necessary. 26% (n=47) of patients were found to have LVA, but more frequently in those with persistent atrial fibrillation (35% vs. 10% if paroxysmal). These were distributed in patches throughout the atria but occasionally were diffusely distributed. Age, male gender, persistent AF and low left atrial appendage (LAA) flow velocity in sinus rhythm were independently associated with the presence of LVA. Ablation consisted of septal lines (51%), roof with box line (51%) and multiple targeted combinations. Freedom from recurrent arrhythmia at 12 months was 70% in those with LVA and 62% in those without (p=0.09). When compared to the cohort control group, only 27% were free from recurrence. However, there was no comparison of extent of LVA or distribution.(84) Despite interest in this area however, it must be noted that the majority of this cohort were not found to have regions of low voltage and yet still experienced high rates of arrhythmia recurrence. Furthermore, there appears to be fairly poor correlation between AF duration and the presence of fibrosis, with some patients with longstanding AF demonstrating scar-free atria, whilst some with only brief episodes have highly scarred atria.(94) EAVM does not tell the whole story.

Non-invasive imaging using magnetic resonance imaging (MRI) to detect regions of late-gadolinium enhancement (LGE) has also been explored as a means of characterising the atrial anatomic substrate and correlates with findings on EAVM.(95, 96) In keeping with data from EAVM, more extensive late-gadolinium enhancement correlates with higher rates of recurrence following catheter ablation.(95, 97, 98) Interestingly, in contrast with some EAVM data, duration and type of AF appear to correlate poorly with the degree of fibrosis identified on MRI.(97-99) The DECAAF study graded fibrosis on a scale from 1-4, with 1 representing <10% of the atrial wall, grade 2 ≥10% but <20%, grade 3 ≥20% but <30% and grade 4 ≥30%. 81% of patients demonstrated at least 10% fibrosis (18.9% stage 1, 41.2% stage 2, 30.8% stage 3, 9.2% stage 4) with hypertension being the only baseline predictor of fibrosis burden.(97) Similarly, McGann et al prospectively performed LGE-MRI in 426 patients prior to a first ablation procedure using the same staging methodology.(98) Although patients with persistent AF were more represented

amongst those with higher stage LGE, each stage of LGE included a diverse mix of phenotypes.(98)

Although LGE-MRI and EAVM findings appear to correlate, they are clearly not equivalent. When compared to MRI, EAVM appears to underestimate fibrosis burden. In the DECAAF study described above and in the cohort studied by McGann et al, 81% and 66% of patients respectively had >10% fibrosis in contrast to only 26% of patients undergoing EAVM demonstrating low voltage areas.(82, 97, 98) Using a cut-off of 0.05mV, only 6% of patients undergoing first time PVI demonstrate regions of scar.(83) EAVM therefore appears to lack the sensitivity for tissue characterisation possible through MRI. It must be remembered that the results of EAVM purely represent signals recorded at the endocardial surface. Mid wall and more epicardially distributed fibrosis may not result in low signal amplitude at the endocardial surface and regions of patchy LGE may similarly retain relatively preserved voltage amplitude.

1.4.2 Dynamic substrate

Both EAVM and LGE-MRI provide tools to evaluate the anatomic atrial substrate and identify structural modelling without providing assessment of the electrophysiological processes. As well as, and in close relationship with, structural changes responsible for AF are alterations in electrophysiological properties that promote fibrillatory mechanisms and may broadly be termed the dynamic substrate.

Electrical remodelling

A key early observation in the study of AF electrophysiology was the concept that “AF begets AF”.(100) Following clinical observations that patients with paroxysmal AF frequently progressed to persistent AF, Wijffels et al. conducted experiments in goats that were instrumented with electrodes sutured to the epicardium with the leads tunnelled exteriorly allowing repeated stimulation with rapid pacing to induce and maintain AF. Atrial effective refractory period (AERP) and conduction velocities were measured at baseline, and after varying periods of AF. Longer periods of pacing-maintained AF resulted first in shortening of the AFCL and subsequently longer durations of sustained AF with loss of spontaneous termination after the longest periods. Although little change in conduction velocities was observed, dramatic shortening in refractory periods occurred with increasing AF duration. Importantly, these electrophysiological changes reversed following a period of sinus rhythm.(100)

Many of these changes have since been identified in human AF, and a significant body of work has gone into identifying a multitude of molecular and cellular alterations

responsible for these electrophysiological adaptations. Reduced expression of depolarising L-type calcium channels alongside increased expression of inward rectifier potassium channels have been identified, potentially responsible for significant shortening of action potential duration.(101) Although these changes may be thought of as promoting re-entry, this does not necessarily support re-entry mechanisms within a hierarchical AF theory but may rather provide the environment to promote increased probability of re-entry waves occurring as stochastic regenerative renewal processes.(102)

Autonomic influence

The effect of vagal stimulation on atrial electrophysiology has long been recognised. Indeed, the early experiments conducted by Moe showed vagal stimulation was necessary for the maintenance of AF in dog studies and Garey had extensively discussed the importance of vagal stimulation many years earlier. Further animal studies showed this to largely be the result of shortening action potential duration and refractoriness promoting re-entry.(103) Adrenergic stimulation may also play a role, perhaps through promotion of enhanced triggered activity.(101)

Cardiac autonomic innervation is through a complex network of ganglionated plexi and are particularly concentrated around the PV and PV-LA junction.(101, 104) High-frequency stimulation of these sites has been shown to trigger both ectopy arising distant to the stimulation site as well as AF, generating further interest in the role of “upstream” autonomic mechanisms.(105)

1.4.3 Structure and Function Reconciled

Although the dynamic and structural substrate have so far been considered separately, the key to understanding AF mechanisms most likely lies in identifying how electrophysiology and anatomy interact and evolve over the natural history of the arrhythmia. Neither are stable factors. Structural atrial remodelling resulting in fibrosis is consistently observed in conditions also known to be associated with AF such as hypertension, obesity, heart failure, aging and sleep apnoea.(106) Similarly, AF itself may result in both fibrotic and electrical remodelling.(100, 101) As discussed, electrophysiological changes observed including abnormalities in calcium handling resulting in altered action potentials and refractory periods, as well as abnormalities of gap junction distribution and cellular conduction, combine with myofiber disarray resulting from interstitial fibrosis to add to the ingredients for re-entry.(101, 107)

Therefore, although structural changes occur both leading to and in the context of AF, the issue of key mechanistic importance is the functional effect of these alterations. Conduction velocity is known to be reduced in regions of bipolar electrogram amplitude

<0.5mV during EAVM of patients with AF.(108, 109) Regions of fibrosis have also been shown to result in non-uniform conduction slowing in optical mapping studies of explanted diseased hearts as well as in epicardial contact mapping in animal models.(110, 111) In explanted human hearts, zones of fibrosis were shown to anchor intramural re-entry through sub-centimetre tracts in the altered tissue architecture.(110) Similar observations have been made in regions of abrupt muscle fibre orientation changes in the left atrium(112), consistent with the recognition of exaggerated direction dependent changes in conduction velocity in patients with AF.(113) Recent work characterising AF “driver” regions identified using emerging technology, Cartofinder, has also shown these to be preferentially located in regions of maximal rate dependent conduction slowing and predominantly in regions of low bipolar voltage amplitude.(109)

Further evidence from cardiac MRI also suggests anchoring of rotational sources to structural heterogeneities.(114) Although the phenotype seen in advanced atrial remodelling is one of dense fibrosis, it may be that regions with patchy fibrosis and relatively preserved electrogram amplitude are most important from the perspective of potential ablation targets. It is here and in scar border zones that highly abnormal and fractionated electrograms may be observed although the mechanistic significance of regions with fractionation is questionable.(114, 115) However, the focus for much of this work described has been in the left atrium with relatively little work exploring the contribution of the right atrium.

1.4.4 Right versus left atrium

The landmark discovery of pulmonary vein ectopy triggering AF has resulted in much of the mechanistic focus remaining on the left atrium.(44) Related to this is the recognition that other regions of the left atrium, particularly the posterior wall share embryological origins with the pulmonary veins, helping to explain the importance of antral ablation and the role of the PV-LA junction in anchoring re-entry mechanisms.(73, 74) Similarly, dominant frequency studies suggest a hierarchical contribution with higher dominant frequencies seen in the left atrium. However, this gradient is lost as AF progresses, suggesting a diminishing role of the LA alone.(116, 117) As the role of the pulmonary veins diminish, the atrial substrate takes over, resulting in a substrate driven phenotype. This substrate is not restricted to the left atrium. Indeed, the loss of DF gradients results from acceleration in the right atrium (RA) and homogenisation between chambers rather than a slowing in activation rate in the left atrium.(116)

Early efforts to characterise AF electrophysiology in the cardiac catheter laboratory (then superseded by interest in the pulmonary veins) focussed on the right atrium with

limited and often indirect assessment of the left atrium (either via a patent foramen ovale or measurements in the left pulmonary artery).(118) In patients with induced AF, earliest activation appeared to be within the RA with evidence of conduction slowing and possible re-entrant mechanisms at the onset of the arrhythmia.(118) However, the mapping conducted was of limited density, focussed on AF initiation alone and largely neglected the left atrium. The same group developed this approach in early work adopting non-contact mapping technology. Again, direct LA mapping was limited in the absence of routine trans-septal access and therefore restricted to those with patent foramen ovale.(119) In the 45 in whom spontaneous atrial premature beats (APBs) were observed, 85 sites were identified, 60 of which were localised to the right atrium. In addition, they analysed segments during sustained AF in which electrograms organised into identifiable atrial tachycardias. In 56% of patients, this appeared to be right sided in origin.(119) This high incidence of atrial premature beats however conflicts with many physicians' clinical observations and it isn't clear how iatrogenic ectopy induced by catheter manipulation could be excluded, particularly considering 4-6 recording catheters in addition to the non-contact array balloon were used. Only sequential bi-atrial mapping was conducted using the non-contact array. However, these efforts served as an important step in attempting to characterise the biatrial electrophysiological substrate involved in AF propagation. They suggested that a key element distinguishing more persistent forms of the arrhythmia was the evolution to extensive and alternating atrial tachycardia circuits.

Subsequent work has explored the distribution of abnormal structural substrate identifying a lower mean electrogram voltage amplitude in the LA compared to the RA.(120) However, it is not clear whether this represents a difference in distribution of pathology or a physiological difference between the two structures. The development of techniques for in vivo AF mapping has also demonstrated a biatrial distribution in the dynamic properties of AF propagation. Early trials of the addition of linear ablation in patients with persistent (and longstanding persistent) AF suggested improved outcomes with the addition of RA ablation compared to LA ablation alone.(121) Early interest in identifying regions of complex electrogram fractionation suggested a high incidence in the RA and evaluation of approaches adopting biatrial ablation revealed 26% of patients reverted to sinus rhythm following RA ablation.(122, 123) This figure is in keeping with more recent work examining non-pulmonary vein AF drivers. In trials using FIRM mapping (discussed in more detail below), approximately 25% of driver sites are in the right atrium, with 85% of patients having at least one RA driver.(124, 125) In 22% of cases in which AF terminated with focal driver ablation, this was achieved with RA ablation.(125) Using non-invasive mapping, 31% of re-entry mechanisms and 29% of focal drivers were seen in the

right atrium in one study, which was consistent with a later multicentre study in which 27% of drivers localised to the RA.(126, 127)

So far however, studies have evaluated each chamber sequentially and identified the presence of mechanisms independent of each other. There has been no systematic work exploring how the atria interact in maintaining AF and how the temporal variation in driver dynamics may influence propagation between chambers. Experimental work in animal models have assessed regional dominant frequencies across interatrial connections suggesting a gradient across Bachmann's bundle (BB).(65) Indeed, this is a well recognised inter-atrial connection widely thought to be responsible for rapid conduction between chambers. Delayed conduction across BB has been associated with development of atrial arrhythmias.(128) Additional inter-atrial pathways have also been identified including the septopulmonary bundle, posterior interatrial connections, infero-posterior pathways between the coronary sinus and inferior pulmonary veins, and via musculature around the fossa ovalis.(129-131) However, their role during AF has not been characterised. In fact the action potential duration of BB myocytes is prolonged in canine studies.(101) This suggests longer refractoriness, which in the presence of rapid activation during AF may diminish the conductive role of BB and shift conduction to alternative sites.

1.5 Strategies for AF ablation beyond the pulmonary veins

As discussed in detail, the cornerstone of AF ablation is pulmonary vein isolation, which has evolved into an empiric strategy of wide area circumferential isolation. This has proved successful in patients with paroxysmal AF,(132, 133) but significantly less effective in patients with persistent AF.(134, 135) This suggests a fundamental difference in the critical fibrillatory mechanisms involved, with less dependence on pulmonary vein ectopy and increasing contribution of non-pulmonary vein arrhythmia substrate. This has resulted in exploration of additional ablation strategies in patients with persistent AF that include both empiric and individualised approaches. As our understanding of the mechanisms of fibrillation have evolved alongside parallel technological advances, increasing interest has been directed towards identifying individualised mechanisms that can be targeted by ablation.(136) Key to this approach is the ability to translate novel experimental findings into the clinic to identify and target the individualised mechanisms involved in AF propagation. A number of approaches have emerged with this objective at their core.

1.5.1 Empiric strategies

Linear ablation

In part following early observations by Garrey and in line with the multiwavelet hypothesis of AF propagation, the addition of linear ablation lesions to PVI gained much attention, with the theoretical aim of creating a degree of atrial segmentation and encouraging coalescence of wavelets or disruption of re-entry resulting in AF termination. Early studies evaluated the addition of linear mitral isthmus ablation with or without a roof line to pulmonary vein isolation alone or in combination with cavo-tricuspid isthmus (CTI) ablation in mixed populations of patients with both paroxysmal and/or persistent AF.(137-142) Although a number of these studies suggested benefit in terms of freedom from AF, an increase in atypical left atrial flutter was frequently associated with the addition of ablation beyond the pulmonary veins. The addition of linear ablation lesions became a key aspect of a stepwise ablation approach proposed by the Bordeaux group that sought to achieve a slowing in AFCL and AF termination, which appeared to result in improved clinical outcomes.(143, 144) These results were supported by results of subsequent meta-analyses.(145)

The majority of the benefit observed with the addition of linear ablation in these studies was in patients with persistent rather than paroxysmal AF in whom pulmonary vein isolation alone appeared efficacious. Interest was therefore focussed on this group, but despite the promising early data, the pivotal STAR-AF2 trial showed no incremental benefit of linear ablation, using a combination of roof and mitral isthmus lines, compared to PVI alone. In this study, a single PVI procedure resulted in a 59% freedom from arrhythmia (AF or AT) recurrence over a follow up of 18 months.(135)

Reasons for this lack of benefit are unclear. However, it should be noted that significant technological advances had occurred since the earliest studies of circa 2004-8, particularly with the advent of 3-dimensional mapping. These advances may have resulted in improved delivery of pulmonary vein isolation thereby eliminating the benefit seen from additional ablation achieved in un-blinded single centre studies. Outcomes may also have been limited by ability to achieve durable conduction block across linear lesions, particularly in the posterolateral mitral isthmus where this can be notoriously difficult to achieve.(146)

Posterior wall isolation

As alluded to in previous sections, observation of shared embryological origins between the pulmonary veins and posterior LA wall as well as early suggestion of clustering of high frequency sources to the posterior LA made posterior wall isolation (PWI) an attractive target for additional empiric ablation.(147)

Single centre observational studies in patients with both paroxysmal and persistent AF provided initially encouraging results, with mixed results in early randomised controlled trials.(148, 149) One of the challenges of interpreting this data however is significant variation in the technique employed to obtain PWI including a single ring incorporating the PVs and posterior wall, a box lesion around the posterior wall itself, and point by point ablation eliminating all signals on the posterior wall, which may be termed a debulking approach. This variation is evident in high rates of posterior wall reconnection, reaching 63% in pooled analysis, although may be lower if a debulking approach is employed.(148, 150) The first randomised studies largely included patients with paroxysmal AF in whom it may be harder to improve upon results of PVI alone, in contrast to the first study in patients only with persistent AF in whom a significant benefit was identified.(149) Unfortunately, further randomised multicentre studies have not been able to reproduce these benefits. The POBI investigators randomised 213 patients with persistent AF across 5 centres in South Korea to compare a strategy of box PWI to PVI alone. Over average follow up of 16 months, freedom from arrhythmia recurrence without the use of antiarrhythmic drugs was 50.5% in the PVI group and 55.9% in the PWI group (p=0.522).(151) In a smaller studies of patients with persistent AF changed to paroxysmal with the use of antiarrhythmic drugs, and those with persistent AF undergoing repeat procedures following index PVI alone, no additional benefit has been demonstrated.(152, 153) Of note, the only randomised study performed using a strategy of posterior wall debulking, using a cryoablation approach, demonstrated significant improvement in freedom from recurrent AF, but this was balanced by an increase in AT, although this was a small study with only 55 patients in each arm.(154)

Overall, there is still much debate as to the incremental benefit of PWI including the optimal approach to its delivery. Results of larger, multi-centre studies are eagerly anticipated.(155)

Left atrial appendage isolation

The arrhythmogenic role of the left atrial appendage (LAA) has emerged from identification of possible re-entry triggers responsible for emergence of atrial tachycardia in patients undergoing ablation for persistent AF.(156) Since then, a number of studies have evaluated the role of LAA isolation (LAAI) in patients with persistent and long-standing persistent AF using either radiofrequency ablation, exclusion with a Lariat device or cryo-ablation. A meta-analysis of these studies suggests significant benefit from LAA isolation with a freedom from recurrent arrhythmia at 12 months of follow up of 75.5% compared to 43.9% in patients not receiving LAA isolation.(157) However, of the 7 studies included in this analysis only the BELIEF trial was a prospective randomised study.(158)

The BELIEF trial evaluated the addition of LAAI to a control strategy of PVI, PWI including ablation down to the coronary sinus, superior vena cava isolation and ablation of triggers identified using high dose isoproterenol infusion in 173 patients with longstanding persistent AF. LAA ablation was permitted in the control arm if triggers were identified using isoproterenol but was only performed in 9% of patients in this group. At 12 months follow up, 56% of patients in the LAAI group were free of recurrent arrhythmia compared to 28% in the control group (p=0.001).(158) Notably, albeit in a challenging group of patients, the results in the LAAI group were modest when compared to contemporary data using other approaches with the statistically significant benefit really arising from the particularly poor results in the control arm.

A major complication with the adoption of LAAI is the risk of stroke arising from thrombus formation within an electrically isolated and non-contractile appendage. Although reported stroke rates were low in the BELIEF trial, this was over only a short period of follow up with diligent use of antithrombotic drugs. Others report rates of LAA thrombus of 23% with rates of combined LAA thrombus and/or thromboembolism of 28%, despite anticoagulation over a longer follow up period.(159) Many consider LAAI to mandate LAA occlusion presuming a significant risk of thrombus formation with even a short interruption of anticoagulation.

Vein of Marshall ethanol ablation

The vein of Marshall (VOM) is a branch atrial vein draining into the coronary sinus that courses along the epicardial LA through the lateral ridge between the LAA and left upper PV, and the posterolateral mitral isthmus in a region rich in autonomic innervation that has been implicated in the origin of ectopic foci and is traditionally targeted from the endocardium during mitral isthmus ablation as outlined above. Considering both the putative arrhythmogenic properties of this region in combination with challenges of durable mitral isthmus conduction block with endocardial radiofrequency ablation, Valderabanno developed a technique of selective VOM cannulation, balloon occlusion and ethanol injection to achieve ablation. In canine studies, both feasibility and efficacy were shown in conjunction with a significant blunting of autonomic responses as evidenced by lack of change in AERP with vagal stimulation after VOM ethanol infusion.(160) Feasibility in humans was also demonstrated with electroanatomic voltage mapping revealing significant areas of low voltage on the posterior wall and posterolateral mitral isthmus.(160, 161)

The Bordeaux group have subsequently incorporated VOM ethanol ablation into a broader strategy for the treatment of patients with persistent AF termed the Marshall plan

that includes VOM ethanol injection, ablation with the aim of eliminating local electrogram signals within the coronary sinus, PVI, and linear endocardial ablation to the roof, mitral isthmus, and CTI.(162) Single centre evaluation of this strategy in a prospective cohort of 75 patients with persistent AF showed promising results with 72% of patients free from recurrent arrhythmia at 12 months, following a single procedure.(163)

Adjunctive VOM ethanol has also been evaluated in the VENUS randomised controlled trial. A total of 343 patients were randomised to a strategy of catheter ablation alone compared to catheter ablation in addition to VOM ethanol ablation. Although non-PV ablation was not mandated within the protocol, approximately 96% of patients in both groups received additional empirical ablation, which in between two thirds and three quarters of patients consisted of PWI. A statistically significant benefit was observed with 38% of patients in the catheter ablation group and 49.2% in the VOM ablation group free from recurrent arrhythmia over 12 months, rising to 51.6% when only patients in VOM ethanol could be achieved were included.(164)

Challenges of empiric strategies

As outlined above, a number of trials evaluating various empiric strategies have yielded statistically significant benefit, particularly the BELIEF and VENUS studies. Notably, neither of these studies test the addition of a single adjunctive strategy against PVI alone with the control arms of both studies consisting of ablation strategies that have not themselves been shown to be superior to a limited strategy of PVI. The benefit observed in the study intervention groups resulted largely from particularly (and unexpectedly) poor outcomes in the control arm rather than overwhelmingly improved success rates associated with the study intervention. It is of course difficult to identify what the explanation for this may be but a degree of unconscious bias on the part of investigators carrying out the procedures cannot be ruled out. It should also be noted that both these strategies involve extensive destruction of (left) atrial myocardium with associated loss of contractile properties.

1.5.2 Individualised strategies

Methods of identifying the structural atrial changes involved with AF are based around MRI to identify LGE and invasive EAVM to identify low voltage areas, both of which have been discussed above. However, with advancing experimental evidence of AF mechanisms, approaches to analyse the underlying electrophysiology with the aim of guiding patient specific ablation strategies have emerged. Unfortunately, methods employed in the experimental “bench” setting cannot always be translated to the clinical electrophysiology laboratory. A vital tool of experimental electrophysiology is optical

mapping using potentiometric dyes, however, the toxicity of these dyes precludes their use clinically. The challenge in the clinical setting is one of both recording the electrophysiological data during AF and, crucially, processing the complex fibrillatory signals.

Conventional 3-dimensional electroanatomical mapping systems now in widespread use rely on manipulating recording electrodes around the atrial endocardial surface to undertake activation mapping, referred to as point-by-point mapping. In stable arrhythmias, this is able to create a visual model of wavefront propagation. AF however is characterised by chaotic wavefront propagation with significant variation in spatiotemporal distribution of atrial activation. This limits the ability of conventional techniques to evaluate whole chamber activation during atrial fibrillation and therefore their usefulness for identifying patient specific mechanisms. A number of techniques aimed at overcoming these challenges have emerged.

Complex fractionated electrogram ablation

One of the earliest attempts to develop an ablation approach guided by individualised electrophysiology was the targeting of complex fractionated atrial electrograms (CFAE). Nadamanee hypothesised that CFAEs represented sites of slow conduction and/or pivot points around regions of functional block and that ablation at these sites should prevent wavelet re-entry and therefore AF perpetuation.(122) This approach was incorporated into the stepwise strategy developed by the Bordeaux group with targeting of CFAE resulting in high rates of AF termination.(144)

A particular limitation however is the lack of specificity of identified ablation targets, with electrogram fractionation influenced by several factors including wavefront collision, slow conduction, wavefront direction and anisotropy, size and spacing of mapping catheter electrodes, as well as possible arrhythmogenic mechanisms. Randomised controlled trial evaluation of this approach showed no clinical benefit, alongside high rates of ablation induced complex atrial flutters.(135)

Ganglionic plexus ablation

The role of the autonomic nervous system has attracted significant attention as an attractive “upstream” target for ablation. Use of high frequency stimulation allows mapping of GP sites with effects on both atrio-ventricular conduction and ectopy induction.(105, 165) A small study of individualised GP ablation without PVI compared to PVI alone in patients with paroxysmal AF showed interesting results. Although not statistically significant, GP ablation alone resulted in a high rate of arrhythmia recurrence, but less requirement for antiarrhythmic drugs.(166)

Although mapping of GPs using high frequency stimulation provides an individualised approach, the concentration of ectopy triggering GPs around the PVs suggest an inadvertent targeting of these sites during PVI that may account for some of the benefit seen beyond simply electrically isolating the PVs.(104) Harnessing this observation has also resulted in improvements in outcomes in patients with paroxysmal AF through the addition of empiric extension of the PVI encirclement at specific anatomic sites associated with GP clusters, although these approaches have not been systematically evaluated in patients with persistent AF.(167)

Dominant frequency

The concept of dominant frequency (DF) analysis emerged from early optical mapping evidence of focal re-entry which revealed cycle lengths that correlated with the electrogram frequency at these regions on spectral analysis.(168) The principle relies on identifying the activation rate of the main atrial signal at any given site. The region with the highest frequency of its main signal represents the site of a putative rotational driver.(169) In practice, this involves conversion of atrial electrograms from the “time domain” to the “frequency domain”. In the clinical electrophysiology laboratory, an electrogram signal is recorded in the time domain, whereby the amplitude is plotted against time. The principle underpinning DF analysis is that the electrogram is made up of a set of sinusoidal waves, each with a specific frequency and amplitude, which are identified using a Fast Fourier Transform followed by a set of filtering steps.(169) These frequencies are then plotted as a power spectrum. The frequency with the highest power is the dominant signal at that site and represents the activation rate.

Following on from results in animal models, studies during catheter ablation have suggested a gradient of dominant frequency from the left to right atrium with highest frequency at the PV-LA junction in patients with paroxysmal but not persistent AF.(116, 170) Furthermore, segmental pulmonary vein isolation in patients with paroxysmal AF appears to abolish this gradient, whilst patients with persistent AF who have a baseline LA-RA frequency gradient have better rates of long term freedom from AF following PVI.(117) This confirms the importance of the PVs in patients with paroxysmal AF and potentially explains why PVI alone is successful in a proportion of patients with persistent AF. These findings have been supported in work by Atienza et al which included ablation aimed at targeting the highest DF sites in both the LA and RA in 50 patients with a mix of paroxysmal and persistent AF.(171) A global reduction in DF and abolition of the LA-RA gradient, when present was associated with improved freedom from AF.(171) However, a randomised study has since shown no incremental benefit in adding ablation of highest DF sites to PVI in patients with persistent AF, essentially confirming the importance of

PVI.(172) To date therefore, DF analysis appears to identify patients in whom PVI alone is less efficacious but the evidence that high DF sites outside the PVs represent critical drivers in humans is weak, whilst there is no evidence that ablation of these sites is beneficial.(173)

Phase analysis

Phase is a technical descriptor that facilitates the tracking of a specified region of myocardium through the action potential thereby enabling analysis of spatiotemporal changes during atrial fibrillation.(174) Evaluating the distribution and pattern of phase over time is used to provide insights into mechanisms of fibrillation.(174) Regions of particular interest are those identified around which phase is seen to transition through a complete cycle from –π to +π.(174) Here, the phase is indeterminate and the propagating wave is rotating around this hinge point in an organized manner. This central region with indeterminate phase is referred to as the singularity.(174)

This method relies on computing the phase of a unipolar electrogram at each instant of time and calculation of a phase shifted signal, most commonly using a mathematical approach known as the Hilbert Transform. Plotting of the 2 signals against each other should create a circular loop when there is a consistent relationship between the instant and time delayed samples allowing the calculation of the phase angle as the system traverses this plotted loop.(175) Subsequent analysis of the phase of all the electrograms acquired during a recording at every instant in time facilitates identification of potential spatial organization. Recognition of a progressive transition in space through the entire phase cycle from –π to +π as mentioned above suggests the presence of a rotor.(174)

This method does however possess a number of limitations. Each unipolar electrogram that forms the basis of the phase analysis is obtained from the integration of electrical potential signals within a small region of myocardium.(174) Highly localized activation patterns such as local micro-reentry may not be detected. Similarly, unipolar electrograms are highly susceptible to far-field signals and noise, which may particularly be the case in regions of scar, thereby disrupting the spatial distribution of phase.(176, 177) Sensitivity and specificity for rotor detection are also highly affected by inter-electrode distance, which is very sensitive to changes in basket spline position during manipulation within the atria.(177, 178) Bunching of splines particularly affects the equatorial electrodes resulting in interspline distances ranging between 1.5 to 85.1mm.(177) Interpolation then fills the space between electrodes, with this reliability falling with increasing distance from the recording electrode. Although this may not limit

the sensitivity of rotor detection, it significantly reduces specificity with a high rate of false rotor detection.(176-179) A similar problem is seen with signal filtering methods, of which a consistent approach is lacking. Band-pass filtering (at highest dominant frequency) can affect sensitivity and specificity of rotor detection resulting in false detection of rotors and falsely increasing both spatial and temporal stability of detected rotors.(179-181)

Focal Impulse and Rotor Modulation

Narayan et al. pioneered a system using a 64 pole basket catheter to conduct global atrial contact mapping.(182, 183) Contact electrograms are processed using complex proprietary software based around phase mapping to identify and ablate focal impulses and rotors thought to represent drivers of AF, in a process referred to as focal impulse and rotor modulation (FIRM).(184) They have identified rotors in both the left and right atria, with ablation of these sites in combination with PVI resulting in good outcomes both acutely and in longer term follow up.(124, 184, 185) However, such positive results have not always been replicated and other studies have not revealed the stable rotors described.(181, 186, 187) More recent clinical evidence does not support this approach.(188, 189) This may in part be due to difficulties with electrode contact. Although different size baskets are available, it is often difficult to ensure good electrode contact with the endocardium. Some studies have reported coverage of only 50% of the atrial endocardial surface with rotors falsely identified in regions without electrode contact.(190, 191) These technical considerations result in highly limited spatiotemporal resolution in comparison to optical mapping possibly explaining the limited benefit seen and variation in results compared to laboratory experimental data.

Electrocardiographic Imaging

In contrast to invasive catheter based FIRM mapping, electrocardiographic imaging (ECGI) is a non-invasive mapping approach. Using the ECVUE System (CardioInsight, Medtronic, MN, USA), unipolar body surface potentials are recorded from the torso using a vest made up of 252 electrodes. Computed tomography is then used to generate images of electrode position and atrial anatomy. Using this data, virtual epicardial surface electrograms can be derived using a complex mathematical inverse solution to Laplace's equation. Activation maps are then displayed based on activation time annotation using the maximum -dV/dt and further signal processing including phase mapping may be conducted to characterise propagation patterns.(192)

This technique has been used to identify driver mechanisms that may represent targets for catheter ablation with some evidence of improved outcomes.(126, 193) However, given that the mapping is performed prior to an ablation procedure and without

conventional 3-dimensional electroanatomic mapping, precise localization of driver regions for ablation can be difficult. This is compounded by a localization error introduced by the inverse solution methodology and the fact that it is not clear whether epicardial activation also reflects endocardial activation.(176) Moreover, recent validation work comparing to epicardial contact mapping has raised questions about the overall accuracy of the approach.(194) Finally, the septum cannot be visualised.

Non-contact charge-density mapping

The AcQMap system (Acutus Medical, CA, USA) is a high resolution combined imaging and electrophysiological mapping system that uses catheter based ultrasound crystals to generate atrial endocardial surface anatomy onto which electrical activation maps are visualized. This is a basket type catheter comprising 6 splines, each of which incorporates 8 ultrasound transducers and electrodes. When positioned in the centre of either atrium, a 3-dimensional image of the atrial surface is acquired by ultrasound through processing of up to 115,000 points per minute allowing the entire anatomy to be generated within a few minutes. The 48 electrodes are then used to record raw intracardiac unipolar signals. The entire chamber field is recorded at a rate of 150,000 samples/second. An inverse solution is applied to recreate signals on the generated endocardial surface anatomy. The use of regularisation and normalisation techniques as well as the close proximity of the electrodes to the potential source on the atrial endocardium serve to limit the errors introduced in the solution to the inverse problem.

Uniquely, this system uses charge density mapping to provide more focused, high resolution visualisation of cardiac activation in comparison with voltage signals.(195) A dipole is a localised entity of two closely spaced oppositely charged particles. As an action potential is generated within the myocardium, facilitated by the movement of ions across the cell membrane, a small dipolar charge imbalance is created in the region of the adjacent extracellular space. The initial depolarization is followed by recruitment of adjacent cells and spreads outwards, where the dipole layer directly represents the propagating wavefront. There is then a fundamental difference between the voltage signal and charge, as the mere presence of these dipole charges results in the distribution of voltage extending beyond their localised physical boundary.(195) These local charges represent the sources of the potential field measured as an electrogram by conventional electrophysiological recording systems or as an electrocardiogram when measured on the body surface. Therefore, although the raw signals recorded are intra-cavitary potential signals, knowledge of the relationship between potential and charge defined by Poisson's equation, and utilization of the inverse solution enables the dipolar charge sources on the

endocardial surface to be derived and displayed as an activation wavefront across the atrial surface.(196)

Annotation of the negative slope of the charge signal, which correlates with phase 2 of the action potential, identifies the zone of depolarisation at any instant in time and enables construction of a propagation map.(195) This is visualized as a moving leading edge of a wavefront displayed as an isochronal map, with differing isochronal spacing representing changing conduction velocities. Interpretation of the propagation map is assisted by inbuilt AcQTrack™ software. This is an automated algorithm that tracks and evaluates conduction at every vertex of the anatomy (approximately 3,500 in total) thereby removing any subjectivity from the classification and quantification of activation patterns. The distance between each vertex is approximately 2mm, which represents the spatial resolution. Whilst planar activation wavefront are excluded, this enables identification of directional changes in propagation to be identified and characterised. Three distinct patterns of propagation are identified including focal firing (FF), localised rotational activation (LRA) and localised irregular activation (LIA).

The advantage of this technology is that it allows panoramic mapping of AF propagation without requiring a timing reference or uniform catheter contact. The charge (rather than voltage) approach results in sharper signals and reveals complex propagation patters not visualised using other systems and particularly missed by a phase analysis approach which attempts to impose a transition from –π to +π which is not present in regions of complex irregular conduction. To date, this technology is limited to only a few centres in the UK as well as Europe and North America. However, the first multinational, single arm clinical trial evaluating its use (UNCOVER-AF) has revealed promising results.(197) No studies have sought to explore the significance of the propagation patters identified or evaluate their relationship to the underlying atrial substrate.

1.6 Summary and Research Questions

Whilst the pulmonary veins and PV-LA junction are the key targets for AF ablation, it is clear that additional mechanisms are involved resulting in limited efficacy of pulmonary vein isolation alone. This additional substrate includes fixed structural changes in the form of atrial fibrosis, identified with the use of late gadolinium enhancement on cardiac MRI or low voltage electrograms during invasive electroanatomic mapping, and dynamic electrophysiological mechanisms that may be either passive processes of fibrillatory conduction or mechanistic “drivers” responsible for AF maintenance.

One of the major challenges in developing ablation strategies for AF is a clear understanding of the arrhythmia mechanisms involved. Although this section has outlined

in detail many of the competing theories and factors identified in AF initiation and maintenance, there is significant heterogeneity between patients that extend beyond simple classifications of paroxysmal and persistent, which are of course based purely on the time it takes for the earth to rotate rather than on any measure of electrophysiology. A great deal of effort, as evidenced by the literature reviewed here has gone into trying to describe a unifying hypothesis for the mechanism of AF. However, given such observed clinical heterogeneity it may likely be that a universal mechanism does not exist, but rather any number of factors combine and vary in individual patients

Furthermore, technological considerations have limited the translation of laboratory experimental methods of AF mapping into human studies, also contributing to some of the disparity in results. The emergence of charge density non-contact mapping overcomes many of the limitations of alternative technologies and facilitates global mapping of AF propagation to identify a range of complex propagation patterns. However, it is not clear what these patterns of propagation represent in terms of mechanistic processes and their relationship to the underlying structural changes that may be present. In addition, the relative role of the right and left atrium in AF maintenance as well as the dynamics of interatrial conduction during AF have not been clearly characterised.

This work therefore seeks to:

1. Develop tools for analysis and quantification of complex patterns of AF propagation identified using AcQMap charge density mapping that can be applied to compare patients
2. Evaluate these tools to explore the effect of adenosine on wavefront propagation patterns during AF
3. Explore the spatiotemporal properties of AF activation and relate these to properties of atrial conduction and structure during sinus rhythm
4. Perform simultaneous bi-atrial mapping in patients with both persistent and paroxysmal AF to reveal patterns of interatrial communication and the relative role of the LA and RA to arrhythmia maintenance
5. Develop novel techniques for assessment of AF electrophysiological phenotype based on whole chamber recordings of AF activation
6. Explore clinical outcomes in a real world cohort of patients undergoing individualised charge density guided ablation of persistent AF.

2 Methodology development

2.1 Introduction

In this chapter the methods for collection of clinical mapping data applicable to much of the further work described is outlined. This is followed by a detailed description of activation pattern identification and the development of custom tools for the quantification of electrophysiological substrate properties.

A crucial tool in quantifying complex propagation patterns is the adoption of defined criteria based on conduction properties that can be used to provide an objective method for identification of specific phenomena. The focus of prior work attempting to identify local sources acting as drivers responsible for maintenance of AF, has been on identification of either focal activations or sites of spiral wave re-entry (or “rotors”).(126, 183) However, fibrillatory conduction beyond possible driver mechanisms is complex and poorly characterised. Non-contact signal acquisition however allows visualisation of whole chamber activation and the identification of additional features of fibrillatory conduction. The integration of a system of wavefront activation tracking allows classification of these conduction patterns, which is crucial to objective identification and quantification.

Key to many of the research goals within this project is the ability to quantitatively analyse patterns of AF propagation to allow comparisons between AF maps both within and between patients. It is hypothesised that the complex propagation patterns revealed using the AcQMap mapping system represent features of the underlying atrial substrate and that the dynamic patterns are affected by structural properties. If these patterns are of mechanistic importance then it is crucial that a method of quantification is possible that can guide ablation strategies. Therefore, both global measures and methods to localise specific regions are needed. We sought to develop tools using both new methods and the application of established techniques to this specific dataset that will facilitate the desired comparisons.

2.2 Clinical study procedures and data acquisition

2.2.1 Patient selection

Patients undergoing clinically indicated catheter ablation for symptomatic atrial fibrillation were recruited following informed consent and approval from the appropriate Research Ethics Committee. All study procedures complied with the principles of the Declaration of Helsinki.

2.2.2 Clinical mapping and ablation procedures

All procedures were performed under general anaesthetic and high-frequency jet ventilation to aid catheter stability in line with local clinical practice. Transoesophageal echocardiography was used to exclude left atrial appendage thrombus. Bilateral femoral venous access was obtained using direct ultrasound guidance. A decapolar catheter (Inquiry, Abbott Medical) was positioned within the coronary sinus to serve as a positional reference and for analysis for coronary sinus bipolar electrograms. For initial procedures, an additional quadripolar catheter was advanced into the inferior vena cava (IVC) and below the diaphragm to serve as a unipolar reference. Subsequently a dedicated access sheath (AcQRef, Acutus Medical) was used which included a unipolar reference electrode on the distal tip of the access sheath, through which the coronary sinus decapolar catheter was placed.

A single trans-septal puncture was performed under trans-oesophageal echocardiogram guidance using a Brockenbrough needle through a SL0 sheath, through which an ablation catheter was also passed. Heparin was administered as an initial bolus followed by continuous infusion to maintain an ACT of 350s throughout. The trans-oesophageal echocardiogram probe was then removed and an oeshophageal temperature probe placed.

The SL0 sheath was exchanged over the guide wire for an AcQGuide sheath (Acutus Medical) through which the AcQMap imaging and mapping catheter was advanced.

2.2.3 Atrial geometry and noncontact signal acquisition

Atrial chamber anatomy was generated using ultrasound integrated onto the AcQMap catheter. A technique of catheter roving and rotation is used to collect reflected ultrasound signals and define the endocardial surface as shown in figure 2.1. Post-processing of the raw surface generated results in generation of a triangular surface mesh comprising approximately 3,500 vertices forming the corners of the constituent triangular faces. The mitral annulus and pulmonary vein ostia can be defined and manually cut out to form the final anatomical reconstruction.

Acquisition of AF signals is carried out from a static central position within the chamber, identified by visualisation of equal distribution of ultrasound signals in relation to the adjacent chamber surface. Raw signal recordings were obtained, and segments of AF propagation calculated for durations specific to the requirements of specific analyses described in subsequent sections. Raw signals are visually inspected to identify spurious signals resulting from possible damage to catheter recording electrodes during insertion

and manipulation, which are then excluded. A 100Hz low pass and 50Hz notch filter together with smoothing algorithm are applied. Callipers are used to select a QRS-T wave template and applied to the algorithm for subtraction of ventricular far-field signals prior to calculation of charge density and generation of a propagation history map. Propagation history maps were generated using the default method of activation time annotation based on identification of the maximum negative dv/dt. A time threshold of 70ms was applied representing a conservative value for presumed refractoriness and a window width for visualising the lead and trailing edge of an activation wavefront was set at 80ms.

In all patients, initial mapping data acquisition was performed prior to any catheter ablation. Recordings of AF were obtained at the start of the procedure in patients attending in AF, whilst in patients attending the procedure in sinus rhythm recordings of atrial pacing were obtained initially where required and AF then induced using burst atrial pacing from the coronary sinus. Maps of atrial pacing were otherwise obtained following direct current cardioversion (DCCV) if required.

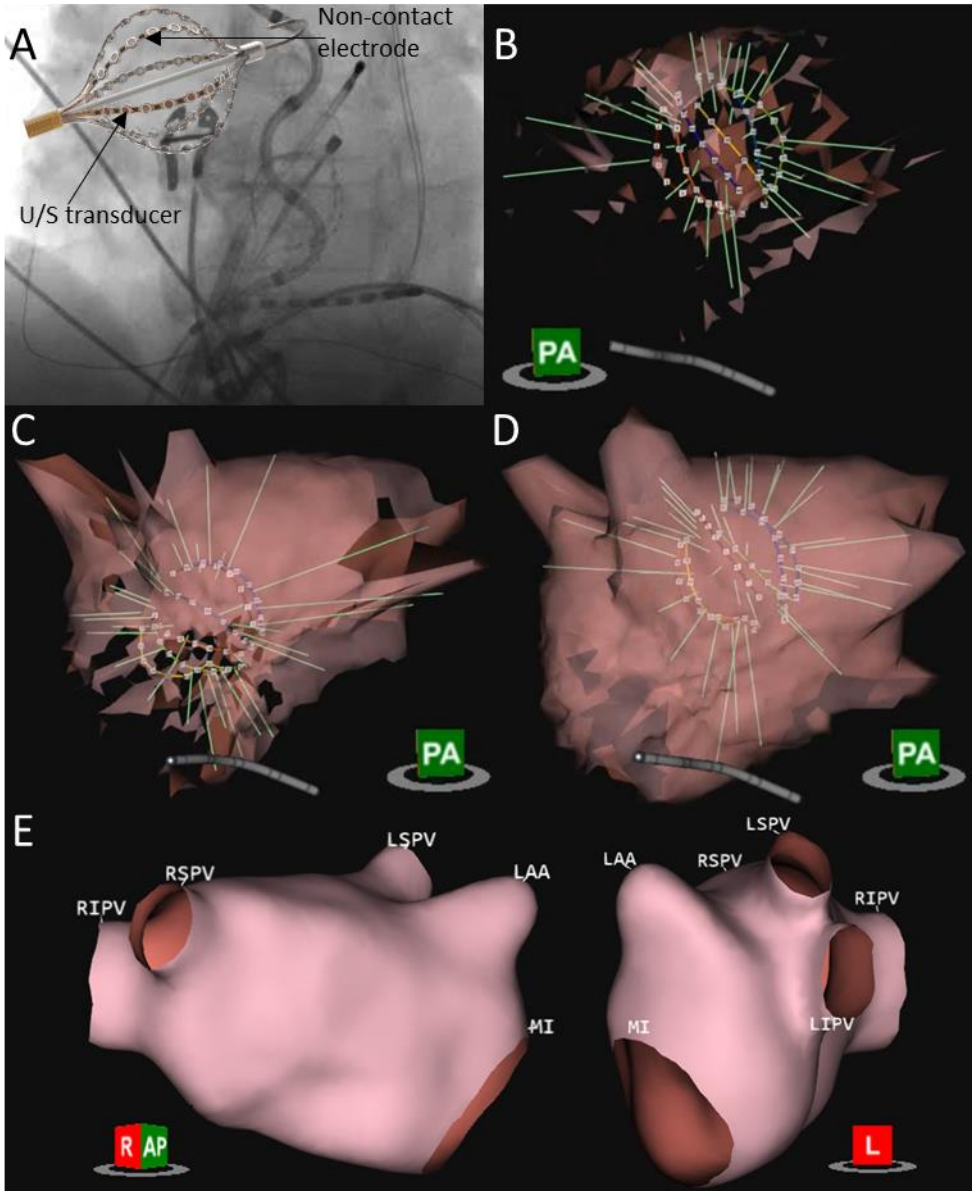

Figure 2.1 Collection of ultrasound chamber geometry. Fluoroscopic view of the AcQMap catheter *positioned within the left atrium (A) and (inset) with the 8 ultrasound (U/S) transducers and 8 electrodes shown on the 6 splines of the catheter. Ultrasound is used to generate the chamber anatomy (B-D) with the ultrasound beams illustrated by green lines emanating from the basket transducers. Following post-processing, the final anatomy is generated (E). AP, antero-posterior; L, left lateral; LAA, left atrial appendage; LIPV, left inferior pulmonary vein; LSPV, left superior pulmonary vein; MI, mitral isthmus; PA, postero-anterior; RIPV, right inferior pulmonary vein; RSPV right superior pulmonary vein.*

2.2.4 Multi-position non-contact mapping of atrial pacing

Where appropriate specific to the study outlined in further sections atrial pacing was conducted from up to three atrial sites including the left atrial appendage, high right atrium and proximal coronary sinus. A protocol consisting of a 4-beat drive train at 800ms cycle length followed by a single extrastimulus with coupling interval 20ms above the

effective refractory period and was used and mapped using the AcQMap multi-position non-contact “SuperMap” algorithm.

SuperMap data acquisition is obtained using multi-position recording. The non-contact catheter is manoeuvred throughout the chamber and in turn positioned in close proximity to all portions of the endocardial surface. Adequate proximity to the chamber surface is indicated by a change in colour on the portions of the surface at which adequate coverage has been obtained with additional proximity indicators highlighting when inadvertent contact of the recording electrodes and chamber surface is made. Catheter localisation is achieved based on the impedance field.

During recording, contact unipolar signals recorded from the decapolar catheter positioned within the coronary sinus are continually collected and analysed according to both signal morphology and cycle length. From this analysis, coronary sinus electrograms are automatically binned (this does not require a user defined template) into beat groups up to a maximum of four unique groups. Simultaneously obtained non-contact unipolar signals are “binned” according to the coronary sinus beat group identified and signals obtained from each point in the chamber can then be combined according to the relevant beat group to form a whole chamber activation map. A minimum of 10 beats are required to form a unique beat group. This allows the ability to collect and identify different paced cycle lengths collected simultaneously.

Propagation history maps generated are visualised as a moving leading edge of an activation wavefront with a trailing colour band to aid interpretation, as explained above for AF propagation maps. The width of this colour band (in milliseconds [ms]) can be manually adjusted according to user preference. Default settings for map calculation exclude signals recorded within 5mm of the endocardial surface thereby ensuring exclusion of inadvertently collected contact signals. In the case of low amplitude signals, for example in highly scarred atria, a high-sensitivity calculation can be selected, which incorporates signals recorded at a distance up to but no less than 0.5mm from the chamber surface. An example of SuperMap acquisition during pacing is shown in figure 2.2.

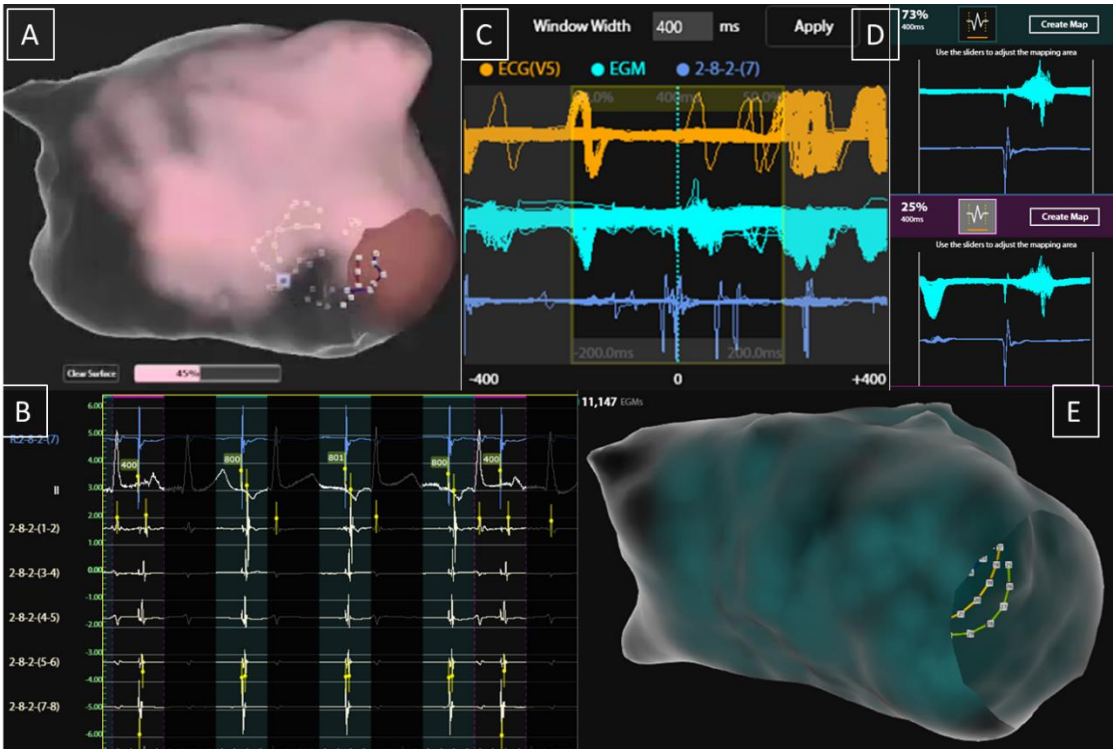

Figure 2.2 Example of SuperMap acquisition during pacing using a repeating 3-beat drive train at 800ms cycle length followed by a single extrastimulus at 400ms cycle length. SuperMap non-contact multi-position atrial electrogram data is obtained during continuous manipulation of the AcQMap catheter throughout the chamber with the surface illuminating once adequate proximity has been obtained (A). The proportion of the surface covered is updated throughout. Each cycle detected is grouped according to coronary sinus electrogram cycle length and morphology, with 800ms paced beats highlighted in green and extrastimulus beats in pink (B). The window of interest can be adjusted as required (C) and the proportion of data within each beat group identified (D). The group of interest can be selected to show the density and number of non-contact electrograms included (E) and generate a propagation history map of wavefront activation.

2.3 Developing tools for quantification of activation patterns during atrial fibrillation

2.3.1 Propagation pattern characterisation

Localised patterns of activation, as highlighted above are identified using AcQTrack, an integrated platform within the AcQMap system. The propagation history map is first generated based on virtual dipole signals from each of approximately 3,500 vertices on the chamber surfaces and derived from biopotential signals recorded on 48 non-contact electrodes. This map allows visualisation of wavefronts over the atrial surface. AcQTrack evaluates the propagation of these wavefronts to identify specific patterns of activation. Every vertex of the chamber is continuously analysed during the display of the propagation history map thereby allowing real-time identification of regions of interest, which can be displayed as both a dynamic map (where each activation pattern is highlighted during playback of the propagation history) and a cumulative map, where a sliding scale allows adjustment to the display according to the frequency of each pattern

detected at any localised site. Patterns of activation identified include focal firing (FF), localised irregular activation (LIA) and localised rotational activation (LRA), with the specific algorithm used for their detection described below. Representative examples of these patterns are seen in figure 2.3. Wavefronts that do not meet these definitions (for example smooth planar wavefronts) are discounted.

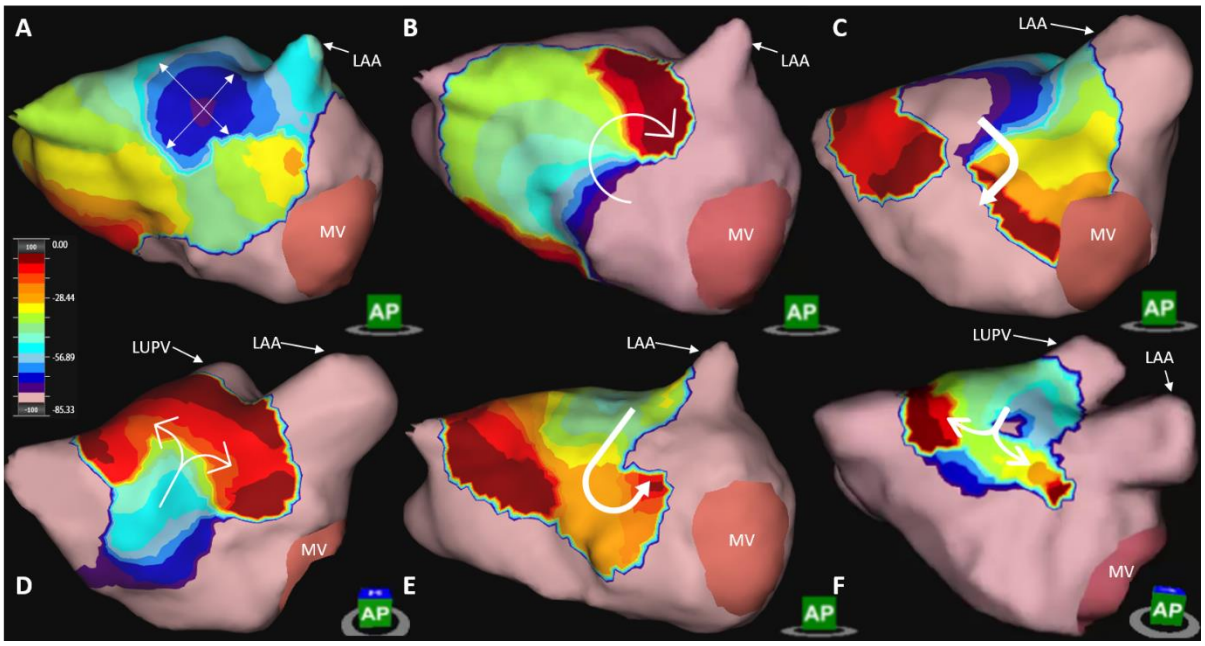

Figure 2.3 Examples of dynamic AcQTrack analysis. Each activation pattern is identified including focal firing (FF) (A) characterised by radial activation from a central earliest point, localised rotational activation (LRA) (B) where smooth rotational activation of >270° is observed; and localised irregular activation (LIA) (C). LIA includes a range of specific patterns of activation, all characterised by changing wavefront direction of >90° (C-F, dynamic AcQTrack detection not shown). Colour scale depicts the leading (red) to trailing edge (purple) of a wavefront with the full colour spectrum occupying 80ms. LAA: Left atrial appendage; LUPV: Left upper pulmonary vein; MV: Mitral valve.

Focal firing (FF)

- The focal activation algorithm determines whether an activation at a vertex came from a previous cardiac wavefront, or whether activation spontaneously started from the current activation. Focal activation is detected at a vertex if an activation is earlier than its neighbors' activation by at least 2-5 ms (default 3ms), and conduction spreads outward from the early activation.
- Activations are connected as a wavefront if the time difference between the two activation times would produce a conduction velocity greater than 0.05 m/s.

Localised irregular activation (LIA)

- The localised irregular activation algorithm computes the difference in angle between cardiac conduction entering and leaving a confined region, as illustrated

in figure 2.4. If the angle difference of conduction entering and leaving a confined region exceeds 90 degrees, localised irregular activation is detected in the region.

- An area of approximately 200-300 mm^2 is considered a confined region
- Wavefronts are considered to be passing through the region if the activation times differences between the border of the confined region and the central vertex would result in a conduction velocity between 0.3 m/s to 3.0 m/s.
- Activations are grouped into entering and leaving the region based on the activation time with comparison to the central vertex. A mean conduction vector entering the region and leaving the region are then computed. Angle difference between the vector entering and leaving the region are computed and if the difference exceeds 90 degrees, LIA is detected.

Localised rotational activation (LRA)

- The localised rotational activation algorithm computes the degrees of conduction propagation around a central point by summing the angle differences of sequential conduction velocity vector directions around the central point, as illustrated in figure 2.5. If the rotational angle of conduction vector changes exceeds 270 degrees, equating to total angle of propagation change of 360 degrees, rotation is detected at the central point. An area of approximately 200-300 mm^2 around the central point is considered.
- To ensure smooth propagation around the central point, an r^2 of a linear fit of activation time to position around the central vertex must exceed 0.7.
- Conduction velocity vector directions changes cannot exceed 45 degrees per position change around the vertex
- Activation time difference around the central obstacle must be greater than 50ms.

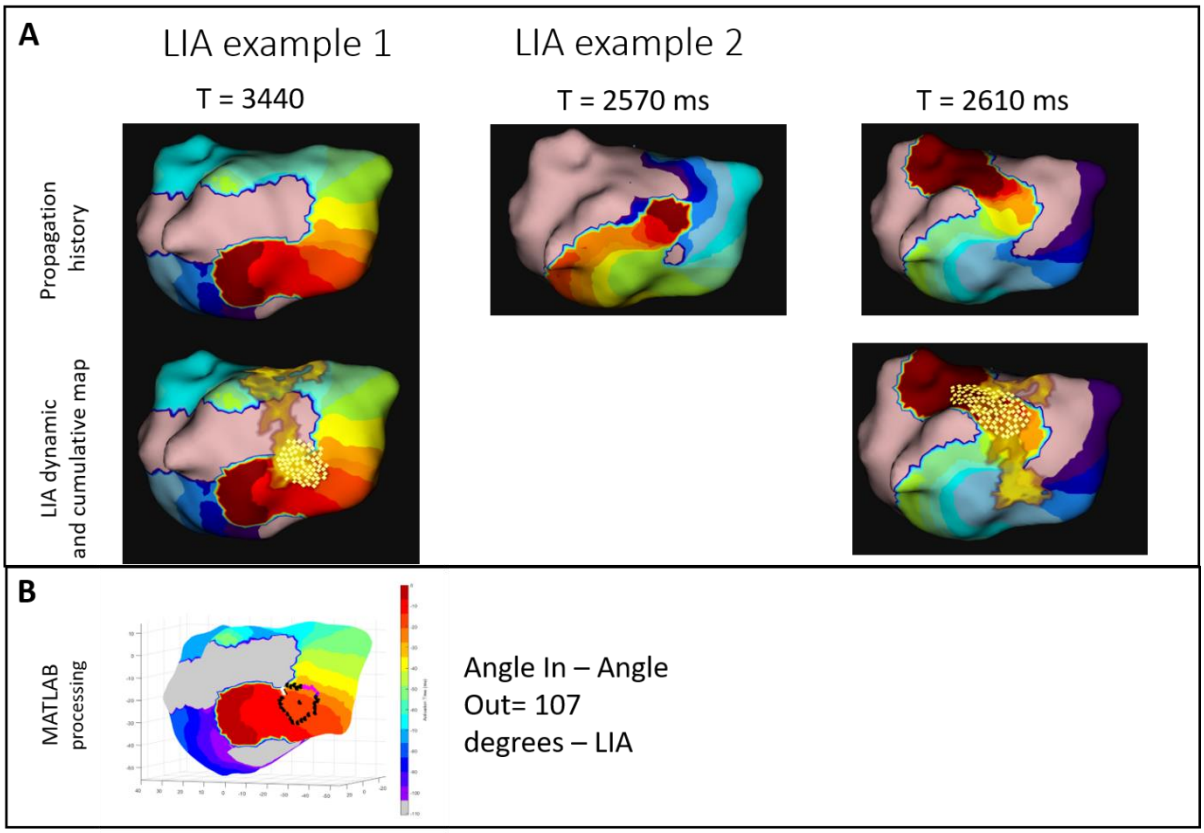

Figure 2.4 AcQTrack identification of LIA.Examples of patterns characterised as LIA are shown in A. Top row shows static images of a propagation history map taken at 3 time points with the row below including the dynamic view of LIA detection (yellow dots) and the cumulative map (yellow patch overlay) highlighting a region over the posterior wall where a frequency of LIA above a specified (user defined) threshold was detected. Panel B illustrates the computational processing that results in LIA classification for example 1. Red denotes the leading edge of the wavefront and purple the trailing edge. The time difference used for this display can be adjusted manually (here it is set to 100ms).

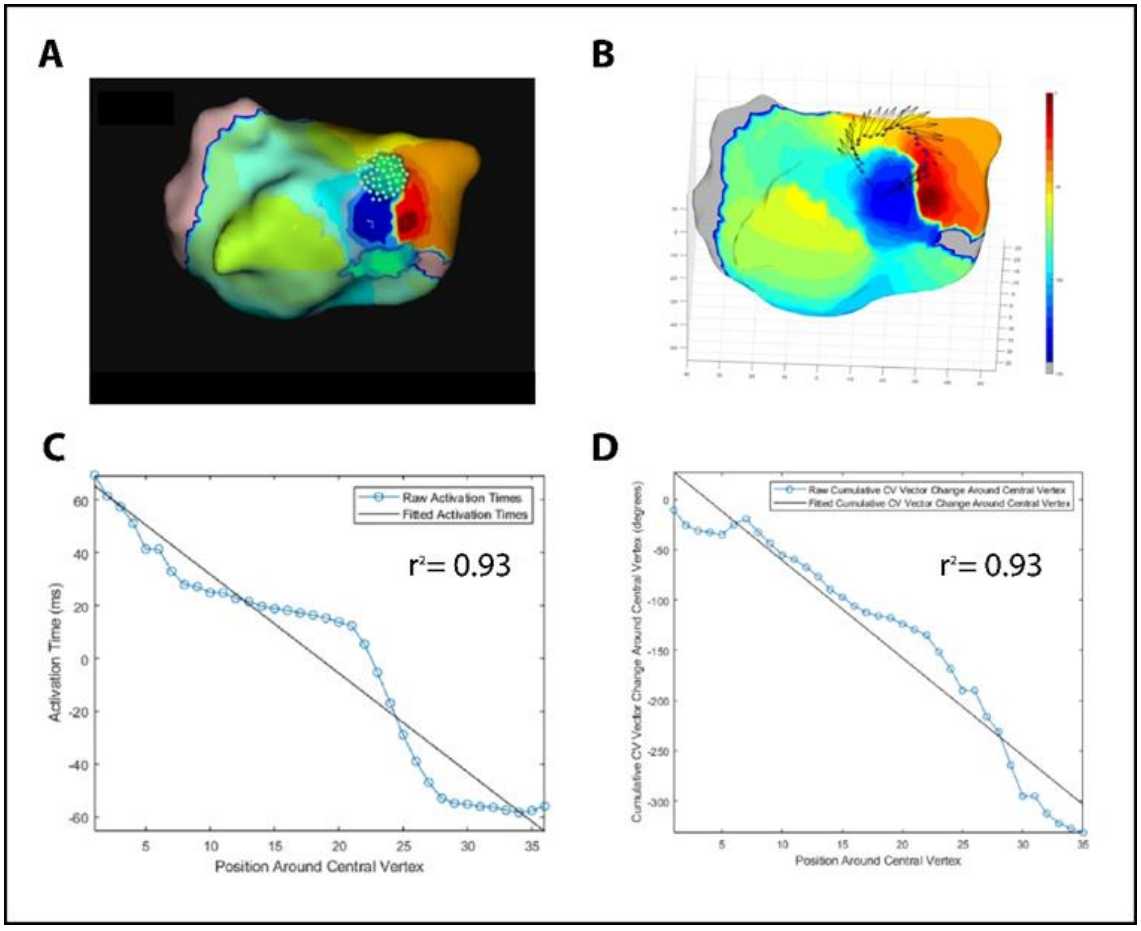

Figure 2.5 AcQTrack identification of LRA. (A) shows a static propagation history map including the dynamic view of LRA detection (green dots) and the cumulative map (green patch overlay) highlighting a region where a frequency of LRA above a specified (user defined) threshold was detected. (B) illustrates the processing and where activation times (C) and vectors (D) are plotted at points around a central vertex within the algorithm.

2.4 AcQTrack pattern quantification

For each pattern identified by AcQTrack, a specific surface area of the anatomy is considered when detecting the parameters necessary to qualify as that pattern and when these are met the vertices of the chamber surface within that area are highlighted for the duration that the activation pattern remains, as illustrated by the dynamic display seen in figures 2.4 and 2.5.This data is recorded within the mapping system console and can be exported for analysis.

Highly specific features are needed to satisfy the parameters for LRA and focal firing detection that are outlined above. However, the parameters for LIA detection are far less stringent (as the features of this propagation pattern are more varied) resulting in more false positive occurrences potentially caused by wavefront collision or mapping artefacts. Occurrences of these activation patterns in any given recording are often distributed widely across the chamber at low frequency with clustering of patterns at higher frequency. However, the specific frequency threshold that differentiates localised

regions of most repetitive activation is highly variable between patients and maps. Whilst in one recording of a fixed duration a specified frequency threshold may be suitable, in another recording the frequency across the whole chamber may be above this threshold (as a result of different properties of AF propagation between patients/recordings) meaning that no activation occurrences are excluded and the region with the most repetitive patterns is therefore not differentiated. In view of this, a method to analyse and quantify these propagation patterns has several requirements:

1. Be able to quantify global chamber occurrences to quantify "substrate properties"
2. Able to exclude infrequent occurrences that may represent false positive detections or isolated findings unlikely to be mechanistically significant
3. Include a dynamic adjustment individualised for each recording and specific to the overall properties of each map obtained
4. Identify localised regions with the most repetitively occurring patterns that may be used to guide targeted ablation
5. Provide output according to the number of occurrences of each pattern, the proportion of time the patterns were present, and the proportion of the chamber surface area affected

The AcQTrack data can be exported from the mapping system console and a custom designed programme was developed with the aim of meeting these requirements. The process is outlined in figure 2.6. Initially, all AcQTrack data is exported to create a static map quantifying every pattern occurrence at each vertex of the chamber anatomy for the entire recording duration (2.6A). Each single occurrence of an activation pattern identified by AcQTrack is represented as a patch of the chamber surface that occupies all vertices within the specific confined zone (of 200-300mm^2) at which the activation pattern is detected by AcQTrack (as outlined above) and for the specific period of time that the pattern remains (2.6B). The number of these unique patches equates to the number of occurrences of the specified propagation pattern (2.6C). When taken over the duration of the recording, the proportion of time in which activation patterns are detected on the chamber surface represents the time parameter (2.6C). Similarly, the proportion of the chamber in which an occurrence is detected represents the surface area affected (2.6D).

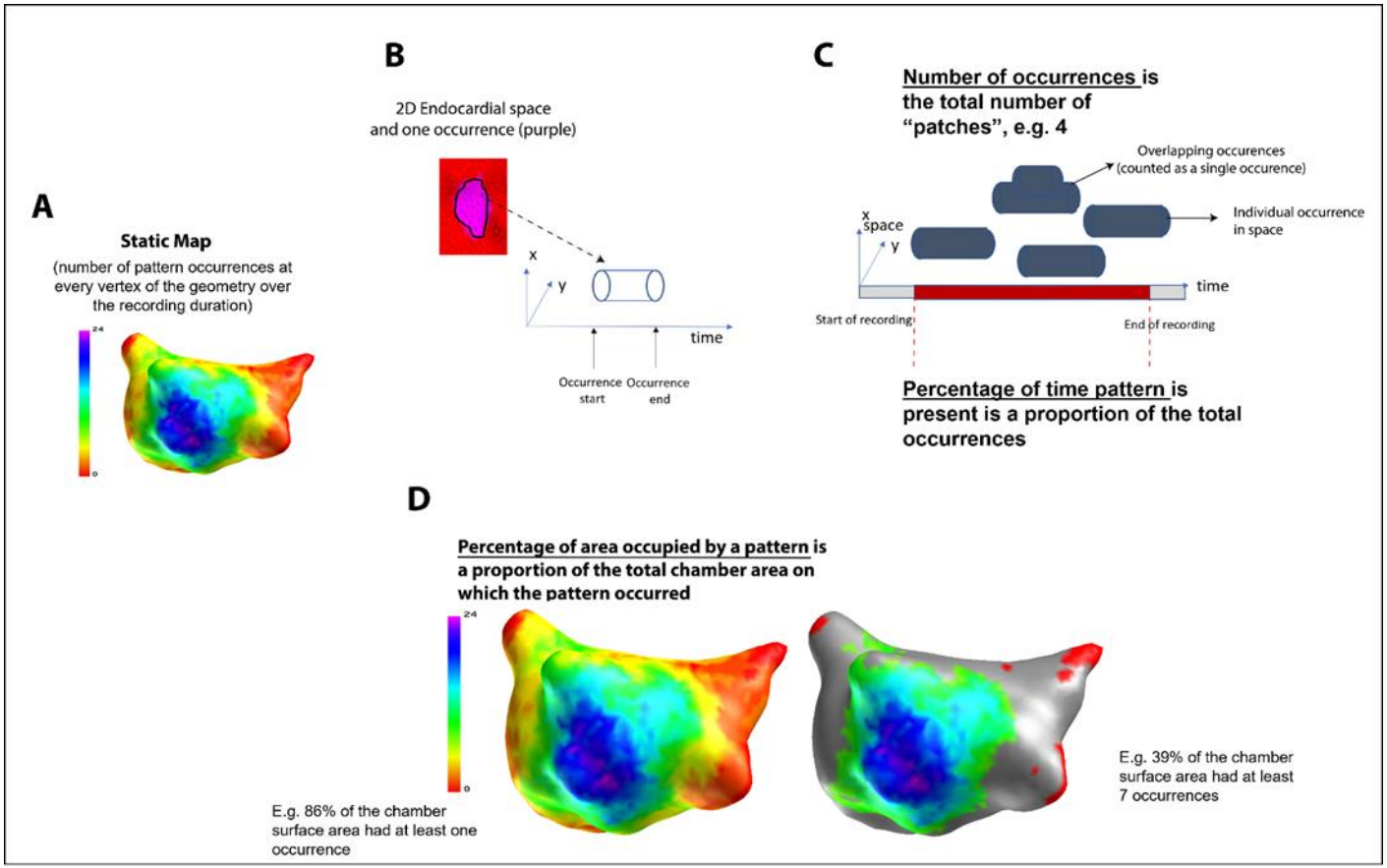

Figure 2.6 Method for AcQTrack pattern quantification. A static map is generated (A) demonstrating all pattern occurrences. Each occurrence is identified in space as the confined zone on the endocardial surface at which the activation pattern is detected by AcQTrack (in B shown as a purple patch on the red chamber surface and represented for illustrative purposes by a single cone) for the duration of time that the pattern remains (B) allowing calculation of the total number of occurrences and the percentage time they are present (C), as well as the proportion of the chamber surface area affected (D). Grey shows the region with pattern occurrences excluded when applying the cut off (explained in text below)

The next step is to identify a suitable cut off threshold to correct for false positive pattern detection and isolated occurrences as well as to identify those regions in which specified activation patterns are repeatedly observed. The number of occurrences in each region and the proportion of time that they are present are known. These factors are therefore used to determine the optimum threshold as outlined in figure 2.7. The initial static map displays all occurrences with no cut off applied (in figure 2.7; zero on the x axis i.e. every occurrence is counted). The percentage of the recording time with the relevant pattern is shown on the Y axis. As the cut off is increased along the X axis, i.e. only regions with increasing numbers of occurrences are included, the proportion of time these are present decreases. A standardised cut off for the minimum absolute number of occurrences in any region does not allow for a relative correction for the varying total numbers between patients. For example where very high numbers are detected in one map with a minimum of five occurrences in any single region, then a cut off of 4 would not exclude any outlying data, compared to another map where very few detections were seen and the same cut off disproportionately excludes important data. Furthermore, an absolute cut off does not take into account the recording duration analysed. The approach developed applies a threshold relative to the total time pattern occurrences are present, as illustrated in figure 2.7. Thresholds can then be applied that result in an exclusion of occurrences resulting in a reduction in the percentage of time that the pattern is present. The highest threshold identifies the region with only the most repetitive activation pattern occurrences.

For the example used in figure 2.7, a colour coded representation of the number of LIA occurrences for each of the (approximately) 3500 vertices on the left atrial geometry is provided. Cut-offs were then used to eliminate the low frequency vertices, which is also those in which LIA activity was present for a relatively small proportion of the total percentage time any LIA activity was present at any part of the whole chamber. The X axis has all 3500 vertices grouped by the minimum number of individual LIA occurrences seen at that vertex during that 5-second recording. The Y axis represents the percentage of time that at least 1 of the 3500 vertices displayed LIA activity during the 5-second segment. In this example the chart indicates that for 91% of the time, any vertex which showed 1 or more LIA occurrences during the recording was exhibiting that activity (thus, for 9% of the 5 second recording there was no LIA activity at any site). To eliminate those vertices which only very infrequently displayed occurrences, a 5% cut off is introduced. This is a relative 5% of the overall percentage time that one or more occurrences were present during the recording and thus the threshold moves down from 91% to 86.5% of the overall percentage time. This has the impact of excluding

those low frequency vertices which contributed very little to the total time that one or more LIA were present, eliminating the red and most of the orange and yellow colours. To illustrate areas where occurrences are excluded at each cut-off, these regions are coloured grey in this figure in contrast with red which represents the background colour of the chamber surface and therefore where there were no pattern occurrences detected irrespective of cut-off.

When the threshold is increased to a 10% cut-off (and drops to a total percentage time of 81.9%), this has the effect of excluding all of the vertices which had 5 or fewer LIA occurrences, eliminating more yellow and green colour-coded areas. Finally, a 20% cut off moves the threshold of percentage time LIA were present at any point on the whole chamber from 91% down to 72.8% and in doing so in this patient's recording excludes all of those vertices which displayed 8 separate LIA occurrences or fewer and the colour coding on the map is focused in on the green and dark blue areas.

What can be demonstrated in the bar chart is that the small area in purple, surrounded by dark blue, that demonstrated the most individual LIA occurrences, occupied less than 10% of the recording segment time, i.e. the 21 individual LIA occurrences occurring in those vertices had a cumulative time of less than 0.5 of a second. This is because LIA activity is a depolarisation phenomenon and will not be present during repolarisation, which takes up the majority of the cycle length. The very nature of slow, pivoting and stuttering propagation may also lead to one very disorganised wavefront being counted as multiple LIA occurrences, hence the need to incorporate percentage time as a modifier. If it was desirable to show all vertices which showed 5 or more LIA occurrences during the analysed segment, the threshold would need to be decreased to less than 5% (i.e. no cut-off) and a much larger number of vertices would be shown across a wider colour range and percentage time of the recording.

Further impetus for the dynamic cut-off approach is that there may not be a fixed relationship between the frequency of pattern occurrences and the duration that the patterns are present. Fewer occurrences may persist for longer (e.g. multiple rotations of LRA) in one recording whilst a higher frequency in another recording (e.g. short-lived pivoting LIA) may last for shorter durations. This is illustrated in figure 2.8. In scenarios with a high frequency of pattern occurrences and a high degree of clustering a threshold method of either a fixed percentage of occurrences or the dynamic thresholding method explained above produce similar results (2.8A). However, in examples with a less clearly delineated cluster or a lower frequency of occurrences, a fixed percentage method

resulted in exclusion of areas with a high number of occurrences that persist for a longer duration and therefore may be mechanistically important (2.8B, C).

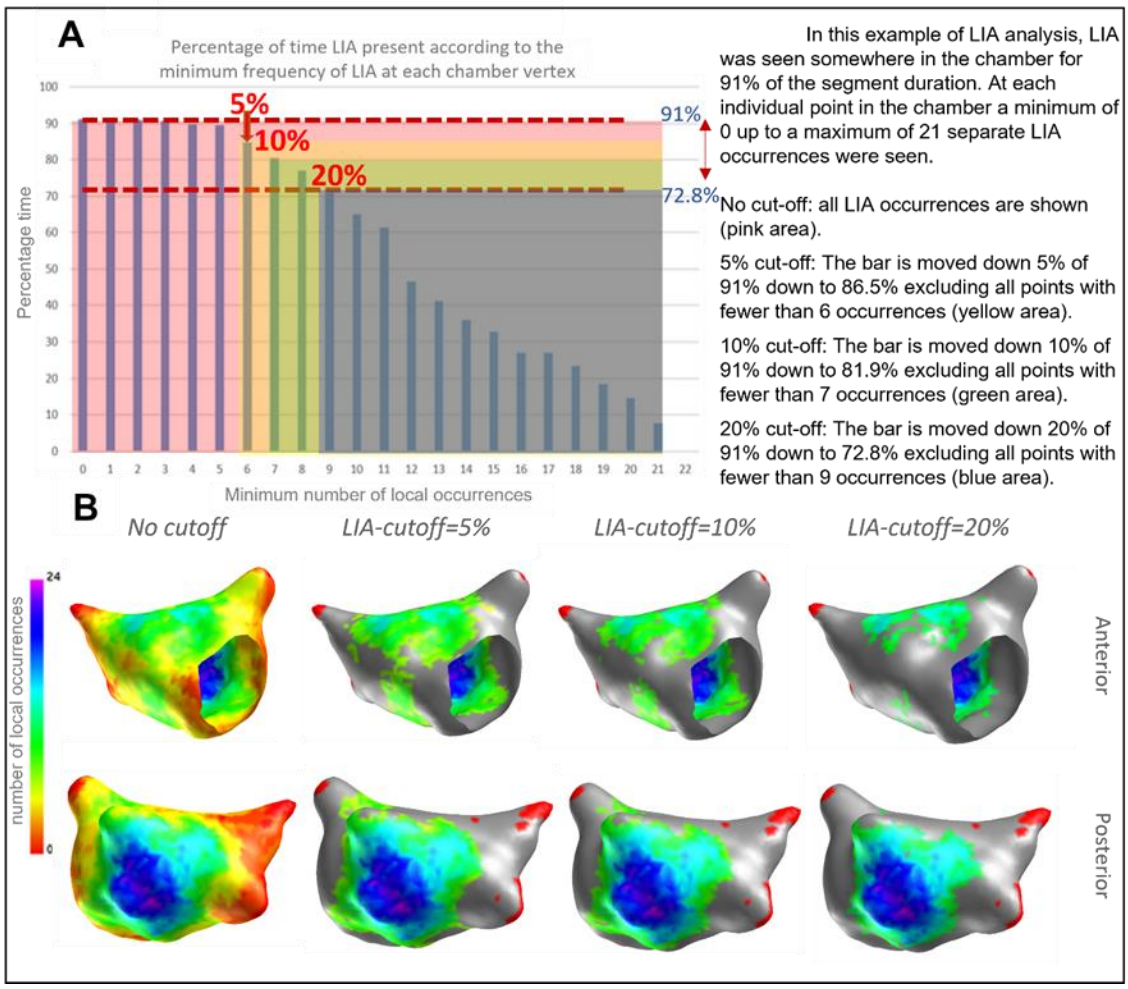

Figure 2.7 Threshold method. With no cut off applied, all occurrences are counted and the percentage of time occupied calculated (y-axis). Cut offs are then applied based on this analysis. Applying a 5, 10 and 20% relative reduction in the total time that patterns are present results in gradual exclusion of the least frequent occurrences below the minimum number of local occurrences (at each vertex) shown on the x-axis. (B). In this example the 5% cut off results in excluding regions with fewer than 6 LIA occurrences, with increasing exclusion with higher cut offs. (Regions with excluded occurrences are shown in grey for illustrative purposes, red shows areas with no occurrences irrespective of cut-off, i.e. background colour of the chamber surface). (See text for detailed explanation)

Initial analyses suggested that the technique as described above resulted in an overestimation of the frequency of both LIA and LRA. As outlined above, every vertex of the anatomy is analysed by the AcQTrack tool to identify propagation patterns that meet the necessary criteria. A wavefront with changing direction or rotation often features a pivot point that drifts across a region rather than remaining at a single anatomical vertex. This results in a propagating wavefront meeting the specific LIA or LRA parameters in multiple adjacent vertices creating overlapping patches when seen during dynamic propagation and illustrated in figure 2.9. The method was therefore adapted to merge

overlapping discs and count these as a single occurrence. In addition, a 5ms inclusion tolerance is included where occurrences are detected separately but within the same location less than 5ms apart. This is to ensure that an occurrence isn't counted twice where a short period is seen during which the AcQTrack parameters are not met but the time duration is too short to account for a separate wavefront activating that region. When this is applied to the threshold regions to quantify pattern occurrences within these zones, only "patches" where the centre falls within the specified zone is counted rather than any occurrences that purely overlap that region (figure 2.9B and C).

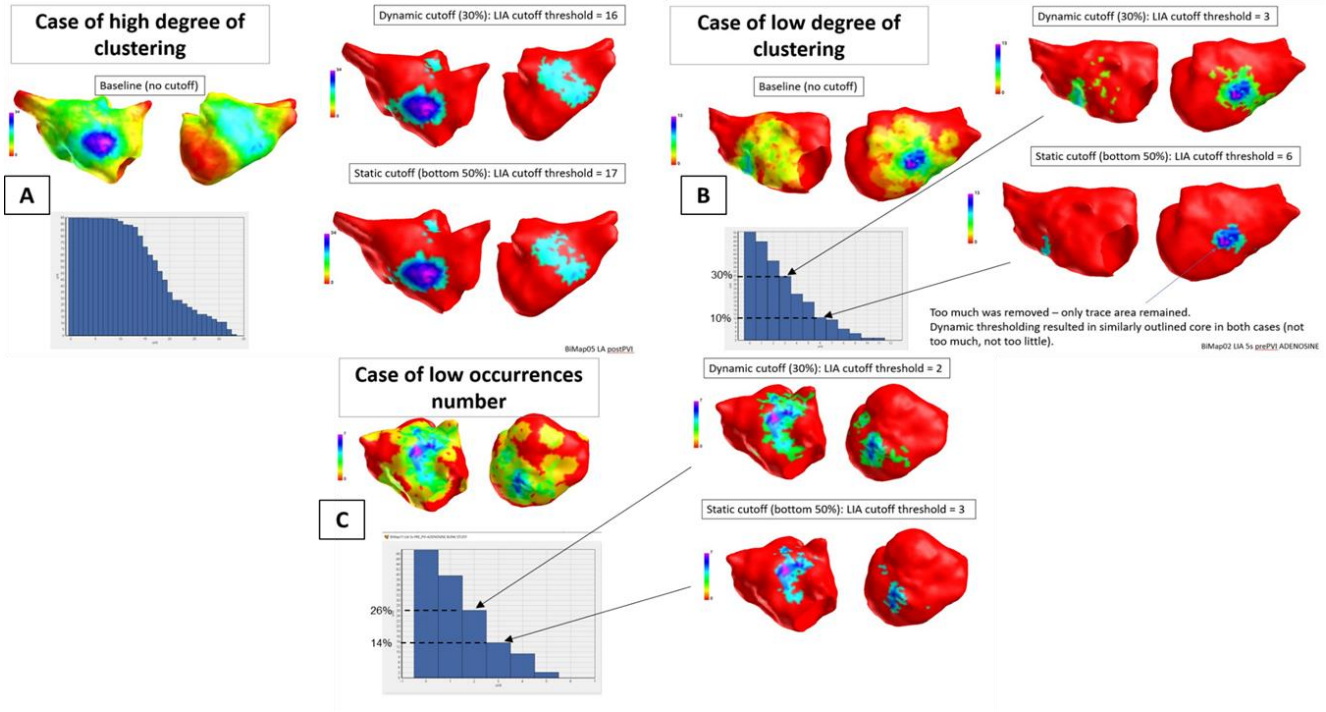

Figure 2.8 Effect of clustering pattern on thresholding.In a case with a high frequency of occurrences and high degree of clustering both a percentage frequency and a dynamic threshold approach produce similar results (A). However, where there is less clear clustering (B) a fixed percentage approach excludes regions where patterns occur for a significant duration i.e. exclusion is too high therefore potentially excluding areas of importance. This may also be the case in an example with a low frequency of patterns that last for a relatively longer period of time (C).

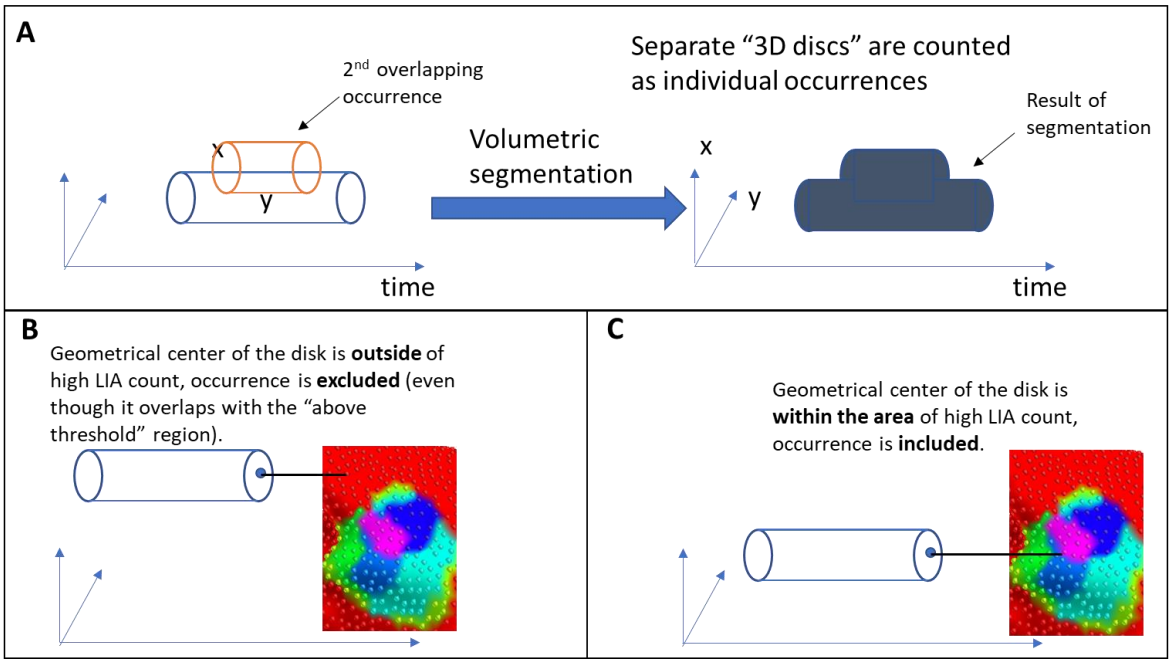

Figure 2.9 Adaptation to quantification method to combine overlapping occurrences as a single count (A) and then identify the geometric centre of each occurrence disc (B). Only if the centre of this disc falls within a threshold cut off zone is this occurrence included in the analysis (C).

2.5 Signal processing methods

2.5.1 Phase processing

Established methods for analysis of fibrillatory signals include phase mapping. The AcQMap system reconstructs virtual dipoles on the chamber surface. In terms of phase mapping signal processing techniques, these can be approached in the same way as unipolar electrograms. We sought to apply phase mapping methods to the AcQMap data in order to calculate global measures of AF cycle length, identify phase singularities and calculate mean phase coherence.

Virtual electrograms were filtered and phase reconstruction achieved using a method of sinusoidal recomposition and the Hilbert transform as previously described.(198) Phase singularity detection and lifespan calculation is then completed in line with previously described methods.(199) Virtual electrograms from each triangular vertex of the surface mesh making up the reconstructed anatomy are analysed for calculation of atrial fibrillation cycle length (AFCL). The cycle length at each vertex is calculated and results for all signals combined to provide the mean and standard deviation of global AFCL.

2.5.2 Dominant frequency

Following filtering, calculated charge density signals for each vertex of the anatomy were exported for spectral analysis using a custom designed programme in Matlab (Mathworks 2019a). Fast Fourier Transform was performed and the frequency-power spectrum for each signal plotted. The maximum peak within a presumed physiological range between 4 and 10Hz was identified and the frequency at that power assigned as the dominant frequency (DF) for that signal and displayed as a colour coded value to that vertex of the anatomy as illustrated in figure 2.8. Where sites of abrupt transition in DF were identified, the signals were manually inspected to exclude spurious results resulting from harmonics within the frequency domain. If identified, then the next peak within the range 4-10Hz was identified and assigned as the DF. The mean of all DF values for every vertex of the chamber was calculated and used as the global DF value for each map. Sites of high DF were identified defined as a localised zone on visual inspection of the DF plot with DF value higher than all surrounding regions.

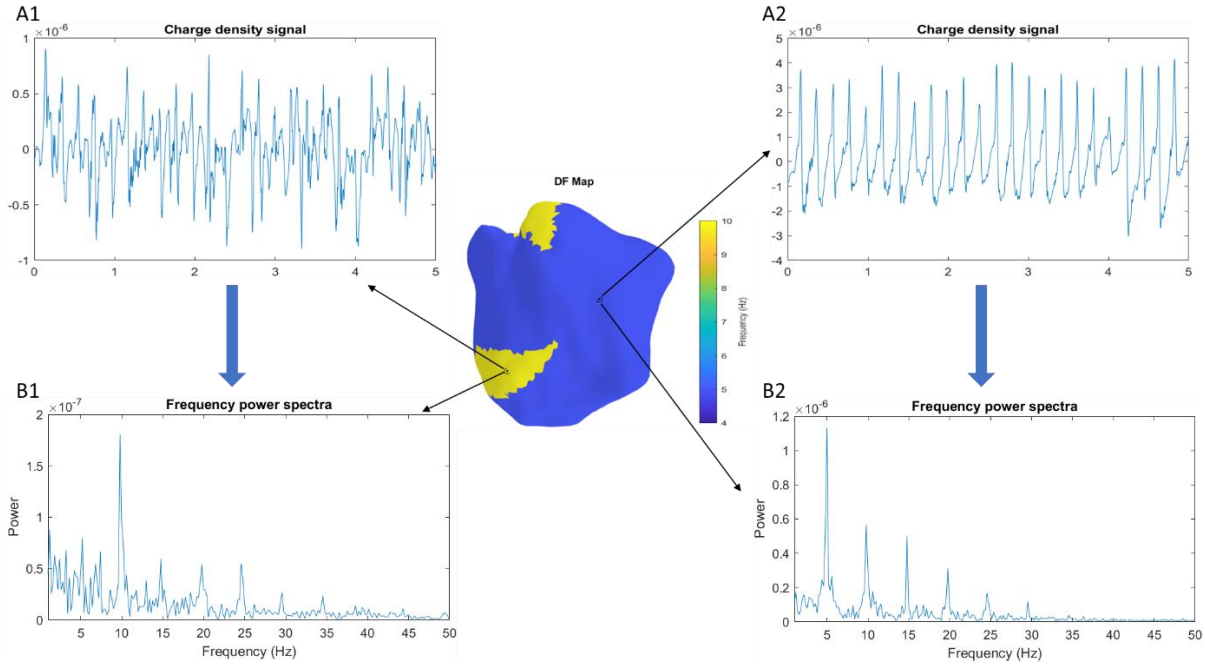

Figure 2.10 Generation of DF plots was performed based on analysis of the exported charge density signals (A1, A2). Frequency power spectra are plotted following Fast Fourier Transform and the highest power within the frequency range 4-10Hz identified (B1, B2). The frequency at that power was assigned as the DF for the signal at each vertex of the chamber surface.

2.6 Validation

One of the challenges in the implementation and evaluation of novel technologies to the field of AF mapping is validation of the tools themselves. These challenges relate to both the lack of a “gold-standard” against which to compare and a lack of understanding of AF propagation, which includes uncertainties in the interpretation of complex fibrillatory

electrograms. Previous iterations of non-contact mapping technology including the Ensite Array catheter were validated against contact unipolar electrograms for electrogram morphology, amplitude and annotation of activation time during both sinus rhythm and AF.(200) The use of the inverse solution (described above) to calculate endocardial signals has many similarities between this older technology and the AcQMap system.

Shi et al have performed detailed validation of the AcQMap system using a similar approach to prior work using the Ensite Array.(201) Comparison was performed between reconstructed voltage signals and contact unipolar electrograms recorded by a multipolar circular mapping catheter during both sinus rhythm and AF.(201) Validation measures assessed included both electrogram morphology and timing. During sinus rhythm, median morphology cross-correlation and timing difference was 0.85 (IQR: 0.71, 0.94) and 6.4ms (IQR: 2.6, 17.1), respectively, with values of 0.79 (IQR: 0.69 to 0.88) and 14.4ms (IQR: 6.7 to 26.2), for morphology and timing difference during AF.(201) Similar to prior studies, the radial distance between the centre of the AcQMap catheter and the atrial surface significantly impacted results, particularly at distances ≥40mm (see figure 2.11), with correlation values falling significantly beyond this point.(201)

The key aspect of the AcQMap system however is the use of charge density reconstruction and conversion to maps of AF propagation. Although the maps generated are fundamentally derived from the inversely calculated “virtual” electrograms, significant proprietary signal processing steps are required to generate the final propagation map that is analysed to identify patterns of AF activation and determine ablation targets. However, validation of the accuracy of the AF propagation maps generated is challenging in view of both the lack of a comparative “gold standard” technique and associated lack of knowledge of AF mechanisms, as alluded to above. Validation of accuracy of activation maps is therefore limited to sinus rhythm, pacing and organised arrhythmias (such as atrial tachycardia/atrial flutter) that can be analysed with conventional contact mapping techniques.

Our initial experience of the AcQMap system involved cases of typical cavotricuspid isthmus (CTI) dependent atrial flutter in order to gain familiarity with the technology, which was employed in conjunction with contact mapping using the Abbot Ensite Precision system. Right atrial geometry was generated followed by recording of right atrial electrical activation from a central position in the chamber (as done during AF). Maps of atrial activation were calculated from segments following T waves and preceding the subsequent QRS complex (the “TQ” interval) and consistently revealed clear patterns of macro-re-entry involving the CTI, with the mechanism confirmed by conventional

contact mapping, entrainment and termination during completion of linear ablation to achieve CTI block. In one patient, the AcQMap system revealed an atypical circuit consisting of an “upper loop” re-entry mechanism around the SVC as well as identifying an anomalous pulmonary vein (later confirmed on computed tomography). Ablation of the critical isthmus posteriorly resulted in change of the tachycardia circuit to typical CTI dependent flutter.(202)

Design of the protocol employed during simultaneous biatrial mapping included the recording of sinus rhythm propagation as well as during pacing from multiple sites and at different pacing cycle lengths. Contact mapping was also performed during sinus rhythm. Single beat propagation maps were calculated from central position recordings of each paced rhythm in the first 9 patients in this study and visually analysed for patterns of atrial activation and to identify the site of pacing. The earliest activation site was clearly identified consistent with the pacing site in all maps generated with a clear pattern of biatrial activation consistent with progressive conduction across the chambers as anticipated. Sinus rhythm maps clearly identified the origin of activation consistent with the anatomical location of the sinus node and correlated with the findings of contact maps. This provided a degree of validation of AcQMap propagation maps, albeit without a suitable measure during AF.

The multi-position “SuperMap” algorithm was also compared to the results of high density contact maps in patient with organised atrial arrhythmias, primarily for speed of generation but also for concordance of mapping findings and accuracy when compared to the results of entrainment and response to ablation. “SuperMap” was accurate in 92% of maps generated with non-contact and contact map findings producing concordant results in 79%.(203)

Although we did not therefore carry out further formal validation studies, results of work done by others appeared to be consistent with expected findings in the context of previous literature on non-contact mapping. Furthermore, single position activation maps during sinus rhythm, pacing and organised arrhythmias was consistent with both anticipated mapping appearances and results obtained by complementary techniques, including high density contact mapping.

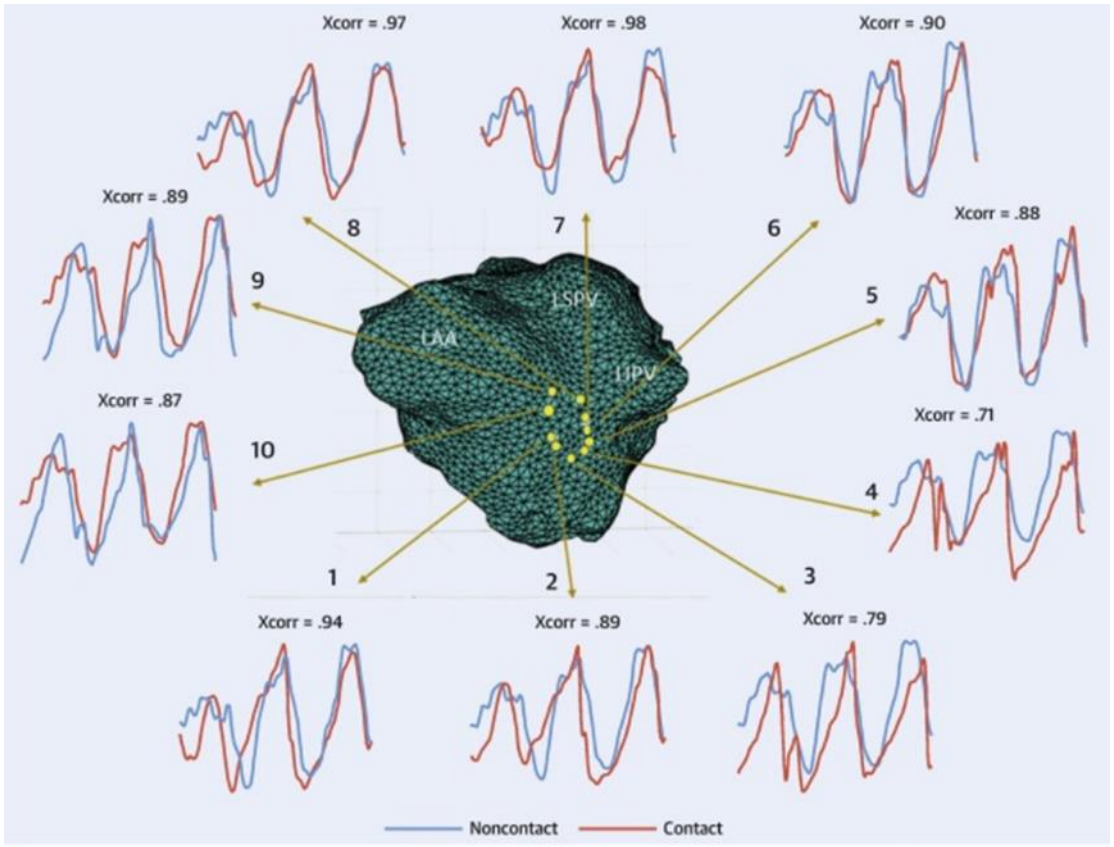

	Sinus Rhythm		Atrial Fibrillation	
	Correlation	Timing Difference	Correlation	Timing Difference
N = 20	0.85 (0.71-0.94)	6.4 (2.6-17.1)	0.79 (0.69-0.88)	14.4 (6.7-26.2)
Radial distance (r) from center of noncontact catheter				
≤40 mm	0.87 (0.72-0.94)	5.7 (2.6-15.4)	0.81 (0.69-0.89)	12.3 (5.9-21.8)
>40 mm	0.73 (0.56-0.88)	15.1 (4.1-27.7)	0.67 (0.45-0.82)	28.3 (16.2-36.0)
p Value	<0.01	<0.01	<0.01	<0.01

Figure 2.11 Validation of inversely derived non-contact voltage electrograms against contact unipolar electrograms for both morphology and timing during sinus rhythm and AF. Accuracy diminishes significantly at radial distances ≥40mm from the centre of the AcQMap catheter. Adapted from Shi et al.(201)

3 Impact of Adenosine on Wavefront Propagation in Persistent AF

3.1 Introduction

Although pulmonary vein ectopy is widely recognised as the prevalent trigger for atrial fibrillation (AF), mechanisms responsible for maintaining AF and resulting in the progression from paroxysmal to persistent phenotypes are poorly understood. Adenosine is known to shorten atrial myocardial action potential duration and refractoriness, and it's administration may provoke AF.(204-207) This effect is mediated by specific G-protein coupled cell surface receptors and activation of outward potassium currents.(206, 208) These are the same currents activated by cholinergic stimulation through the binding of acetylcholine to muscarinic receptors but despite the ionic basis for this effect being well recognised, the impact on the properties of dynamic wave-front propagation during AF are less clear. Spatially limited dominant frequency mapping studies showed adenosine (or acetylcholine) infusion resulted in increased dominant frequency with differential effects between atrial sites potentially due to the heterogenous distribution of adenosine receptors across the atrial myocardium.(72, 209) This has been proposed as indirect evidence of high frequency re-entry mechanisms maintaining AF and accelerated by adenosine.(72, 170) Hansen et al recently examined the effect of adenosine on AF in explanted human hearts (with and without a history of AF) and 10 patients in whom ablation confirmed "drivers" had been identified.(210) They postulated that adenosine could be used to reveal "driver" sites that can then be targeted by ablation. However, the direct functional effect of adenosine on dynamic wave-front propagation in a broader population of patients undergoing ablation for persistent AF has not been evaluated.

Adenosine is frequently used during non-contact mapping to cause transient atrio-ventricular block reducing the effect of far-field ventricular signals. In conjunction with knowledge of its pharmacological effect on atrial myocardium, we sought to evaluate the effect of adenosine on atrial propagation patterns in patients undergoing catheter ablation for symptomatic persistent AF. The aim was to apply the analytical methods devised as outlined in section 2 to both further examine the mechanisms involved in AF maintenance, establish the extent to which atrial propagation is altered by adenosine thus potentially restricting the clinical utility of adenosine to aid AF mapping, and explore the potential for adenosine to reveal sites of potential AF "drivers".

3.2 Methods

3.2.1 Patients

Patients undergoing elective catheter ablation for persistent atrial fibrillation using the AcQMap system were included in the analysis. This included patients enrolled in parallel research studies (RECOVER-AF; NCT03368781 and BiMap-AF; NCT03812601) and undergoing both first time and repeat procedures for recurrent AF. These studies were approved by the local ethics committee and conducted according to the principles of the Declaration of Helsinki. All patients gave written informed consent. Patients with a clinical contraindication to adenosine administration were excluded.

3.2.2 Electrophysiological mapping procedure

Procedures were carried out under general anaesthetic in line with standard institutional practice. With the exception of amiodarone, antiarrhythmic drugs were stopped a minimum of five days prior to the procedure. Heparin boluses were administered prior to trans-septal puncture followed by continuous heparin infusion to maintain an ACT >350s. A decapolar catheter (Inquiry, Abbott Medical) was inserted into the coronary sinus and the AcQMap mapping catheter was inserted into the left atrium. A circular mapping catheter (Inquiry Optima, Abbott Medical) was used to guide pulmonary vein isolation. In patients attending the procedure in sinus rhythm, AF was induced with burst pacing from the coronary sinus and only sustained AF was mapped for inclusion in the analysis (no patients demonstrated spontaneous termination following induction). A 3-dimensional ultrasound generated anatomy of the left atrium was reconstructed and electrophysiological recordings from 48 non-contact electrodes obtained using the AcQMap system as previously described.(195, 196) Recordings were taken at one or more of three timepoints during the procedure for each participant: prior to pulmonary vein isolation (in those undergoing first time procedures), immediately following pulmonary vein isolation, and following non-pulmonary vein left atrial ablation. At each time point, an additional recording was obtained during the administration of a bolus of 15mg of adenosine with pharmacological effect confirmed by the observation of transient atrioventricular conduction block and/or hypotension. Radiofrequency ablation was delivered to achieve pulmonary vein isolation (or re-isolation). Following this, additional non-pulmonary vein ablation was delivered guided by baseline AcQMap propagation maps targeting regions with highly repetitive patterns of FF, LIA or LRA over several map segments as determined by the operator.

3.2.3 Propagation map construction, export and analysis

Electrophysiological recordings before and after adenosine administration were processed for construction of propagation history maps. For each time period, a five

second segment was taken, which in the case of adenosine corresponded with maximal atrioventricular conduction block. A 100Hz low pass filter and 50Hz notch filter was applied, outlier electrode signals were excluded following manual interrogation (to identify spurious signals as a result of electrode damage during catheter insertion/preparation), and the QRS-T wave subtraction algorithm applied for all recordings (including those obtained following adenosine administration). Propagation maps were calculated and displayed using the default minimum amplitude sensitivity of 0.02mV, time threshold of 70ms (representing a conservative value for minimum atrial refractoriness) and window width of 80ms (determining the duration of display of propagating wavefronts). Wave-front propagation patterns were evaluated using the AcQTrack system and data exported for analysis in custom designed software.

For each five second map, AcQTrack data for LRA, LIA and FF were extracted and quantified in line with the methods described in section 2.2.

3.2.4 Signal Processing and Dominant Frequency Analysis

Virtual electrograms from each vertex of the surface mesh (approximately 3500 in total) making up the reconstructed anatomy were also exported for analysis and calculation of atrial fibrillation cycle length (AFCL) and identification of phase singularities (PS). Virtual electrograms were filtered and phase reconstruction achieved using a method of sinusoidal recomposition and the Hilbert transform as previously described.(198) Phase singularity detection and lifespan calculation was then completed in line with previously described methods.(199) For AFCL calculation, the cycle length at each nodal point was calculated for the 5s recording from the phase signals and results for all signals combined to provide the mean global AFCL over the duration of the 5s segment.

Virtual charge density signals were exported from each vertex of the chamber and dominant frequency (DF) identified as the maximum peak of the frequency-power spectrum at values within a presumed physiological range between 4 and 10Hz following Fast Fourier Transform performed in Matlab (Mathworks 2019a). The mean and standard deviation for all signals across the chamber were calculated to give the chamber DF value for comparison. Regions of high DF, defined as a localised zone with DF higher than all surrounding regions, were identified and compared to regions of high frequency LRA. A detailed description is included in section 2.4.2.

3.2.5 Clinical outcomes

Clinical outcomes were assessed according to acute procedural effects resulting in ablation terminating atrial fibrillation (either directly, or via an organised atrial tachycardia)

or requiring direct current cardioversion (DCCV) to restore sinus rhythm. Differences in propagation patterns before and after adenosine were compared on the first map obtained in each patient (i.e., at the earliest stage of the procedure) according to acute procedural outcome.

3.2.6 Statistics

Statistical analysis was performed using SPSS (version 25, IBM) or Matlab (Mathworks, R2019a). Continuous variables were assessed for normality of distribution using the Shapiro-Wilk test and expressed as mean ± standard deviation. Data were compared using the paired samples t-test comparing each map obtained with and without adenosine. Where differences were not normally distributed data was additionally transformed and analysed using a one-sample t test. If the results are concordant then the paired sample t-test is reported. Categorical data are expressed as a number and percentage.

3.3 Results

3.3.1 Patients

Twenty-two patients with persistent AF were included in the analysis. Mean age of the population was 60±12 and 68% were male. Other characteristics are shown in table 3.1. Maps with and without adenosine were created prior to pulmonary vein isolation in 11 participants, immediately following pulmonary vein isolation in 15 participants and following additional left atrial ablation in 9 participants resulting in a total of 35 paired maps. In all cases, a clear effect of adenosine on atrioventricular conduction was observed with a mean longest RR interval of 5708±2933ms.

Table 3.1 Patient characteristics (n=22)

Age, years	60±12
Male, n (%)	15 (68)
Body Mass Index (BMI, kg/m^2), median (IQR)	29 (25-30)
Amiodarone peri-procedure, n (%)	6 (27)
Ejection fraction, (%), median (IQR)	55 (54-60)
Left atrial diameter, (mm), median (IQR)	45 (39-50)
Time since diagnosis (years), median (IQR)	3.5 (2-5)
First time procedure, n (%)	8 (36)
In AF at procedure start, n (%)	14 (64)

3.3.2 Wavefront Propagation Patterns

At baseline, the number of LIA occurrences was 99±20 (within the 5s of recorded segment), which increased to 109±26 with adenosine, a statistically significant difference of 10 (95% confidence interval 2 to 19, p=0.012). When a 5% cut off was used, LIA occurrences with adenosine were 83±16 compared to 76±15, reflecting a statistically

significant difference of 7 (95% CI 2.5-11, p=0.003). At 10, 20, 30 and 40% cut offs there was no difference in the number of LIA occurrences with adenosine (71±13 from 67±11, difference 4, 95% CI -1.1-7.7, p=0.133; 53±9 from 51±9, difference 2, 95% CI -1.8-4.7, p=0.372; 41±8 from 41±7, difference 0, 95% CI -2.8 – 3.1, p=0.906; and 32±5 from 32±5, difference 0, 95% CI -2.8-2.3, p=0.840 for 20, 30 and 40% cut offs respectively - see table 3.2). When analysed as a percentage of time over which LIA occurred, adenosine resulted in a small but statistically significant increase in time LIA was present at all but the 40% cut offs. The percentage of left atrial surface area in which LIA occurred was not affected by adenosine except for a small decrease in the surface area at the 30% (19.2±5.6 to 16.4±3.5, difference 2.8, 95% CI 0.5-5, p=0.019) and 40% (14.0±5.4 to 11.6±3.0, difference 2.4, 95% CI 0.4-4.3, p=0.021) cut offs.

Irrespective of cut off value, there was a significant increase in LRA with adenosine. The smallest increase in LRA occurrences was from 8.4±5.2 to 14.1±5.7 observed at the 20% cut off (5.7, 95% CI 2.7-8.6, p<0.0005), with the largest effect from 16.1±7.6 to 24.2±8.1 detected with no cut off applied (8.1, 95% CI 4.1-12, p<0.0005). The same pattern was observed when measured as a percentage of time LRA was present as illustrated in figure 3.1. Adenosine administration resulted in a small increase in the proportion of the LA surface area in which LRA occurred. See table 3.2 for full results. Examples of the effect of adenosine are shown in figure 3.2.

Although differences were observed at all stages, this did not reach statistical significance at baseline, and was most pronounced post-PVI and following non-PV ablation (see figure 3.3 and table 3.3).

Adenosine had no significant effect on the number of focal firings observed (24.5±8.2 vs 22.0±7.3 at baseline, difference -2.5, 95% CI -6 – 1.2, p=0.18).

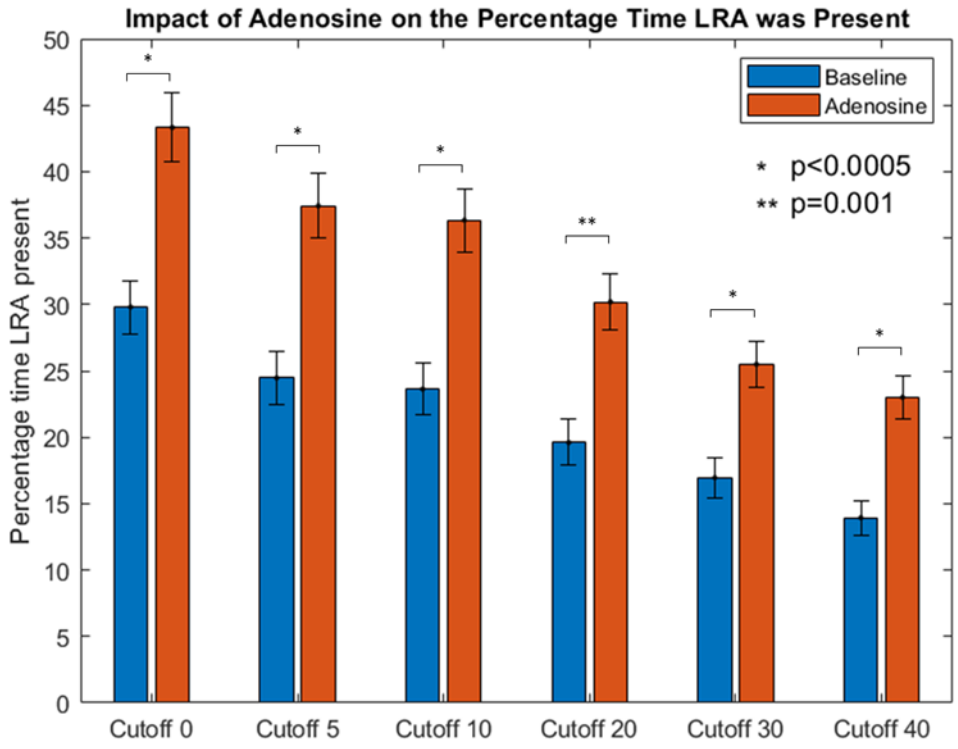

Figure 3.1 Effect of adenosine on percentage time of LRA occurrences. (LRA, localised rotational activation. Bars represent standard error).

Table 3.2 Table of full results for the effect of adenosine on LIA, LRA and FF (Abbreviations as in text).

	Cut off	Baseline (SD)	Adenosine (SD)	Difference (95% CI)	P value
LIA number of occurrences	0%	99±20	109±26	10.0 (2 - 19)	0.012
	5%	83±16	76±15	7 (2.5 – 11.0)	0.003
	10%	67±11	71±13	3.3 (-1.1 – 7.7)	0.133
	20%	51±9	53±9	1.5 (-1.8 – 4.7)	0.372
	30%	41±7	41±8	0.2 (-2.8 – 3.1)	0.906
	40%	32±5	32±5	-0.3 (-2.8 – 2.3)	0.840
LIA % time	0%	76.4±11.1	79.9±12.4	3.5 (0.5 – 6.7)	0.025
	5%	69.9±12.6	74.2±12.3	4.3 (1.5 – 7.2)	0.004
	10%	66.2±11.2	70.2±11.0	4.0 (1.1 – 6.8)	0.007
	20%	57.7±10.2	61.1±9.1	3.4 (1.0 – 5.8)	0.007
	30%	50.1±8.2	52.9±9.6	2.7 (0.2 – 5.3)	0.035
	40%	41.6±7.4	44.0±7.4	2.4 (-0.2 – 5.1)	0.072
LIA % surface area	0%	85.8±11.3	86.1±13.8	0.3 (-3.5 – 4.0)	0.889
	5%	46.1±10.0	46.4±10.2	0.3 (-3.6 – 4.2)	0.887
	10%	37.9±7.8	35.6±8.4	-2.3 (-6.3 – 1.6)	0.242
	20%	25.5±5.2	23.5±5.9	-2.0 (-4.5 – 0.4)	0.096
	30%	19.2±5.6	16.4±3.5	-2.8 (-5.0 - -0.5)	0.019
	40%	14.0±5.4	11.6±3.0	-2.4 (-4.3 - -0.4)	0.021
LRA number of occurrences	0%	16.1±7.6	24.2±9.8	8.1 (4.1 – 12)	<0.0005
	5%	11.3±6.5	18.6±8.1	7.3 (3.7-10.7)	<0.0005
	10%	10.7±6.3	17.9±7.9	7.2 (4.0-10.5)	<0.0005
	20%	8.4±5.2	14.1±6.4	5.7 (2.7-8.6)	<0.0005
	30%	6.8±4.1	11.6±4.9	4.8 (2.6 – 6.7)	<0.0005
	40%	5.5±3.3	10.2±4.3	4.7 (2.8 – 6.5)	<0.0005
LRA % time	0%	29.8±11.8	43.3±15.5	13.5 (7.1 – 19.9)	<0.0005
	5%	24.5±11.6	37.4±14.5	12.9 (6.8 – 19.0)	<0.0005
	10%	23.6±36.3	36.3±14.1	12.7 (6.9 – 18.5)	<0.0005
	20%	19.6±10.3	30.1±12.5	10.5 (4.9 – 16.3)	0.001
	30%	17.0±9.0	25.5±10.3	8.5 (4.3 – 12.8)	<0.0005
	40%	13.9±7.6	23.0±9.5	9.1 (5.0 – 13.1)	<0.0005
LRA % surface area	0%	22.3±8.3	29.6±10.2	7.3 (3.3 – 11.3)	0.001
	5%	12.7±6.5	16.0±6.7	3.3 (0.19 – 6.5)	0.038
	10%	11.1±5.4	14.8±6.3	3.7 (1.1 – 6.2)	0.007
	20%	7.7±3.3	10.1±4.1	2.4 (0.6 – 4.2)	0.012
	30%	6.0±2.5	7.7±3.7	1.7 (0.6 – 3.0)	0.005
	40%	4.7±2.2	6.3±2.8	1.6 (0.6 – 2.7)	0.004
FF numbers		24.5±8.2	22.0±7.33	-2.5 (-6 – 1.2)	0.18

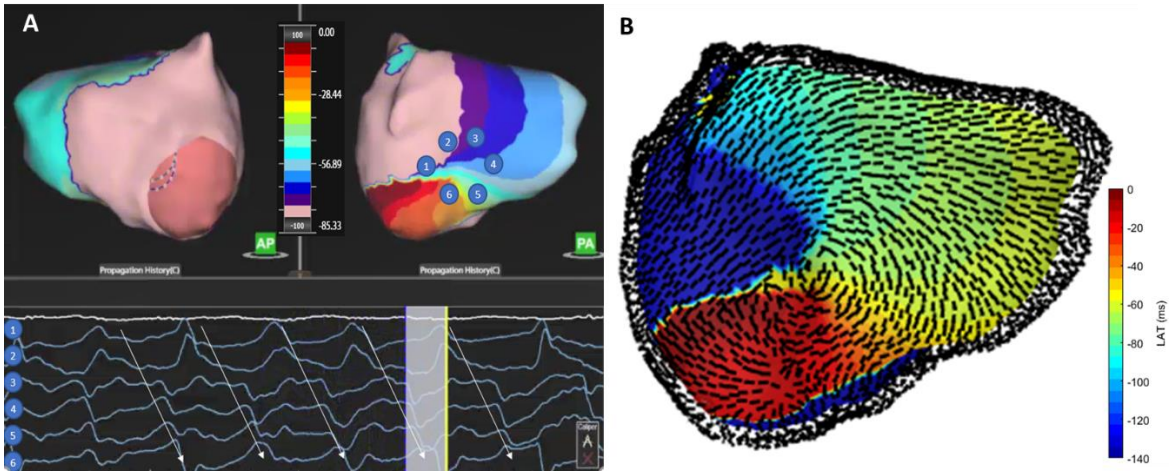

Figure 3.2 Example activation map of a zone of LRA on the infero-posterior LA seen following adenosine injection (A). Dipole signals around this rotational pivot point demonstrate progressive activation. The conduction velocity vector map (B) demonstrates the angles of propagation around the central point. (Thanks to Nathan Angel, Acutus Medical, for generation of the conduction velocity vector image)

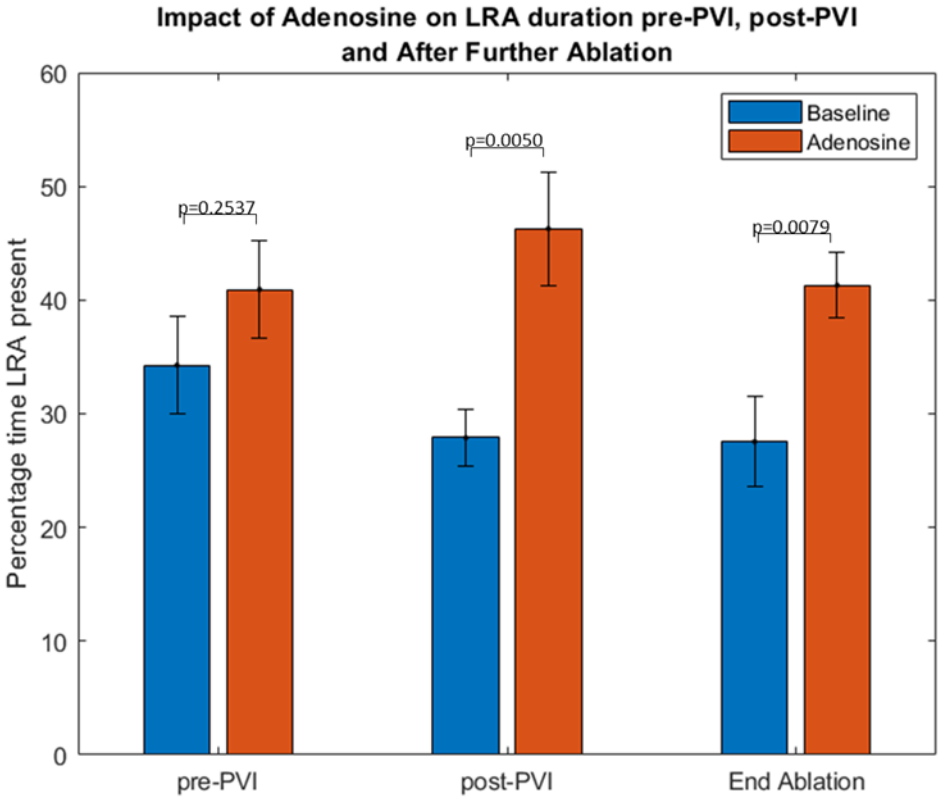

Figure 3.3 Effect of adenosine on LRA duration before and after pulmonary vein isolation and following non-pulmonary vein ablation. Bars represent standard error.

3.3.3 Atrial Fibrillation Cycle Length

At baseline, AFCL was 181.7±14.3ms, which reduced to 165.1±16.3ms with adenosine, a mean shortening of 16.6ms (95% CI 11.3 – 21.9, p<0.0005). The value for

the 5th percentile of AFCL in each map was also analysed to reflect the fastest activation rates, proposed as a surrogate of refractoriness. Adenosine resulted in a similar shortening of the 5th percentile of AFCL from 135.0±11.1ms to 127.5±12.2ms, a mean reduction of 7.5ms (95% CI 3.8 – 11.2, p<0.0005). The coefficient of variance of AFCL (SD/mean) was 0.072±0.028 at baseline, and 0.052±0.016 with adenosine (difference 0.020, 95% CI 0.01 – 0.03, p<0.0005).

There was a concomitant increase in global DF with adenosine from a mean of 6.0±0.7 to 6.6±0.8, a statistically significant mean difference of 0.6 (95% CI 0.4 – 0.9, p<0.0005). Coefficient of variance in DF reduced with adenosine from 0.08±0.05 to 0.06±0.02, but this was not statistically significant (mean difference 0.02, 95% CI -0.003 – 0.03, p=0.0915).

3.3.4 Phase Singularities

Multiple short-lasting phase singularities were found in all recordings. There were a greater number of phase singularities seen with adenosine (36.6±9.3) compared to baseline (30.1±7.8), which represented a statistically significant mean difference of 6.5 (95% CI 2.6 to 10.0, p=0.002). There was a small but statistically significant increase in the lifespan of phase singularities with adenosine from 509±161 to 599±245ms (90; 13-167; p=0.023).

3.3.5 Spatial distribution of LRA

In light of the observation of LRA occurring over a greater LA surface area with adenosine, each map was visually inspected at the highest cut off to identify whether regions with repetitive LRA remained spatially consistent or were changed with adenosine use. At baseline, a region of repetitive LRA could be identified in 89% (31 of the 35) of maps, with 61 zones identified in total (1.7±1.1 per map). Following adenosine infusion, 70 zones were identified across all 35 maps (2±1 per map), with 42 of these zones (60%; 1.2±1.0 per map) localized to the same site as LRA in baseline maps. Figure 3.4 illustrates regions of repetitive LRA in two patients before and after adenosine infusion. Regions of high frequency LIA and LRA may overlap, given that multiple wavefronts over different AF cycles may or may not satisfy criteria for LRA within the same confined region (e.g., partial rotation through 180°) and be classified as LIA. 81% of sites with high frequency LRA with adenosine coincided with sites where high frequency LIA was seen on baseline maps. There were 11 maps (in 9 patients) where the zones of LRA observed in adenosine maps were all in different sites from the baseline maps. In 4 of these, there were no regions of repetitive LRA seen at baseline.

In those patients where mapping was performed at more than one timepoint during the procedure (n=12; 1 patient had maps at all 3 timepoints), regions with the highest frequency of LRA seen on adenosine maps were compared. Across maps, 54 sites were identified, with 15 (28%) of these present at more than one timepoint during the procedure.

Across 26 maps at baseline, 40 sites of high DF were identified with 13 of these (33%) correlating with sites of high frequency LRA. After adenosine injection, 44 high DF sites were identified (in 30 maps), with 12 (27%) of these aligning with sites of high frequency LRA (see figure 3.5).

3.3.6 Clinical outcomes

Ablation resulted in acute termination to sinus rhythm in 6 (27%), with the remainder undergoing direct current cardioversion at the end of the procedure. Those in whom DCCV was required had more LRA on baseline maps compared to patients in whom ablation terminated AF. This was most prominent at 20% cut off when measured as a number of LRA occurrences (9.0±5.2 vs 3.7±2.3, 95% CI 0.7 – 10, p=0.0270), proportion of time LRA was present (20.8±10.8 vs 10.3±6.5, 95% CI 0.6 – 20.5, p=0.0380) or the surface area affected (8.3±3.3 vs 3.9±2.3, 95% CI 1.3 – 7.5, p=0.0080). There was no difference between the 2 groups on adenosine maps on any measure. See tables 3.4 and 3.5 for full results.

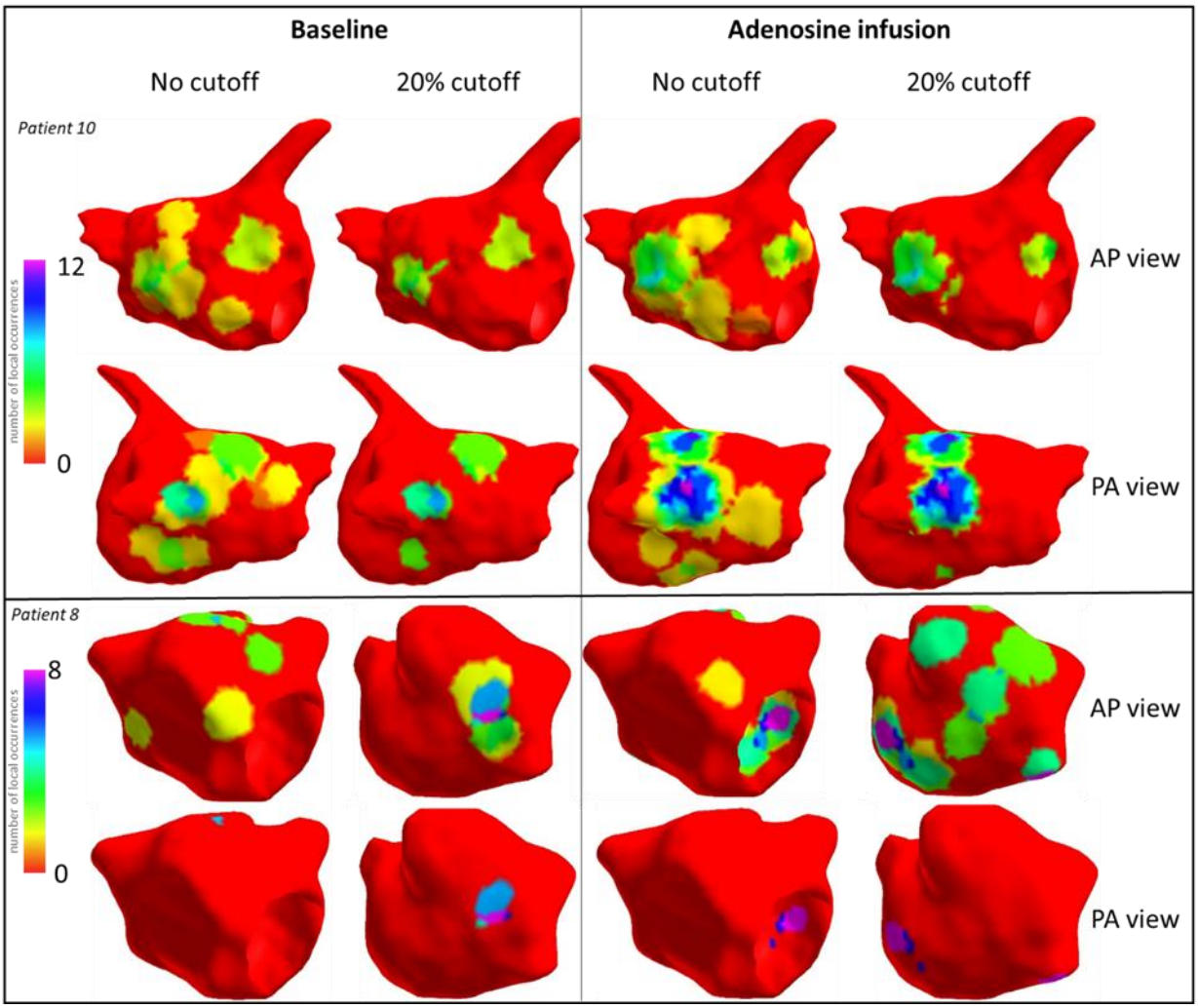

Figure 3.4 Regions of highly repetitive LRA following adenosine infusion identified at 20% cut off threshold (in pink/purple) occur at regions of LRA at baseline at lower frequency. (LRA, localised rotational activation).

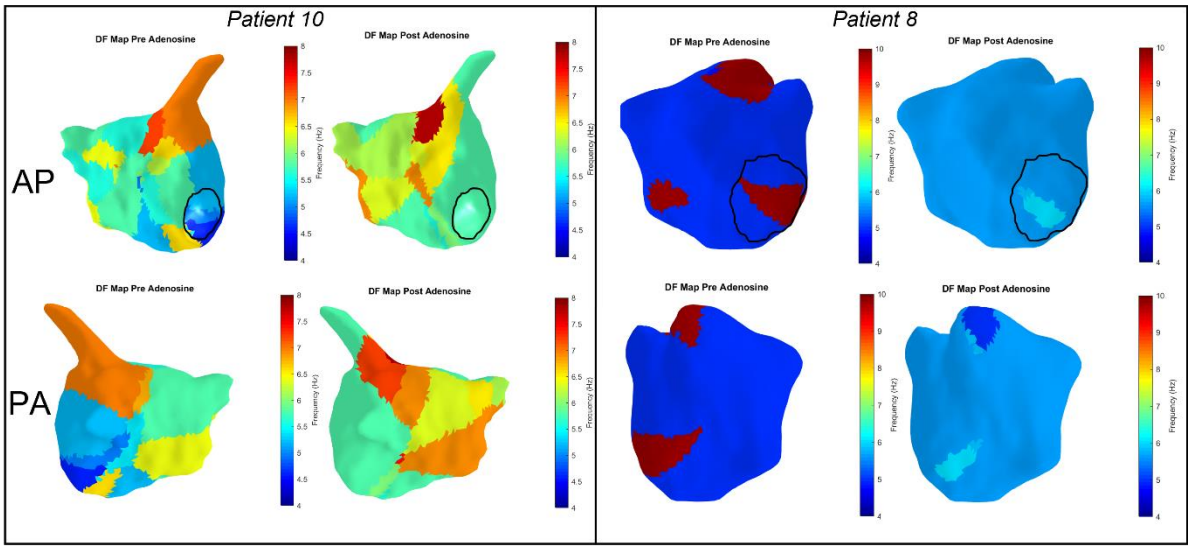

Figure 3.5 Dominant frequency (DF) maps for the same patients included in figure 3.4. A zone of highest DF in patient 10 is seen at the base of the LAA in the AP view both before and after adenosine injection, which does not correlate with the region of high frequency LRA seen on the posterior wall (see figure 3.4). Zones of high DF are also seen in patient 8 in the septum, roof and mitral isthmus at baseline. A region of high frequency LRA is seen on the roof of the LA (figure 3.4) but there is no correlation with other zones of high DF. A region of high DF in the postero-lateral mitral isthmus following adenosine correlates with a site of LRA.

3.4 Discussion

The main findings of this study are that intravenous adenosine injection has the following effects on AF: (i) AFCL shortening with increase in DF, (ii) a modest increase in wave propagation irregularity (as defined by LIA parameter), (iii) marked increase in the number of short-lasting rotating waves (assessed both by activation time and phase singularity mapping), and (iv) an increase in the lifespan of rotating waves. We found no effect of adenosine on focal firing frequency. Although the majority (60%) of regions found to have high LRA counts on adenosine maps were consistent with the zones identified at baseline, 40% of regions seen were only revealed with use of adenosine and only 28% were consistent across multiple mapping time points.

The mechanisms responsible for maintenance of persistent AF are poorly understood. Early studies in animal models led to the description of localised rotors, defined as organised and repetitive re-entry circuits thought to represent organised drivers.(66, 67, 211, 212) In recent years, efforts have focussed on developing techniques to map these sources to guide additional ablation beyond the pulmonary veins in a bid to improve clinical outcomes. Although early results of this strategy were promising,(124-126, 184) recent randomised studies evaluating this approach have been disappointing.(189) Furthermore, these methods have primarily relied on a phase mapping approach applied either to multi-electrode basket catheters or non-invasive body surface electrodes, which aim to identify phase singularities representing the pivot point of

localised rotors.(174) Further studies and evaluation of this technique have revealed contrasting results and highlighted the limitations of this approach.(177, 178, 180, 187)

The non-contact mapping employed in this study reveals patterns of propagation based on charge density reconstruction.(195) Uniquely, this system allows visualisation of the dynamics of wavefront propagation during AF and reveals recurrent patterns of partial rotation, directional changes, conduction slowing and focal firing with a high degree of spatial stability.(195) Whilst the ionic effects of adenosine have been well defined, the functional impact of these changes on wavefront propagation are less clear. The presumption that hyperpolarising the atrial myocardial cell membrane, as well as shortening action potential duration and refractoriness, promotes re-entry appears theoretically sound and is supported by our results with the predominant effect of adenosine being a promotion of LRA.(213) Hansen et al showed that adenosine promoted local re-entry at sites of AF termination or cycle length slowing, proposed as evidence of adenosine unmasking sites of re-entry driving AF propagation(210). However, although 9 of the 15 sites identified (in the 10 patients studied) were more pronounced with adenosine, 6 were not(210). We found that only 28% of sites identified with adenosine were stable between recordings. Moreover, the rotational activation promoted by adenosine was evident both in regions with repetitive patterns (as identified using the higher cut-offs) but also distributed more widely through the chamber (seen with no cut off applied). Patients in whom ablation terminated AF had less rotational activation at baseline but the effect of adenosine was the same irrespective of acute procedural outcome, which is not in keeping with the theory that sites revealed with the use of adenosine represent arrhythmogenic sources responsible for AF propagation. The degree of rotational activation measured following adenosine appears to represent the pharmacological properties of the drug, independent of the individual substrate properties of the patient. The degree of rotational activation prior to adenosine administration was however lower in patients in whom ablation achieved sinus rhythm. It may be that the degree of rotational activation seen serves as a surrogate marker of atrial functional electrophysiological properties that impact the likelihood of acute termination, but these are concealed by use of adenosine rather than revealed and does not provide evidence that targeting ablation to areas identified with the use of adenosine are likely to yield improved procedural outcomes.

Sites of high frequency LRA and LIA may overlap as these both represent localised directional changes in propagation. 81% of LRA zones identified using adenosine occurred in regions with high frequency LIA at baseline. Re-entry mechanisms have been shown to anchor to structural heterogeneities(110, 114), whilst LIA zones are

highly stable between recordings, perhaps reflective of local structural abnormalities or anatomical complexities, (214) which results in directional change in propagation at these sites. Shortening of atrial refractoriness with adenosine enables the directional change to complete >270° of rotation and persist for longer therefore appearing as LRA. Importantly these are generally short-lived patterns of incomplete rotation rather than stable complete re-entry. Zaman et al. reviewed reconstructed isochronal maps from sites of acute AF termination during ablation of persistent AF guided by focal impulse and rotor modulation (FIRM) mapping. The predominant activation pattern seen was that of incomplete rotation (in 46%) with stable rotational sources identified in only 21%, in keeping with high density contact mapping studies.(215, 216) We did not find stable rotating waves using both approaches (LRA and PS mapping). It may be that regions of high frequency LIA best reflect anatomical properties that impact wavefront propagation, with LRA determined by functional atrial properties. Importantly, the patterns of LRA promoted by adenosine occur in a spatiotemporally diverse distribution and are therefore of limited clinical relevance when devising ablation strategies.

No effect on focal firing was observed. Hyperpolarisation of the atrial myocardial cell membrane results in slowing in the rate of diastolic depolarisation thus reducing automaticity. In addition, adenosine is known to inhibit catecholaminergic sensitive L-type inward calcium currents within the atria.(213) Importantly however, all the patients included in our analysis had persistent AF. Adenosine appears to have differential effects in patients with paroxysmal versus persistent arrhythmia possibly due to the relative difference in aetiological contribution of the pulmonary veins and wider atrial myocardial substrate.(72, 208) Increased pulmonary vein firing following adenosine infusion is well described but is likely to be of greater significance in paroxysmal AF and not observed during persistent arrhythmia.(217, 218) Furthermore apparent focal firing during persistent AF may be related to epicardial to endocardial breakthrough rather than automaticity (which is not affected by adenosine).(62) Re-entry mechanisms may occur at the micro-anatomic level, only detectable using high resolution optical mapping(110) and not revealed at the resolution of the clinical mapping system used in this study. However, if present, and promoted by adenosine then it would be anticipated that this would manifest as an increase in focal activations appearing on the endocardial surface, which was not observed.

These results suggest a global acceleration of AF within the left atrium as demonstrated by a reduction in mean AFCL with significant (albeit small) reduction in variation of AFCL from 7.2 to 5.2% (measured by coefficient of variance of AFCL), which is supported by the concomitant increase in DF. This suggests a global atrial

pharmacological effect rather than limited focal changes which would be expected to cause greater heterogeneity in AFCL (or DF) across the chamber.

3.4.1 Limitations

These results are restricted to analysis of left atrial propagation. The distribution of adenosine receptors is heterogenous(209) and in persistent AF, an increase in dominant frequency with adenosine was demonstrated only in the high right atrium.(72) The right atrium is known to represent sites of mechanistic significance in a proportion of patients with AF and a differential effect of adenosine on right atrial propagation cannot be excluded.(125, 127)

Only short segments of maps (5 second duration) were analysed. Spatiotemporal variation in AF propagation may mean that patterns of propagation change during different or longer map durations. The differences observed following adenosine administration were highly consistent suggesting this was not simply the result of a different time period of measurement. Although an increase in LIA was also observed, these changes were small, only significant (in terms of number of pattern occurrences) in raw analysis and 5% cut off, and not likely to be clinically significant. Given the whole chamber acceleration in AFCL, a greater number of AF cycles would be expected over the same recording period and a small increase in the occurrences of infrequent spatially diverse irregular activation may therefore be observed. Furthermore, the proportion of time LIA patterns were present increased by only 3.2-3.8% which is unlikely to be significant and may also be driven by the reduction in refractoriness.

The technology used in this study is based on the resolution of local charge density derived through application of the inverse solution to multiple simultaneously recorded intracavitary unipolar electrograms(195). Electrical activity on the endocardial surface (discretized as approximately 3500 vertices) is obtained as an inverse solution based on measurements of 48 electrodes of the basket catheter. This is a unique approach aimed at achieving a more accurate local representation of cardiac activation and has been validated against contact unipolar recordings(201). However, the precise implication of this technique on the visualised map of atrial activation, compared to alternative techniques is difficult to discern and requires further extensive comparison given the lack of sufficient validation of activation patterns against contact recordings or optical mapping during AF.

It is difficult to establish the effect of ablation. The effects on LRA were consistent at all stages of the procedure but not statistically significant prior to any ablation. The primary analysis was intended to detect an effect across all maps and may have been

underpowered to detect differences with sub-analyses. The difference in statistical significance was driven in part by a reduction in LRA observed post-PVI, which may be the result of pulmonary vein ablation incorporating sites of LRA. However, this difference was not statistically significant and if PVI eliminated rotational sites it would be anticipated that this would also reduce the impact of adenosine, which was not observed. Although the number of rotational activation patterns were lower in patients in whom ablation was acutely successful, it is difficult to draw further conclusions about the process of sinus rhythm restoration, which was not seen to occur instantaneously following ablation delivery. It cannot therefore be determined whether the first area targeted, or the last, or a combination of all of them was the critical mechanism maintaining AF. Furthermore, although we report acute procedural outcomes, these may not correspond to clinically meaningful long-term outcomes, which would require further analyses beyond the scope of this study.

3.4.2 Conclusion

These results suggest that rotational activation, in contrast with focal firing, and much less so LIA, is influenced by adenosine. This is likely to be as a result of its effect on the refractory period of local tissue with a shortening of refractoriness allowing for a higher density of rotating wavefronts at spatially variable sites throughout the left atrium and shorter global cycle length with increase in DF. The degree of rotational activation may serve as a surrogate measure of individual atrial functional properties, with little evidence that rotational activation seen with adenosine represents promising targets for ablation aimed at arrhythmogenic sources of AF perpetuation within the left atrium particularly as there is little stability in LRA sites within patients. Caution should be exercised when interpreting maps obtained following adenosine administration to guide non-pulmonary vein ablation.

Table 3.3 Impact of adenosine on LRA frequency, duration and surface area, pre-pulmonary vein isolation, post-pulmonary vein isolation and following non-pulmonary vein ablation. LRA: Localised rotational activation; PVI: pulmonary vein isolation; SA: surface area

Variable	Cut off	Pre-PVI				Post-PVI				Post non-PVI ablation			
		Baseline (SD)	Adenosine (SD)	Difference (95% CI)	p value	Baseline (SD)	Adenosine (SD)	Difference (95% CI)	p value	Baseline (SD)	Adenosine (SD)	Difference (95% CI)	p value
LRA number	0	18±8.5	22.5±8.5	4.8 (-2.9 – 12.0)	0.2044	15.9±8.0	25.6±12.4	9.7 (2.0 – 17.5)	0.0173	14.2±5.8	24.0±6.3	9.8 (5.5 – 14.1)	0.0007
	5	12.9±6.7	17.1±7.3	4.2 (-1.5 – 9.9)	0.1360	11.5±7.0	20.1±10.1	8.6 (1.4 – 15.8)	0.0230	9.1±5.2	17.8±5.2	7.9 (4.4 – 12.9)	0.0016
	10	11.9±6.9	16.9±7.2	5.0 (-0.6 – 10.6)	0.0749	10.7±6.6	18.9±9.8	8.2 (1.5 – 14.8)	0.0203	9.1±5.2	17.6±5.2	8.5 (3.9 – 13.0)	0.0027
	20	8.2±6.3	13.4±4.4	5.5 (0.5 – 9.9)	0.0345	9.0±5.4	14.5±8.4	5.5 (-0.6 – 11.6)	0.0720	7.8±3.8	14.1±5.3	6.3 (1.9 – 10.8)	0.0116
	30	7.3±5.0	10.9±3.9	3.6 (-0.1 – 7.4)	0.0551	6.5±4.0	11.5±6.1	5.0 (1.3 – 8.6)	0.0118	6.9±3.4	12.3±4.3	5.4 (1.3 – 9.6)	0.0156
	40	6.5±4.4	9.3±3.3	2.8 (-0.6 – 6.0)	0.0935	4.8±2.9	10.7±5.5	5.9 (2.2 – 9.5)	0.0040	5.3±2.1	10.2±3.5	4.9 (2.9 – 6.9)	0.0005
LRA time	0	34.2±14.2	40.9±14.3	6.7 (-5.6 – 18.9)	0.2537	27.8±9.7	46.3±19.4	18.5 (6.5 – 30.3)	0.0050	27.5±11.9	41.3±8.7	13.8 (4.7 – 22.8)	0.0079
	5	28.8±13.0	34.4±13.3	5.6 (-5.3 – 16.6)	0.2810	23.4±10.1	41.3±17.9	17.9 (6.2 – 29.4)	0.0053	20.9±11.6	34.7±8.3	13.8 (5.4 – 22.3)	0.0054
	10	27.4±13.5	34.0±13.0	6.6 (-4.1 – 17.3)	0.2011	22.5±9.4	39.3±17.6	16.8 (6.0 – 27.6)	0.0048	20.9±11.6	34.3±8.2	13.4 (4.4 – 22.3)	0.0090
	20	19.8±12.5	28.8±10.5	9.0 (-2.0 – 20.0)	0.0991	19.9±9.6	32.4±16.3	12.5 (1.4 – 23.6)	0.0301	18.9±9.8	28.2±6.7	9.3 (1.2 – 17.5)	0.0297
	30	18.6±10.9	24.6±8.7	6.0 (-3.1 – 14.9)	0.1722	15.7±7.8	26.4±13.4	(10.7 (3.4 – 17.9)	0.0069	17.0±9.0	25.2±6.5	8.2 (0.6 – 15.7)	0.0381
	40	17.5±10.1	21.8±7.7	4.3 (-3.6 – 12.3)	0.2491	11.9±6.0	24.7±11.9	12.8 (5.0 – 20.6)	0.0033	13.1±5.4	21.7±7.1	8.6 (4.5 – 12.8)	0.0014
LRA SA	0	25.6±8.7	28.0±10.2	2.4 (-4.9 – 9.7)	0.4776	21.1±8.0	30.9±12.2	9.8 (1.7 – 17.8)	0.0213	20.2±8.1	29.5±6.7	9.3 (5.6 – 13.0)	<0.0005
	5	16.0±6.9	15.8±7.6	-0.2 (-5.6 – 5.3)	0.9414	12.1±6.3	16.8±7.4	4.7 (-1.8 – 11.2)	0.1407	9.5±4.8	14.9±4.3	5.4 (3.3 – 7.4)	<0.0005
	10	13.5±6.2	15.5±7.7	2.0 (-3.2 – 7.8)	0.4105	10.3±4.9	14.4±6.6	4.1 (-0.9 – 9.2)	0.0990	9.5±4.8	14.3±4.1	4.8 (2.0 – 7.5)	0.0041
	20	7.7±4.1	10.9±4.1	3.2 (0.3 – 6.2)	0.0342	7.9±3.3	9.6±4.8	1.6 (-2.2 – 5.6)	0.3788	7.5±2.7	10.1±3.3	2.6 (0.6 – 4.5)	0.0162
	30	6.8±2.5	8.6±4.7	1.8 (-0.9 – 4.7)	0.1633	5.1±2.3	6.9±3.5	1.8 (-0.2 – 3.8)	0.0733	6.4±2.8	7.8±2.3	1.4 (-0.6 – 3.6)	0.1312
	40	5.8±1.9	6.8±3.1	1.0 (-0.6 – 2.6)	0.1843	3.7±2.0	6.1±3.1	2.4 (0.1 – 2.6)	0.0417	5.0±2.3	6.1±2.3	1.1 (-0.3 – 2.6)	0.1097

Table 3.4 Difference in localised rotation activation frequency, duration, and surface area at baseline according to acute procedural outcome.

Variable	Cut off	Group	n	Mean	Standard deviation	p-value	95 % Confidence interval
LRA number	0	DCCV	16	16.9	7.9	0.0760	-0.8 – 13.8
		Sinus with ablation	6	10.3	5.0		
LRA percent time	0	DCCV	16	31.8	13.1	0.0970	-2.1 – 23.1
		Sinus with ablation	6	21.3	10.9		
LRA percent SA	0	DCCV	16	23.7	8.4	0.0380	0.5 – 16.6
		Sinus with ablation	6	15.1	6.8		
LRA number	5	DCCV	16	12.3	6.0	0.0590	-0.2 – 11.2
		Sinus with ablation	6	6.8	4.8		
LRA percent time	5	DCCV	16	26.8	12.2	0.0760	-1.2 – 22.1
		Sinus with ablation	6	16.3	10.0		
LRA percent SA	5	DCCV	16	14.6	7.0	0.0490	0.0 – 13.1
		Sinus with ablation	6	8.0	5.0		
LRA number	10	DCCV	16	11.1	5.8	0.1280	-1.3 – 9.8
		Sinus with ablation	6	6.8	4.8		
LRA percent time	10	DCCV	16	25.2	12.2	0.1270	-2.8 – 20.6
		Sinus with ablation	6	16.3	10.0		
LRA percent SA	10	DCCV	16	11.7	5.5	0.1690	-1.7 – 9.1
		Sinus with ablation	6	8.0	5.0		
LRA number	20	DCCV	16	9.0	5.2	0.0270	0.7 – 10.0
		Sinus with ablation	6	3.7	2.3		
LRA percent time	20	DCCV	16	20.8	10.8	0.0380	0.6 – 20.5
		Sinus with ablation	6	10.3	6.5		
LRA percent SA	20	DCCV	16	8.3	3.3	0.0080	1.3 – 7.5
		Sinus with ablation	6	3.9	2.3		
LRA number	30	DCCV	16	7.1	4.4	0.0780	-0.4 – 7.6
		Sinus with ablation	6	3.5	2.6		
LRA percent time	30	DCCV	16	17.4	9.7	0.0940	-1.4 – 16.8
		Sinus with ablation	6	9.8	7.3		
LRA percent SA	30	DCCV	16	6.1	2.5	0.0450	0.1 – 5.1
		Sinus with ablation	6	3.5	2.7		
LRA number	40	DCCV	16	6.1	4.1	0.1410	-1.0 – 6.6
		Sinus with ablation	6	3.3	2.5		
LRA percent time	40	DCCV	16	15.4	9.8	0.1740	-3.0 – 15.2
		Sinus with ablation	6	9.2	6.8		
LRA percent SA	40	DCCV	16	5.0	2.2	0.1220	-0.5 – 4.2
		Sinus with ablation	6	3.2	2.7		

Table 3.5 Difference in localised rotational activation frequency, duration and surface area following adenosine according to acute procedural outcome.

Variable	Cut off	Group	n	Mean	Standard deviation	p-value	95 % Confidence interval
LRA number	0	DCCV	16	22.7	9.1	0.738	-7.8 – 10.9
		Sinus with ablation	6	21.2	10.1		
LRA percent time	0	DCCV	16	40.7	14.5	0.971	-15.3 – 15.9
		Sinus with ablation	6	40.5	18.5		
LRA percent SA	0	DCCV	16	27.4	8.9	0.986	-10.5 – 10.3
		Sinus with ablation	6	27.5	14.1		
LRA number	5	DCCV	16	17.5	8.0	0.731	-6.6 – 9.3
		Sinus with ablation	6	16.2	7.9		
LRA percent time	5	DCCV	16	34.8	13.8	0.988	-14.3 – 14.5
		Sinus with ablation	6	34.7	16.2		
LRA percent SA	5	DCCV	16	15.1	6.0	0.943	-6.9 – 7.4
		Sinus with ablation	6	14.9	9.9		
LRA number	10	DCCV	16	16.9	7.6	0.715	-6.4 – 9.1
		Sinus with ablation	6	15.5	8.2		
LRA percent time	10	DCCV	16	34.0	13.7	0.998	-14.5 – 14.5
		Sinus with ablation	6	33.9	16.7		
LRA percent SA	10	DCCV	16	14.0	5.6	0.897	-7.6 – 6.7
		Sinus with ablation	6	14.4	10.3		
LRA number	20	DCCV	16	13.4	6.3	0.772	-5.3 – 7.1
		Sinus with ablation	6	12.5	5.8		
LRA percent time	20	DCCV	16	27.9	12.5	0.795	-14.4 – 11.2
		Sinus with ablation	6	29.6	13.7		
LRA percent SA	20	DCCV	16	10.1	4.5	0.941	-4.6 – 4.9
		Sinus with ablation	6	9.9	5.4		
LRA number	30	DCCV	16	11.2	4.9	0.388	-2.8 – 6.8
		Sinus with ablation	6	9.2	4.4		
LRA percent time	30	DCCV	16	23.2	10.0	0.88	-11.1 – 9.6
		Sinus with ablation	6	23.9	11.5		
LRA percent SA	30	DCCV	16	8.0	4.1	0.324	-2.2 – 6.2
		Sinus with ablation	6	6.0	4.4		
LRA number	40	DCCV	16	10.3	4.6	0.238	-1.9 – 7.2
		Sinus with ablation	6	7.7	4.4		
LRA percent time	40	DCCV	16	21.8	9.6	0.767	-8.6 – 11.5
		Sinus with ablation	6	20.3	11.3		
LRA percent SA	40	DCCV	16	7.0	3.0	0.126	-0.7 – 5.4
		Sinus with ablation	6	4.7	3.1		

4 Bi-atrial Assessment of Spatiotemporal Variability of Complex Propagation Patterns

4.1 Introduction

The limited efficacy of pulmonary vein isolation for the ablation of persistent atrial fibrillation (persAF) has resulted in concerted efforts to identify non-pulmonary vein mechanisms responsible for AF maintenance. This has led to the development of techniques to facilitate mapping of the underlying atrial electrophysiology with the aim of revealing fibrillatory mechanisms and guiding targeted ablation.(126, 184, 187, 197, 219, 220)

Non-contact charge-density mapping allows visualisation of whole chamber activation. Ultrasound is used to generate a high resolution 3-dimensional reconstruction of the atrial chamber anatomy based on a triangular mesh structure comprising constituent corners (termed vertices) of triangular faces, which form the unique points for calculation of inverse derived charge density signals. Wavefront patterns are scrutinised in real time at every vertex of the chamber surface (approximately 3,500) by in an inbuilt application (AcQTrack, Acutus Medical), as described above. Non-planar, complex localised patterns of propagation are identified and characterised as localised rotational activation (LRA), localised irregular activation (LIA) and focal firing (FF)(see chapter 2).(196) To be classed as LRA, a smooth depolarisation wavefront has to rotate 360 degrees around a central point. LIA is characterised by a difference in angle between conduction that enters and leaves a confined region exceeding a threshold of 90 degrees (and not meeting the criteria for LRA above). In contrast, FF is defined as activation of a primary vertex that precedes adjoining neighbours and extends centrifugally from this primary vertex.

A catheter ablation approach aimed at targeting these zones has been evaluated in one prospective observational study.(197) Within this study, mapping durations of approximately 5-seconds were used to identify ablation targets, but little work has been done exploring the spatial and temporal stability of these electrophysiological phenomena. It is unclear to what extent the patterns of AF propagation involved represent stable features of the underlying substrate and are therefore consistent over separate AF epochs or are more dynamic potentially affected by physiological influences or even mapping artefacts, knowledge of which is crucial in developing an optimal approach.

The properties of atrial regions demonstrating these activation patterns during AF have not previously been explored in sinus rhythm using traditional methods of contact mapping. Electroanatomical voltage mapping has been employed extensively as a method of examining cardiac tissue, with low voltage amplitude representing a surrogate measure of tissue fibrosis. However, although presence of low voltage is associated with poorer outcomes from catheter ablation(83), both sensitivity and specificity of voltage mapping is poor and influenced by multiple technical and physiological factors, as explained above.(86, 87) In addition, many patients do not exhibit regions of fibrosis, measured either by bipolar voltage or MRI.(84, 95) The concept of gross fibrotic structural remodelling is therefore inadequate when attempting to explain the pathophysiological process responsible for maintenance and progression of AF and bipolar voltage mapping alone is unlikely to identify more subtle abnormalities in the absence of dense scar. These subtle abnormalities may represent regions with abnormal conduction properties but preserved voltage amplitude, that can be revealed during pacing at different rates and vectors to reveal regions of anisotropy and delayed conduction.

We have performed the first study employing simultaneous mapping of AF activation in both the left and right atria using the AcQMap system and sought to investigate the spatial stability between 2 separate 30-second recordings of left and right atrial AF propagation and the effects of increasing duration of AF recording length on the degree of variability in mechanisms observed. Properties of atrial regions with the most stable patterns were explored using long and short cycle length pacing and electroanatomic voltage mapping in sinus rhythm.

4.2 Methods

4.2.1 Simultaneous Bi-Atrial Mapping

Patient selection

Patients between the ages 18-80 undergoing first time catheter ablation for either paroxysmal (n=5) or persistent (n=17) AF were recruited following appropriate ethical approval (REC reference 18/SC/0409). Exclusion criteria include prior cardiac surgery, congenital cardiac abnormalities and severe valve disease. Additional exclusions included pregnancy or planning pregnancy around the time of the procedure or anatomical abnormalities that may preclude the use of 2 AcQMap catheters and bilateral femoral venous access.

Electrophysiological mapping and ablation

Procedures were carried out under general anaesthetic. With the exception of amiodarone, antiarrhythmic drugs were stopped a minimum of five days prior to the procedure. Venous access was obtained via bilateral femoral vein puncture under direct ultrasound guidance. Heparin boluses were administered prior to trans-septal puncture followed by continuous heparin infusion to maintain an ACT >350s. A decapolar catheter (Inquiry, Abbott Medical) was inserted into the coronary sinus through an AcQRef (Acutus Medical) sheath which includes a distal electrode used as a unipolar reference. The first AcQMap catheter was advanced over a 0.032 guide wire into the RA via an AcQGuide (Acutus Medical) sheath and ultrasound used to reconstruct the right atrial chamber anatomy as previously described.(196) The ablation catheter (Tacticath, Abbott Medical) was advanced via an Agilis sheath into the left atrium across the single transseptal puncture site. The second AcQGuide sheath was then exchanged for the transseptal access sheath over the guide wire and a second AcQMap catheter advanced into the LA (see figure 2). The LA anatomy was then generated with ultrasound. A circular mapping catheter (Inquiry Optima or Advisor Variable Loop, Abbott Medical) was used to undertake electroanatomic voltage mapping and guide pulmonary vein isolation as outlined below.

In patients attending the procedure in sinus rhythm AF was induced using burst atrial pacing, otherwise all AF recordings were obtained prior to DCCV. Once AF was established, recordings of 2 minutes duration were generated and time alignment between systems facilitated using a below threshold pacing stimulus from the coronary sinus catheter of 4 beats at 1000, 800 and 600ms intervals and 12 second rest period. Pulmonary vein isolation was performed using contact force guided radiofrequency ablation using 40-50 Watts (Tacticath ablation catheter, Abbott Medical). Simultaneous biatrial AF mapping was repeated following completion of PVI. Additional ablation and AF mapping was undertaken at the discretion of the operator.

Propagation Map Calculation and Data Export

Raw electrode biopotential signals were visually inspected to identify outlying or corrupted signals (likely resulting from electrode damage during catheter preparation and insertion), which were then manually excluded. A low pass filter at 100Hz as well as a 50Hz notch filter and smoothing algorithm were applied followed by selection of a QRS-T wave template for subtraction. The AcQMap system allows operators to define separate mapping segments of any duration up to a maximum of approximately 14-15s, limited by software processing capability. For this study, three consecutive 10-second mapping segments were created for simultaneous left and right atrial mapping, synchronised using the coronary sinus low amplitude pacing spike. This process was repeated to create two

30-second AF maps following splicing together of each 10s segment. Propagation maps were calculated using the default timing method (based on -dv/dt of dipole signals), window width (for isochronal colour bars) of 80ms and time threshold of 70ms (representing presumed minimum refractoriness). AcQTrack propagation patterns were calculated for each segment and data exported for offline analysis.

Propagation Pattern Quantification

Complex propagation patterns described above (LIA, LRA and FF) were identified using the AcQTrack (Acutus Medical) system during AF to ensure objective classification of activation patterns, as outlined in chapters 1-2. As previously explained, every wavefront was scrutinised at each vertex of the anatomy. Planar wavefronts were discarded, whilst if the parameters for LIA, LRA and FF are met within a discreet zone ($300mm^2$ for LRA and $200mm^2$ for LIA) the vertices within this zone are highlighted and recorded by the system.

These data were exported and analysed using the methods outlined in chapter 2 to allow quantification of activation pattern frequency, duration of time present and the surface area over which they occur.

The results obtained using this method were applied to allow analysis of spatiotemporal stability as outlined below and define regions for further analysis using bipolar electroanatomic voltage mapping and analysis of conduction properties during pacing as explained below.

4.2.2 Spatiotemporal Variability Analysis

Spatial stability

Spatial stability was assessed by correlating the frequency of propagation patterns (LIA, LRA and FF) at each vertex of the chamber anatomy over 2 separate 30s recordings taken at baseline prior to any ablation. The value for the number of pattern occurrences were plotted for each vertex of the anatomy for each recording. A linear best fit line was plotted, and R^2 calculated to assess the strength of the linear correlation between the two mapping segments. Stability of regions with the most repetitive patterns identified using the 30% threshold value for each 30s map were compared using Cohen's kappa statistic.

Temporal Stability/Optimal Mapping Duration

We sought to identify the minimum mapping duration required to identify the sites that are shown over the full 30s analysis to represent regions with the highest frequency and therefore most repetitive activation for each of the specific patterns described. The

region with the highest frequency of each propagation pattern may be considered as reflecting an optimum target for ablation. This was identified using the 30% cut off to identify the relevant zone on maps of increasing duration up to 30 seconds. Each vertex of the anatomy contained within and outside this region (at 30% cut off) was used to calculate the kappa statistic to quantify the consistency between these zones against the zone identified during a full 30 second segment. Kappa values were calculated and plotted at both 1-second and 5-second increments with a value of 0.8 considered excellent consistency compared to the result obtained at 30-seconds. The duration at which a kappa value of 0.8 was reached was extracted for each map and used for comparisons.

In a subset of 15 patients, additional analyses were undertaken using alternative methods to confirm that the results obtained were consistent between methods used. LIA, LRA, and FF were quantified for occurrence frequency, percentage time present and percentage of the chamber surface area affected (for FF only frequency was assessed) at increasing durations, also in 1-second increments up to 30-seconds. At each incremental recording duration, the percentage change in each variable was calculated. For occurrence frequency the results for every possible combination of maps of increasing duration within the 30s recording were compared (e.g. the frequency of a pattern was measured over 5-seconds and compared with all possible maps of 5-second duration within the full 30-second recording). For occurrence time and surface area a 5s moving average at 1s increments was calculated. Heatmaps were created for each pattern allowing a visual representation of the effect of duration on variability.

4.2.3 Electroanatomic Voltage Mapping and Geometry Registration

Electroanatomic voltage mapping was performed in sinus rhythm with DCCV used following collection of all AF data in patients attending the procedure in AF. If DCCV was unsuccessful then data was obtained during AF. Mapping was performed using a circular mapping catheter (Inquiry Optima; 20x 1mm band electrodes with 2mm tip electrode and 1-4.5-1mm electrode spacing, or Advisor Variable Loop 20x 1mm electrodes with 1-4-1 spacing, Abbott Medical) and the Ensite Precision electrophysiological mapping system (Abbott Medical). Interpolation threshold was set to 7mm with internal and external projection limited to 5mm.

Bipolar voltage amplitude data together with chamber geometry was exported and re-constructed offline using a custom designed software application. Voltage points collected within the pulmonary veins and left atrial appendage were excluded as these regions are not visualised using the AcQMap system and provide non-representative

results for comparison. Bipolar amplitude was measured from peak to peak in local electrograms. AcQMap and Precision anatomies were co-registered using a system of anatomical fiducial points and scaling of the Precision anatomy to minimise the average distance between chamber surfaces as shown in figure 4.1. Each vertex of the AcQMap anatomy was aligned with its nearest neighbour point on Precision to allow comparison and the corresponding voltage amplitude assigned to that vertex. Regions of high frequency LIA identified using the 30% cut off threshold were identified and the mean bipolar voltage amplitude corresponding to these regions was compared to the average for the rest of the chamber using the paired t-test.

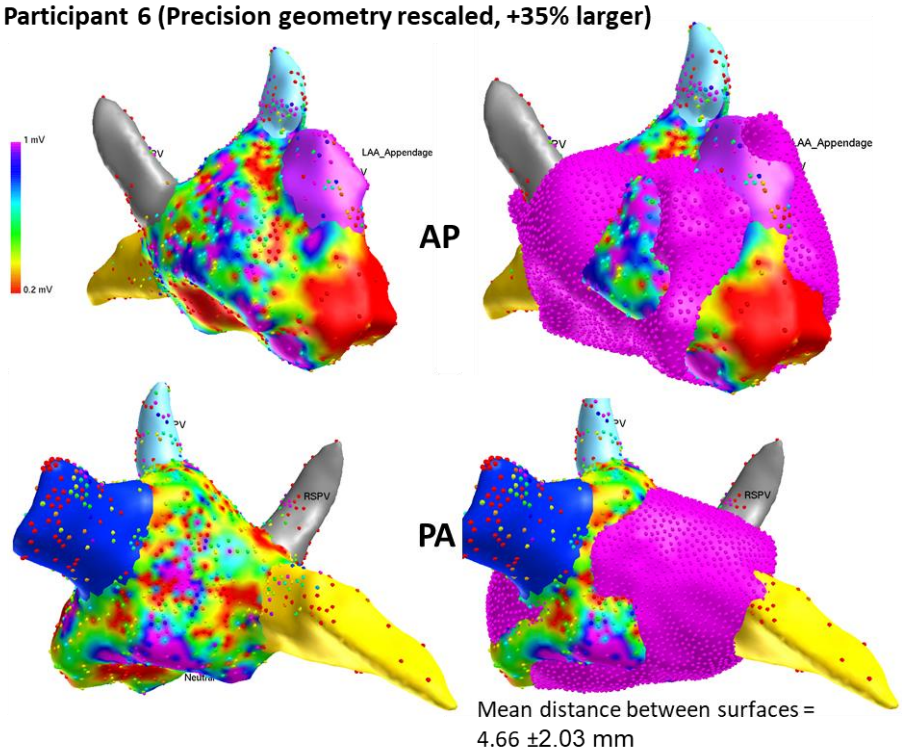

Figure 4.1 Fused contact and non-contact geometries. Anteroposterior (AP) and posteroanterior (PA) views of the scaled Precision left atrial geometry (left 2 images) and the merged Precision and AcQMap geometries (right 2 images).

4.2.4 SuperMap and Conduction Heterogeneity Calculation

Activation mapping was performed during pacing using the AcQMap "SuperMap" algorithm (Acutus Medical) in a subset of 9 patients recruited following the introduction and clinical release of this mapping algorithm designed for high density multi-position non-contact mapping of organised rhythms. The pacing protocol involved a repeating 4-beat drive train followed by a single extrastimulus at a coupling interval of 20ms longer that the effective refractory period with no rest period, using a pacing output of twice the diastolic threshold. This was conducted at up to 3 sites including the high right atrium, left atrial appendage (both using the ablation catheter positioned at these sites), and the most

proximal coronary sinus bipoles positioned within the LA. If AF was induced by the pacing protocol, DCCV was used to restore sinus rhythm, but pacing was abandoned if AF was repeatedly induced and only data collected up to that point analysed.

The “SuperMap” algorithm allows continuous data collection across multiple paced cycles. The AcQMap basket was roved throughout the chamber for a minimum duration of 3 minutes to ensure full and even coverage of the entire chamber. Each paced beat (drive train and extrastimulus) is identified automatically using the morphology and cycle length of unipolar signals detected with the coronary sinus catheter electrodes and local chamber electrogram data is “binned” according to the corresponding group identified by the coronary sinus signals. This allows simultaneous mapping of both paced cycle lengths and was repeated for each pacing site and within the LA and RA.

Local activation time (LAT) data from each map created was exported and analysed using a custom application programme. The LAT difference between each vertex and every neighbouring vertex at a 5mm radius was calculated and the maximum value assigned to that local point. Values <1ms or >100ms were excluded as these were deemed to suggested non-physiological conduction of either <0.05m/s or >5m/s. When applied to the whole chamber, or specific regions, a histogram of LAT differences could be generated and the median value for that specific region calculated to give the median activation time difference (MAT). The conduction heterogeneity index (CHI) was derived from the difference between the 95^{th} and 5^{th} percentile values divided by the MAT as illustrated in figure 4.2 and described previously(221). As high frequency LIA zones were found to be stable across maps, these regions were identified on the 1^{st} AF map obtained in each participant and an additional 5mm radius added to this region. The difference in MAT and CHI between each paced cycle length was compared within this region and in the remainder of the chamber.

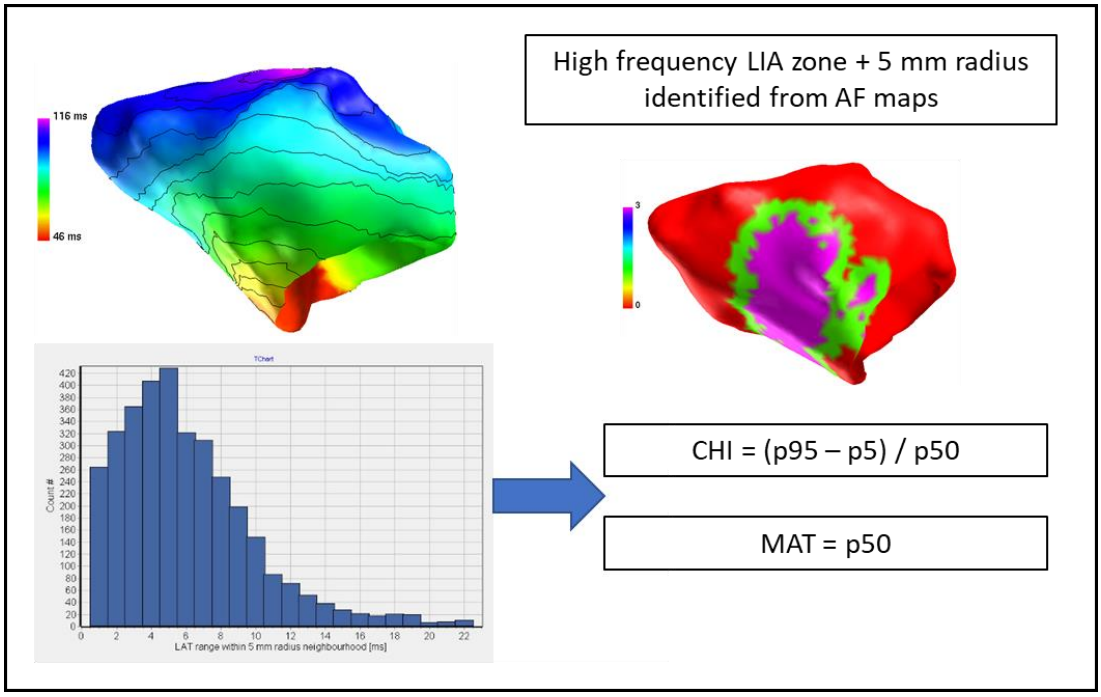

Figure 4.2 Method of CHI calculation. Local activation time maps are obtained using SuperMap during pacing and regions with high frequency LIA are identified during AF. LAT differences at a radius of 5mm from every point on the chamber surface are calculated allowing generation of a histogram for whole region concerned (e.g. LIA or LRA zones). The conduction heterogeneity index (CHI) and median activation time difference (MAT) are calculated from this histogram.

4.2.5 Statistics

Continuous variables are expressed as mean ± standard deviation or median and interquartile range depending on distribution. Between group comparisons were performed using independent samples t-test or Wilcoxon rank sum test depending on distribution as assessed using the Kolmogorov-Smirnov test. A two-sided p value of <0.05 was considered significant. Statistical analysis was performed using SPSS (IBM v25) or Matlab (R2019a, MathWorks) and figures created using Matlab.

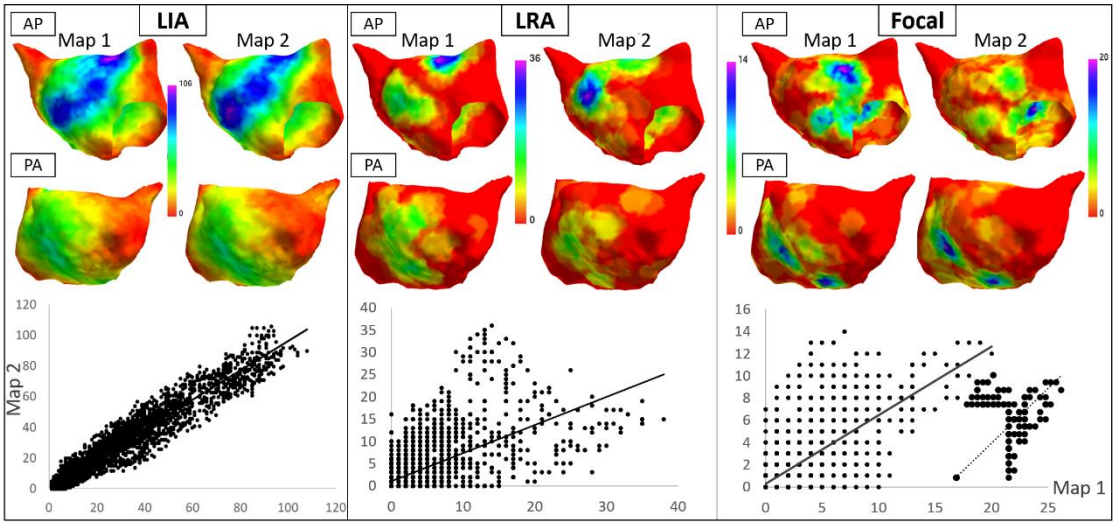

Figure 4.3 Example of spatial stability of LIA, LRA and FF in the LA. Antero-posterior (top row) and postero-anterior (lower row) views of the left atrium showing the density and distribution of localised irregular activation (A), localised rotational activation (B) and focal firing (C) (red=no occurrences, purple=highest density) in patient 10. Each pair of images represent 2 sequential 30s maps. Graphs below represent correlation plots for each anatomy vertex (1st map X axis, 2nd Y axis) with R^2 for LIA 0.92, LRA 0.39 and FF 0.49. Inset graph shows correlation for regions with FF frequency ≥1 every 3s on the first map with R^2 of 0.74.

4.3 Results

4.3.1 Patient Characteristics and Map Segments Obtained

The characteristics of all patients recruited to the study are outlined in table 4.1. One patient (patient 9) was excluded from analysis as only organised atrial tachycardia could be induced when attending for the procedure. In all but one patient (patient 12), two 30-second maps of AF were obtained at baseline. Patient 12 had varying QRS morphology as a result of left bundle branch block and only one 30s segment could be obtained with sufficient quality of QRS-T wave subtraction to allow analysis. Maps following pulmonary vein isolation were obtained in 12 patients and a further 8 recordings were obtained following non-pulmonary vein ablation providing a total of 62 simultaneous AF recordings in the left and right atrium. Mapping duration and temporal variability analysis was performed on all maps obtained (a total of 124 maps including both chambers). Spatial variability analysis was performed by comparing the two 30s maps obtained at baseline in the 20 patients.

Table 4.1 Characteristics of patients recruited to the study. Data is expressed as n(%), medians, 1st and 3rd quartiles or mean±standard deviation. Patient 9 was excluded from analysis as only atrial tachycardia could be induced. (AF: atrial fibrillation; BMI: Body mass index; LA: Left atrium; LV: left ventricle)

Characteristic	Distribution
AF Type	16 Persistent, 5 Paroxysmal
Sex	41% Female
Age	61 (56-66)
BMI (kg/m^2)	30 (26-33)
CHADs-VASc	1.3±1.3
Prior Anti-Arrhythmic Drugs	Sotalol: 2 (9.5%) Amiodarone: 7 (33%) Flecainide: 4 (19%)
LA Diameter (mm)	43 (38-51)
LV Ejection Fraction (%)	60 (55-60)
Time Since AF Diagnosis (Months)	48 (20-60)
Rhythm at baseline	SR: 11, AF: 10

4.3.2 Spatial Variability

LIA demonstrated the greatest spatial stability between each 30s recording with R^2 of 0.83(0.71-0.88) across all maps analysed. This was consistent across both chambers with values of 0.81(0.75-0.88) and 0.84(0.61-0.88) in the LA and RA respectively. Median R^2 for LRA and FF were 0.39(0.24-0.57) and 0.64(0.54-0.73) respectively. Multiple low frequency focal firings were seen widely distributed across the atrial surface (see figure 4.3). For high frequency FF, defined as occurring ≥10 times over the 30s, R^2 was 0.83(0.68-0.85). Detailed results are outlined in table 4.2.

Stability of regions across both maps with the highest frequency patterns identified at 30% cut off was also greatest for LIA in both the LA and RA. Cohen kappa statistic for LIA in the LA and RA respectively was 0.75 (0.64-0.78) and 0.75 (0.58-0.79). Full kappa statistic results for all patients are outlined in table 4.3.

The anatomical regions with maximal LIA were the anterior and posterior LA (in 46% and 27% of maps respectively) and the lateral and septal RA (in 46% and 32% respectively). LRA showed similar distribution with the zone of highest LRA frequency in the posterior LA in 41% and the anterior LA in 34%. In the RA, the lateral wall was the most common site (in 37%) followed by the septum and posterior walls (each in 24%). A similar distribution was observed for FF, most commonly involving the anterior and posterior LA (in 34% and 29% respectively), followed by the LA septum (20%). In the RA, the highest frequency of FF was seen in the septum in 59% and the lateral wall in 22%.

4.3.3 Mapping duration results

Figure 4.4 demonstrates the effect of increasing map duration on kappa statistic values for LIA, LRA and FF respectively compared to maps of 30 seconds. Analysis was conducted on all 124 recordings (62 in the LA and 62 in the RA) obtained. LIA showed the highest kappa value at all time periods with a value of 0.66 (0.57-0.70) at 5s, rising to 0.93 (0.91-0.95) at 25s. LRA demonstrated the lowest value of 0.32 (0.17-0.43) at 5s, with a maximum of 0.85 (0.79-0.91) at 25s. A kappa value of 0.8 can be considered excellent correlation. Figure 4.4D shows kappa values at 1-second increments for LIA, LRA and FF. A value for 0.8 was reached by 12-seconds (IQR 6) for LIA compared to 19-seconds (IQR 7) for FF ($p<0.0005$) and 22-seconds (IQR 8) for LRA ($p<0.0005$).

The duration of mapping required to achieve a kappa value of 0.8 was compared between the left and right atria, in patients with paroxysmal and persistent AF, before and after pulmonary vein isolation and in patients on or off amiodarone. There was no difference for any parameter between the left and right atria. In patients with persistent AF, LIA stabilised earlier than in patients with paroxysmal AF (11±6 versus 15±4, difference 4-seconds, 95% confidence interval 0.6-5.6, $p=0.004$). There was no difference between any groups for stability of LRA. The frequency of focal firing stabilised after 17.2±5.6 seconds following pulmonary vein isolation compared to 19.1±3.7 seconds prior to pulmonary vein isolation, a difference of 1.9-seconds (95% CI 0.3-3.6, $p=0.023$). Full results for all comparisons are in figures 4.5 and 4.6 and tables 4.2-4.4.

Heatmaps for the subset of 15 patients are shown in figure 4.7. When measured as either a frequency, proportion of time the propagation pattern was present or a proportion of the atrial surface area that patterns occurred, variability in LIA fell rapidly, followed by FF and LRA. A significant degree of variability in LRA patterns was observed, particularly when measured as a proportion of the atrial surface affected up to durations of 20-25s.

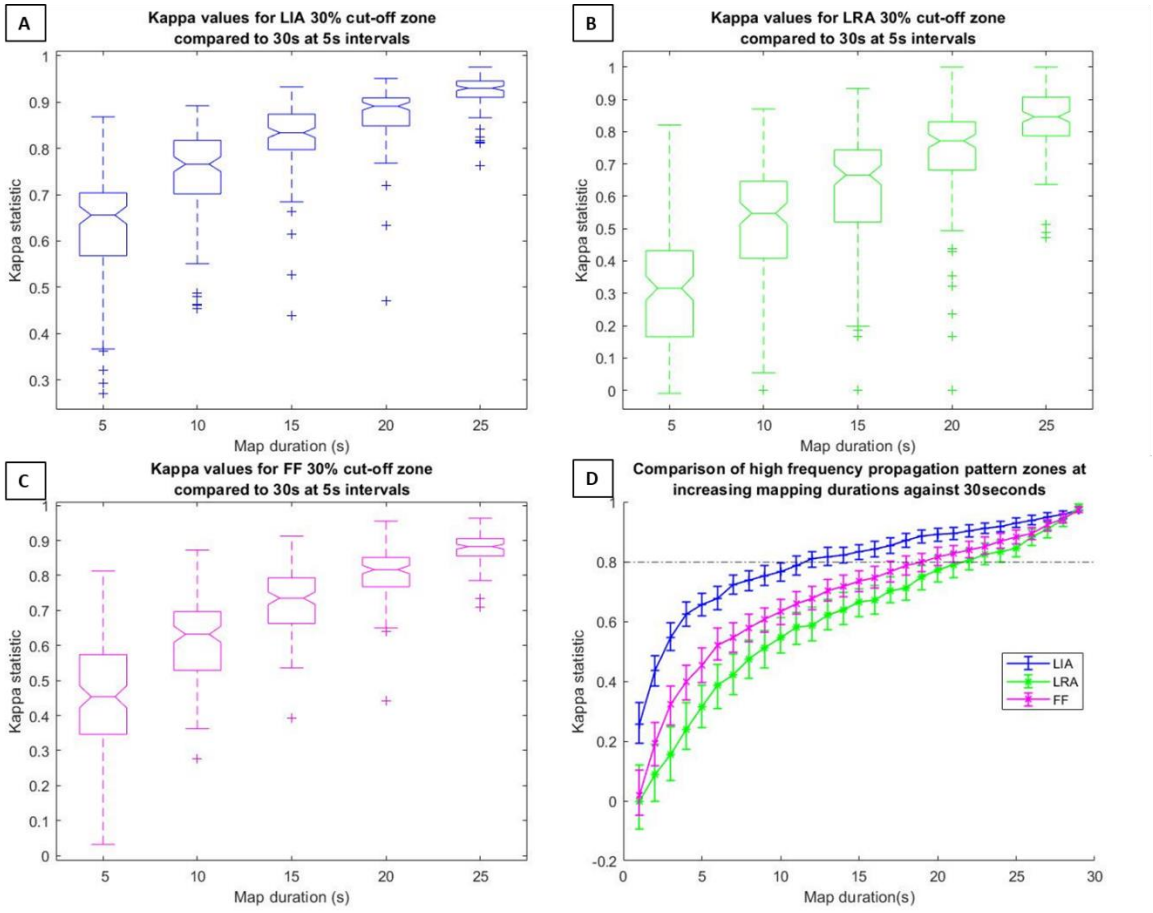

Figure 4.4 Kappa values for effect of time on identification of repetitive zones of LIA, LRA and FF. Boxplots (A-C) showing the distribution of kappa values in 5-second increments for regions with high frequency (at the 30% cut off) LIA, LRA and FF respectively compared to the result after 30-seconds. Kappa values for the LIA, LRA and FF are shown at 1-second increments in (D) showing the point at which the kappa value (representing a very good level of agreement) reaches 0.8. LIA: Localised irregular activation, LRA: Localised rotational activation, FF: Focal firing.

Table 4.2 Differences in time to reach a kappa value of 0.8 between zones of high frequency LIA compared to 30-seconds.

Group		Time to reach kappa 0.8	Difference (95% CI)	P value
AF classification	Paroxysmal	15(4)	4 (0.6-5.6)	0.004
	Persistent	11(6)		
Chamber	LA	12.4(4.3)	0.1 (-1.7 – 1.5)	0.898
	RA	12.5(4.8)		
Ablation stage	prePVI	13.0(4.9)	1.5 (-0.3-3.1)	0.099
	postPVI	11.5(3.5)		
Antiarrhythmics	On amiodarone	10(6)	3 (0.1-3.6)	0.007
	Off amiodarone	13(6)		

Table 4.3 Differences in time to reach a kappa value of 0.8 between zones of high frequency LRA compared to 30-seconds.

Group		Time to reach kappa 0.8	Difference (95% CI)	P value
AF classification	Paroxysmal	19.8 (5.4)	1.5 (-4.3 – 1.4)	0.314
	Persistent	21.3 (5.4)		
Chamber	LA	20.7 (4.9)	0.7 (-2.6 – 1.2)	0.491
	RA	21.3 (5.8)		
Ablation stage	prePVI	21.1 (4.6)	0.2 (-1.8 – 2.3)	0.822
	postPVI	20.9 (6.7)		
Antiarrhythmics	On amiodarone	21.1 (6.0)	0.0 (-2.0-2.0)	0.985
	Off amiodarone	21.1 (5.1)		

Table 4.4 Differences in time to reach a kappa value of 0.8 between zones of high frequency FF compared to 30-seconds.

Group		Time to reach kappa 0.8	Difference (95% CI)	P value
AF classification	Paroxysmal	19.9 (3.4)	1.6 (-0.8 – 3.4)	0.186
	Persistent	18.3 (4.7)		
Chamber	LA	18.6 (4.2)	0.2 (-1.4 – 1.9)	0.828
	RA	18.4 (4.9)		
Ablation stage	prePVI	19.1 (3.7)	1.9 (0.3 – 3.6)	0.023
	postPVI	17.2 (5.6)		
Antiarrhythmics	On amiodarone	18.6 (4.8)	0.2 (-1.5 – 1.9)	0.835
	Off amiodarone	18.4 (4.4)		

4.3.4 Voltage and Conduction Properties

The median distance between merged chamber surfaces was 6.0mm (IQR 3.4-10.7). The voltage in regions of high frequency LIA was 1.09mv (IQR 0.55-1.94) compared to 1.07mv (IQR 0.51-1.94) in the remainder of the chamber (p=0.9936).

A total of 53 paired maps at long and short cycle length were obtained for the LA and RA in a subset of 9 patients (in 1 participant only 2 sites were obtained due to AF induction). Having identified LIA as spatially stable, conduction properties during pacing were analysed within these regions. The MAT across all maps obtained in regions with high frequency LIA was 7.5ms (IQR 6.6-8.9) compared to 6.0ms (IQR 5.2-7.7) in the remainder of the chamber, a statistically significant difference of 1.5ms, p<0.0005. Extrastimulus pacing resulted in a significant increase in CHI in regions of high frequency LIA from 3.3 (IQR 2.3-4.4) to 4.0 (IQR 3.1-5.4) (p=0.0480), but no increase in the remainder of the chamber (p=0.4636) as shown in figure 4.8.

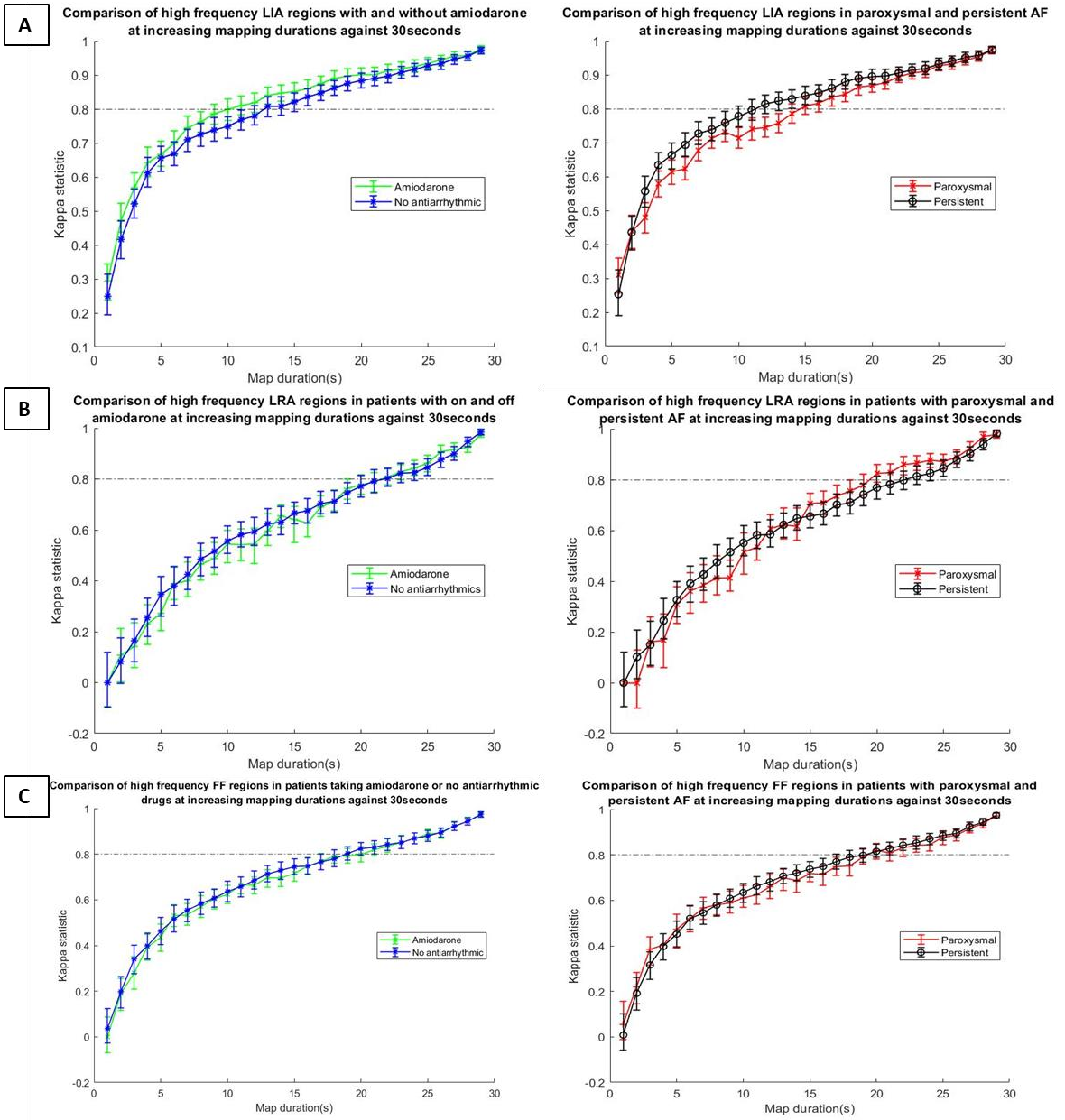

Figure 4.5 Comparison between patients on or off amiodarone and with paroxysmal or persistent AF on the agreement between zones with high frequency LIA, LRA and FF (A-C respectively) at incremental mapping durations against 30s.

4.4 Discussion

This study demonstrates that regions with LIA patterns show high spatiotemporal stability. In contrast rotational activation patterns, closest to the 'rotors' identified using other mapping techniques, show the least spatiotemporal stability. Regions of high frequency FF are relatively more stable whereas infrequent FF is not. Mapping durations of 20-25s are required to identify all temporally variable propagation patterns although shorter durations will identify the most stable LIA and FF. Although bipolar voltage amplitude in these regions is normal, they demonstrate an increase in conduction heterogeneity during short coupled extrastimulus pacing.

The aim of technologies designed to facilitate electrophysiological mapping and ablation of AF mechanisms is to identify repetitive patterns within a characteristically disorganised rhythm. The total duration analysed has a significant impact on how a repetitive pattern is defined and there have been limited efforts previously to determine the optimum duration required. Shi et al have previously described the distribution and frequency of charge density activation patterns within the LA but used short R-R interval segments within a 30s recording precluding a robust assessment of either spatial or temporal stability.(222) Studies often do not report the duration of AF mapped but may report that patterns identified are stable over several minutes and separate recordings.(125, 183, 184) Other studies have used recording durations of between 10 seconds and 5 minutes,(187, 220, 223) whilst an analysis of the mapping duration required to identify sites at which ablation terminated AF suggested a duration of between 4 and 30s was required.(224) However, the shorter duration suggested relied on a driver definition requiring only very transient occurrence (present for >0.4s within a 4s period) insufficient to result in discrimination between other regions of similarly low frequency when analysed prospectively, without the prior knowledge of the effect of ablation at that site. Of note a retrospective analysis where 5 minute initial recordings were used found that 89% of the mechanistic sites identified were also seen when 30s recording durations were analysed.(225) However, shorter durations than this were not assessed. It may be revealing that when only 10s recording durations have been chosen, in the study by Child et al using a technique of basket contact mapping and phase singularity analysis, spatially stable patterns were not identified.(187) Rotational activation patterns demonstrate the least stability between and during recordings, with 10s of mapping showing only very moderate correlation with the results obtained from 30s mapping (kappa 0.55) and a variability in rotational activation pattern frequency of approximately 20% at a duration of 10s. The fact that the region that appears to represent the highest frequency of LRA after 10s of analysis is significantly different from the region identified when longer durations are used highlights the transient and variable nature of these activation patterns. Of note, of course, is that durations beyond 30s were not assessed and it may be that accuracy improves yet further if longer analyses are performed.

Traditional electrophysiological assessment has involved mapping of either the endocardial or epicardial surfaces. There is increasing recognition that the remodelling involved in the development and progression of AF is a three-dimensional process resulting in activation time differences between atrial surfaces.(61, 62) In this context, epicardial propagation that results in local breakthrough conduction will manifest as a focal activation pattern on the endocardial surface. The sites of epicardial breakthrough

are likely to either be randomly distributed, if arising from chaotic 3-dimensional propagation, or recur at specific sites where the remodelling process promotes breakthrough to the endocardial surface. Sporadic focal activations and random breakthroughs are likely to display minimal consistency across recordings whilst high frequency activations or sites of recurrent breakthrough are likely to be consistent. This was supported by the finding of much greater correlation at high frequency sites (R^2 value 0.83, IQR 0.17) than when all activations are considered (R^2 0.64, IQR 0.19). However, distinguishing between a site of recurrent breakthrough and true focal activation is not possible using the mapping methods described here. There similarly appears to be earlier stabilisation of focal firing variability following pulmonary vein isolation. This suggests a greater degree of stability in non-pulmonary vein sites of focal activation.

The spatial consistency of LIA detection between separate recordings is illustrated in figure 4.3. Bipolar voltage amplitude in these regions is normal, which suggests that the activation properties observed are not the result of dense fibrosis. However, bipolar voltage amplitude is a relatively crude tool and is highly dependent on both rate and vector of activation(88). Wong et al performed electroanatomic mapping in a mixture of patients with paroxysmal and persistent atrial fibrillation during pacing from the coronary sinus and pulmonary veins.(88) Pulmonary vein pacing resulted in a significant change in bipolar amplitude compared to coronary sinus pacing (1.04 ± 0.43 mV vs. 1.47 ± 0.53 mV; $p = 0.01$) and shortening of cycle length brought about similar changes in amplitude, in keeping with previous studies by Williams et al.(226).

Studies using late gadolinium enhanced magnetic resonance imaging reveal patchy areas of fibrosis out of keeping with the burden seen on voltage mapping studies(84, 97) suggesting the existence of interstitial fibrosis that is not revealed by measuring bipolar voltage amplitude. The MAT during pacing within LIA zones was longer, suggestive of slower conduction velocity, and short coupled extrastimulus pacing resulted in an increase in CHI in these regions that was not observed in the remainder of the chamber. Although these sites may represent anatomically normal regions of changing fibre orientation resulting in anisotropic conduction, they may represent disrupted conduction caused by underlying atrial interstitial fibrosis resulting in fibre disarray and rate dependent conduction abnormalities that manifest as local irregular activation patterns during AF. In the same study by Wong et al highlighted above, a shortening of pacing cycle length was also associated with a global reduction in conduction velocity (30.4 ± 13.0 cm/s vs. 38.6 ± 14.0 cm/s; $p < 0.001$).(88) This slowing was most pronounced in regions that also demonstrated a reduction in bipolar amplitude and was most frequently seen in the region of the posterior left lower pulmonary vein

antrum, posterior wall and inferior wall. This highlights that abnormal conduction properties are closely linked to activation rate and may in part explain results of previous studies that showed reduction in CV only in low voltage zones during sinus rhythm.(108) Of note, these findings were most evident in patients with either long lasting paroxysmal AF and earlier persistent AF in whom high rate pacing provided the electrophysiological stress needed to reveal their presence. Patients with earlier or more advanced disease may either not yet exhibit significant remodelling, or this process is advanced to the extent that the abnormalities are severe enough to be detected without the need for 'conduction stressing'.

In a study by Walters et al. using surgically placed epicardial plaques in patients with longstanding persistent AF, disorganised activation was frequently observed, which did not satisfy criteria for either rotors or focal activations but was stable over multiple recordings of 10s duration taken over a period of 10 minutes(227). This disorganised activation may represent similar propagation patterns to the irregular activation observed using charge density mapping, which was similarly stable even at short mapping durations. Walters also reported that rotors were frequently transient, in keeping with the results outlined here.

Both the non-hierarchical multiple-wavelet hypothesis and the competing "mother-rotor", or focal driver, hypothesis describe a process of wave-break in the formation of fibrillatory wavefronts involved in maintenance of cardiac fibrillation.(52, 67) Tissue homogeneity is thought to play a significant role in the susceptibility to fibrillation(228) with regions of structural inhomogeneity likely responsible for the wave-break that results in fibrillatory conduction.(229) The anatomical regions demonstrating stable LIA patterns identified in this study may therefore reflect sites of structural heterogeneity responsible for wave-break, and therefore play an important role in AF maintenance.

Importantly, this study was not designed to assess ablation strategy or effectiveness and is not able to determine the impact of the phenomena identified on AF maintenance. This requires further detailed work. However, an understanding of the transient properties of rotational activity and low frequency focal activations observed in short mapping segments is crucial to designing ablation strategies that can be tested in clinical trials and suggests they are unlikely to occur as a result of anatomical substrate, such as scar or myofibre architecture. Targeting a fixed therapy to transient, migratory activation patterns is likely to be ineffective. The effect of atrial size on differences in activation patterns detected was also not assessed and would be of limited value given a relatively small sample size. Although there is some variation in correlation between

contact unipolar electrograms and inverse derived electrograms, the distance of the atrial endocardium from the recording electrodes of the AcQMap catheter significantly influences this and may therefore have some impact on the activation patterns detected.(201) However, a significant reduction in correlation occurs at distances greater than 40mm. The median LA diameter of patients in our study was 43mm resulting in significantly lower radial distances from the AcQMap catheter and therefore greater accuracy in reconstructed inverse electrograms.

It must be acknowledged that the method of conduction heterogeneity quantification used provides an assessment of conduction over a broad area without accurate assessment of highly localised conduction properties. Local conduction velocity measurements considering both speed and direction were not assessed although an effect of directionality was incorporated by using including measurement from multiple pacing sites. Specific validation of conduction velocity measurement using AcQMap non-contact mapping has not been performed and would be susceptible to small errors in localisation introduced into the impedance field or resulting from minor defects in the ultrasound generated anatomy (either resulting from manual errors in post processing or erroneous ultrasound deflections from local structures such as other catheter within the chamber) hence use of activation time annotation alone was used for this analysis.

4.4.1 Conclusion

Charge density mapping facilitates identification of complex patterns of wavefront propagation during atrial fibrillation. Although irregular activation patterns characterised by changing wavefront direction, and high frequency focal firing are spatially stable, rotational activations, closest to the ‘rotors’ identified using other mapping techniques, are transient and meandering, with low spatial stability. A minimum duration of 20s is required to identify. These stable regions of irregular activation may best reflect underlying atrial structural abnormalities and represent important sites for catheter ablation approaches. The duration of mapping recording used significantly impacts the results obtained. Mapping durations of 20-25s are required to identify regions of repetitive but transient rotational activation whilst shorter segments will accurately reveal regions with high frequency irregular and focal activation.

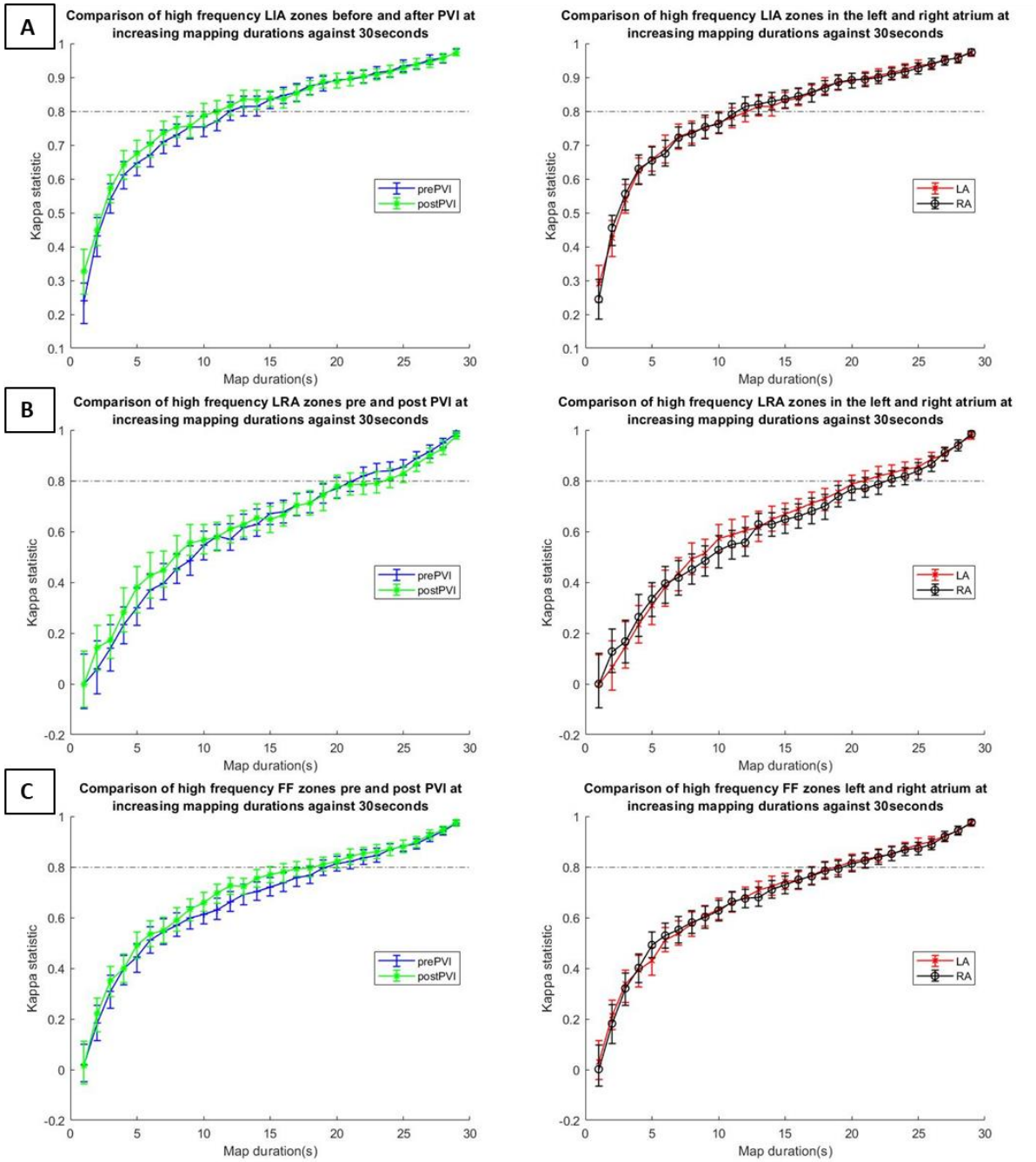

Figure 4.6 Comparison between patients before and after pulmonary vein isolation and in the left compared to the right atrium on the agreement between zones with high frequency LIA, LRA and FF (A-C respectively) at incremental mapping durations against 30s.

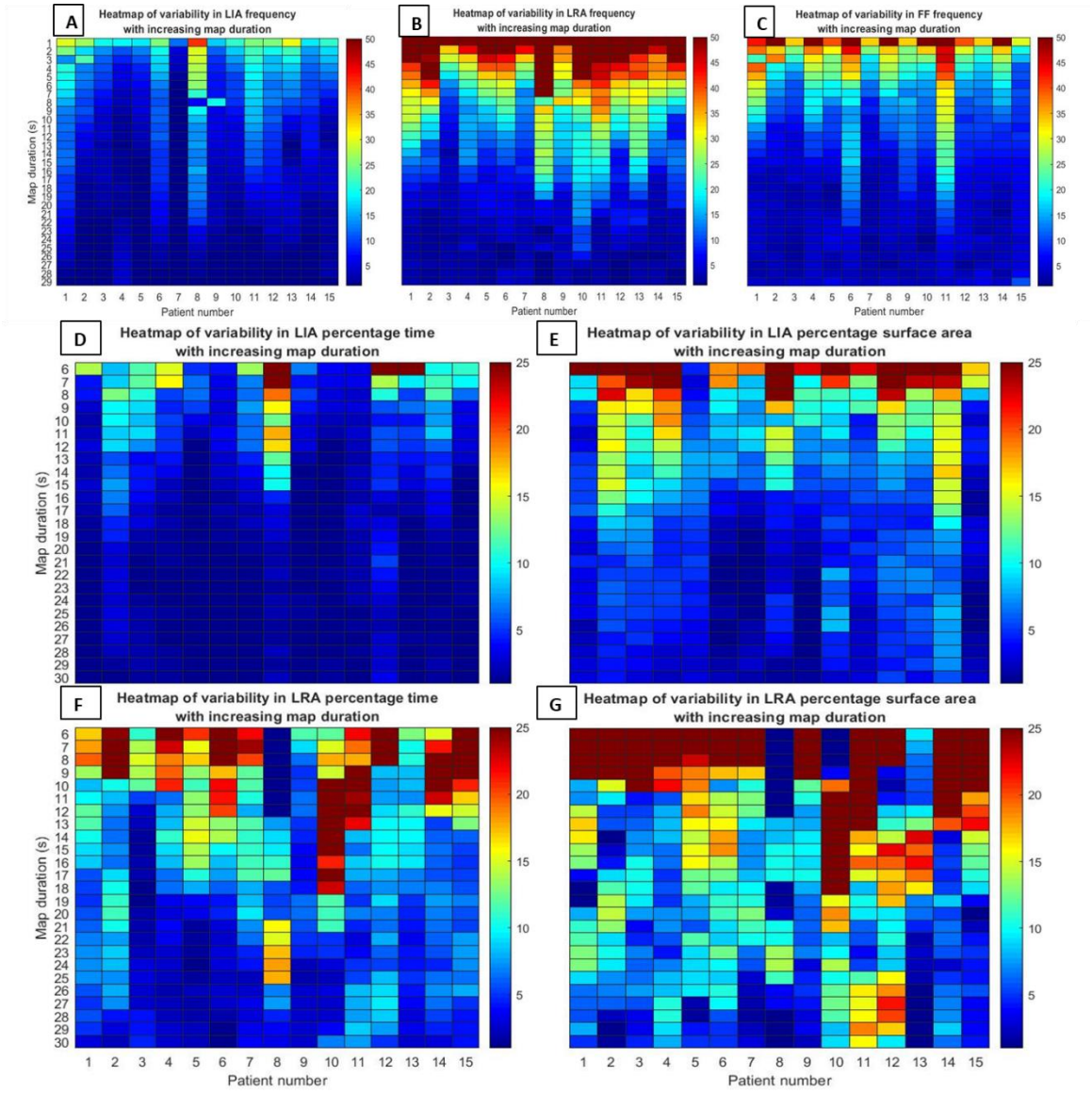

Figure 4.7 Heatmaps showing the variability in frequency of LIA, LRA and FF (A-C) in a subset of 15 patients studied with colours representing the percentage change in each pattern at incremental recording duration. The variability of patterns within the highest frequency regions identified using the 30% cut off are shown as a percentage time and a proportion (%) the atrial surface area over which it occurs for both LIA (D-E) and LRA (F-G).

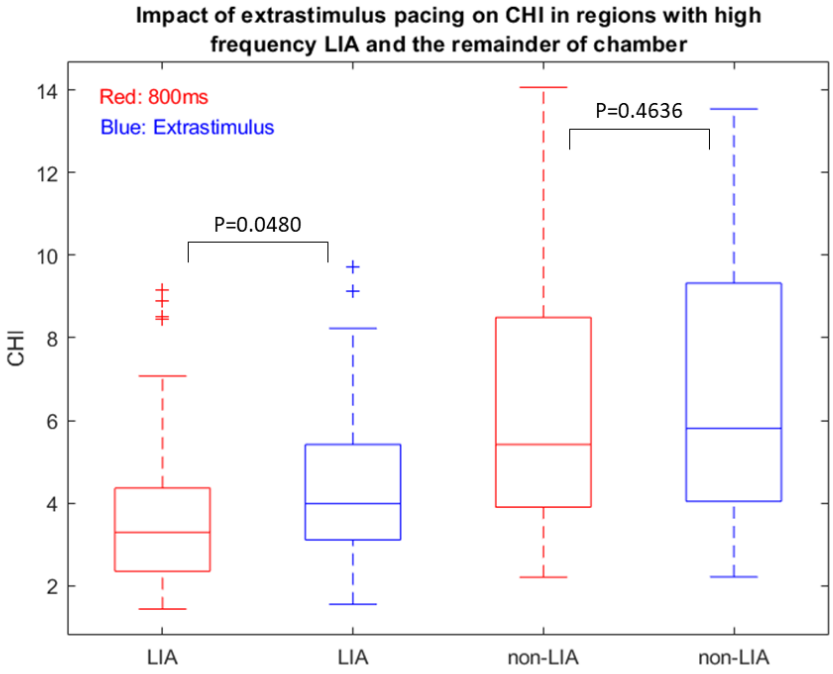

Figure 4.8 Boxplot of the effect of pacing cycle length on conduction heterogeneity (CHI) in regions with high frequency LIA and the remainder of the chamber.

5 Insights into Bi-Atrial Mechanisms during Atrial Fibrillation

5.1 Introduction

Early evidence of pulmonary vein triggers initiating AF has resulted in a very left atrium-focused approach with efforts to improve results of catheter ablation. Little work has been done to characterise the role of the right atrium in AF maintenance.

The few recent studies that exist describing the biatrial electrophysiological substrate during atrial fibrillation have focussed around quantification of “driver” sites using either multipolar basket catheters, body-surface potential mapping, or a combination of the two.(124, 126, 187, 230) These methods have relied on phase mapping and singularity detection, which depends heavily on the mapping tools used and the signal processing methods applied.(178, 180) This is in large part due to the difficulties in mapping the complex rhythm of atrial fibrillation in terms of both providing whole chamber simultaneous visualisation and accurate processing of fibrillatory electrograms. The AcQMap system employs non-contact mapping to provide a solution to the former of these two problems, whilst use of the Laplacian, specific regularisation techniques and the shift to revealing local dipolar charge sources attempt to overcome the latter.(195)

Identification of apparent drivers using sequential left and right atrial mapping does not provide data on the interaction between chambers during AF propagation. Anatomical work has explored the conduction pathways responsible for inter-atrial propagation however, their functional contribution during AF is less clear and the role of dynamic processes propagating between chambers in sustaining AF has not been examined in vivo.

Earlier sections have shown regions of LIA to be spatially stable possibly reflecting underlying atrial structural properties, whilst LRA is often transient and provoked by adenosine, suggestive of a relation to tissue refractoriness. Anatomical work has explored the conduction pathways responsible for inter-atrial propagation. However, their functional contribution during AF is less clear and the role of dynamic processes affecting and propagating between chambers in sustaining AF has not been examined. In this section, a detailed characterisation of biatrial propagation patterns is carried out systematically exploring the dynamic role of complex activation patterns in AF maintenance and the respective roles of the LA and RA.

5.2 Methods

5.2.1 Patient selection

Patients included were enrolled in the prospective study BiMap-AF (REC reference 18/SC/0409) and undergoing first time ablation for paroxysmal (n=5) or persistent (n=16) atrial fibrillation. Exclusion criteria included prior cardiac surgery, congenital cardiac abnormalities, and severe valvular heart disease.

5.2.2 Mapping procedure and data analysis

A detailed description of the electrophysiological mapping procedure is outlined in section 4 above. In brief, venous access was obtained via bilateral femoral vein puncture and heparin boluses followed by continuous infusion were used to maintain an ACT >350s. A decapolar catheter (Inquiry, Abbott Medical) was inserted into the coronary sinus through an AcQRef (Acutus Medical) sheath which includes a distal electrode used as a unipolar reference. The first AcQMap catheter was advanced over a 0.032 guide wire into the RA via an AcQGuide (Acutus Medical) sheath and ultrasound used to reconstruct the right atrial chamber anatomy based around a triangular mesh structure where each vertex (corner) of the constituent triangular faces form a unique point for calculation of charge density using the inverse solution as previously described.(196) The ablation catheter (Tacticath, Abbott Medical) was advanced via an Agilis sheath into the left atrium across the single transseptal puncture site. The second AcQGuide sheath was then advanced into the LA (see figure 5.1). The LA anatomy was then generated with ultrasound. A circular mapping catheter (Inquiry Optima or Advisor Variable Loop, Abbott Medical) was used to perform bipolar voltage mapping of the LA and RA during sinus rhythm and this data processed as outlined in section 4 above.

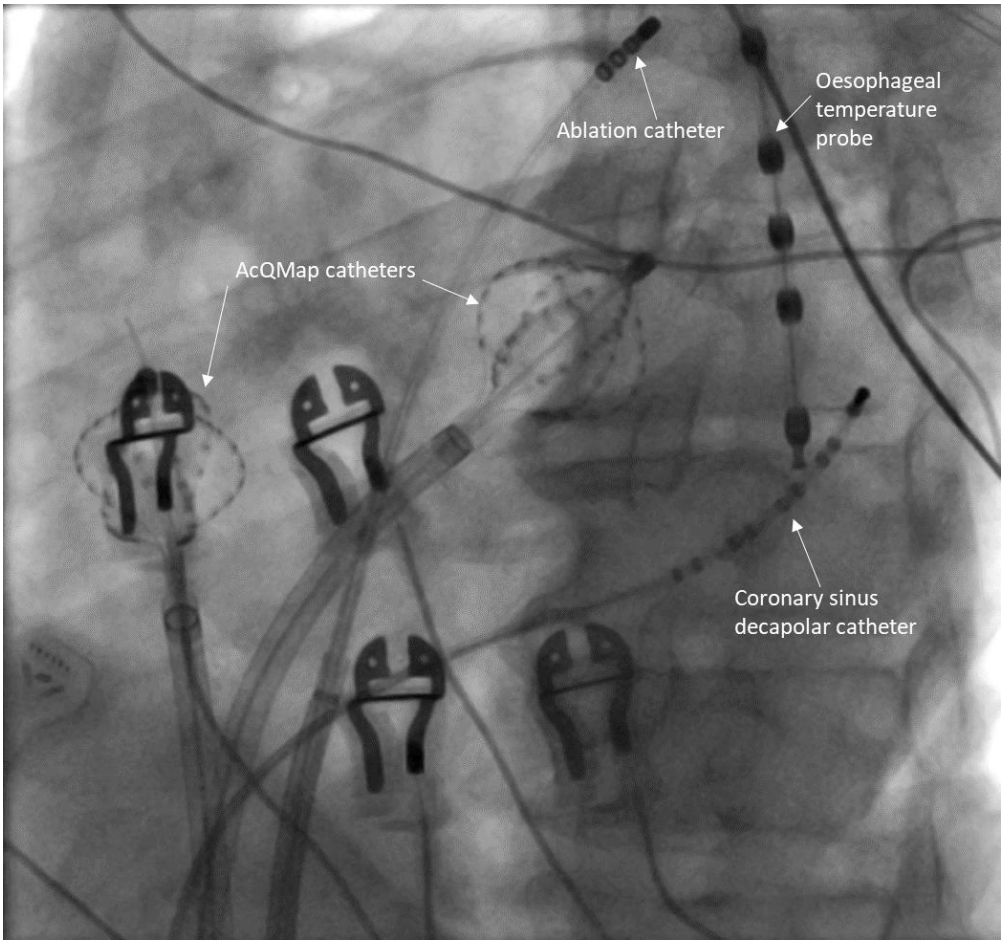

Figure 5.1 Fluoroscopic image of simultaneous biatrial mapping using 2 linked AcQMap systems.

Initial mapping was performed prior to any catheter ablation. In patients attending the procedure in sinus rhythm, AF was induced using burst atrial pacing. Once AF was established, recordings of 2 minutes duration were generated and time alignment between LA and RA systems was facilitated using a below threshold pacing stimulus from the coronary sinus catheter of 4 beats at 1000, 800 and 600ms intervals and 12 second rest period. Pulmonary vein isolation was performed using contact force guided radiofrequency ablation using 40-50 Watts (TactiCath ablation catheter, Abbott Medical). Simultaneous biatrial AF mapping was repeated following completion of PVI and following further non-PV ablation when delivered. PV encirclement was extended to incorporate regions of interest in close proximity to the PV antra and additional ablation and AF mapping was undertaken, targeting regions of maximal LRA, FF or LIA stability across repeated map segments, over a minimum of 2 mapping epochs. Regions of high frequency focal activation were preferentially targeted followed by regions with spatiotemporally consistent LIA and LRA. Where focal activation was targeted distant to other ablation lesions, then limited focal ablation was delivered, whilst larger areas were targeted with wider ablation

to the core of regions of interest and extension to connect to regions of conduction block (either PV encirclement or anatomical boundaries) as previously described.(231)

5.2.3 Propagation Map Calculation and Data Export

Raw AcQMap electrode biopotential signals were visually inspected to identify outlying or corrupted signals, which were then manually excluded. A low pass filter at 100Hz as well as a 50Hz notch filter and smoothing algorithm were applied followed by selection of a QRS-T wave template for subtraction. Three consecutive 10-second mapping segments were created for simultaneous timepoints in both the left and right atria, confirmed relative to the coronary sinus low amplitude pacing spike. This process was repeated to create two 30-second AF maps following splicing together of each 10s segment. Propagation maps were calculated using the default timing method (based on -dv/dt of dipole signals), window width (for isochronal colour bars) of 80ms and time threshold of 70ms (representing presumed minimum refractoriness). AcQTrack propagation patterns were calculated for each segment and data exported for offline analysis.

5.2.4 Propagation Pattern and Substrate Quantification

As previously described above, AcQTrack data for identification of patterns of FF, LIA and LRA were exported and analysed using a custom designed programme to allow quantification of both the number of occurrences of each pattern and, for LIA and LRA, the proportion of time they are present. In addition, atrial fibrillation cycle length (AFCL) was measured for signals at each vertex of the anatomy as described in section 3 and averaged over 30s.

5.2.5 Interatrial communication

Anatomical and electrical connection between left and right atria is complex and extensive. How LA and RA influence each other during AF is unclear. Several questions can be posed: (1) Is there a single channel of communication through which electrical activity in one chamber affects the other, or does whole LA-RA contact area take part in interaction? (2) If such channel exists, is it anatomically stable or does it vary between patients? (3) Is there a consistent direction of wave propagation through such channel or does it vary in time?

To answer these questions, the parameter of Mean Phase Coherence (MPC) was used. MPC has previously been used to analyse electroencephalograms in patients undergoing neurosurgery for epilepsy where high values correlated to sites of epileptogenic foci, and has since been applied to the assessment of spatial alignment of electrodes during simultaneous endocardial and epicardial contact mapping of AF.(232)

MPC quantifies the degree of coherence between sequences of activations in two signals with a value ranging between 0 and 1. A value of 1 denotes a scenario in which there is perfect synchronisation between activation times in both signals, whilst a value of 0 denotes a complete absence of coherence/coordination. We assumed that if a communication channel exists, MPC between a point within the channel and the other chamber should be higher (than if a point outside the channel was selected). Therefore, data points within the channel should be in the greatest coherence/coordination with the opposite chamber.

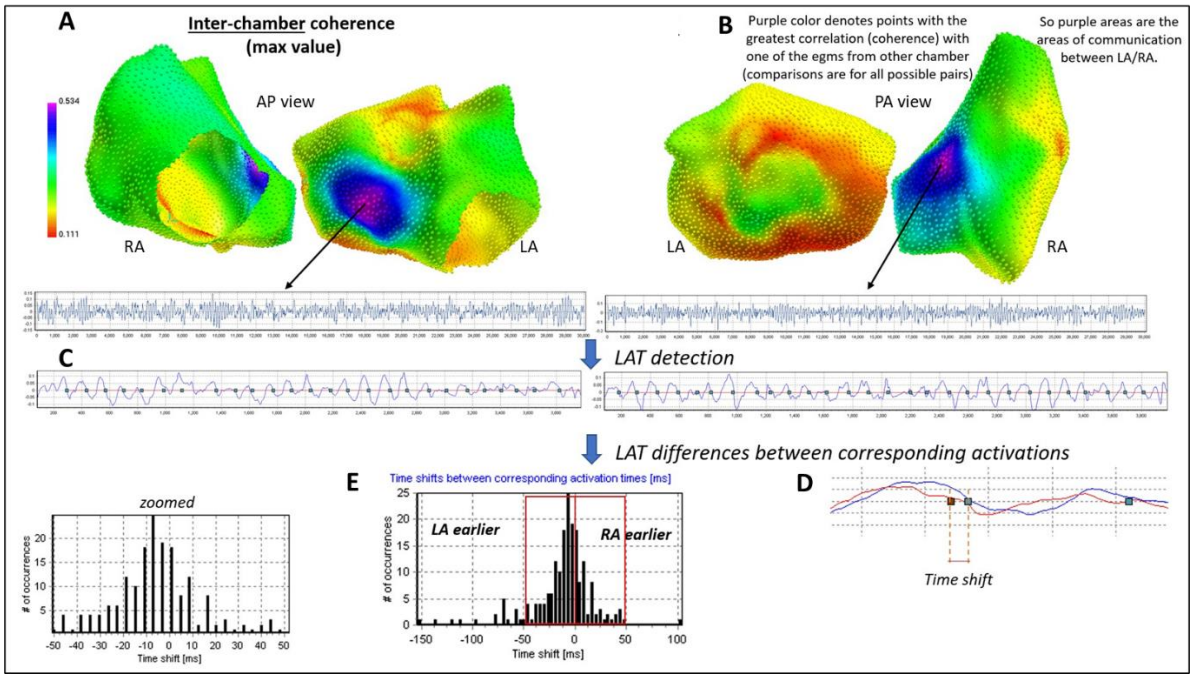

Figure 5.2 Method to characterise inter-atrial propagation. Mean phase coherence (MPC) is calculated for each point on the anatomy and every point on the surface of the opposite chamber. The maximum MPC value is assigned to this local point on the left atrium (A) and right atrium (B). Local activation times (LAT) are assigned via phase analysis (C) and the time shift between local activations at the point of highest MPC calculated (D). A histogram of time shifts between chambers is plotted (E) with a normal distribution suggesting a consistent relationship between chambers. (AP, antero-posterior; LA, left atrium; PA, postero-anterior; RA, right atrium)

A custom designed programme was created in which virtual electrograms from every vertex of the reconstructed left and right atrial (LA, RA) anatomies were exported and phase calculated for the 30s recordings. For each vertex, coherence between activations at this point and every other point on the opposing chamber was calculated using MPC. The maximum of all MPC values was assigned to this local point to estimate the degree of coherence between activity at a given point and the opposing chamber. The region with highest MPC value represents the dominant channel of communication.

In order to determine which chamber is leading, activation times at the centres (points with the highest MPC value) within the channels of both chambers were

investigated. For each local activation, the time difference between the LA and RA was determined to identify the direction of propagation (see figure 5.2). In the case of no communication between atria, a histogram of time differences is expected to be uniform (any time difference is equally probable). When communication is present, normal distribution is expected (there is a dominant time difference between activations at the channels of both atria). If seen to be preceding the opposite chamber for ≥60% of the recording, then the chamber was deemed to be leading.

5.2.6 Analyses performed and statistical methods

Patients were grouped according to paroxysmal or persistent phenotype and rhythm at the start of the procedure therefore differentiating induced versus baseline AF. Analysis was performed on all maps obtained prior to ablation. Substrate was quantified using the combined variables of AFCL, FF frequency, LRA time and LIA time either with no cut-off or the 30% cut-off. Additional analysis used the frequency of LRA and LIA in place of their duration. Maps and patients in which a leading chamber could be identified were documented and changes in inter-atrial propagation were identified following delivery of ablation.

Statistical analysis was performed using SPSS (version 27, IBM corporation) and R statistical software (version 4.0.3) with figures produced in Matlab (Mathworks, R2019a). Two-way MANOVA testing was used to explore the effect of clinical AF phenotype (paroxysmal and persistent) and chamber mapped on electrophysiological substrate measured by combined variables as explained above. Further two-way MANOVA testing was used to explore the effect of baseline rhythm and chamber mapped on the same combined dependent variables. In each analysis scatterplots were used to test for linearity between dependent variables and multicollinearity excluded using Pearson correlation coefficient providing $r<0.9$ and >0.1. Univariate outliers were identified through inspection of a boxplot and multivariate outliers assessed using Mahalanobis distance ($p>0.001$). Dependent variables were assessed for normality of distribution using the Shapiro-Wilk test and Bonferonni correction for the number of variables included ($p>0.0125$). Homogeneity of covariances matrices was assessed using Box's M test and homogeneity of variances assessed using Levene's Test of Homogeneity of Variances. A p-value of <0.05 was considered significant. Figures are expressed as mean±standard error unless otherwise stated.

Binomial logistic regression was used to identify predictors of acute procedural outcome. Univariate analysis was performed for all the combined variables included in exploratory MANOVA testing and with and without a cut-off applied. Analysis was carried

out considering each chamber independently and together, as well as including only patients with persistent AF. Multivariate analysis was performed using AFCL, FF frequency, LIA time and LRA time with separate models for results with no cut-off and using the 30% cut-off. The log odds, p-value and Akaike Information Criterion (AIC) were calculated for each variable included in the univariate analysis. For each multivariate model, the AIC value as well as AUC-ROC (area under the curve – receiver operating characteristics curve) for the model, and the log odds and p-value for each independent variable were calculated to indicate the predictive accuracy of the model and the contribution of each variable.

Following identification of predictors of acute procedural outcome, two-way ANOVA testing was carried out to explore the interaction effect of chamber and ablation outcome on those variables identified as significant univariate predictors.

5.3 Results

5.3.1 Baseline Characteristics

A total of 22 patients were enrolled in the study including 5 patients with paroxysmal and 17 patients with persistent AF. One patient with persistent AF had been taking amiodarone and only organised atrial tachycardia could be induced on the day of the procedure, and they were excluded from all analysis. Of the remaining 21 patients, characteristics are shown in table 4.1 above.

5.3.2 Ablation delivered and acute outcome

Additional non-PV ablation was delivered in 14 of the 21 patients included with an average of 1.8±1 regions of interest ablated. In 6 patients, ablation was performed in the RA. Acute AF termination following ablation was achieved in 10/21 (48%) of patients, including 5/16 (31%) of those with persistent AF.

5.3.3 Paroxysmal vs persistent AF

A two-way MANOVA assessed the effect of clinical AF phenotype and chamber mapped on electrophysiological substrate. There was no significant interaction effect on the combined dependent variables but there was a significant main effect of AF phenotype whether activation pattern frequency or proportion of time present were measured and irrespective of cut-off applied ($p<0.0005$). Follow up univariate two-way ANOVA testing for the main effect of AF phenotype revealed a significant effect for LRA ($p<0.0005$ for both LRA frequency and time) and FF frequency ($p<0.0005$) but no effect for AFCL ($p=0.318$) or LIA ($p=0.769$). Patients with paroxysmal AF had less rotational activation compared to patients with persistent AF whether measured as occurrence frequency (39±18 vs. 72±4,

difference of 33, 95% confidence interval 16-50, p<0.0005) or percentage of time present (14±3 vs 24±1, difference 10, 95% CI 5-16, p<0.0005). These findings remained when the 30% cut off was applied (23±4 vs. 42±2 occurrences, difference 19, 95% CI 9-29, p<0.0005; and 8±2% vs 16±1% for the proportion of time present, difference 8%, 95% CI 4-11, p<0.0005). At the 30% cut off patients with persistent AF had more sites of LRA (1.9±0.1 vs 1.0±0.2, difference 0.9, 95% CI 0.5 – 1.4, p<0.0005). Patients with paroxysmal AF had a higher number of focal firings both when all occurrences were included (222±14 vs 144±7, difference 78, 95% CI 46 – 109 p<0.0005) and when only high frequency sites (at 30% cut-off) were included (140±9 vs 90±5, difference 50, 95% CI 29-70, p<0.0005). There were more high frequency focal firing sites in patients with persistent AF (4.7±0.2 vs 3.6±0.6); but this difference was not statistically significant (difference 1.1, 95% CI -0.02 - 2.11, p=0.055). See tables 5.1-5.3 for full results.

5.3.4 Rhythm at the start of the procedure

There was a statistically significant interaction effect between chamber and baseline rhythm on the combined dependent variables (p=0.007). Univariate analysis showed a significant interaction effect on LRA time (p=0.018) but not for AFCL (p=0.114), FF frequency (p=0.512) or LIA time (p=0.557).

In the RA of patients in AF at the start of the procedure rotational activation was present for 31±2% of time compared to 12±2% in patients presenting in SR, an absolute difference of 19% (95% CI 13-24, p<0.0005). A smaller difference was observed in the LA (27±2% vs 17±2%, absolute difference of 10%, 95% CI 4-15, p=0.0001, figure 5.3A). In the RA, patients in AF at the start of the procedure had significantly fewer focal activations compared to those in SR (122±14 vs 176±14, 95% CI 14-94, p=0.008), but there was no significant difference in the LA (155±14 vs 190±14, 95% CI -4 – 75, p=0.079, figure 5.3B). These differences remained when only high frequency occurrences using the 30% cut off were included. See tables 5.4-5.6 for full results.

Patients in whom AF was induced had a significantly longer mean AFCL (201±2 vs 181±2, difference 20, 95% CI 13-27, p<0.0005). There was no significant difference in the patterns of LIA based on either chamber or baseline rhythm.

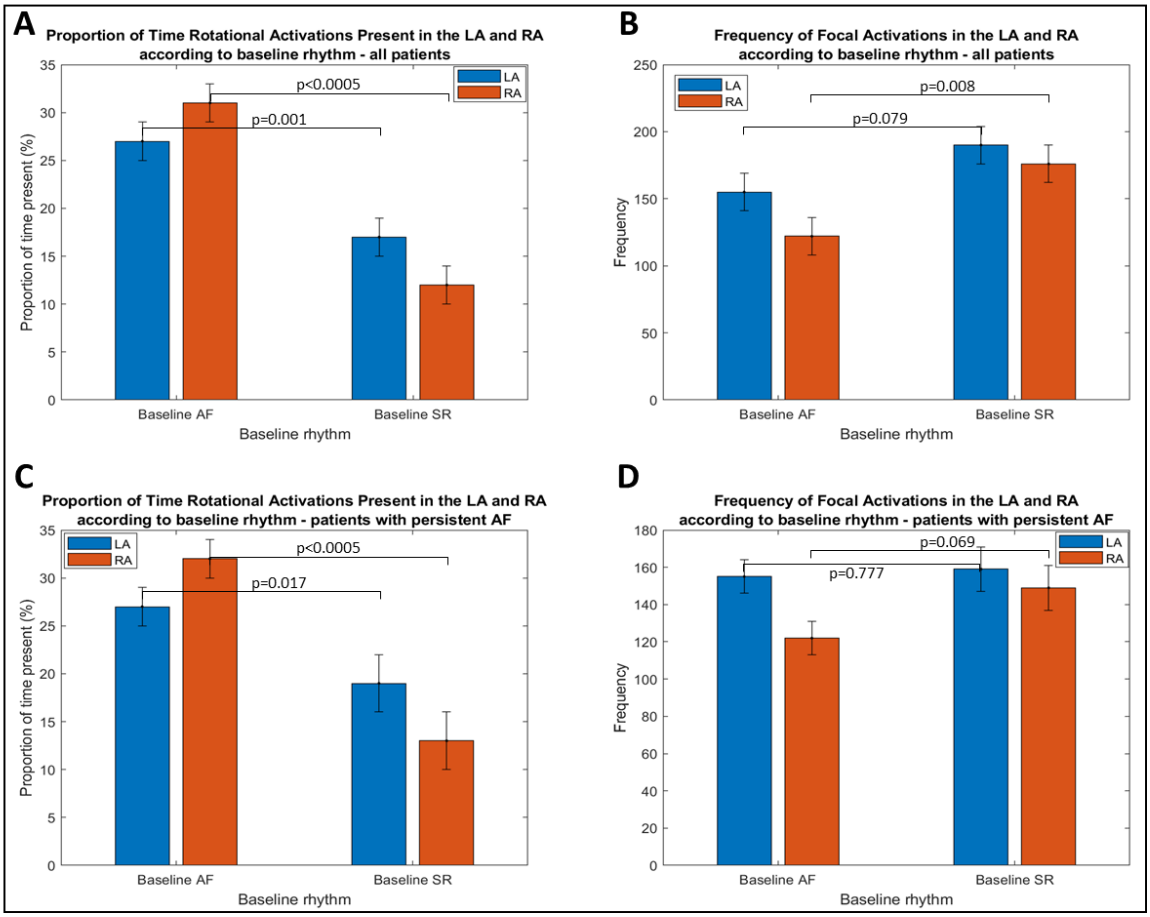

Figure 5.3 Interaction between chamber mapped and baseline rhythm on the duration of LRA and the frequency of focal firing across all patients (A-B) and only in patients with persistent AF. LA, left atrium; LRA, localised rotational activation; RA, right atrium. Bars represent standard error

Table 5.1 Effect of AF type and chamber on electrophysiological substrate. p-values for the results of interaction and main effects of AF type and chamber on the combined dependent variables expressed as both frequency and time using no cut-off and a cut-off at 30%.

Variable	Cut off	Interaction	AF type	Chamber
Time present	0	0.65	<0.0005	0.202
	30	0.485	<0.0005	0.072
Frequency	0	0.967	<0.0005	0.084
	30	0.863	<0.0005	0.061

Table 5.2 Difference in AFCL and propagation patterns in patients with paroxysmal and persistent AF. Figures expressed as mean±standard error.

Variable	Cut off	Paroxysmal AF	Persistent AF	Difference (95% CI)	p value
AFCL	N/A	195±4	190±2	5 (-5 – 15)	0.318
LRA frequency	0	39±8	72±4	33 (16 – 50)	<0.0005
	30	23±4	42±2	19 (9 – 29)	<0.0005
LRA time	0	14±3	24±1	10 (5 – 16)	<0.0005
	30	8±2	16±1	8 (4 – 11)	<0.0005
LIA frequency	0	399±29	423±15	24 (-41 – 89)	0.466
	30	204±10	210±5	6 (-17 – 29)	0.599
LIA time	0	58±3	59±2	1 (-9 – 6)	0.769
	30	40±2	40±1	0 (-6 – 5)	0.869
FF frequency	0	222±14	144±7	78 (46 – 109)	<0.0005
	30	140±9	90±5	50 (29 – 70)	<0.0005

Table 5.3 Difference in LRA and FF patterns in the LA and RA of patients with paroxysmal and persistent AF. Figures expressed as mean±standard error.

Variable	Cut off	Chamber	Paroxysmal AF	Persistent AF	Difference (95% CI)	p value
LRA frequency	0	LA	42±11	75±6	33 (8 – 56)	0.009
		RA	36±11	70±6	34 (10 – 58)	0.006
	30	LA	26±6	43±3	17 (3 – 31)	0.020
		RA	21±6	41±3	20 (6 – 35)	0.005
LRA time	0	LA	15±4	24±2	9 (1 – 17)	0.022
		RA	12±4	24±2	12 (4 – 20)	0.004
	30	LA	9±2	16±1	7 (1 – 11)	0.027
		RA	7±2	16±1	9 (3 – 14)	0.003
FF frequency	0	LA	232±20	156±11	76 (13 – 120)	0.001
		RA	211±20	132±11	79 (35 – 124)	0.001
	30	LA	150±13	98±7	52 (24 – 80)	<0.0005
		RA	130±13	83±7	47 (19 – 75)	0.001

Table 5.4 Influence of baseline rhythm and chamber mapped on electrophysiological substrate. p-values for the results of interaction and main effects of baseline rhythm and chamber on the combined dependent variables expressed as both frequency and time using no cut-off and a cut-off at 30%.

Variable	Cut off	Interaction	Baseline rhythm	Chamber
Time present	0	0.007	<0.0005	0.023
	30	0.006	<0.0005	0.010
Frequency	0	0.014	<0.0005	0.004
	30	0.081	<0.0005	0.037

Table 5.5 Difference in AFCL and propagation patterns according to baseline rhythm. Figures expressed as mean±standard error.

Variable	Cut off	Baseline AF	Baseline SR	Difference (95% CI)	p value
AFCL	N/A	181±2	201±2	20 (13 – 27)	<0.0005
LRA frequency	0	86±4	45±4	-41 (-54 – 30)	<0.0005
	30	50±3	27±3	-23 (-30 - -16)	<0.0005
LRA time	0	29±1	15±1	-14 (-18 – -11)	<0.0005
	30	19±1	9±1	-10 (-12 - -7)	<0.0005
LIA frequency	0	438±19	397±19	-41 (-94 – 12)	0.131
	30	218±7	201±7	-17 (-35 – 3)	0.090
LIA time	0	60±2	58±2	-2 (-9 – 4)	0.421
	30	41±2	39±2	-2 (-6 – 3)	0.468
FF frequency	0	138±10	183±10	45 (17 – 73)	<0.0005
	30	86±6	115±6	29 (11 – 47)	0.002

Table 5.6 Difference in AFCL LRA and FF patterns in the LA and RA according to baseline rhythm. Figures expressed as mean±standard error.

Variable	Cut off	Chamber	Baseline AF	Baseline SR	Difference (95% CI)	p value
AFCL	N/A	LA	183±4	198±3	15 (5 – 24)	0.004
		RA	178±4	204±3	26 (16 – 36)	<0.0005
LRA frequency	0	LA	84±6	52±6	-32 (-48 - -15)	<0.0005
		RA	89±6	38±6	-51 (-69 - -35)	<0.0005
	30	LA	47±4	31±4	-16 (-27 - -6)	0.002
		RA	52±4	22±4	-30 (-40 - -19)	<0.0005
LRA time	0	LA	27±2	17±2	-10 (-15 - -4)	0.001
		RA	31±2	12±2	-19 (-24 - -13)	<0.0005
	30	LA	18±1	11±1	-7 (-10 - -2)	0.001
		RA	21±1	8±1	-13 (-17 - -9)	<0.0005
FF frequency	0	LA	155±14	190±14	35 (-4 – 75)	0.079
		RA	122±14	176±14	54 (14 – 94)	0.008
	30	LA	96±9	122±9	26 (1 – 51)	0.045
		RA	77±9	108±9	31 (6 – 57)	0.016

5.3.5 Patients with persistent AF

There was a statistically significant interaction effect of baseline rhythm and chamber on the combined dependent variables (p=0.033). In univariate testing, this interaction was significant for LRA time (p=0.019) but not AFCL (p=0.060), LIA time (p=0.272) or FF frequency (p=0.272). In the RA, LRA was present for 32±2% of the map in patients in AF at baseline compared to 13±3% in those where AF was induced (difference 19, 95% CI 12 – 25, p<0.0005). A significantly smaller difference was observed

in the LA (27±2 vs 19±3, difference 8, 95% CI 1-14, p=0.017). See figure 5.3C-D and tables 5.7-5.9.

5.3.6 Acute procedural outcome

Univariate predictors of acute AF termination with ablation included longer AFCL and a higher frequency of focal activations, whilst more LRA, both in frequency and measured as a proportion of time present, was predictive of the need for DCCV. When each chamber was analysed independently, only RA measures were predictive of acute outcome. See table 5.10 for full results. In multivariate analysis with AFCL, LIA time, LRA time and FF frequency with no cut off applied, the overall model accurately predicted acute outcome in 82.9% of cases with AUC-ROC of 0.86 and AIC of 87.8 with a residual deviance of 77.8 on 77 degrees of freedom given the null deviance of 113.2 on 81 degrees of freedom. In this multivariate model, longer AFCL (log-odds 0.0626, p=0.0328) and greater LIA frequency (log-odds 0.096, p=0.0005) were significant predictors of AF termination with ablation. When the 30% cut off was applied acute outcome was accurately predicted in 82.9% with AIC 86.6 and AUC-ROC of 0.86 with a residual deviance of 76.5 on 77 degrees of freedom. Longer AFCL (log-odds 0.0769, p=0.0139), increasing LIA time (log-odds 0.141, p=0.0004) and higher frequency of focal activations (log-odds 0.025, p=0.0366) were independent predictors of AF termination with ablation. Patients requiring DCCV compared to those in whom ablation terminated AF had significantly more rotational activation in the RA with correspondingly fewer focal activations and shorter AFCL but no significant difference in the LA. See figure 5.4 and table 5.11.

In patients with persistent AF, LRA in the RA, whether measured as frequency (log-odds -0.0313, AIC 38.1, p=0.038) or proportion of time present (log-odds -0.099, AIC 36.9, p=0.0238), and FF in the RA (log-odds 0.0428, AIC 36.2, p=0.0159) were significant predictors of acute outcome. The multivariate model with no cut-off applied accurately predicted ablation outcome in 81% with AIC of 35.2 and AUC-ROC 0.86. With the 30% cut off, accuracy improved to 84% with AIC of 34.9 and AUC-ROC of 0.88. No measures of LA substrate were significant.

Table 5.7 Effect of AF type and chamber on electrophysiological substrate. p-values for the results of interaction and main effects of AF type and chamber on the combined dependent variables expressed as both frequency and time using no cut-off and a cut-off at 30% in patients with persistent AF.

Variable	Cut off	Interaction	Baseline rhythm	Chamber
Time present	0	0.033	<0.0005	0.017
	30	0.033	<0.0005	0.023
Frequency	0	0.014	<0.0005	0.010
	30	0.115	<0.0005	0.075

Table 5.8 Difference in AFCL and propagation patterns according to baseline rhythm in patients with persistent with AF. Figures expressed as mean±standard error.

Variable	Cut off	Baseline AF	Baseline SR	Difference (95% CI)	p value
AFCL	N/A	181±2	205±3	24 (17 – 32)	<0.0005
LRA frequency	0	86±4	49±6	-37 (-52 - -23)	<0.0005
	30	50±3	29±3	-21 (-30 - -12)	<0.0005
LRA time	0	29±1	16±2	-13 (-18 - -9)	<0.0005
	30	19±1	10±1	-9 (-12 – 06)	<0.0005
LIA frequency	0	438±19	397±25	-41 (-105 – 22)	0.193
	30	218±7	199±9	-19 (-42 – 5)	0.114
LIA time	0	60±2	57±3	-3 (-10 – 5)	0.449
	30	41±1	39±2	-2 (-7 – 3)	0.461
FF frequency	0	138±6	154±8	16 (-5 – 37)	0.136
	30	86±4	97±6	11 (-4 – 24)	0.159

Table 5.9 Difference in AFCL, LRA and FF patterns in the LA and RA according to baseline rhythm in patients with persistent AF. Figures expressed as mean±standard error.

Variable	Cut off	Chamber	Baseline AF	Baseline SR	Difference (95% CI)	p value
AFCL	N/A	LA	183±3	201±4	18 (7 – 28)	<0.0005
		RA	178±3	210±4	32 (21 – 42)	<0.0005
LRA frequency	0	LA	84±6	60±8	-24 (-45 - -4)	0.022
		RA	89±6	39±8	-50 (-71 - -30)	<0.0005
	30	LA	47±4	35±5	-12 (-25 – 0)	0.044
		RA	52±4	23±5	-29 (-41 - -16)	<0.0005
LRA time	0	LA	27±2	19±3	-8 (-14 - -1)	0.017
		RA	32±2	13±3	-19 (-25 - -12)	<0.0005
	30	LA	18±1	12±2	-6 (-10 - -1)	0.016
		RA	21±1	8±2	-13 (-17 - -8)	<0.0005
FF frequency	0	LA	155±9	159±12	4 (-25 – 34)	0.777
		RA	122±9	149±12	27 (-2 – 57)	0.069
	30	LA	96±6	101±8	5 (-15 – 25)	0.626
		RA	77±6	92±8	15 (-5 – 35)	0.133

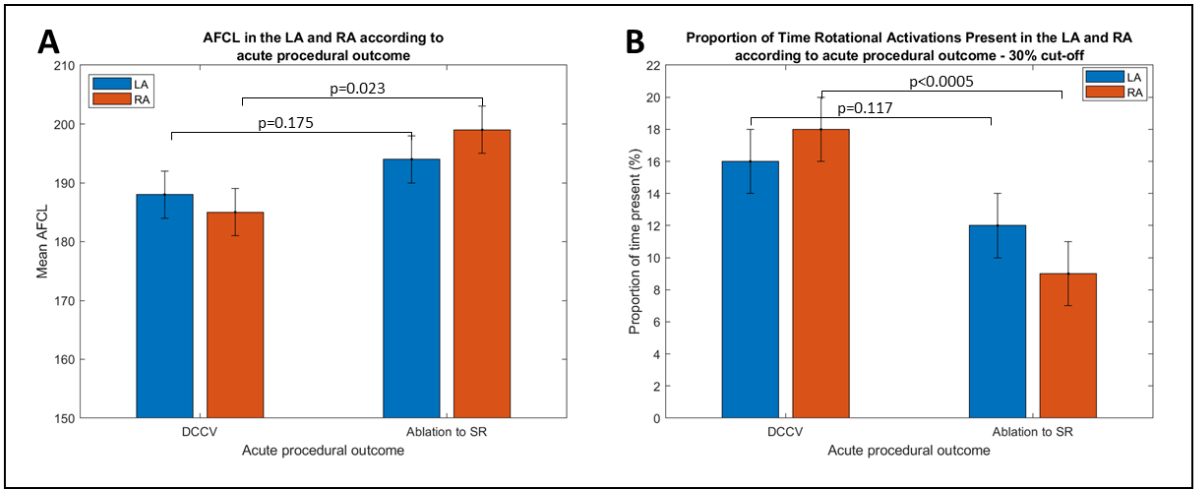

Figure 5.4 Difference in AFCL and LRA according to acute outcome. Difference in AFCL (A) and proportion of time LRA was present in high frequency (30% cut-off) zones (B) for the LA and RA in patients requiring DCCV and in whom ablation resulted in AF termination. Bars represent standard error.

Table 5.10 Univariate predictors of acute procedural outcomes across both chambers and LA and RA independently. Abbreviations as in text.

Variable	Combined			LA			RA		
	Log-odds	AIC	p value	Log-odds	AIC	p value	Log-odds	AIC	p value
AFCL	0.0303	111.4	0.0211	0.0214	59.3	0.2555	0.0383	55.7	**0.0409**
LRA time (0 cut-off)	-0.0854	102.1	0.0005	-0.049	57.9	0.1102	-0.1379	45.2	**0.002**
LIA time (0 cut-off)	0.0193	115.6	0.2098	0.0131	60.2	0.5000	0.0332	59.0	0.2219
LRA frequency (0 cut-off)	-0.03	102.4	0.0006	-0.0183	56.9	0.0708	-0.045	47.0	**0.0035**
LIA frequency (0 cut-off)	0.0009	117.0	0.6028	-0.0005	60.6	0.8241	0.002	30.2	0.543
FF frequency (0 cut-off)	0.0133	105.9	0.0048	0.0079	57.6	0.1046	0.0412	45.7	**0.0044**
LRA time (30 cut-off)	-0.1175	103.1	0.0006	-0.0633	58.4	0.1438	-0.195	45.5	**0.0019**
LIA time (30 cut-off)	0.0301	115.3	0.1695	0.0194	60.1	0.4876	0.0525	58.6	0.1702
LRA frequency (30 cut-off)	-0.0404	105.7	0.0017	-0.0223	58.5	0.1613	-0.070	48.1	**0.0038**
LIA frequency (30 cut-off)	0.0027	117.0	0.6094	-0.0014	60.1	0.8482	0.0069	59.8	0.3676
FF frequency (30 cut-off)	0.0204	106.0	0.0045	0.0128	57.2	0.0853	0.0588	47.2	**0.0076**

Table 5.11 Difference in AFCL, LRA, LIA and FF patterns in the LA and RA according to acute procedural outcome. Figures expressed as mean±standard error.

Variable	Cut off	Chamber	Ablation to SR	DCCV	Difference (95% CI)	p value
AFCL	N/A	LA	194±4	188±4	6 (-18 – 5)	0.275
		RA	199±4	185±4	14 (2 – 25)	0.023
LRA frequency	0	LA	57±7	77±7	20 (1 – 40)	0.042
		RA	44±7	79±7	35 (15 – 55)	0.001
	30	LA	34±4	43±4	9 (-3 – 21)	0.123
		RA	26±4	46±4	20 (8 – 32)	0.001
LRA time	0	LA	19±2	25±2	6 (-1 – 12)	0.088
		RA	15±2	28±2	13 (7 – 20)	<0.0005
	30	LA	12±2	16±2	4 (-1 – 8)	0.117
		RA	9±2	18±2	9 (5 – 13)	<0.0005
LIA frequency	0	LA	449±28	439±26	10 (-67 – 86)	0.802
		RA	401±28	383±26	18 (-58 – 95)	0.629
	30	LA	211±12	213±9	2 (-25 – 30)	0.852
		RA	213±10	201±9	12 (-15 – 40)	0.372
LIA time	0	LA	64±3	60±3	4 (-6 – 12)	0.453
		RA	58±3	54±3	4 (-4 – 13)	0.299
	30	LA	44±2	41±2	3 (-4 – 8)	0.447
		RA	40±2	36±2	4 (-2 – 10)	0.226
FF frequency	0	LA	194±15	155±13	39 (-1 – 78)	0.052
		RA	179±15	123±13	56 (17 – 95)	0.006
	30	LA	124±9	96±9	28 (2 – 52)	0.034
		RA	111±9	78±9	33 (8 – 59)	0.010

5.3.7 Bipolar Voltage

There was a low burden of low amplitude signals in all patients (table 5.12) with 2.1% <0.5mv in patients with pAF and 5.9% <0.5mv in patients with persAF (p<0.0005). Mean bipolar voltage amplitude was consistently lower in the RA compared to the LA but amplitudes were normal in both chambers (mean 1.87±1.71 v.s 1.98±2.0 [p<0.0005] in the RA and LA respectively in patients with pAF and 1.27±1.27 vs 1.32±1.31 [p<0.0005] in patients with persistent AF) (see table 5.13).

Table 5.12 Proportion of chamber with low voltage amplitude according to AF phenotype, baseline rhythm and acute procedural outcome.

		Points <0.5mv (%)	p-value	Points <0.1mv (%)	p-value
AF phenotype	pAF	2.1	<0.0005	0.05	<0.0005
	persAF	5.9		0.14	
Baseline rhythm	SR	2.8	<0.0005	0.07	<0.0005
	AF	8.4		0.20	
Response to ablation	SR	3.3	<0.0005	0.08	<0.0005
	DCCV	6.6		0.16	

Table 5.13 Difference in mean bipolar voltage amplitude in the LA and RA according to AF phenotype, baseline rhythm and acute procedural outcome. Figures are expressed as mean±standard deviation.

Variable		LA	RA	Difference (95% CI)	p value
AF phenotype	pAF	1.98±2.0	1.87±1.71	0.11 (0.07-0.15)	<0.0005
	persAF	1.32±1.31	1.27±1.27	0.05 (0.03-0.08)	<0.0005
	Difference	0.66 (0.62-0.69)	0.60 (0.56-0.63)		
	p value	<0.0005	<0.0005		
Baseline rhythm	SR	1.84±1.89	1.66±1.54	0.18 (0.15-0.20)	<0.0005
	AF	1.07±0.99	1.11±1.20	0.04 (0.01-0.08)	0.0040
	Difference	0.77 (0.74-0.80)	0.55 (0.51-0.58)		
	p value	<0.0005	<0.0005		
Acute response to ablation	SR	1.79±1.92	1.60±1.53	0.19 (0.16-0.21)	<0.0005
	DCCV	1.20±1.10	1.23±1.29	-0.03 (-0.07-0.00)	0.0864
	Difference	0.59 (0.56-0.62)	0.37 (0.34-0.41)		
	P value	<0.0005	<0.0005		

5.3.8 Interatrial Propagation and Effect of ablation

At baseline, 41 maps were obtained. A dominant chamber was identified in 11 maps (in 9 patients). Of these, 5 maps (in 4 patients) were LA dominant, and 6 maps (in 5 patients) were RA dominant. The remainder showed balanced interatrial propagation. The channel of communication was in the septum in 29 (71%), over Bachmann's bundle in 7 (17%), through the coronary sinus in 3 (7%) and over multiple channels in 2 (5%).

In the 4 patients with LA dominant propagation, PVI resulted in AF termination in 1, and in another transient organisation with clear RA dominance. In the other 2, the LA remained dominant and further LA ablation was delivered resulting in a change to balanced propagation and DCCV restored SR. In 3 of the 5 patients with RA dominance, the RA remained dominant following PVI. In 2 of these, further ablation to the LA and RA restored sinus rhythm whilst DCCV was needed in 1. Of the remaining 2, balanced propagation was seen post PVI in one patient where further LA ablation was delivered and DCCV used to restore SR, and in the other, extensive LA ablation was delivered and SR restored (without RA ablation). In a further patient, PVI resulted in a change from balanced propagation to RA dominance and RA ablation was then delivered prior to DCCV (see figure 5.5 for detailed outline).

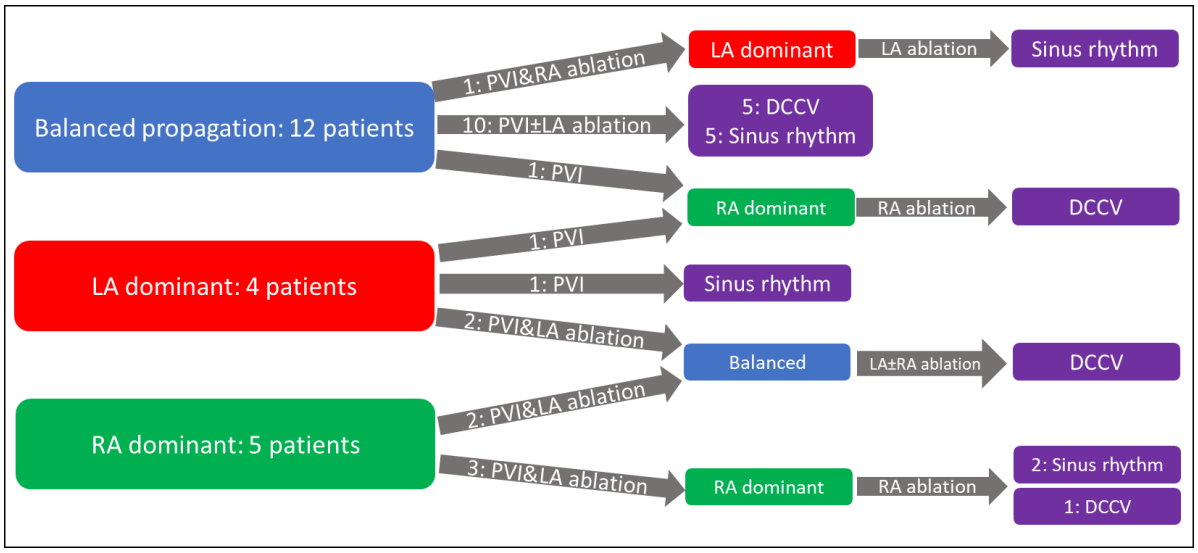

Figure 5.5 Patterns of interatrial propagation and changes following ablation.

5.4 Discussion

In combination with AFCL, a frequently used marker of AF electrophysiological substrate, this data contributes to the quantification of the bi-atrial electrophysiological activation patterns involved in AF maintenance. The main findings of this analysis are as follows:

1. Patients with either persistent AF (compared to paroxysmal) or those who present in AF (compared to those presenting in SR) exhibit more LRA patterns when measured either as a number of individual occurrences, a proportion of time these patterns are present, or number of sites of high frequency LRA.

2. Patients with paroxysmal AF, or persistent AF in whom AF is induced, demonstrate higher numbers of focal activation.
3. Mean AFCL is the same in patients with paroxysmal vs persistent AF but significantly shorter in patients presenting for their procedure in AF vs SR.
4. In the majority of patients, AF is maintained by dynamic, balanced propagation between chambers. When a dominant chamber was identified prior to ablation this was the LA in 4 patients and the RA in 5 patients.
5. Right atrial, but not LA, electrophysiological substrate, quantified by either AFCL, FF frequency or LRA time predicted acute procedural outcome, including in patients with persistent AF.

Initial comparisons were made between patients identified as paroxysmal or persistent AF. Reported outcomes after ablation of paroxysmal AF are significantly better than for persistent AF and indeed the best outcomes appear to be in patients with the shortest (<24 hours) paroxysms.(77, 233, 234) This strongly points towards differences in AF phenotypes between these groups brought about by changes in the underlying mechanisms of AF propagation. These differences appear to largely be driven by changes in the relative contribution of focal and rotational activation patterns with no difference in irregular activation. Given knowledge of the difference in clinical outcomes between these groups, the observed changes are likely to represent genuine variations in AF mechanisms.

Superior outcomes following catheter ablation for persistent AF have been observed when patients were in sinus rhythm at the start of their procedure.(235) What is unclear is whether this is a result of beneficial reverse remodelling brought about by sustained sinus rhythm or whether the very fact that patients are able to remain in sinus rhythm following cardioversion implies an inherently milder AF phenotype. The same differences observed in patients with paroxysmal AF were seen in patients with persistent AF presenting in sinus rhythm, suggesting an AF phenotype in these patients more closely resembling paroxysmal AF. This is further supported by measures of AFCL. There was no difference in mean AFCL in patients with paroxysmal versus persistent AF, but patients in persistent AF at the start of the procedure had a significantly faster AFCL than those in sinus rhythm, a discrepancy arising from patients in sinus rhythm appearing more closely aligned in terms of AFCL with paroxysmal AF than those with truly persistent AF at the time of the procedure. This suggests similarities in the mechanisms sustaining AF in these patients and may explain the observation that a strategy of catheter ablation limited

to pulmonary vein isolation, with recognised efficacy in patients with paroxysmal arrhythmia, is also effective in a significant proportion of patients with persistent AF.(135)

Measures of RA electrophysiological properties were significant predictors of ablation outcome, but this was not the case for LA measures. Patients requiring DCCV demonstrated significantly more LRA and fewer FF in the RA, as well as a shorter RA AFCL than those in whom AF terminated with ablation. This inverse relationship between LRA and FF appears to mirror the differences observed based on clinical AF phenotype and suggests that these parameters represent genuine markers of the electrophysiological substrate.

It is important to recognise however that the differences observed are associative and not necessarily causative. The key from a clinical perspective is distinguishing between mechanistically important phenomena that can be impacted by ablation, and simply markers of disease severity or electrophysiological remodelling. Increasing rotational activation and shortening of AFCL appear to closely correlate and are both univariate predictors of acute outcome. AFCL has previously been suggested as a marker of arrhythmogenic substrate using a stepwise ablation approach in addition to identifying patients in whom AF termination is achieved through more limited ablation.(236, 237) A shortening of AFCL suggests shorter refractory periods and is likely to represent a marker of electrical remodelling. What appears to be a close association between AFCL and rotational activation patterns suggests that this represents a similar marker of electrical remodelling, with shorter refractory periods providing the optimal electrophysiological environment for re-entry.

Of particular interest is that it appears to be measures of RA electrophysiological substrate that identify ablation- refractory patients. Importantly, this does not take into consideration the effect of the ablation delivered to terminate AF. Five of the 11 patients in whom DCCV was needed to restore sinus rhythm underwent ablation to areas of interest in the RA. It is unclear whether further right atrial ablation would necessarily confer benefit or whether the differences observed are markers of progressive electrophysiological remodelling resulting in an ablation refractory state. Although the bipolar voltage amplitude in the RA was lower than the LA this was still well within the physiological range and not suggestive of a fibrotic RA substrate that would explain the differences observed.

The number of focal activation patterns appears to inversely correlate with the degree of rotational activation, however, in contrast to LRA, in multivariate analysis, a higher number of activations in zones with repetitive focal firings remained an independent predictor of successful AF termination with ablation, as was a longer AFCL and greater

proportion of time LIA was present. Both LIA and LRA represent directional changes in propagation and sites of repeated LRA often overlap with zones of more stable LIA, perhaps as a result of anchoring to structural heterogeneities responsible for complex patterns of conduction.(114, 238) The degree of directional change in wavefront propagation within these regions may reflect functional atrial properties influencing the relative balance of irregular and rotational patterns. A greater balance of LIA may represent a milder phenotype less able to sustain re-entry, resulting in a greater likelihood of ablation terminating AF. In most patients with high frequency FF, these were targeted with ablation, resulting in AF termination suggesting a possible mechanistically important role of these phenomena that represent attractive ablation targets.

Where regions with repetitive, high frequency focal activation were identified, these were preferentially targeted with ablation. However, in one patient a region of highly repetitive FF was identified on post-procedure analysis that was not identified and ablated in real time. In this patient, 2 other areas of FF in the LA were ablated and DCCV used to restore SR. This suggests a spectrum of different AF phenotypes, characterised at one end by sites of high frequency focal activation that represent mechanistically important phenomena, perhaps resembling “drivers” identified in previous studies, where ablation is more likely to result in acute AF termination. At the other end of the spectrum represents a more complex substrate dependent state with shorter AFCL and dynamic patterns of LRA.

Although right atrial substrate properties predicted acute procedural outcomes, AF maintenance predominantly involved balanced propagation between atria. Efforts to identify drivers responsible for maintenance of AF have evolved from identification of high frequency spiral wave re-entry mechanisms in animal models(66, 168, 211) and subsequent application of dominant frequency (DF) mapping aimed to identify high frequency sources responsible for hierarchical activation of the atria.(169, 170) However, a frequency gradient between chambers is mainly found in patients with paroxysmal AF, and ablation of high DF sites has not been shown to confer clinical benefit.(172, 173) The balanced propagation between chambers observed in the majority of patients in our study suggests a more complex interaction of bi-atrial mechanisms not in keeping with high frequency drivers. Furthermore, even in patients with a dominant chamber at baseline, ablation of mechanisms identified in that leading chamber resulted in AF termination in only 3 of 9. Of the remainder, 5 showed a change to either balanced propagation or dominance of the opposite chamber (1 remained RA dominant despite LA and RA ablation and received DCCV). Two patients with RA dominance at baseline changed to LA dominance without any RA ablation. This supports the concept of a critical mass of substrate responsible for maintaining AF propagation. The extent to which ablation is

required to terminate the arrhythmia is dependent on the functional atrial substrate properties that determine this threshold. Ablation limited to PVI is sufficient in a proportion, whilst in others, additional ablation resulting in incremental depletion of individual mechanisms across both chambers is required.

Better classifying these patient groups is important in determining ablation strategy. Arrhythmia recurrences include both organised atrial tachycardia and AF. Achieving improved long-term outcomes is likely to be obtained by a combination of minimising ablation where possible whilst limiting more extensive non-pulmonary vein ablation to patients with more advanced atrial substrate where this is likely to be required.

Importantly, this analysis was based on propagation patterns in AF and seeks to understand mechanisms related to arrhythmia maintenance rather than initiation. Ectopy (arising from the pulmonary veins) has been demonstrated to trigger AF but ectopy alone is insufficient to result in sustained arrhythmia.(44) A vulnerable atrial substrate is required to result in AF initiation, without which only the ectopy remains. Mechanisms must then exist to sustain the arrhythmia. Given that the atria are intricately linked, and the arrhythmia is seen to sustain in both of these chambers one may expect the processes that sustain the arrhythmia to be observed in both chambers and mechanistic processes be shared between patients with paroxysmal and persistent AF. The differences in electrophysiological substrate observed may reflect the point at which an ablation approach limited to eliminating the arrhythmia trigger becomes ineffective and additional substrate modification is required.

It is important to acknowledge that AF termination does not necessarily translate into long term freedom from arrhythmia recurrence.(235) However, the purpose of this study was primarily to explore bi-atrial mechanisms involved in AF maintenance. As such, arrhythmia termination is a useful indicator of the effect of ablating these mechanisms and identifying different substrate phenotypes. These results provide evidence of the role of both chambers in sustaining AF, with right atrial mechanisms representing a marker of substrate progression. Empirical treatment strategies focussed on the left atrium may therefore always result in limited clinical gains when the right atrium is ignored. Where a dominant chamber was identified, the precise mechanism responsible for this was difficult to elucidate, but in 8 of these 9 patients, ablation resulted in a clear change in interatrial propagation pattern, suggesting a hierarchy of interdependent processes. Ablation delivered to mechanisms in the dominant chamber result in a change to the balance of remaining mechanisms and therefore the balance of propagation between chambers. PVI followed by targeted ablation limited to the dominant chamber directly terminated AF in

only 2 of these patients further supporting the importance of multiple co-existing mechanisms in most patients rather than a single dominant driver. Identifying and targeting all of the regions may be important to eliminate the substrate responsible for maintaining AF and therefore conferring improved long-term outcomes.

In conclusion, this data suggests that maintenance of AF predominantly involves bi-atrial mechanisms characterised by an electrophysiological phenotype that can be identified based on a combination of global AFCL and the relative contribution of focal and rotational activation patterns. Termination of AF following catheter ablation appears to be determined primarily by electrophysiological properties of the RA, perhaps reflecting a state of more advanced electrophysiological remodelling.

6 Recurrence Matrix Mapping – Novel Approach to Characterising Atrial Fibrillation Phenotype

6.1 Introduction

Atrial fibrillation (AF) is a highly complex arrhythmia. Despite extensive research, there remains little consensus on the mechanisms responsible for AF propagation beyond agreement on the role of pulmonary vein ectopy in arrhythmia initiation(44). Apart from triggers however, appropriate electrophysiological conditions, the so-called atrial substrate, are required to sustain the arrhythmia, especially when persistent. Although eliminating pulmonary vein triggers is more successful in reducing arrhythmia recurrence in patients with paroxysmal AF(133, 233, 239) compared to those with persistent AF(135, 145), with the best results in patients with the shortest paroxysms(234), duration of AF episodes is not always a reliable predictor of response. These differences in outcome suggest a spectrum of AF phenotypes, from pulmonary vein, trigger dependent, to a substrate dependent, trigger independent arrhythmia(240).

Several approaches have been developed aimed at characterising the non-pulmonary vein substrate, but none has yet definitively identified the mechanisms responsible for AF maintenance(95, 126, 184, 223, 230). One of the significant challenges in the study of electrophysiological mechanisms of AF is the development of accurate methods for the analysis of fibrillatory signals. Phase analysis has been widely applied to both basket catheter signals and body surface potential mapping, mainly for the identification of rotational activations, thought to represent “drivers”(126, 174, 184, 187). Phase coherence has previously been used to analyse the complex signals seen in electroencephalogram recordings of patients with epilepsy(241), and applied to invasive simultaneous endocardial and epicardial mapping of AF in order to quantify the synchronicity between signals on each surface of the atrial chamber(232). The concept of recurrence analysis is used to identify patterns within complex dynamical systems and, through use of recurrence plots allows visualisation of recurrences within these systems(242). Recently, phase coherence has been used to generate recurrence plots to identify repetitive patterns of activation during localised epicardial mapping of AF(243). However, this technique has never been applied to whole chamber mapping of atrial fibrillation. In this study, we sought to apply the novel tool of recurrence plot analysis to whole chamber biatrial recordings of atrial fibrillation in order to quantify the degree of repetitiveness/organisation in AF propagation that may help to reveal individualised AF phenotypes and predict acute procedural outcomes.

6.2 Methods

6.2.1 Patient selection

Data was obtained from patients recruited to the BiMap-AF study, the main results of which are included in chapters 4-5 above (REC reference 18/SC/0409). This included patients aged 18-80 undergoing first time catheter ablation for either paroxysmal (n=5) or persistent (n=16) atrial fibrillation. Patients were excluded for previous cardiac surgery, congenital cardiac abnormalities, or severe valvular heart disease. The study complied with procedures laid out in the declaration of Helsinki.

6.2.2 Electrophysiological mapping procedure

Detailed procedures have been outlined in sections 4-5 above. Procedures were carried out under general anaesthetic and antiarrhythmic drugs (excepting amiodarone) were stopped a minimum of 5 days prior to the procedure. Electrophysiological mapping was performed using two linked AcQMap non-contact charge density mapping systems (Acutus Medical; CA, USA), with AcQMap mapping catheters positioned in both the right and left atrium to allow simultaneous bi-atrial recording and a decapolar catheter (Inquiry, Abbot Medical) was inserted into the coronary sinus. Ultrasound was used to generate left and right atrial anatomies as previously outlined in detail(196).

In patients in sinus rhythm at the start of the procedure, AF was induced using burst atrial pacing and sustained AF was mapped for study analysis. Both AcQMap catheters were placed in a static central position in each chamber and non-contact recordings of atrial activation were generated for 2 minutes. Time alignment of the two systems was achieved using a below threshold pacing stimulus from the coronary sinus.

Raw AcQMap electrode biopotential signals were visually inspected to identify outlying or corrupted signals, which were then manually excluded. A low pass filter at 100Hz as well as a 50Hz notch filter and smoothing algorithm were applied followed by selection of a QRS-T wave template for subtraction. Three consecutive 10-second segments were created for simultaneous timepoints in both the left and right atria, confirmed relative to the coronary sinus low amplitude pacing spike. This process was repeated to create two 30-second AF maps following splicing together of each 10s segment. Recordings were obtained at the start of the procedure and following wide antral circumferential ablation to achieve pulmonary vein isolation. Additional ablation guided by AcQMap propagation patterns was performed with direct current cardioversion used to restore sinus rhythm if not achieved with ablation alone. AcQMap ablation targets were identified based on operator determined stability over repeated map segments focussing on regions with repetitive focal and irregular activation patterns. The resultant whole

chamber computed dipole electrograms were exported, together with the atrial anatomical meshes for processing and generation of recurrence plots (described below).

6.2.3 Clinical outcomes

The primary clinical outcome was the acute response to ablation. Termination with ablation included either direct conversion from AF to sinus rhythm following ablation or via an organised atrial tachycardia that was then ablated to achieve sinus rhythm. Otherwise, direct current cardioversion (DCCV) was used.

6.2.4 AcQMap Propagation Map Calculation and Activation Pattern Quantification

Propagation maps were calculated in the AcQMap system from the computed dipole signals using the default timing method (based on -dv/dt of dipole signals), window width (for isochronal colour bars) of 80ms and time threshold of 70ms (representing presumed minimum refractoriness). AcQTrack (Acutus Medical) was used to identify specific propagation patterns including focal firing (FF), localised irregular activation (LIA) and localised rotational activation (LRA) as explained previously in section 2.

6.2.5 Symbolic Dynamics

Whole chamber and regional complexity were quantified by analysing the relationship between occurrences of the propagation patterns described above (LIA, LRA and FF) to provide a value of the measure of variability in activation pattern transitions termed symbolic dynamics entropy (SDE). For every occurrence of an activation pattern, the preceding and following activation patterns detected within a threshold of 200ms are recorded to provide a two or three component activation pattern sequence (for example FF → LRA → LIA for the scenario where a focal activation is followed by a rotational and then irregular occurrence; or FF → FF → FF for a sequence of successive focal activations; or FF → LIA for a two component sequence). Three pattern long sequences were analysed including patterns occurring across the whole chamber and two pattern long sequences were generated within each atrial anatomical segment resulting in global and regional measures. The number of times each possible sequence occurs were counted to generate a histogram illustrating the distribution of each activation pattern transition sequence. The Shannon entropy of the histogram is calculated to give the SDE value to provide a measure of the variability of pattern transitions. Where a repetitive sequence of activation patterns repeatedly recurs, this provides a low value, whilst a high variability in activation pattern sequences results in a high value and suggests greater overall complexity.

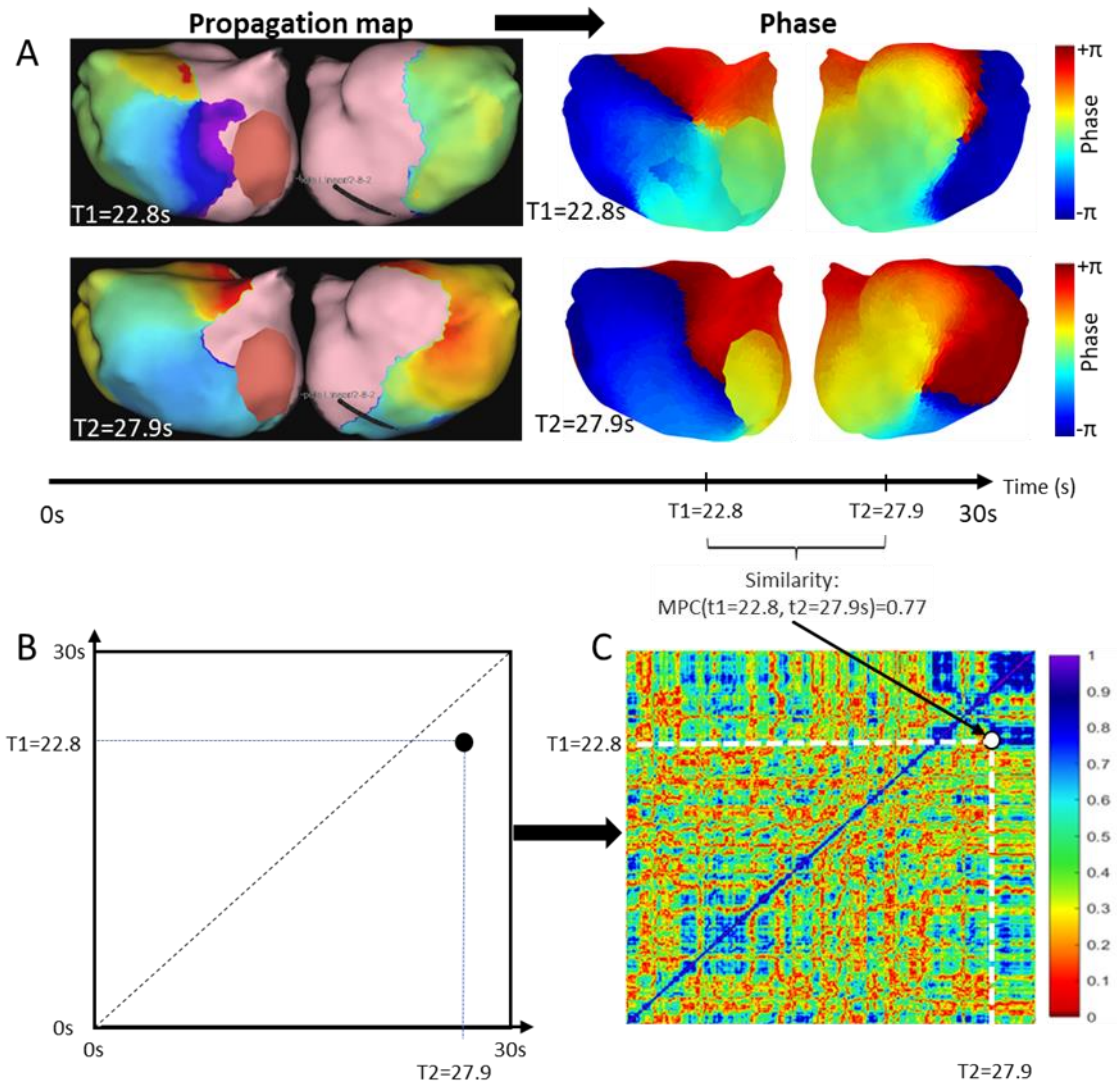

Figure 6.1 Schematic of recurrence distance matrix calculation. The recurrence matrix presents similarity between conduction patterns (as expressed by phase maps) between all possible pairs of time points. Examples of activation maps at two different time points, (A) which are first converted to phase. Similarity between those two maps calculated using mean phase coherence (MPC) was equal to 0.77. This value becomes a single point (with color-coded) value on recurrence distance matrix at coordinates (T1, T2) corresponding to time points of those two maps (B). Computation of MPC between all possible pairs of time points results in the full matrix (C).

6.2.6 Signal Processing and Recurrence Plot Generation

Processing of charge density signals and recurrence plot generation was performed using a custom designed software application. Electrogram phase was calculated from the exported charge density electrograms from each vertex of the chamber using sinusoidal recomposition and Hilbert transform(198). Mean phase coherence (MPC) was calculated using phase values for each vertex of the anatomy at a given timepoint and similarity in conduction patterns at two timepoints was determined using the following equation:

$$MPC(t_1, t_2) = \frac{1}{N}\sum_{k=1}^{N} exp(\, i(\phi_k(t_1) - \phi_k(t_2))) \quad (241)$$

where k denotes the virtual electrode index on the anatomy, t represents the timepoint, φ represents phase, and N is the number of points on the anatomy. In the case of an organised repetitive rhythm with a stable spatial distribution of phases between every timepoint (e.g. sinus rhythm [SR] or macro-re-entrant tachycardia) this would result in a value approaching 1.0 whilst a scenario with no similarity between spatial distributions would result in a value approaching zero. The MPC value for all time points was plotted to generate a recurrence matrix and the mean value calculated to give a measure of repetition of whole chamber propagation patterns, termed recurrence index (RI) (figure 6.1).

The recurrence index for atrial anatomical segments was calculated following generation of local recurrence maps. For each vertex of the chamber, a locality consisting of neighbouring vertices within a radius of 20mm was defined and the recurrence plot generated for that locality. The mean value was then assigned to that central vertex. Applying this to the whole chamber generates a local recurrence map and the mean value for every vertex within an anatomical segment results in the regional RI.

The whole chamber phase processed signals were additionally used to measure mean cycle length over 30s at each vertex of the chamber. The mean of all vertices represents the whole chamber AF cycle length (AFCL).

Following development, recurrence matrix analysis was tested in a recording of macro-reentrant atrial tachycardia to assess the proof of concept. A sample matrix from a recording of mitral isthmus dependent flutter is shown in figure 6.2. This demonstrates the matrix properties seen in repeating identical patterns of activation resulting in a RI of 0.80±0.11

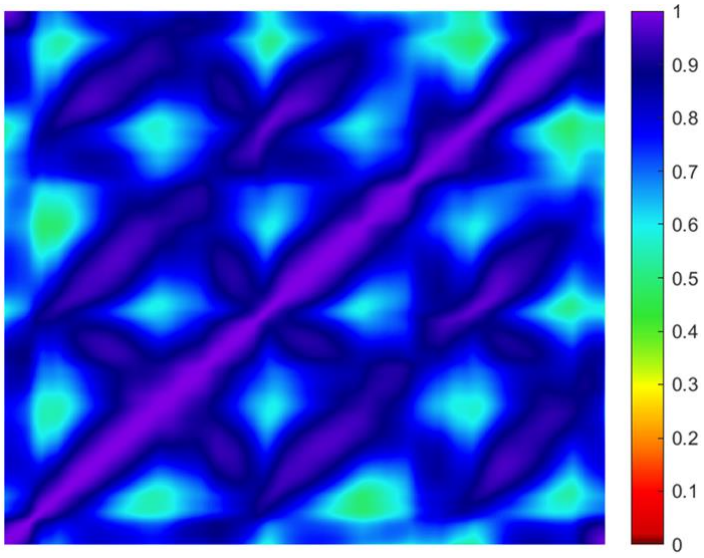

Figure 6.2 Flutter recurrence matrix. Recurrence matrix for a recording of 3-cycles of mitral isthmus dependent left atrial flutter. RI value for the matrix is 0.80±0.11. The parallel lines on the plot with MPC value approaching 1 (purple) demonstrate repeating, identical patterns of activation.

6.2.7 Analyses performed

For each map generated, recurrence plots and RI for the whole chamber and anatomical segments (left atrium: anterior, septum, roof, lateral, posterior and inferior; right atrium: septum, anterior, lateral and posterior) were generated. The frequency of LIA was measured at each vertex to quantify the degree of complexity of wavefront propagation as visualized on AcQMap propagation history maps, which was correlated with the RI at each vertex. The SDE value for the whole chamber and each atrial segment was calculated, with a high value suggesting a high degree of variation in activation pattern sequences and therefore more complex propagation, with a low value suggesting recurring sequences and a lower degree of complexity.

Statistical analyses were performed using Matlab (Mathworks, R2019a), SPSS (IBM, v25) and R statistical software (version 4.0.3). Following normality testing using the Shapiro-Wilk test, comparisons were made between patients with paroxysmal and persistent arrhythmia and according to the rhythm at the start of the procedure using the two-sided Wilcoxon rank-sum test. The impact of pulmonary vein isolation on whole chamber RI was also compared using the two-sided Wilcoxon rank-sum rest. Correlation between complexity measured by RI and the frequency of LIA patterns as well as the SDE was measured in each region using the Spearman correlation coefficient. Regional RI values were compared using ANOVA testing and changes in LA and RA recurrence index before and after PVI were compared using the paired t-test. Binomial logistic regression was used to identify predictors of acute ablation outcome. The whole chamber RI, whole chamber SDE, frequency of LRA, LIA and FF, and mean AFCL were included for

univariate and multivariate analysis. As a higher rate of acute arrhythmia termination would be expected for patients with paroxysmal AF, models were repeated including only patients with persistent AF to test the applicability to this patient group alone.

A p-value of <0.05 was considered significant. Figures are expressed as medians (25th and 75th percentile) or mean and standard deviation according to distribution.

6.3 Results

6.3.1 Patient characteristics and acute procedural outcomes

Table 6.1 summarises the characteristics of the 21 patients enrolled in the study. Eleven patients attended the procedure in SR. Two 30-second maps of AF were obtained at baseline in all but one patient in whom rate dependent left bundle brunch block resulted in variation of QRS morphology preventing adequate and consistent QRS-T wave subtraction for a duration long enough to obtain signals of sufficient quality to permit analysis. In this patient, only one 30s segment was used. Maps following pulmonary vein isolation were obtained in 12 patients with persistent AF. In 10 patients (48%), ablation resulted in termination to SR whilst 11 (52%) required DCCV.

Table 6.1 Patient Characteristics. Data is expressed as n (%), medians, 1st and 3rd quartiles or mean±standard deviation. (AF: atrial fibrillation; BMI: Body mass index; LA: Left atrium; LV: left ventricle)

Characteristic	Distribution
AF Type	16 Persistent, 5 Paroxysmal
Sex	41% Female
Age	61 (56-66)
BMI (kg/m^2)	30 (26-33)
CHADs-VASc	1.3±1.3
Prior Anti-Arrhythmic Drugs	Sotalol: 2 (9.5%) Amiodarone: 7 (33%) Flecainide: 4 (19%)
LA Diameter (mm)	43 (38-51)
LV Ejection Fraction (%)	60 (55-60)
Time Since AF Diagnosis (Months)	48 (20-60)

6.3.2 Recurrence plot characteristics

Examples of different recurrence plot phenotypes are shown in figure 6.3. Varying patterns were observed. These ranged from highly complex, disorganised patterns (figure 6.3A) which show a speckled appearance of red-green colour with no discernible repetition to highly organised repetitive patterns of propagation that was interrupted with

short periods of complexity (figure 6.3C-D). Variation within one recording can be observed (as in figure 6.3B) where a period of complexity is followed by a period of organisation. Patterns between chambers were sometimes very different (figure 6.3E-F) with a high degree of organisation observed in one chamber in contrast to a highly disorganised pattern in the contralateral chamber. Regional changes could also be observed as illustrated in figure 6.4. Although a high degree of complexity could be seen in whole chamber plots, when each region of the chamber was examined, areas of both high complexity and organisation could be observed.

Propagation history maps for periods of maximal organisation (as illustrated in circled regions in figure 6.3) were examined. This included 8 separate segments in 5 patients. In all segments, the period of organisation coincided with the emergence of a dominant site of focal firing that remained for the duration of the organised period with a stable cycle length. Average cycle length variation across these segments was 4.7±1.6%. In 6 segments (in 4 patients) the driver mechanism appeared to be focal with a clear QS charge density signal seen at the point of origin, as shown in figure 6.5. In one patient the mechanism appeared to represent localised re-entry re-set by repeated focal activation arising near the base of the left atrial appendage. In all segments, cessation of the focal activation resulted in degeneration to more complex atrial activation with a concurrent change in appearance of the recurrence matrix.

6.3.3 Recurrence Index

Prior to any ablation, a higher whole chamber RI was observed in patients with paroxysmal AF (0.40; 25^{th}-75^{th} percentile: 0.36-0.44) compared to persistent AF (0.35; 0.33-0.38) ($p<0.0005$). Patients in whom AF was induced also had a higher RI (0.40; 0.36-0.44) compared to patients in AF at the start of the procedure (0.34; 0.32-0.35) ($p<0.0005$). These differences were observed in both the LA ($p=0.016$) and RA ($p=0.0094$) in patients with paroxysmal vs. persistent AF as well as in both chambers in patients in AF at baseline vs. induced AF ($p<0.0005$ for both chambers).

Greatest complexity was observed in the anterior, septal and posterior regions of the LA and the septal and lateral RA, whereas the lateral LA and anterior RA showed the most organisation (figure 6.6A). A significant inverse correlation was observed between local RI and the frequency of LIA patterns (correlation coefficient $r = -0.6590$, $p<0.0005$, figures 6.4C and 6.6B) and with regional SDE ($r=-0.5424$, $p<0.0005$).

Pulmonary vein isolation resulted in an increase in RI in both the LA (0.33 – 0.41; difference 0.08, 95% confidence interval 0.01-0.10, $p=0.018$) and RA (0.35 – 0.39; difference 0.04, 95% CI 0.03-0.07, $p<0.0005$, figure 6.6C).

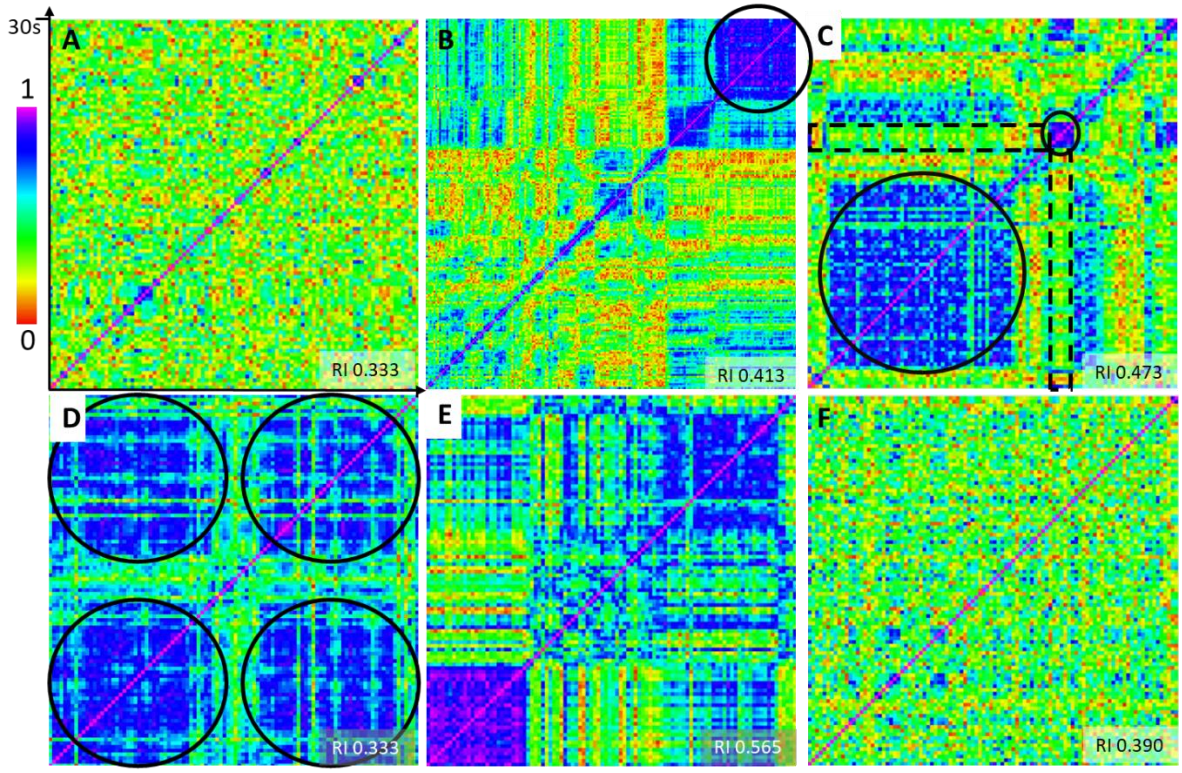

Figure 6.3 Recurrence plot phenotypes. Patterns include highly disorganised complex propagation (A), and periods of organised patterns (circled, B) following greater complexity. In (C), a period of organisation is followed by another shorter segment (circled) that are very different to each other as denoted by the red-green bands (dashed boxes) which show that the pattern within the first ~2-15s has very low coherence with the pattern at ~18-20s and ~28-30s. In (D), 2 periods of organisation are repeated with a period of highly complex conduction between. (E-F) show the plots for the same patient's left atrial (LA) (E) and right atrial (RA) (F) propagation. Whilst a high degree of organisation is seen in the LA, a greater degree of complexity is observed in the RA. Colour bar shows purple to represent a high degree of organised repetitive propagation whilst red represents highly complex disorganised propagation.

6.3.4 Predictors of acute procedural outcome

In univariate analysis, RI was the strongest predictor of acute procedural outcome (AIC 97.0, p=0.0007). See table 6.2 for full results. In multivariate analysis, the overall model attained residual deviance of 65.03 on 75 degrees of freedom, given the null deviance of 113.24 on 81 degrees of freedom, with AIC of 79.03, and accurately predicted ablation outcome in 89% of cases. In this multivariate model, only RI retained statistical significance (log odds 20.15, p=0.0078). When only patients with persistent AF were included, RI remained a statistically significant predictor of ablation outcome (log odds 14.8, AIC 72.8, p=0.0076) in univariate analysis. The multivariate model in this group attained residual deviance of 52.97 on 57 degrees of freedom, given the null deviance of 79.50 on 63 degrees of freedom, with AIC of 67.0 and accurately predicted ablation

outcome in 91% of cases. Only RI remained statistically significant (log odds 18.0, p=0.0279).

In 4 of the 5 patients in whom a period of highly organised activation was observed in association with a dominant focal mechanism, this focal activation was identified and ablated during the procedure, resulting in AF termination. In 1 patient, this mechanism was not identified and therefore not ablated and DCCV was required to restore sinus rhythm.

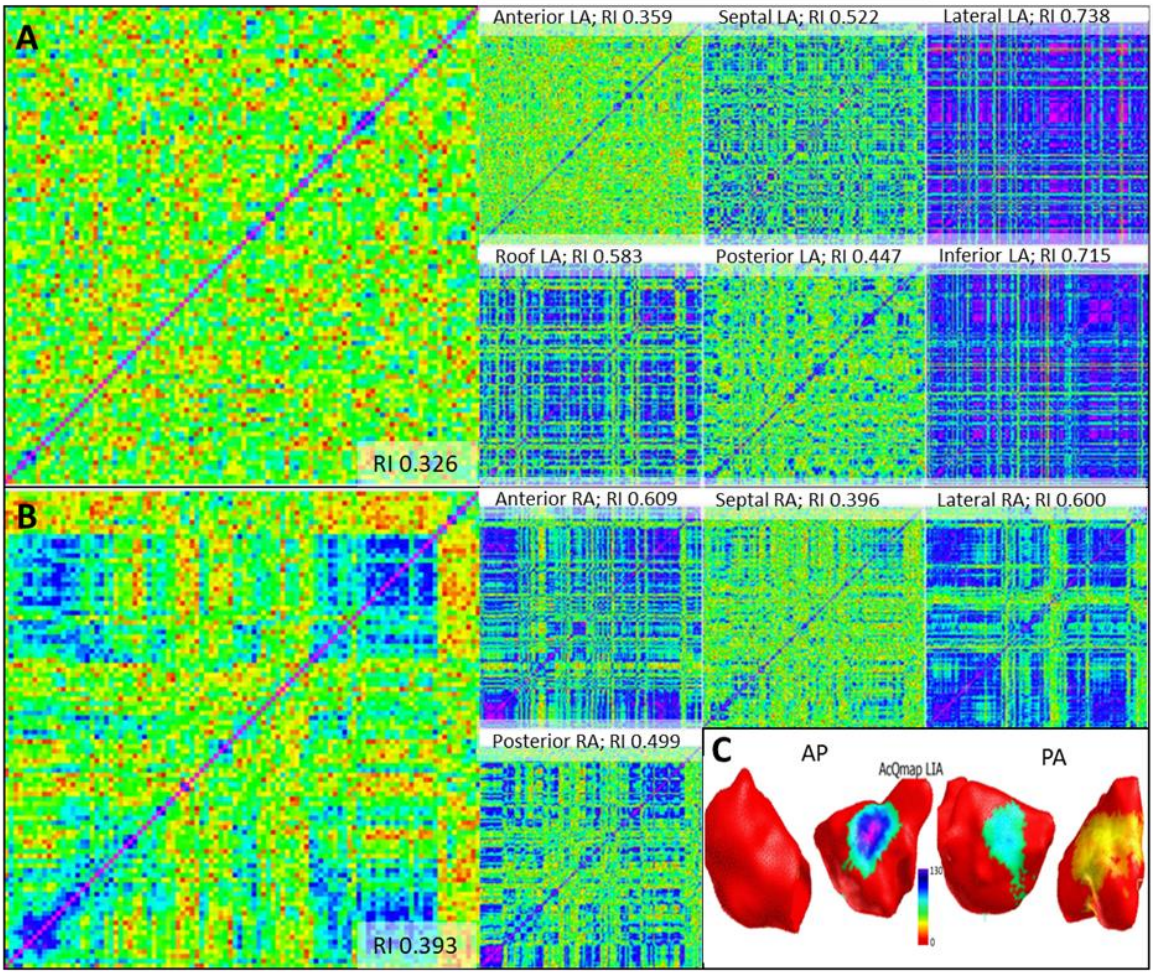

Figure 6.4 Examples of whole chamber and regional recurrence plots. Different patterns observed in the LA (A) and RA (B) and atrial segments. The anterior and posterior LA, and the septal RA show the greatest complexity. A high degree of organisation is seen in the lateral and inferior LA, and the anterior and lateral RA. (C) shows the regions with maximal frequency of localised irregular activation patterns in both chambers.

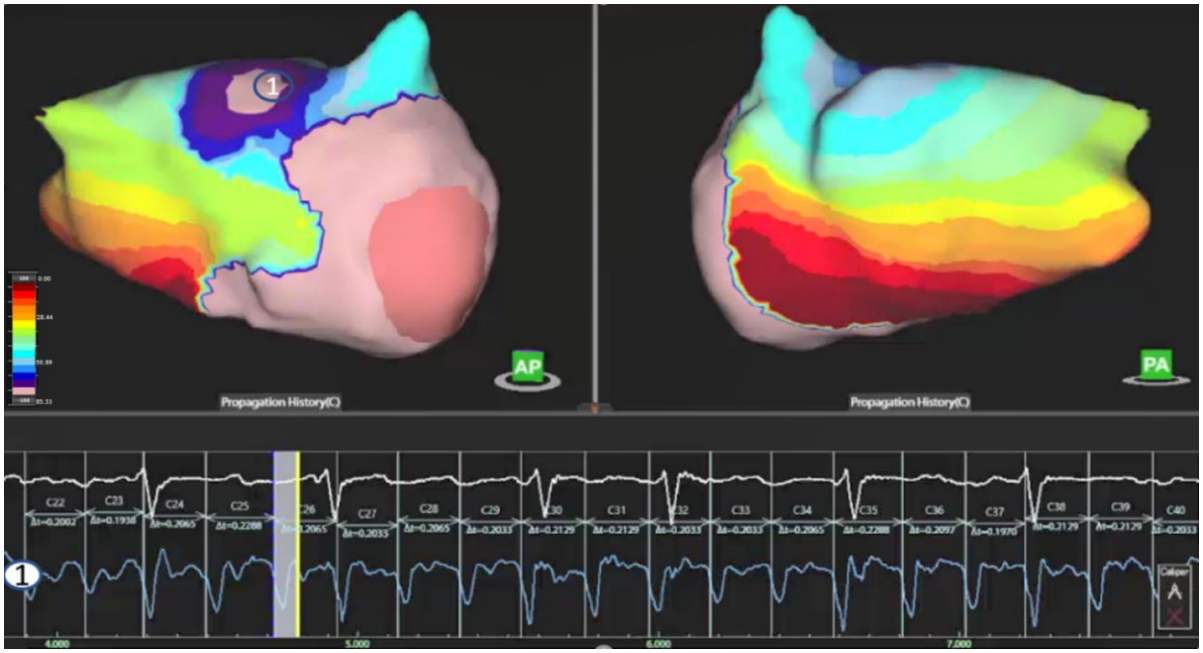

Figure 6.5 Propagation map showing focal driver from the anterior roof with QS signal on the virtual dipole electrogram (1) and cycle length of 208±7.0ms, as illustrated on the recurrence matrix (circled) in figure 3B.

Table 6.2 Results of univariate and multivariate analysis of predictors of acute procedural outcome. AFCL, atrial fibrillation cycle length; FF, focal firing; LIA, localised irregular activation; LRA, localised rotational activation.

Variable	Univariate analysis			Multivariate analysis	
	log odds	AIC	p value	log odds	p value
Recurrence index	20.4	97.0	0.0007	20.15	0.0078
Symbolic dynamics entropy	-5.4794	101.0	0.0007	-0.8570	0.7985
LIA frequency	0.0009	117.0	0.6028	0.0116	0.0779
LRA frequency	-0.0284	102.4	0.0006	-0.0223	0.4124
FF frequency	0.0133	105.9	0.0048	0.0163	0.0937
AFCL	0.0303	111.4	0.0211	0.0257	0.4004

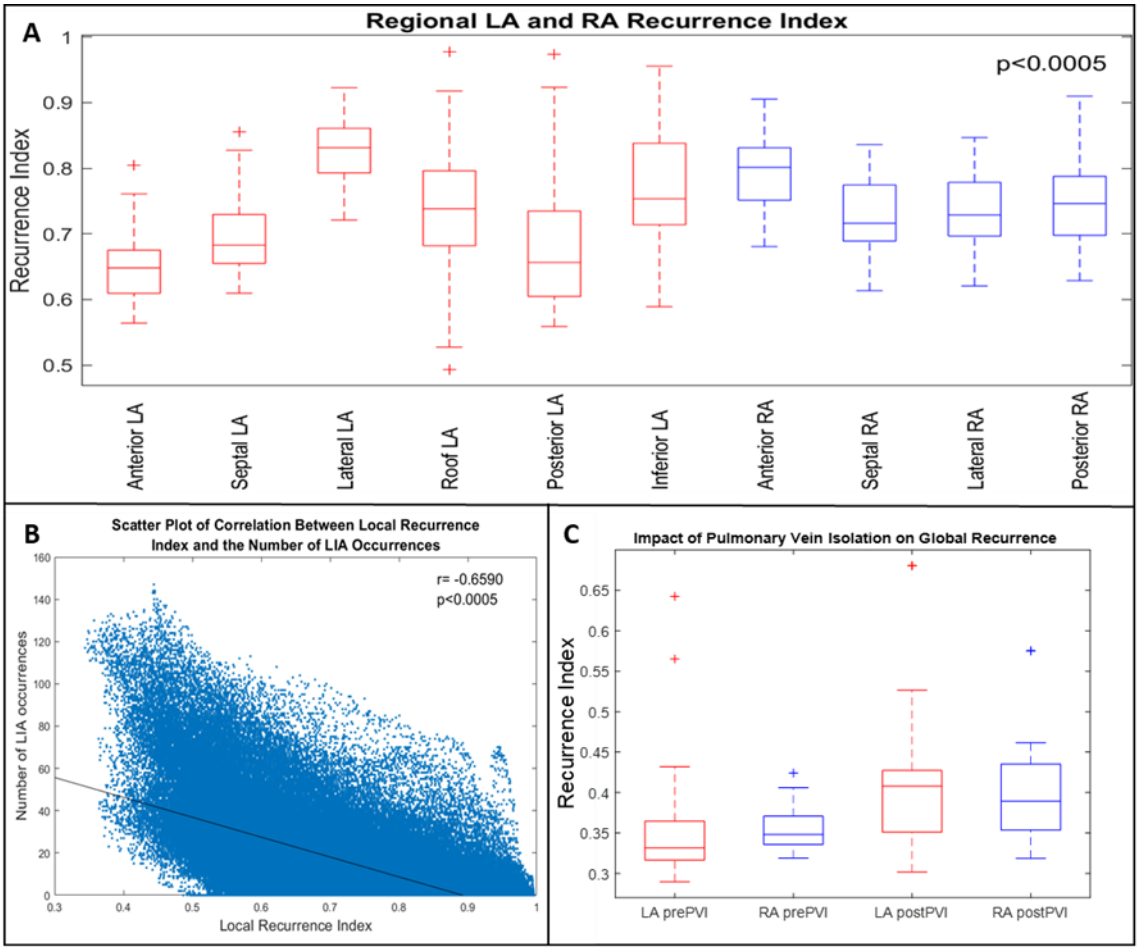

Figure 6.6 Regional recurrence values, correlation with LIA and effect of PVI. Regional recurrence values for the left atrium (red) and right atrium (blue) are shown in (A). (B) shows the correlation between regional recurrence value and the complexity of AF propagation as shown on AcQMap propagation maps measured by the frequency of localised irregular activation patterns in each region. The effect of pulmonary vein isolation of mean recurrence values in the LA and RA is shown in (C).

6.4 Discussion

In this study we have demonstrated the application of recurrence analysis to allow characterisation of AF propagation. Whole chamber recurrence plots reveal patterns of activation within a complex rhythm. The RI can distinguish clinical AF phenotype and is the optimal predictor of acute procedural outcome in both univariate and multivariate analysis. There is significant regional variation of AF complexity identified using recurrence analysis, which strongly correlates with complexity identified using AcQMap propagation maps as defined by the regional frequency of localised irregular activation patterns and SDE. Transient periods with high whole chamber RI coincide with the emergence of a dominant focal mechanism that appears to result in organised activation of the remainder of the chamber.

Handa et al have recently described what they term the “electrophenotype spectrum” responsible for the fibrillatory mechanisms involved in the maintenance of

ventricular fibrillation(244) and propose similar processes in the atrium(245). Whilst a high degree of disruption to gap junction coupling together with compact myocardial fibrosis results in highly disorganized fibrillation, a more organised phenotype sustained by localised drivers is observed in those with patchy interstitial fibrosis and preserved gap junction coupling(245). Atrial fibrosis, whether identified using the surrogate of electrogram voltage amplitude, or non-invasively using late-gadolinium enhanced magnetic resonance imaging (LGE-MRI), is associated with poor outcomes following catheter ablation(83, 98). This is likely to occur via both interruption to myocardial architecture, and by direct intercellular interaction or paracrine effects effecting myocyte electrophysiology(89). Fibrosis is not a binary phenomenon but occurs along a spectrum from interstitial through to dense, compact scar, associated with different arrhythmic potential(90). It follows that additional aspects of the arrhythmogenic substrate, including gap junction coupling and ion handling also cover a broad spectrum and the combination of all these factors results in a range of AF phenotypes in which different mechanisms predominate. The range of recurrence plot characteristics observed in our study supports this hypothesis with the electrophenotypic spectrum extending from more organised repetitive patterns of propagation to highly chaotic and complex appearances.

Superior outcomes from catheter ablation are seen in patients with paroxysmal compared to persistent AF(135, 233, 234). This is likely to represent differences in severity of the arrhythmogenic substrate and therefore differences in fibrillatory mechanisms involved. Differences have also been observed between patients with recurrent persistent AF who maintain a period of SR up to their ablation procedure (following cardioversion) compared to those remaining in AF(235), suggesting either a beneficial effect of a period in SR resulting from reverse re-modelling or a fundamental difference in disease substrate that differentiates those able to maintain SR and those in whom AF spontaneously recurs or cardioversion is unsuccessful. Significant differences in the whole chamber RI were observed between these groups, supporting the concept of different fibrillatory phenotypes that correlated with the underlying atrial substrate.

Whole chamber RI, as a measure of AF organisation, was the best predictor of acute procedural outcome in both univariate and multivariate analysis. This observation remained when excluding patients with paroxysmal AF, all of whom reverted to SR following pulmonary vein isolation alone. It is acknowledged that acute procedural outcomes may not correlate with longer term success and freedom from arrhythmia(235). The ablation approach in this study involved pulmonary vein isolation followed by targeting of regions of interest identified using AcQMap until either SR was achieved or no further ablation targets were identified. Therefore, although inferences about long term outcomes

cannot be drawn, this does support the ability of recurrence matrix analysis to differentiate the electrophysiological phenotype, which is likely to reflect those substrate properties that impact the response to ablation. In addition, these electrophenotypic differences appear to extend beyond those that can be identified according to clinical AF categorisation as either paroxysmal or persistent.

The AcQMap system allows visualisation of whole chamber propagation, depicted as a leading edge of a depolarising wavefront. Complex patterns of LIA have been shown to be highly stable(214) and were used here to quantify regional variation in AF propagation complexity. Regional recurrence analysis correlated well with the degree of complexity measured by the frequency of LIA patterns and SDE.

The whole chamber RI increased in both the LA and the RA following PVI. Wide antral circumferential ablation results in additional substrate modification by incorporating regions of complex myofiber structure at the pulmonary vein-LA junction that may potentiate re-entry(69, 71). Eliminating the impact of the pulmonary veins in AF maintenance may explain the increase in the degree of organisation seen in the LA but does not necessarily account for the effect seen in the RA. The critical mass theory was postulated by Garrey in 1914 following the observation that the fibrillatory potential of myocardial tissue was highly dependent on tissue mass, with the hearts of large mammals much more prone to fibrillation compared to those of rats and mice(48). More recent work in both animal and computer models of fibrillation have corroborated this concept and form the foundation for the surgical Maze procedure(246, 247). Wide antral pulmonary vein ablation results in a reduction in functional atrial volume, which may limit the formation of fibrillatory waves resulting in the increase in organisation evident across both chambers. In addition, there has been considerable interest the role of the autonomic nervous system in AF arrhythmogenesis and incidental ablation of atrial ganglionic plexuses during PVI may account for a physiological “upstream” effect of left atrial ablation that accounts for the increase in right atrial RI that was observed(248).

The greatest clinical utility of this approach may be in the ability to guide individualised treatment strategies. A high RI, in keeping with low AF complexity may reflect a more trigger dependent phenotype that will respond well to pulmonary vein isolation alone or targeting of patient specific non-pulmonary vein triggers or “drivers” if identified. Additional ablation in these patients may provide little modification to fibrillatory mechanisms whilst creating iatrogenic substrate for atrial tachycardias. Low RI suggests more complexity-inducing conduction patterns that sustain AF, requiring ablation aimed at the underlying AF substrate properties rather than upstream drivers/triggers alone

illustrated by a lower likelihood of acute termination in these patients. At the extreme end of the spectrum, an ablation approach may be futile, or require antiarrhythmic drugs in combination with extensive atrial de-bulking that causes such severe loss of atrial contractile function as to counter act the clinical benefits of SR restoration. Regional analysis may be able to guide ablation strategies in combination with concurrent mapping approaches (including identification LIA zones), although the optimal approach would need evaluation in clinical trials. Ablation with an aim of homogenising areas with maximal complexity may prevent wave-break and target localised mechanisms involved in AF maintenance, whilst linear ablation through highly repetitive zones may interrupt AF propagation which repeatedly requires this channel therefore impeding the ability of the arrhythmia to self-sustain.

6.4.1 Limitations

An important limitation is the use of acute ablation response as the primary clinical outcome. The relationship between acute AF termination and long-term freedom from arrhythmia recurrence is unclear. Although the method proposed identifies different patterns of AF propagation, their long-term clinical significance cannot be determined and would require additional larger studies and long-term follow up. In addition, application within a larger cohort of patients is required to confirm these findings within the broader population of patients undergoing AF ablation.

Application of this technique was also limited to recordings obtained using the AcQMap system. The recurrence matrix analysis described is dependent on signals obtained simultaneously over the whole chamber, which is facilitated by this non-contact mapping technique. Whole chamber signal acquisition is possible using contact mapping basket catheters but is limited by issues of chamber coverage and bunching of splines impacting recording resolution(177, 186). Application to signals obtained from body surface potential mapping would allow further evaluation of the applicability of the technique.

6.4.2 Conclusion

The application of recurrence matrix analysis to whole chamber recordings of AF allows identification of different phenotypes that appear to represent the underlying atrial substrate. Regional values correlate well with the complexity of AF propagation seen using AcQMap and whole chamber RI was the best predictor of acute AF termination with ablation. Identifying periods with high organisation may help reveal “drivers” that can be targeted with focal ablation.

7 Clinical Impacts of AcQMap-guided ablation of atrial fibrillation

7.1 Introduction

Previous sections have provided mechanistic insights into atrial fibrillation (AF) using global non-contact charge density mapping (AcQMap, Acutus Medical). Properties of complex localised patterns of activation during AF have been studied providing information of temporal properties of AF propagation key to the practical application of AF mapping to clinical ablation procedures. As discussed in previous sections, charge density has been validated against traditional contact mapping for both signal morphology and timing annotation with the calculation of charge density facilitating resolution of sharper local signals compared to a voltage based approach.(195, 201) The insights provided by work contained in previous sections has informed the application of AcQMap charge density mapping to guide an individualised approach to AF ablation in addition to empiric pulmonary vein isolation (PVI) in clinically indicated procedures performed in our centre.

Evaluation of an AcQMap-guided ablation strategy has demonstrated promising results in terms of both safety and 12-month efficacy outcomes in a recent single arm registry study of patients undergoing first time ablation for persistent AF.(197) Similarly promising success rates have been observed over 24-months of follow up in 40 patients with persistent AF when compared to a propensity matched cohort of patients undergoing an empiric approach of pulmonary vein (PV) and posterior wall isolation (PWI).(249) However, there is a paucity of data on outcomes in “real-world” clinical practice taking into account the complex patients frequently selected for this approach in place of traditional empiric strategies and incorporating advances made through the work outlined in previous sections of this thesis.

This section aims to describe the clinical approach to charge density mapping developed following the work outlined above and outline the clinical outcomes achieved through application of this technique to a broad cohort of consecutive patients undergoing AF ablation guided by this technology in our centre.

7.2 Methods

7.2.1 Study design

This retrospective study included all patients undergoing AcQMap-guided ablation for atrial fibrillation at Oxford University Hospitals NHS Foundation Trust from January

2016 to July 2021. Baseline patient characteristics, procedural and imaging data (transthoracic echocardiography [TTE]) were collected prospectively. Clinical follow-up data was collected from medical notes at discharge, and at the latest follow-up period. The study complied with the Declaration of Helsinki and was registered and endorsed by the institutional audit governance committee (ID 7052). Procedural data was collected for all procedures performed (including patients undergoing repeat procedures), whilst long term efficacy outcomes were measured following the first procedure performed in each patient (where patients underwent more than one AcQMap-guided procedure).

7.2.2 Procedure workflow and electrophysiological mapping

Procedures were carried out under general anaesthetic. With the exception of amiodarone, antiarrhythmic drugs were stopped a minimum of five days prior to the procedure. Venous access was obtained via bilateral femoral vein puncture under direct ultrasound guidance. Heparin boluses were administered prior to trans-septal puncture followed by continuous heparin infusion to maintain an ACT >350-seconds (s). A decapolar catheter (Inquiry, Abbott Medical) was inserted into the coronary sinus through an AcQRef (Acutus Medical) sheath which includes a distal electrode used as a unipolar reference. A contact force sensing ablation catheter (Tacticath, Abbott Medical; or AcQBlate, Acutus Medical) was advanced via an Agilis sheath into the left atrium across the single transseptal puncture site. An AcQGuide sheath (Acutus Medical) was exchanged for the transseptal access sheath over the guide wire and the AcQMap (Acutus Medical) catheter was advanced over a 0.032 guide wire into the LA. Ultrasound was used to reconstruct the LA chamber anatomy as previously described.(196)

In patients attending the procedure in sinus rhythm (SR), AF was induced using burst atrial pacing at the start of the procedure. In patients undergoing re-do procedures and attending in SR, pulmonary vein conduction was assessed prior to AF initiation to identify the need for PV re-isolation. AcQMap recordings of AF propagation were obtained at baseline prior to any ablation for a minimum of 1-minute, and a minimum of two 10-s maps of AF activation were calculated in order to provide sufficient duration to identify stable patterns of activation guided by results outlined in section 4 and previously published.(250) AF activation patterns were analysed both visually and using AcQTrack™ (Acutus Medical) to identify putative sites of mechanistic significance characterised by patterns of complex activation including focal firing (FF), localised irregular activation (LIA) or localised rotational activation (LRA).

7.2.3 Map interpretation and ablation strategy

Maps of AF propagation were initially analysed prior to PV ablation (when required). An impression of global AF activation phenotype is developed based on patterns of whole chamber activation. Whilst some patients demonstrate highly chaotic appearances with little overall organisation and multiple initiating wavefronts, others show semi-organised patterns of activation with multiple broad, planar wavefronts and localised sites of wave-break resulting in fibrillatory conduction. More organised phenotypes may require less additional non-PV ablation compared to those with more complex global activation.

Sites of localised complex activation patterns were first identified during visual analysis focussing on areas of FF, LIA and LRA as well as regions of repetitive isochronal bunching suggestive of slow conduction, often associated with adjacent patterns of changing wavefront direction (LIA or LRA). Use of multiple mapping segments allows identification of those zones with greatest spatiotemporal stability that can be marked on the chamber surface and inform the approach to identification of ablation targets.

Pulmonary vein isolation (PVI) ablation (or re-isolation when required) was carried out incorporating mechanisms identified in proximity to the PV antra. Repeat AF mapping is then conducted, and further non-PV sites identified. Multiple mapping segments are analysed to identify mechanisms with greatest spatial stability both pre- and post-PV ablation.

A hierarchical approach to ablation targets was adopted based on sites of greatest spatial stability over repeat mapping segments both pre- and post-PVI. Where sites of high frequency FF, defined as >1/second were identified these were preferentially targeted, followed by regions of LIA/LRA. The ablation strategy aimed at ablating the core of mechanistic sites and anchoring these to adjacent non-conducting boundaries (termed a core-to-boundary approach, as previously described).(249) Following initial delivery of ablation to non-PV sites, mapping was repeated to confirm effect of the ablation delivered and/or identify further targets for ablation, termed a map-remap approach. This was repeated until AF terminated or no further mechanistic sites were identified. RA mapping and ablation was performed when no mechanistic targets were identified in the LA or if AF remained following elimination of targets in the LA. The number of cores of mechanistic sites ablated in each chamber was recorded.

7.2.4 Outcome definitions

Acute procedural outcomes assessed included termination of AF following ablation, either directly to SR or via an organised atrial tachycardia that was mapped and ablated resulting in SR.

Major procedural complications recorded included any adverse events requiring intervention or resulting in prolonged hospital stay within 30 days of the index procedure.

Arrhythmia recurrences were defined as any detected occurrence of AF or AT lasting more than 30s after a 3-month blanking period detected either on 12-lead ECG, continuous ambulatory monitoring or implantable cardiac device. Continuous monitoring was performed when clinically indicated or if patients were enrolled in parallel research studies mandating their use, as well as in patients with implantable cardiac devices.

7.2.5 Statistics

Categorial variables were expressed as frequency and percentage. Continuous variables, if normally distributed, were presented as mean and standard deviation, or as median and interquartile range for skewed distributions. Fisher's exact test was used to assess the difference between groups in categorical variables. Predictors of acute and long-term outcomes were assessed using binomial logistic regression. Age, months since AF diagnosis, duration of continuous AF prior to the procedure, BMI, LA diameter, left ventricular ejection fraction (LVEF), CHA_2DS_2Vasc score, rhythm at the start of the procedure, number of LA and RA sites ablated, and the need for RA ablation were included in univariate testing. Acute procedural outcome was additionally included in analysis of long-term outcome. Linearity of the continuous variables with respect to the logit transformation of the dependent variable were confirmed using the Box-Tidwell procedure. Statistically significant univariate predictors were included in the multivariate model. Cumulative probability of freedom from arrhythmia recurrence were estimated with the use of the Kaplan-Meier methods.

Significance was set at 0.05 and all the analyses were two-sided. Statistical analysis was performed using R statistical software version 4.0.3 and IBM SPSS version 27.

7.3 Results

7.3.1 Patients included

Baseline characteristics of patients included are outlined in table 7.1. In total, 139 procedures were performed in 129 patients. Of these 129 patients, 77 were undergoing first-time ablation procedures, with the remainder undergoing repeat procedures (where

previous procedures did not use the AcQMap system). The median age of the whole cohort was 64 (quartile 1-quartile 2: 57-70), with a LA diameter of 45mm (40-50) and 29% had a history of heart failure.

Table 7.1 Baseline characteristics of whole patient cohort and those undergoing first time ablation. Statistics presented: median (1st quartile, 3rd quartile); n (%) (BMI; body mass index, CAD; coronary artery disease, DM; diabetes mellitus, HF; heart failure, HTN; hypertension; VHD, valvular heart disease)

Characteristic	Whole cohort, N = 129	First time ablation, N = 77
Age (years)	64 (57, 70)	64 (55.7, 69
Gender		
Female	38 (29%)	25 (32.5%)
Male	91 (71%)	52 (67.5%)
AF Type		
Persistent	118 (91%)	71 (92%)
Paroxysmal	11 (8.5%)	6 (8%)
First time	77 (60%)	77 (100%)
If re-do, number of previous procedures:		
1	31 (24%)	n/a
2	16 (12%)	n/a
3	5 (3.9%)	n/a
HF	37 (29%)	27 (35%)
DM	6 (4.7%)	5 (6.5%)
HTN	59 (46%)	33 (43%)
CAD	11 (8.5%)	5 (6.5%)
VHD	12 (9.3%)	6 (7.8%)
Stroke	1 (0.8%)	0 (0%)
BMI (kg/m^2)	30.0 (25.9, 33.0)	30.0 (25.7, 34)
LA Diameter (mm)	45 (40, 50)	43 (39, 50)
Ejection Fraction	55 (50, 60)	55 (50, 60)
Time since AF diagnosis (months)	40 (24, 66)	36 (19, 48)
Time in continuous AF (months)	4.0 (1, 8)	6 (3, 9)
AF at procedure start	76 (59%)	46 (60%)
Previous antiarrhythmic drugs:		
Class 3	50 (39%)	36 (47%)
Class 1	13 (10%)	8 (10%)
CHA_2DS_2VASc	2 (1, 3)	1 (1 ,3)
0	27 (21%)	15 (19%)
1	36 (28%)	24 (31%)
2	25 (19%)	18 (23%)
3	24 (19%)	11 (14%)
4	(9.3%)	6 (8%)
5	3 (2.3%)	3 (4%)
6	1 (0.8%)	0 (0%)
7	1 (0.8%)	0 (0%)

Table 7.2 Procedural findings and linear lesions delivered. CTI, cavotricuspid isthmus; PLMI, posterolateral mitral isthmus; other abbreviations as in text.

Procedural findings	n (%)
If re-do procedure, number of veins reconnected (n=62)	
0	33 (53%)
1	10 (16%)
2	11 (18%)
3	3 (5%)
4	5 (8%)
Linear ablation performed:	
PLMI Line	21 (16%)
Roof Line	42 (33%)
CTI	36 (28%)
Number LA cores ablated	
0	17 (13%)
1	17 (13%)
2	27 (21%)
3	40 (31%)
4	21 (16%)
5	6 (4.7%)
6	1 (0.8%)
RA Mapped	57 (44%)
Any RA cores ablated	32 (25%)
Number RA cores ablated	
1	11 (9%)
2	15 (12%)
3	6 (4%)

7.3.2 Procedural characteristics and acute outcomes

The median number of propagation pattern cores ablated across both the LA and RA was 3 (2-4). This was significantly higher in patients undergoing re-do procedures (3 [2-5]) compared to first time procedures (2 [1-3.25]), p<0.0005. RA mapping was performed in 44% of procedures with ablation of RA mechanisms delivered in 25% of all procedures. In patients undergoing first time ablation, RA mechanisms were ablated in 13% versus 42% in patients undergoing re-do procedures, p<0.0005. The median fluoroscopy time for all procedures was 27 minutes (21.5-34). Additional procedural details are included in table 7.2.

Acute AF termination following ablation occurred in 48% of cases but was significantly higher (78%) in patients attending the procedure in sinus rhythm and in whom AF was induced compared to patients in AF at the start of the procedure (26%), p<0.0005.

There was no difference in the rate of acute AF termination between patients undergoing first time procedures versus re-do procedures (52% vs 44%, p=0.3937).

Univariate predictors of acute AF termination with ablation are outlined in table 7.3. Increasing LA diameter and longer duration of continuous AF were significant predictors of requiring DCCV to restore SR (p=0.005 and p<0.0005 respectively), whilst being in SR at the start of the procedure strongly predicted AF termination with ablation (OR 10.00 [4.3 – 23.0], p<0.0005). Fewer LA and RA cores ablated predicted AF termination with ablation. In multivariate analysis only duration of continuous AF (OR 0.84, 95% CI 0.75 – 0.95) and being in SR at the start of the procedure (OR 4.9, 95% CI 1.9 – 12.6) remained significant (p=0.006 and p=0.001 respectively).

Table 7.3 Univariate and multivariate predictors of acute procedural outcome.

Variable	Univariate analysis		Multivariate analysis	
	OR (95%CI)	p value	OR (95%CI)	p value
LA diameter (mm)	0.93 (0.88 – 0.98)	0.005	0.98 (0.92 – 1.05)	0.533
Duration of continuous AF (months)	0.80 (0.72 – 089)	<0.0005	0.85 (0.75 – 0.95)	0.006
SR at baseline	10.00 (4.3 – 23.0)	<0.0005	4.91 (1.92 – 12.55)	0.001
Number LA cores ablated	0.59 (0.44 – 0.78)	<0.0005	0.72 (0.51 – 1.02)	0.062
Number RA cores ablated	0.62 (0.40 – 0.97)	0.034	1.57 (0.48 – 5.11)	0.458
Any RA ablation	0.38 (0.16 – 088)	0.024	0.32 (0.03 – 3.60)	0.354

7.3.3 Major procedural complications

A total of 7 (5%) major procedure-related complications were observed (table 7.4). Pericardial effusion requiring drainage occurred in 4 procedures, in 3 patients. One patient who was undergoing his 3rd and 4th procedures for recurrent AF (initial procedures not AcQMap guided) had particularly challenging anatomy for trans-septal puncture and suffered an effusion during both procedures (despite trans-oesophageal echocardiography guidance). One patient was also undergoing right atrial contact mapping using a circular mapping catheter which became entangled in the tricuspid valve apparatus resulting in damage to the chordae and severe tricuspid regurgitation requiring subsequent surgical repair.

*Table 7.4 Rates of major procedural complications. *Requiring transfusion and prolonged hospitalisation*

Complications	n (%)
Pericardial effusion requiring drainage	4 (2.9)
TIA	1 (0.7)
Groin haematoma*	1 (0.7)
Tricuspid valve injury	1 (0.7)

*Table 7.5 Long term procedural outcomes. *Including only patients with a minimum of 12m follow up*

	Long term outcomes	N (%)
All patients	Any AF/AT recurrence at end f/u	50 (39)
	Any AF/AT recurrence at 12months	40 (31)
	Any AF/AT recurrence at end f/u*	43 (50)
	Any AF/AT recurrence at 12months*	33 (38)
	AF recurrence at end f/u	32 (25)
	AF recurrence at 12months	27 (21)
	AF recurrence at end f/u*	25 (29)
	AF recurrence at 12months*	20 (23)
De-novo ablation only	Any AF/AT recurrence at end f/u	28 (36)
	Any AF/AT recurrence at 12months	23 (30)
	Any AF/AT recurrence at end f/u*	32 (58)
	Any AF/AT recurrence at 12months*	23 (42)
	AF recurrence at end f/u	20 (26)
	AF recurrence at 12months	16 (21)
	AF recurrence at end f/u*	17 (31)
	AF recurrence at 12months*	13 (24)

7.3.4 Long term outcomes

Median follow up duration was 20-m (9-38) and a period of continuous rhythm monitoring was performed in 58% of patients. Results are detailed in table 7.5. At the end of follow up, recurrent arrhythmia (AF or AT) was detected in 39% of patients, including paroxysmal AF or AT in 13% (figure 7.1). Recurrent AF was detected in 25%. Over 12-m of follow up, 31% of patients experienced recurrent arrhythmias, including recurrent AF in 21%. In patients undergoing first time procedures only, at latest follow up recurrent arrhythmias occurred in 36%, including AF in 26%. At 12-m, 26% and 21% of patients experienced any arrhythmia recurrence and AF recurrence, respectively. Kaplan-Meir curves are shown in figures 7.2-7.7.

Increasing LA diameter was a significant predictor of arrhythmia recurrence (OR 1.053, 95% CI 1.002 – 1.107, p=0.042) and remained significant when analysed for only

AF recurrence (OR 1.056, 95% CI 1.000 – 1.115, p=0.048). No other measures, including acute AF termination with ablation, were significant predictors of either AF/AT recurrence or AF recurrence, in either the whole cohort or patients undergoing first time ablation procedures.

At latest follow up, 88% of patients were in SR, 11% in AF and 2% in AT, with 17% of patients taking antiarrhythmic drugs (7% class 1, 10% class 3). Repeat ablation procedures were carried out in 19% of patients.

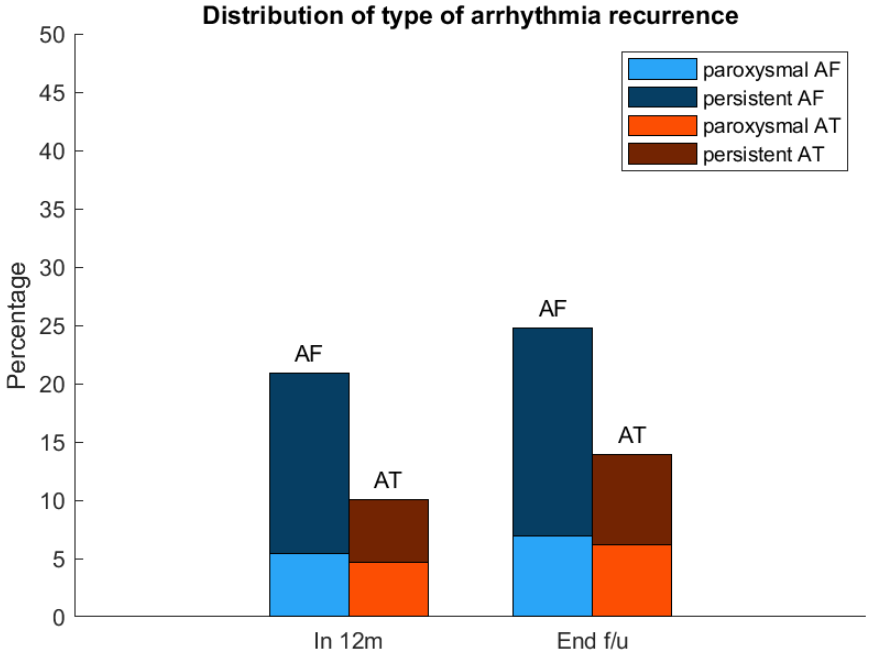

Figure 7.1 Distribution of type of arrhythmia recurrence over the first 12m and whole follow up period.

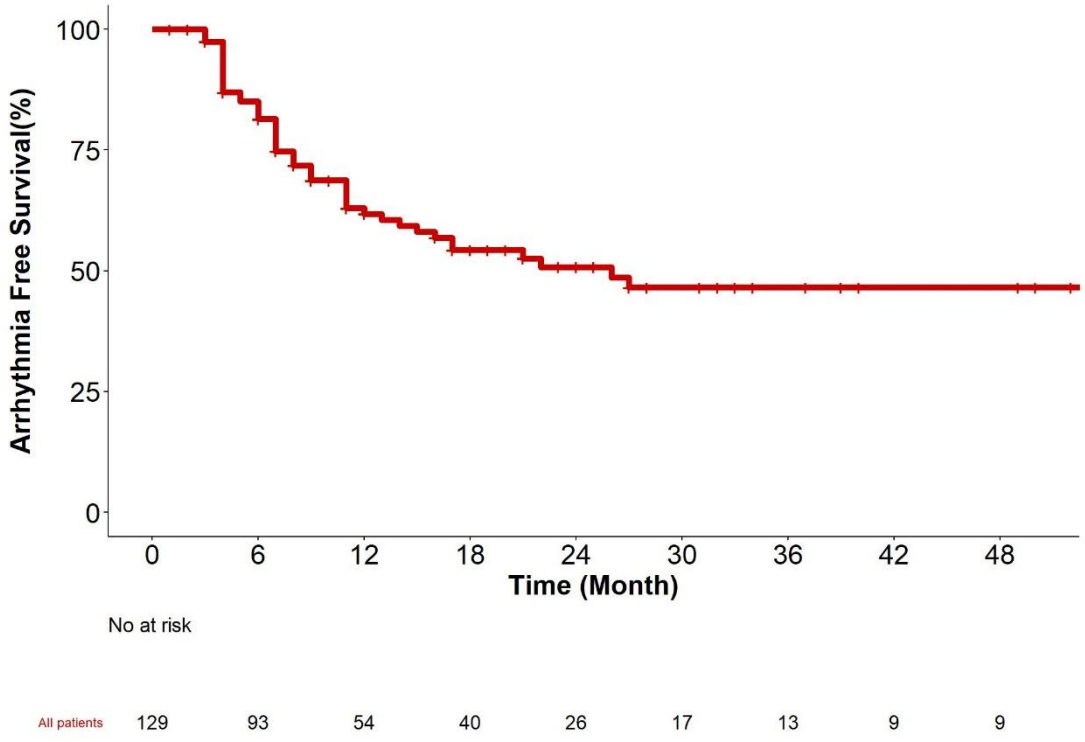

Figure 7.2 Kaplan-Meier curve for any arrhythmia recurrence over the whole follow up period.

7.4 Discussion

In this analysis of "real-world" AcQMap guided AF ablation, major adverse events occurred in 7 out of a total of 139 procedures. Acute AF termination following ablation ocurred in 48% of procedures but was significantly higher in patients in whom AF was induced (78%) compared to those arriving in AF (26%); p<0.0005. Over a median follow up period of 20-m, recurrent arrhythmias were observed in 50 patients (39%), and at 12-m of follow up 40 (31%) of patients experienced arrhythmia recurrence. In patients undergoing first time ablation procedures, arrhythmia recurrences were observed in 30% at 12 months and 36% at latest follow up.

UNCOVER-AF is the largest trial to date evaluating the outcomes of AcQMap guided ablation in patients undergoing first time procedures for persistent AF, but excluded patients with long-standing persistent AF, LA diameter >50mm or LVEF<40%. At 12 months, freedom from AF/AT on or off antiarrhythmic drugs was achieved in 69.2%, with freedom from AF alone in 72.5%.(197) Similar efficacy outcomes observed in the broad cohort of patients included in this study provide further data in support of this approach.

Improving outcomes in AF ablation has proved challenging, with addition of linear lesions or targeting of complex fractionated electrograms delivering no additional benefit

beyond empiric isolation of the pulmonary veins in randomised controlled trials.(135) This has led to concerted efforts to identify novel strategies, either targeting electrophysiological mechanisms thought to represent “drivers” identified using electrophysiological mapping technologies,(126, 184) or by developing further empiric approaches including targeting the LA posterior wall, left atrial appendage (LAA), or ligament of Marshall (LOM).(151, 158, 163, 164) Differences in characteristics of patients recruited to individual studies make direct comparisons unreliable. However, the results in our cohort appear to compare favourably. In the “Substrate and Trigger Ablation for Reduction of Atrial Fibrillation-2” (STAR-AF2) trial, 41% of patients who underwent PVI alone experienced recurrent arrhythmia at 18-m follow up.(135) The cohort included in our analysis was older (64 vs. 58ys), and a higher proportion had a history of heart failure (29% vs. 4%). The VENUS trial evaluated a strategy of additional ethanol ablation of the LOM, resulting in an arrhythmia recurrence rate of 51%.(164) The BELIEF trial (in patients with longstanding persistent AF) analysed the addition of LAA isolation to PVI in addition to PWI, septal and coronary sinus ablation as well as isoprenaline induced trigger ablation, with an arrhythmia recurrence rate in the LAA isolation arm of 44% at 12-m.(158) In a randomised comparison of LA PWI in addition to PVI, versus PVI alone, the addition of PWI resulted in an arrhythmia recurrence rate of 26.5% at mean follow up of 16.2 months.(151)

Additional empiric approaches involve ablation over a large surface area in all patients, yet PVI alone is effective in nearly half of patients undergoing ablation for persistent AF. This suggests that using a broad empiric approach exposes a significant proportion of patients to unnecessary additional ablation. The impacts of extensive LA ablation are poorly understood but include the potential for stiff atrial syndrome.(251) An individualised approach has the potential to allow tailoring of ablation specific to the mechanisms involved in individual patients. The median number of sites targeted in this cohort was 3, with an interquartile range of 2-4, but a higher number in patients undergoing re-do procedures suggesting a more complex non-PV AF substrate in these patients. The majority of trials are conducted in patients undergoing ablation for the first time, with a paucity of data in patients undergoing repeat procedures. Although patients undergoing repeat procedures for recurrent AF frequently have reconnected pulmonary veins, durable PVI is demonstrated in a significant proportion, suggesting non-PV mechanisms responsbile for AF initiation and maintenance.(252, 253) The more complex AF substrate in this patient population creates a particular challenge for ablation strategies, highlighted by lower rates of arrhythmia recurrence when only patients

undergoing first time procedures were analysed. However, further understanding of AF mechanisms are needed before realising the full benefit of this approach.

One of the challenges of an AF-mapping guided approach to individualised AF ablation is an appropriate procedural end point. Ablation resulted in a rate of acute AF termination of 48%, with fewer conduction pattern cores ablated in patients achieving SR. However, acute AF termination did not significantly predict long term freedom from recurrent arrhythmia and was strongly affected by whether AF was induced prior to mapping and ablation. Similar findings have been observed with other techniques. Both linear ablation and ablation of complex fractionated electrograms resulted in higher rates of acute AF termination (22% and 45% respectively) compared to PVI alone in the STAR-AF2 trial, but did not translate to improved outcomes.(235) We did not routinely perform AF induction following termination meaning that patients without AF termination underwent additional map and ablate cycles until elimination of all mechanistic sites. In UNCOVER-AF, increasing number of activation patterns ablated was predictive of long term freedom from arrhythmia recurrence, which may suggest that elimination of all activation pattern mechanisms rather than continued incremental ablation aiming for SR restoration is a more approriate target end point.(197) Although number of activation patterns ablated did not predict long term outcomes in our cohort, we quantified the number of ablation cores delivered rather than the number of discrete activation patterns included, which may account for this difference, bearing in mind the potential for co-localisation of multiple mechanisms at discrete or closely neighboring sites.

Although AF termination doesn't appear to predict long term arrhythmia freedom, it does suggest successful acute modification of mechanisms sustaining fibrillation and therefore provides a degree of indirect validation of the mechanistic importance of activation patterns identified. The pathophysiology of AF is poorly understood, but appears to involve complex interdependent processes of structural and electrical remodeling resulting in a vulnerable substrate able to sustain AF following initiation by ectopic triggers.(89) Recurrent arrhythmia following ablation can therefore result from either failure of ablation allowing ectopic triggers to re-initiate AF (i.e. reconnection of isolated pulmonary veins),(252) failure of the ablation approach to target the relevant mechanistic processes, a lack of durability or effectiveness of ablation delivered to mechanistically appropriate non-PVI targets, or a progression of the disease substrate since the index procedure.(254) Improving clinical outomes therefore requires advancement in all of these areas, with arrhythmia recurrences not necessarily indicating a failure of the ablation strategy alone.

The main limitation of this study is the lack of a control arm and randomisation of treatment strategy. Without this, it is not possible to determine the true incremental benefit of an individualised AcQMap guided approach in comparison to alternative strategies. However, it does provide background data to inform the design of future randomised controlled trials. In addition, the inclusion of a heterogenous group of patients underoing first time procedures as well as re-do, and even 3rd/4th time procedures limits the generalisability to any specific group. In addition, strict rhythm monitoring was not performed in all patients, but rather was included in assessment of recurrences when performed. Increasing rhythm monitoring will result in greater sensitivity to detect additional asymptomatic episodes and continuous monitoring to allow robust measurements of AF burden may provide a more clinically useful measure of procedural success.

In conclusion, this represents a report of the results of a real-world series of patients undergoing AcQMap guided ablation of symptomatic AF in a large UK tertiary centre. Major procedural complications ocurred in 5% of procedures. Over a median follow up period of 20-months, recurrent arrhythmias were observed in 39% of patients, and in 36% in patients undergoing first time ablation procedures. Further randomised controlled trials are needed to fully evaluate the clinical benefit of this approach.

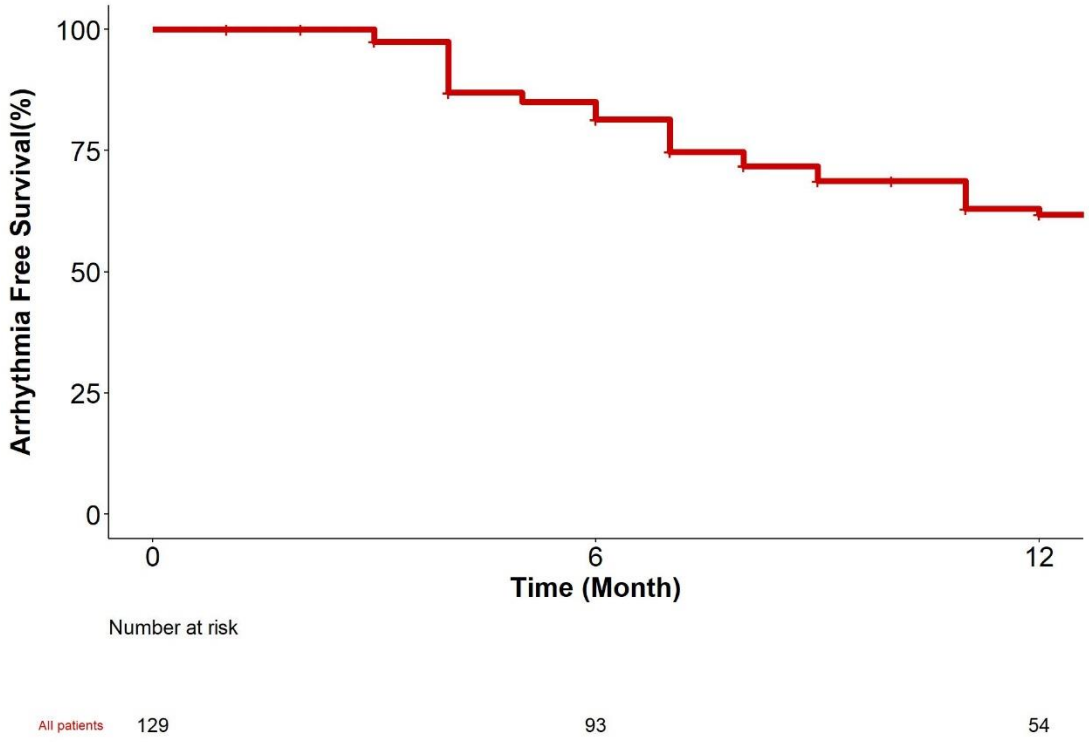

Figure 7.3 Kaplan-Meier curve for any arrhythmia recurrence at 12 months.

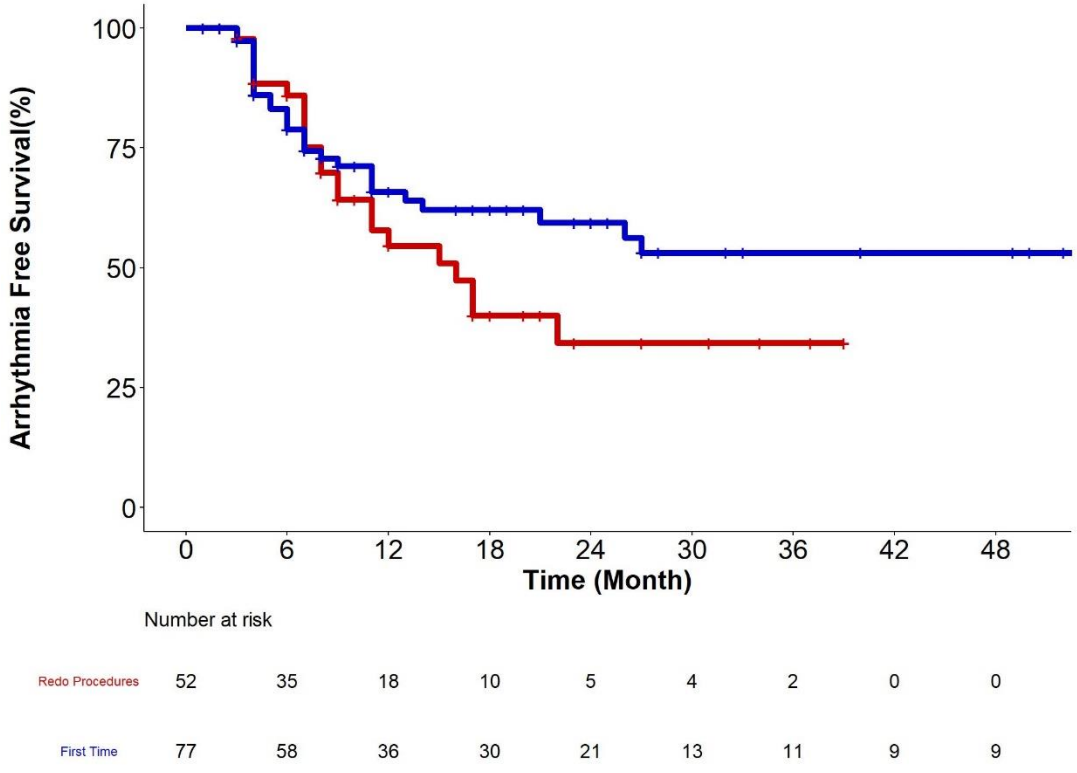

Figure 7.4 Kaplan-Meier curves for arrhythmia free survival in patients undergoing first time and redo procedures over the full follow up period.

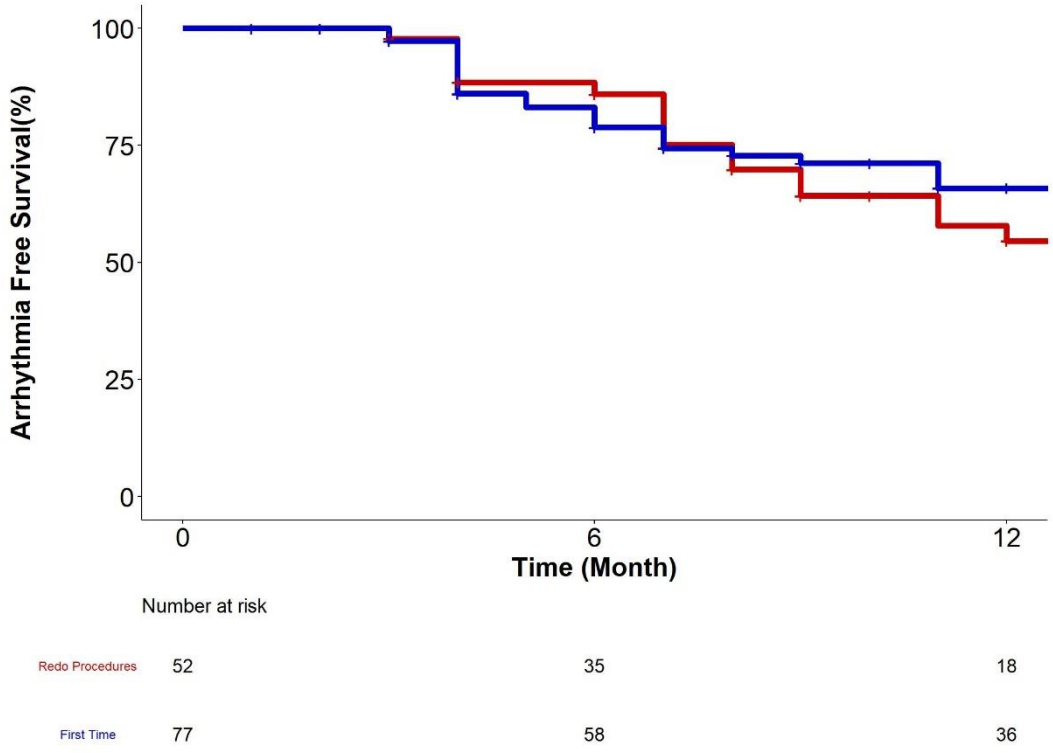

Figure 7.5 Kaplan-Meier curves for arrhythmia free survival in patients undergoing first time and redo procedures over 12m follow up.

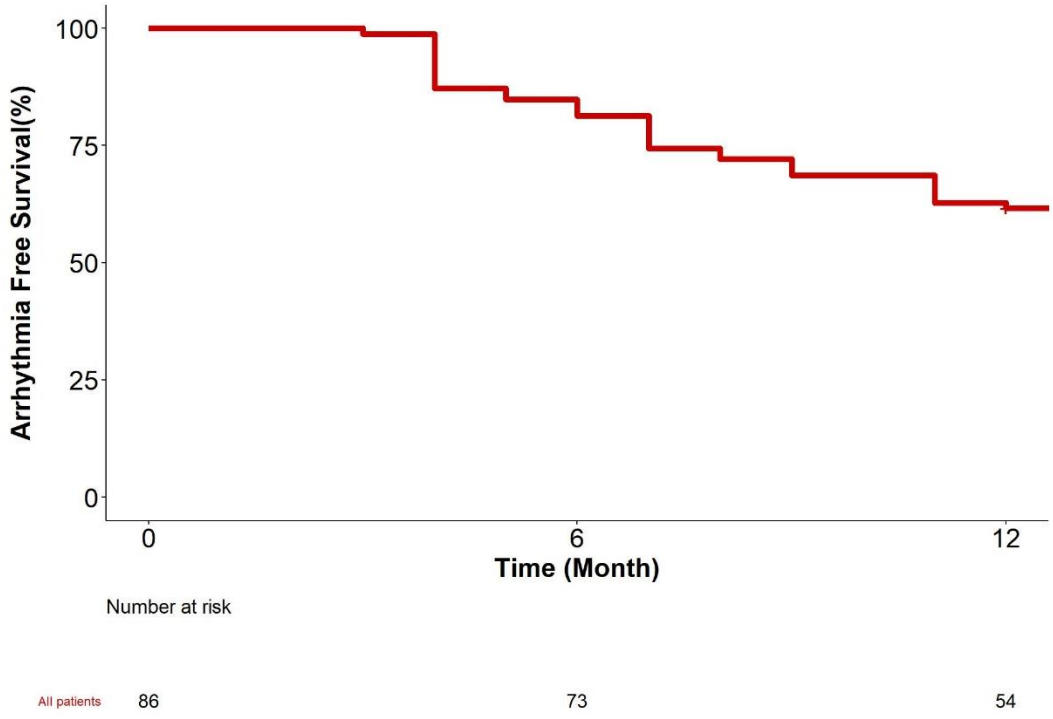

Figure 7.6 Kaplan-Meier curve for any arrhythmia recurrence at 12 months, only including patients with a minimum of 12-months follow up.

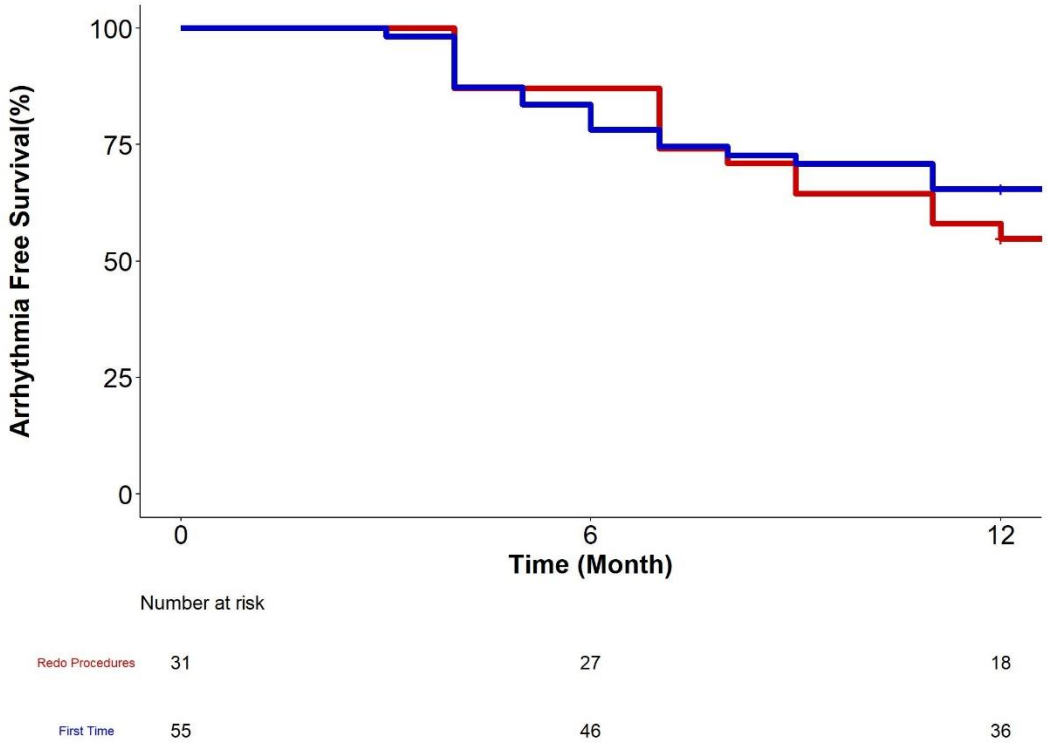

Figure 7.7 Kaplan-Meier curves for arrhythmia free survival in patients undergoing first time and redo procedures over 12-months follow up only including patients with a minimum of 12-months follow up.

8 Conclusions and further work

8.1 Introduction

Strategies for ablation of non-pulmonary vein mechanisms in atrial fibrillation are based around either empiric approaches applying anatomically-based ablation to all patients or individualised approaches based on identification of patient-specific mechanisms. Individualised approaches rely either on identification of electrophysiological mechanisms revealed using electroanatomic mapping tools or delineation of patient-specific fibrotic substrate revealed using non-invasive late gadolinium enhanced magnetic resonance imaging or invasive electroanatomic voltage mapping.(84, 97, 126, 183, 219, 225) In contrast to individualised approaches, empiric strategies assume common mechanisms ubiquitous within the whole patient population. Pulmonary vein isolation ablation is the cornerstone of empiric ablation of AF and is effective in a significant proportion of patients, even with persistent forms.(135) It is therefore inevitable that empirically delivering additional non-pulmonary vein ablation in all patients will include unnecessary therapy, with the associated risk of complications. The potential to individualise therapy is therefore highly attractive.

The major obstacles to the adoption of individualised approaches include limitations in understanding of the mechanistic processes involved in AF initiation and maintenance, and the development of technology able to accurately map fibrillatory conduction. Efforts to advance mechanistic understanding resulted in recognition of the role of atrial scar in the fibrillatory substrate both through direct effects on atrial structural properties and therefore conduction, and through indirect effects on atrial electrophysiological properties.(89) Ablation of regions of atrial fibrosis therefore appears attractive. However, identification of the atrial fibrotic substrate serves more as a surrogate rather than directly revealing areas of mechanistic importance. It is not clear to what extent atrial fibrosis serves as a marker of disease substrate or severity, rather than representing the sites mechanistically key to the mechanistic process. Results of recent randomised trials evaluating the ablation of fibrotic regions identified by cardiac MRI are not encouraging.(255) However technical challenges remain in identifying the fibrotic substrate either invasively or non-invasively and overcoming these may yield advances in mechanistic understanding and, subsequently, ablation approaches.

One of the challenges to technological advancement of electroanatomic mapping of AF has been the inherent limitations of applying traditional techniques of sequential electroanatomic mapping to a rhythm that is characterised by significant variability in

activation between cycles, in contrast to organised atrial rhythms that permit sequential collection of data points that can be aggregated to reveal arrhythmia mechanisms. Although basket catheters, as used for FIRM mapping and in other studies,(184, 187) attempt to overcome this by collecting data from multiple electrodes distributed across the endocardial surface, true global mapping with this approach is not achieved due to insufficient chamber coverage.(177) Non-contact mapping approaches overcome this limitation facilitating panoramic visualisation of whole chamber activation. Recent advances in this technology have been realised with the development of the AcQMap system, which was in the early stages of clinical evaluation at the time of commencement of this work. At this point, no work had been done exploring the application of this technology to the mapping of AF with a view to guiding its practical application and gaining insights to mechanisms of AF, crucial to informing the development of ablation strategies that can then be fully evaluated in randomised clinical trials. This therefore formed the basis of the work contained within this thesis in which methods applied to mapping data acquired are developed followed by practical studies that explore the properties of activation patterns identified. A unique study was undertaken applying this technology to conduct simultaneous bi-atrial mapping and provide insights into the role of inter-atrial communication during AF propagation. A novel technique was then developed to analyse whole chamber recordings of AF and lastly an evaluation of clinical outcomes of procedures guided by charge density mapping and informed by the findings of the above work is outlined.

8.2 Original contributions and implications of work presented

8.2.1 Impact of adenosine on AF activation

In chapter 3, the effect of adenosine on AF propagation was explored. This work has been published.(256) The ionic effects of adenosine have long been recognised and the effect of adenosine on AF mechanisms has attracted interest in part due to similarities between the mechanism of cholinergic atrial stimulation and the mechanism of action of adenosine on atrial electrophysiology. The interest in the potential role of high frequency re-entry sources responsible for AF ignited further interest in this field. Early studies applied dominant frequency mapping, whilst recently more advanced mapping techniques have been applied both ex-vivo and in-vivo. An important hypothesis generated by previous work has been that adenosine is able to reveal re-entry sources and therefore help guide identification of ablation targets.

Although previous studies have shown an effect of adenosine on accelerating AF, this study was the first to incorporate a whole chamber measure of adenosine effect using

both cycle length and dominant frequency. Adenosine was shown to accelerate AF when measured either using whole chamber mean AFCL or dominant frequency. This acceleration appeared to be a global effect rather than selectively impacting localised mechanisms, evidenced by a reduction in the variance of AFCL across the chamber.

The direct effect on dynamic patterns of wavefront propagation is also presented and shows that adenosine promotes rotational activation, but this effect is on the whole chamber rather than revealing stable sites that may be considered localised sources of AF maintenance. 81% of LRA sites identified with adenosine were at sites of repetitive LIA on baseline maps. This refutes some of the findings of recent studies and does not support the hypothesis that adenosine can be used to reveal novel targets for AF ablation. Instead, these results suggest that the degree of rotational activation observed may serve as a marker of atrial electrophysiological properties, particularly refractoriness, that results in a higher degree of directional change in propagation thereby satisfying the definition of LRA with rotation of >270°. This is important to consider when using adenosine to exclude far-field ventricular signals during AF mapping. Sites of rotational activation detected during these periods are likely to reflect the pharmacological effect of adenosine, with ablation of these regions unlikely to yield improved clinical benefits. In contrast, adenosine has no significant effect on frequency of LIA or FF. Where adenosine is required to aid acquisition of non-contact recordings then identification of regions of repetitive LIA and FF should be considered a robust representation of the underlying AF electrophysiological substrate.

Dominant frequency mapping has been proposed as a tool to identify high frequency AF re-entry sources, defined as sites of highest dominant frequency. However, this is a surrogate measure and has not been applied alongside dynamic activation mapping. I present results of whole chamber DF mapping applied to charge density signals compared to sites of repetitive LRA. At baseline, only 33% of high DF sites correlated with sites of LRA, reducing to only 27% following adenosine injection. The poor correlation of high DF sites with regions of LRA refutes previous hypotheses that sites of highest DF represent high frequency re-entry sources of AF and may explain the lack of success of randomised trials aimed at ablating sites of highest DF.

8.2.2 Spatiotemporal stability of AF activation patterns

In chapter 4, this thesis explores the spatiotemporal properties of complex localised patterns of activation in both the LA and RA. This work has been published,(250) with an accompanying editorial discussing the implications of the findings.(257)

Animal studies were the first to suggest stable localised activation patterns during AF, with the subsequent development of in-vivo tools for AF mapping seeking to guide ablation of these sites. Focus has been on rotational and focal mechanisms, in part due to technical limitations of tools to further characterise AF activation. Patterns of partial rotation have been identified using activation mapping but have not been well characterised.

As well as sites of rotational and focal activation, charge density mapping reveals sites of irregular activation (LIA), not previously explored. Development of a successful approach to AF mapping and ablation using this technology requires an understanding of both the spatial and temporal properties of these patterns. The work outlined in chapter 4 covers both issues, suggesting a minimum period of mapping required to reveal stability of each pattern and quantifying the consistency of these sites over time. Important findings of this work are both the lack of stability of LRA sites, and the high stability of both LIA sites and high frequency focal firing in both the LA and the RA. Furthermore, high frequency focal sites stabilise earlier following pulmonary vein isolation, suggestive of greater stability in non-pulmonary vein sites of focal firing. LIA zones did not correlate with dense scar as assessed using contact bipolar voltage mapping but did show increased conduction heterogeneity brought about using close coupled extra-stimulus pacing. No work has previously been done examining these issues using charge density mapping, with only limited studies exploring similar questions using other mapping technologies.

Although reduced bipolar voltage amplitude was not observed at sites of repetitive LIA, the high spatial stability of these sites suggests a relationship to underlying atrial structural properties. In the introduction, methods to identify the structural atrial substrate using both electroanatomic voltage mapping and non-invasive imaging are discussed. Although more advanced substrate identified using these approaches is associated with worse clinical outcomes, this is not a strong predictor, whilst the majority of patients do not demonstrate significant areas of low voltage. In addition, fibrosis identified by these means and electrophysiological mechanisms are poorly correlated. AF propagation must therefore be maintained independent of dense fibrotic mechanisms. Sites of stable LIA may reflect more subtle structural properties such as myo-fibre orientation (anisotropic conduction), disarray or interstitial fibrosis that result in fibrillatory conduction.

The development of techniques to identify patterns of focal and rotational activation, or re-entry, during AF, resulted in a temptation to ablate these sites. The ability of non-contact charge density mapping to identify these patterns, as well as additional sites of complex activation such as LIA results in similar temptations. However, to justify

ablation, mechanisms must be spatially stable and consistent. The findings outlined in this chapter therefore serve to argue against a strategy of targeting LRA zones, in favour of sites of LIA and high frequency focal firing, with the use of mapping durations of a minimum of 20s to facilitate accurate identification of these mechanisms.

8.2.3 Insights into bi-atrial mechanisms of AF propagation

Following the work outlined in chapter 4 exploring spatiotemporal properties of AF activation, further analysis was performed exploring the relative roles of the left and right atrium and inter-atrial communication during AF. Much of the focus in AF ablation and in understanding AF mechanisms has been on the left atrium. Relatively little work has been done characterising mechanisms in the RA. Very few studies have performed simultaneous bi-atrial mapping, with none previously attempting to define patterns of interatrial communication during AF.

The channel of communication between atria was defined using mean phase coherence and activation time differences across this channel were used to identify the direction of propagation between chambers. It was observed that the predominant pattern is one of balanced propagation between chambers with a dominant leading chamber identified in a minority of patients. Furthermore, where a dominant chamber was recognised this was as often the RA as the LA. In addition, the bi-atrial electrophysiological substrate was quantified through analysis of patterns of LIA, LRA, FF, whole chamber AF cycle length, and voltage mapping. The contribution of these measures was assessed in relation to AF type, rhythm at the start of the procedure and acute AF termination with ablation. A spectrum of AF phenotypes was identified according to the relative of balance of LRA and FF. Patients with paroxysmal AF and persistent AF but in SR at the time of the procedure (following DCCV) demonstrated a phenotype characterised by a high frequency of focal firing and less LRA, in contrast to patients with persistent AF in whom more LRA mechanisms were observed in conjunction with a shorter AFCL. These differences were most marked in the RA, rather than the LA, and RA measures, not LA measures, predicted AF termination with ablation.

These findings are important in suggesting a substantial role of the RA in AF maintenance, at least in a significant proportion of patients, particularly those with more persistent forms of AF. It is not clear whether the existence of RA mechanisms is responsible for AF progression, or progression of AF itself results in secondary electrophysiological remodelling of the RA, which then serves as a marker of more advanced disease. However, the results suggest a greater role of the RA than previously recognised and may explain, at least in part, the limited progress achieved with strategies

focused on LA ablation, particularly in patients with persistent and long-standing persistent AF. In addition, theories of AF mechanisms based around localised drivers are based largely on the existence of high frequency sources responsible for downstream atrial activation and fibrillatory conduction. If this theory is correct, the results presented suggest these sources are likely to be evenly distributed between chambers rather than restricted predominantly to the LA, and more focus should be placed on RA mapping in efforts to target localised sources. This may explain the results of prior dominant frequency mapping studies that suggested a lack of DF gradient in patients with persistent AF. Importantly however, even where a dominant chamber was identified, high frequency "drivers" were not observed as the mechanism responsible.

The observation that increasing LRA as well as shorter AFCL are observed in patients with persistent AF and appear to predict a need for DCCV to restore SR must also be interpreted in the context of the results presented in chapters 3 and 4. In these preceding chapters it is shown that adenosine causes functional electrophysiological changes that result in shorter AFCL and increased rotational activation, whilst LRA is spatially and temporally unstable. In results of bi-atrial electrophysiological substrate quantification, increasing LRA was found in patients with persistent AF acutely refractory to ablation. This suggests that rotational conduction during AF, as revealed using charge density mapping, is likely to reflect the functional electrophysiological properties of the atrial tissue, and perhaps the degree of electrical remodelling that has occurred, rather than representing primary mechanisms key to the maintenance of AF. If this is the case, ablation aimed at rotational mechanisms is unlikely to result in clinical benefit.

There was no difference in measures of LIA either between AF clinical phenotypes or between chambers. LIA was the predominant pattern of localised activation occurring at greater frequency and for longer durations than either FF or LRA. In the context of the results presented in chapter 4 this supports the hypothesis that LIA represents structural atrial properties that are shared across patients with AF rather than reflecting the electrophysiological properties of individual patients or AF phenotypes.

8.2.4 Recurrence matrix analysis

In chapter 6, I outline the development of a novel tool for the analysis of AF activation, which was applied to AF signals acquired during the simultaneous bi-atrial mapping described in previous chapters. The data presented up to this point focusses on localised patterns of complex conduction, which is also the focus of most previous studies of AF mapping which aim to identify targets for focal ablation. In this chapter I outline the development and investigation of a new technique to characterise whole chamber

activation patterns and quantify AF complexity. This technique is extended to explore assessment of local complexity compared to the results of propagation history maps and LIA frequency.

Although recurrence matrix analysis has been used previously in complex dynamical systems, it has never been applied to whole chamber recordings of AF. I outline the development of a custom programme to perform this analysis which was retrospectively applied to the dataset obtained from simultaneous bi-atrial mapping. A measure of global AF complexity was devised, termed the recurrence index (RI), which was compared between patients according to clinical AF phenotypes. The RI was significantly higher in patients with paroxysmal AF and those with persistent AF who presented in sinus rhythm and in whom AF was induced at the start of the procedure. This supported the accuracy of the technique in quantifying global complexity given the well-recognised differences between patients with paroxysmal and persistent AF as demonstrated by the significant divergence in outcomes of catheter ablation between these patients. RI was also assessed as a predictor of AF termination alongside the measures of local conduction patterns and AFCL that were evaluated in the previous chapter. Increasing RI was the strongest predictor of AF termination in univariate analysis and remained the only significant predictor in multivariate analysis. This analysis involved all patients recruited to the study, including those with paroxysmal AF, in whom PVI alone resulted in AF termination. A greater RI in these patients was therefore likely to result in the outcomes observed. Of particular interest is the application to only patients with persistent AF. Again, RI was a significant predictor of AF termination in both univariate and multivariate analysis. This supports the validity of this value in a broad group of clinical AF sub-types.

As discussed in previous sections, clinical outcomes within patients with persistent AF are highly variable, suggestive of a range of phenotypes within the broad ECG diagnosis of AF. The RI value developed and outlined in this chapter provides further granularity to the clinical description based on AF duration with the addition of an individualised measure of electrophysiological phenotype that is worthy of further exploration in prospective cohorts.

Additional validity of this measure was provided by the observation of a significant increase in global organisation following PVI. As discussed in chapter 1, this is the only widely accepted ablation strategy known to be effective. Although the precise mechanism by which PVI achieves these results is not entirely clear, it almost certainly extends beyond purely electrical isolation of the pulmonary veins to a wider effect of modification

of the AF substrate. This is evidenced by the increase in organisation measured by RI and observed in both the LA and RA. As also previously discussed, clinical outcomes of PVI are variable. An increase in RI following PVI in the LA or both LA and RA may serve as a further marker of AF phenotype and predict the need for additional non-PV ablation, or specifically RA ablation, and warrants exploration in the context of longer-term clinical outcomes.

Analysis of recurrence matrix patterns provided further insights into AF mechanisms that were explored in conjunction with interpretation of AF propagation history maps obtained from charge density mapping. It was observed that periods of high complexity in whole chamber activation were often interspersed with periods of significant organisation, therefore demonstrating significant temporal variation in AF complexity and mechanisms of whole chamber conduction. Periods of high organisation coincided with the emergence of a dominant mechanism of focal firing with a highly stable cycle length (mean cycle length variation of 4.7±1.6%) that remained for the period of organisation. Interruption of this focal activity coincided with the return of a more complex matrix appearance. Ablation of this focal site, when recognised, resulted in a high rate of AF termination.

These findings provide important data in the context of the localised driver hypothesis of AF propagation and further support the concept of patient-specific phenotypes. A unified hypothesis of AF activation has proven elusive despite a multitude of high quality in-vitro and in-vivo studies over several decades. The variation in characteristics observed on recurrence matrix plots, temporal variability in emergence of sites of stable dominant focal firing, interspersed and contrasted with periods of high complexity, which predominate in many patients points towards variation in mechanisms that cannot be applied universally to all patients with AF. Whilst the localised driver hypothesis may be appropriate in some patients, in others an anarchical description of multi-wavelet propagation may be more accurate. This may explain the inconsistency in findings of clinical studies seeking to identify local drivers and lack of success of empiric ablation strategies beyond PVI.

Recurrence matrix analysis was then conducted using signals from regional atrial anatomical segments to explore quantification of local complexity that may inform localised ablation strategies. Initial development of this approach simply divided the chamber into atrial segments based on anatomical landmarks, which allowed generation of a plot for visual analysis. However, it was observed that the size of the area analysed correlated with the RI calculated. Smaller areas resulted in higher RI, which is perhaps

intuitive given that the smallest area, i.e., a single point compared only to itself, is likely to yield a higher measured phase coherence than when compared to distant sites. The method was therefore adapted into that presented within the Methods section of the chapter to assign a local value to each vertex calculated from a constant endocardial surface area defined as within a radius of 20mm from the index vertex. This allowed calculation of both a RI value for each anatomical segment, and each unique vertex of the chamber, which could be used to generate a global recurrence map and compared to alternative measures of local complexity. The findings outlined in chapter 4 showed that patterns of LIA are highly spatially stable and the frequency of LIA at each vertex of the anatomy over the recording duration could be quantified. This was therefore used as a comparative measure of local complexity. Regional complexity was also quantified by an additional method generated to include a measure of the interaction between co-existing activation patterns, termed symbolic dynamic entropy. Both measures correlated well with local/regional complexity measured using RI. This supports the application of the recurrence method developed to quantify local AF conduction complexity. The results generated from analysis of local complexity could be used in conjunction with findings of global RI to devise ablation strategies. In patients with low global RI and no clear periods of whole chamber organisation, a strategy aimed at sites of maximal local complexity may be appropriate. In contrast, where periods of organisation are observed, an approach aimed at identifying and ablating focal mechanisms potentially representing localised drivers may be appropriate. Although there was some preponderance of maximum complexity zones for certain anatomic sites between patients, these were not uniformly distributed, again arguing against the use of empiric approaches to ablation beyond PVI.

8.2.5 Clinical outcomes of AcQMap-guided ablation

Chapter 7 outlines the clinical outcomes observed in a broad “real-world” cohort of patients undergoing AcQMap-guided ablation for symptomatic AF. Up to this point this thesis has outlined work aimed at exploring AF mechanisms using charge density mapping in selected patients recruited to prospective research studies designed to address specific questions that may inform AcQMap guided ablation strategies. Initial research experience using charge density mapping at our centre led to early adoption of this technique in patients undergoing routine clinical ablation procedures as well as involvement in several industry sponsored registry studies resulting in one of, if not the, largest single centre cohort of patients treated using the AcQMap system worldwide. Published data describing clinical outcomes using this approach are limited to the UNCOVER-AF registry (127 patients) and a small study combining patients from our

centre and one other UK centre with 48-months follow up (40 patients).(249) Both of these studies included only patients undergoing first time procedures.

The clinical characteristics of patients included in this analysis are described and include a mix of patients undergoing first time and re-do ablation procedures. The inclusion of patients undergoing re-do procedures makes this a particularly challenging group given that the only ablation technique with proven clinical benefit (PVI) has already been performed. Beyond re-isolation of re-connected pulmonary veins, no ablation strategy in this group has evidence of clinical benefit. A significant proportion of patients had undergone multiple previous procedures, in whom durable PV isolation is also more likely, suggestive of even more challenging AF substrate.

An acute procedural success rate was measured in terms of arrhythmia termination following ablation and was observed in 48% of patients. However, this was significantly higher (78%) in patients attending the procedure in sinus rhythm and in whom AF was induced compared to patients in AF at the start of the procedure (26%). Beyond baseline rhythm, shorter duration of persistent AF was a univariate and multivariate predictor of AF termination. The number of non-pulmonary vein ablation sites was also reported, and was higher in patients undergoing re-do procedures, further supporting a greater degree of AF complexity in this patient group.

The median follow up period for all patients analysed was 20-months (interquartile range, 9-38) with long-term follow up results presented over both the full follow up period and the first 12-months of follow up. At 12-months, 69% of patients remained free of any arrhythmia recurrence, which reduced to 61% over the full follow up period. Of the 39% experiencing recurrent arrhythmia, 13% had paroxysmal forms (having been persistent prior to the procedure). The only significant predictor of long-term arrhythmia recurrence was increasing LA diameter on pre-procedural transthoracic echocardiography. Acute AF termination with ablation, although suggesting acute modification of the AF substrate, did not predict long-term freedom from arrhythmia recurrence (either AF or AF/AT). Although 39% patients experienced recurrent arrhythmias (26% persistent in nature), only 19% required repeat ablation procedures, perhaps suggesting clinical improvement in arrhythmia burden not quantifiable by binary measures of simple arrhythmia recurrence.

Following presentation of our clinical results, I attempt to put these into the context of results published using other contemporary ablation strategies and the UNCOVER-AF study results. As discussed, this is challenging given differences between characteristics of patient groups enrolled, both measured and unmeasured. The key messages from this data are the need for increased understanding of AF mechanisms and the requirement for

well conducted randomised trials to robustly assess the clinical benefits delivered by novel approaches such as charge density mapping.

8.3 Limitations

One of the main limitations of the findings presented in this thesis is the relatively small number of patients involved. The effect of adenosine was assessed in 22 patients, whilst simultaneous bi-atrial mapping, which generated the data for the analyses conducted in chapters 4-6 was conducted in a further 21 patients. Designing and implementing complex, prospective mechanistic studies is time consuming before even considering recruitment of patients and conduct of the complex procedures required. The mechanistic analyses performed however enable generation of complementary results in different patient groups with the findings explored in analysis of adenosine adding further weight to the results presented using patients undergoing simultaneous bi-atrial mapping. In addition, although the patients involved are the same for the data presented in chapters 4 and 5, the analyses are conducted very differently exploring additional mechanistic questions, the results of which can be anlysed together to provide further context. The development and evaluation of the recurrence matrix mapping technique uses the same patient dataset, but again provides for a very novel analysis approach that can be evaluated independently to the methods and results presented in previous chapters. The inclusion of a much larger group of patients when evaluating longer-term outcomes then allows clinical contextualisation of the mechanistic findings presented.

Acute AF termination with ablation is the clinical outcome used to assess the significance of mechanisms identified in chapters 5-6. Although in chapter 7, I show that AF termination doesn't appear to predict long term arrhythmia freedom, it does suggest successful acute modification of mechanisms sustaining fibrillation and therefore provides a degree of indirect validation of the mechanistic importance of activation patterns identified. As discussed throughout this thesis, the pathophysiology of AF is poorly understood, but appears to involve complex interdependent processes of structural and electrical remodelling resulting in a vulnerable substrate able to sustain AF following initiation by ectopic triggers. Recurrent arrhythmia following ablation can therefore result from either failure of durability of ablation lesions allowing ectopic triggers to re-initaite AF (i.e. reconnection of isolated pulmonary veins), failure to identify the relevant mechanistic processes, failure of durable ablation lesions despite the correct mechanistic ablation targets, or a progression of the disease substrate since the index procedure. Therefore, although acute AF termination may not translate into longer term success, it is perhaps the best measure available to acutely assess arrhythmia mechanisms and is not influenced by either the durability of ablation lesions delivered or progression of disease.

Improving clinical outomes requires advancement in understanding of AF mehanisms revealed using available mapping technology together with development of effective ablation tools and modification of upstream factors responsble for disease progression.

The main limitation of the longer-term clinical outomes presented is the lack of a control arm and randomisation of treatment strategy, as discussed specifically in this chapter. Without this, it is not possible to determine the true incremental benefit of an individualised AcQMap guided approach in comparison to alternative strategies.

8.3.1 Future directions

This thesis outlines some of the insights into mechanisms of AF identified using charge density mapping and the potential benefit this may provide in terms of clinical outcomes. There is much still to learn about the mechanisms of AF and how to translate the results of AF mapping into clinical benefits.

Regions of LIA are shown to be highly stable and likely to represent structural atrial properties, but it is unclear whether these sites are pathological, perhaps related to interstitial fibrosis or myofiber disarray, or are related to normal regions of changing fibre orientation and/or inter-atrial connections. Detailed studies potentially employing histological analysis combined with non-invasive imaging are needed to explore this further.

The optimal ablation approach based on mechanisms identified is also unclear. Should regions of FF be preferentially targeted, in keeping with the hypothesis of focal “drivers”, or should stable regions of LIA be treated as these are the regions of abnormal tissue responsible for fibrillatory conduction? What is the appropriate end point for ablation and how can the effect of ablation be accurately assessed and quantified in real-time to guide therapy?

A novel method of whole chamber measurement of AF complexity is presented, but evaluation to date is limited to the small cohort of patients recruited to this study and compared to acute procedural outcomes. The next step in evaluation of this technique is to test its application to a retrospective cohort of patients in whom both acute and long-term procedural outcomes are known. In addition, the custom programme developed for this analysis is currently only available for offline use and takes approximately 20-minutes to run following export of charge density signals obtained from a recording of 30-seconds in duration. Further improvements in the computational efficiency of this programme are needed to allow integration into the mapping system and enable its practical application. The technique employed is currently based on an approach of phase processing applied

to the calculated charge density signals. However, activation time annotation that is used to generate AF propagation history maps is based on assignment of maximum negative dv/dt to the charge density signals themselves. Altering the approach to apply it directly to the AcQMap propagation history provides an additional avenue for exploration.

Further studies are needed to evaluate clinical applications of this technique. Increasing RI was observed following PVI and both retrospective and prospective analyses are needed to explore the relationship between this and long-term clinical outcomes. Increase in RI may also serve as a useful procedural endpoint, which would require prospective evaluation.

8.4 Conclusion

The research presented in this thesis has involved the study of AF mechanisms identified using whole chamber and bi-atrial charge-density mapping as well as the development and evaluation of a novel technique for the analysis of whole chamber AF activation. The spatio-temporal properties of complex localised patterns of atrial activation are presented together with a systematic analysis of the functional effects of adenosine on dynamic atrial activation as well as traditional markers of AF electrophysiology including cycle length and dominant frequency. The role of the RA in AF propagation is systematically studied, suggesting a critical role, hitherto poorly understood. Application of the insights gained, and methods developed will guide the development of ablation strategies to be employed in clinical studies aimed at improving the treatment of persistent AF.

9 References

1. Adderley NJ, Ryan R, Nirantharakumar K, Marshall T. Prevalence and treatment of atrial fibrillation in UK general practice from 2000 to 2016. Heart. 2019;105(1):27-33.

2. Chugh SS, Havmoeller R, Narayanan K, Singh D, Rienstra M, Benjamin EJ, et al. Worldwide epidemiology of atrial fibrillation: a Global Burden of Disease 2010 Study. Circulation. 2014;129(8):837-47.

3. Go AS, Hylek EM, Phillips KA, Chang Y, Henault LE, Selby JV, et al. Prevalence of diagnosed atrial fibrillation in adults: national implications for rhythm management and stroke prevention: the AnTicoagulation and Risk Factors in Atrial Fibrillation (ATRIA) Study. JAMA. 2001;285(18):2370-5.

4. Kim D, Yang PS, Jang E, Yu HT, Kim TH, Uhm JS, et al. Increasing trends in hospital care burden of atrial fibrillation in Korea, 2006 through 2015. Heart. 2018;104(24):2010-7.

5. Stewart S, Murphy NF, Walker A, McGuire A, McMurray JJ. Cost of an emerging epidemic: an economic analysis of atrial fibrillation in the UK. Heart. 2004;90(3):286-92.

6. Gallagher C, Hendriks JM, Giles L, Karnon J, Pham C, Elliott AD, et al. Increasing trends in hospitalisations due to atrial fibrillation in Australia from 1993 to 2013. Heart. 2019;105(17):1358-63.

7. Friberg J, Buch P, Scharling H, Gadsbphioll N, Jensen GB. Rising rates of hospital admissions for atrial fibrillation. Epidemiology. 2003;14(6):666-72.

8. Wolowacz SE, Samuel M, Brennan VK, Jasso-Mosqueda JG, Van Gelder IC. The cost of illness of atrial fibrillation: a systematic review of the recent literature. Europace. 2011;13(10):1375-85.

9. Johnsen SP, Dalby LW, Tackstrom T, Olsen J, Fraschke A. Cost of illness of atrial fibrillation: a nationwide study of societal impact. BMC Health Serv Res. 2017;17(1):714.

10. Wolf PA, Abbott RD, Kannel WB. Atrial fibrillation as an independent risk factor for stroke: the Framingham Study. Stroke. 1991;22(8):983-8.

11. Investigators RAS. Rivaroxaban-once daily, oral, direct factor Xa inhibition compared with vitamin K antagonism for prevention of stroke and Embolism Trial in Atrial Fibrillation: rationale and design of the ROCKET AF study. Am Heart J. 2010;159(3):340-7 e1.

12. DeVore AD, Hellkamp AS, Becker RC, Berkowitz SD, Breithardt G, Hacke W, et al. Hospitalizations in patients with atrial fibrillation: an analysis from ROCKET AF. Europace. 2016;18(8):1135-42.

13. Benjamin EJ, Wolf PA, D'Agostino RB, Silbershatz H, Kannel WB, Levy D. Impact of atrial fibrillation on the risk of death: the Framingham Heart Study. Circulation. 1998;98(10):946-52.

14. Sankaranarayanan R, Kirkwood G, Visweswariah R, Fox DJ. How does Chronic Atrial Fibrillation Influence Mortality in the Modern Treatment Era? Curr Cardiol Rev. 2015;11(3):190-8.

15. Lee E, Choi EK, Han KD, Lee H, Choe WS, Lee SR, et al. Mortality and causes of death in patients with atrial fibrillation: A nationwide population-based study. PLoS One. 2018;13(12):e0209687.

16. Fauchier L, Samson A, Chaize G, Gaudin AF, Vainchtock A, Bailly C, et al. Cause of death in patients with atrial fibrillation admitted to French hospitals in 2012: a nationwide database study. Open Heart. 2015;2(1):e000290.

17. Giugliano RP, Ruff CT, Braunwald E, Murphy SA, Wiviott SD, Halperin JL, et al. Edoxaban versus warfarin in patients with atrial fibrillation. N Engl J Med. 2013;369(22):2093-104.

18. Granger CB, Alexander JH, McMurray JJ, Lopes RD, Hylek EM, Hanna M, et al. Apixaban versus warfarin in patients with atrial fibrillation. N Engl J Med. 2011;365(11):981-92.

19. Ntaios G, Papavasileiou V, Makaritsis K, Vemmos K, Michel P, Lip GYH. Real-World Setting Comparison of Nonvitamin-K Antagonist Oral Anticoagulants Versus Vitamin-K Antagonists for Stroke Prevention in Atrial Fibrillation: A Systematic Review and Meta-Analysis. Stroke. 2017;48(9):2494-503.

20. Giugliano RP, Ruff CT, Wiviott SD, Nordio F, Murphy SA, Kappelhof JA, et al. Mortality in Patients with Atrial Fibrillation Randomized to Edoxaban or Warfarin: Insights from the ENGAGE AF-TIMI 48 Trial. Am J Med. 2016;129(8):850-7 e2.

21. Odutayo A, Wong CX, Hsiao AJ, Hopewell S, Altman DG, Emdin CA. Atrial fibrillation and risks of cardiovascular disease, renal disease, and death: systematic review and meta-analysis. BMJ. 2016;354:i4482.

22. Freeman JV, Simon DN, Go AS, Spertus J, Fonarow GC, Gersh BJ, et al. Association Between Atrial Fibrillation Symptoms, Quality of Life, and Patient Outcomes: Results From the Outcomes Registry for Better Informed Treatment of Atrial Fibrillation (ORBIT-AF). Circ Cardiovasc Qual Outcomes. 2015;8(4):393-402.

23. Kirchhof P, Benussi S, Kotecha D, Ahlsson A, Atar D, Casadei B, et al. 2016 ESC Guidelines for the management of atrial fibrillation developed in collaboration with EACTS. Eur Heart J. 2016;37(38):2893-962.

24. January CT, Wann LS, Alpert JS, Calkins H, Cigarroa JE, Cleveland JC, et al. 2014 AHA/ACC/HRS guideline for the management of patients with atrial fibrillation: executive summary: a report of the American College of Cardiology/American Heart Association Task Force on practice guidelines and the Heart Rhythm Society. Circulation. 2014;130(23):2071-104.

25. Wyse DG, Waldo AL, DiMarco JP, Domanski MJ, Rosenberg Y, Schron EB, et al. A comparison of rate control and rhythm control in patients with atrial fibrillation. N Engl J Med. 2002;347(23):1825-33.

26. Van Gelder IC, Hagens VE, Bosker HA, Kingma JH, Kamp O, Kingma T, et al. A comparison of rate control and rhythm control in patients with recurrent persistent atrial fibrillation. N Engl J Med. 2002;347(23):1834-40.

27. Calkins H, Hindricks G, Cappato R, Kim YH, Saad EB, Aguinaga L, et al. 2017 HRS/EHRA/ECAS/APHRS/SOLAECE expert consensus statement on catheter and surgical ablation of atrial fibrillation. Heart Rhythm. 2017;14(10):e275-e444.

28. Camm AJ, Lip GY, De Caterina R, Savelieva I, Atar D, Hohnloser SH, et al. 2012 focused update of the ESC Guidelines for the management of atrial fibrillation: an update of the 2010 ESC Guidelines for the management of atrial fibrillation. Developed with the special contribution of the European Heart Rhythm Association. Eur Heart J. 2012;33(21):2719-47.

29. Kirchhof P, Camm AJ, Goette A, Brandes A, Eckardt L, Elvan A, et al. Early Rhythm-Control Therapy in Patients with Atrial Fibrillation. N Engl J Med. 2020;383(14):1305-16.

30. Prabhu S, Taylor AJ, Costello BT, Kaye DM, McLellan AJA, Voskoboinik A, et al. Catheter Ablation Versus Medical Rate Control in Atrial Fibrillation and Systolic Dysfunction: The CAMERA-MRI Study. J Am Coll Cardiol. 2017;70(16):1949-61.

31. Marrouche NF, Kheirkhahan M, Brachmann J. Catheter Ablation for Atrial Fibrillation with Heart Failure. N Engl J Med. 2018;379(5):492.

32. Jones DG, Haldar SK, Hussain W, Sharma R, Francis DP, Rahman-Haley SL, et al. A randomized trial to assess catheter ablation versus rate control in the management of persistent atrial fibrillation in heart failure. J Am Coll Cardiol. 2013;61(18):1894-903.

33. Hunter RJ, Berriman TJ, Diab I, Kamdar R, Richmond L, Baker V, et al. A randomized controlled trial of catheter ablation versus medical treatment of atrial fibrillation in heart failure (the CAMTAF trial). Circ Arrhythm Electrophysiol. 2014;7(1):31-8.

34. Packer DL, Mark DB, Robb RA, Monahan KH, Bahnson TD, Poole JE, et al. Effect of Catheter Ablation vs Antiarrhythmic Drug Therapy on Mortality, Stroke, Bleeding, and Cardiac Arrest Among Patients With Atrial Fibrillation: The CABANA Randomized Clinical Trial. JAMA. 2019;321(13):1261-74.

35. Mark DB, Anstrom KJ, Sheng S, Piccini JP, Baloch KN, Monahan KH, et al. Effect of Catheter Ablation vs Medical Therapy on Quality of Life Among Patients With Atrial Fibrillation: The CABANA Randomized Clinical Trial. JAMA. 2019;321(13):1275-85.

36. Blomstrom-Lundqvist C, Gizurarson S, Schwieler J, Jensen SM, Bergfeldt L, Kenneback G, et al. Effect of Catheter Ablation vs Antiarrhythmic Medication on Quality of Life in Patients With Atrial Fibrillation: The CAPTAF Randomized Clinical Trial. JAMA. 2019;321(11):1059-68.

37. Raine D, Langley P, Shepherd E, Lord S, Murray S, Murray A, et al. Effect of catheter ablation on quality of life in patients with atrial fibrillation and its correlation with arrhythmia outcome. Open Heart. 2015;2(1):e000302.

38. Hakalahti A, Biancari F, Nielsen JC, Raatikainen MJ. Radiofrequency ablation vs. antiarrhythmic drug therapy as first line treatment of symptomatic atrial fibrillation: systematic review and meta-analysis. Europace. 2015;17(3):370-8.

39. Mont L, Bisbal F, Hernandez-Madrid A, Perez-Castellano N, Vinolas X, Arenal A, et al. Catheter ablation vs. antiarrhythmic drug treatment of persistent atrial fibrillation: a multicentre, randomized, controlled trial (SARA study). Eur Heart J. 2014;35(8):501-7.

40. Piccini JP, Lopes RD, Kong MH, Hasselblad V, Jackson K, Al-Khatib SM. Pulmonary vein isolation for the maintenance of sinus rhythm in patients with atrial

fibrillation: a meta-analysis of randomized, controlled trials. Circ Arrhythm Electrophysiol. 2009;2(6):626-33.

41. Nair GM, Nery PB, Diwakaramenon S, Healey JS, Connolly SJ, Morillo CA. A systematic review of randomized trials comparing radiofrequency ablation with antiarrhythmic medications in patients with atrial fibrillation. J Cardiovasc Electrophysiol. 2009;20(2):138-44.

42. Calkins H, Reynolds MR, Spector P, Sondhi M, Xu Y, Martin A, et al. Treatment of atrial fibrillation with antiarrhythmic drugs or radiofrequency ablation: two systematic literature reviews and meta-analyses. Circ Arrhythm Electrophysiol. 2009;2(4):349-61.

43. Asad ZUA, Yousif A, Khan MS, Al-Khatib SM, Stavrakis S. Catheter Ablation Versus Medical Therapy for Atrial Fibrillation. Circ Arrhythm Electrophysiol. 2019;12(9):e007414.

44. Haïssaguerre M, Jaïs P, Shah DC, Takahashi A, Hocini M, Quiniou G, et al. Spontaneous initiation of atrial fibrillation by ectopic beats originating in the pulmonary veins. N Engl J Med. 1998;339(10):659-66.

45. Silverman ME. From rebellious palpitations to the discovery of auricular fibrillation: contributions of Mackenzie, Lewis and Einthoven. Am J Cardiol. 1994;73(5):384-9.

46. Mayer AC. Rhythmical Pulsation in Scyphomedusae. Carnegie Institute of Washington. 1906;47:1-62.

47. Mines GR. On dynamic equilibrium in the heart. J Physiol. 1913;46(4-5):349-83.

48. Garrey W. the nature of fibrillary contraction of the heart - its relation to tissue mass and form. American Journal of Physiology. 1914;33:397-414.

49. Lewis T. Oliver-Sharpey Lectures On The Nature Of Flutter and Fibrillation of the Auricle. Br Med J. 1921;1(3147):590-3.

50. Lewis T. Oliver-Sharpey Lectures On The Nature Of Flutter and Fibrillation of the Auricle. Br Med J. 1921;1(3146):551-5.

51. Moe GK, Abildskov JA. Atrial fibrillation as a self-sustaining arrhythmia independent of focal discharge. Am Heart J. 1959;58(1):59-70.

52. Moe GK, Rheinboldt WC, Abildskov JA. A Computer Model of Atrial Fibrillation. Am Heart J. 1964;67:200-20.

53. Allessie MA, Bonke FI, Schopman FJ. Circus movement in rabbit atrial muscle as a mechanism of trachycardia. Circ Res. 1973;33(1):54-62.

54. Allessie MA, Bonke FI, Schopman FJ. Circus movement in rabbit atrial muscle as a mechanism of tachycardia. III. The "leading circle" concept: a new model of circus movement in cardiac tissue without the involvement of an anatomical obstacle. Circ Res. 1977;41(1):9-18.

55. Krinsky V. Spread of excitation in an inhomogeneous medium (state similar to cardiac fibrillation). Biophysics. 1966;11:676-83.

56. AT W. When Time Breaks Down. Princeton, NJ: Princeton University Press; 1987.

57. Davidenko JM, Kent PF, Chialvo DR, Michaels DC, Jalife J. Sustained vortex-like waves in normal isolated ventricular muscle. Proc Natl Acad Sci U S A. 1990;87(22):8785-9.

58. Pandit SV, Jalife J. Rotors and the dynamics of cardiac fibrillation. Circ Res. 2013;112(5):849-62.

59. Gray RA, Pertsov AM, Jalife J. Incomplete reentry and epicardial breakthrough patterns during atrial fibrillation in the sheep heart. Circulation. 1996;94(10):2649-61.

60. de Groot NM, Houben RP, Smeets JL, Boersma E, Schotten U, Schalij MJ, et al. Electropathological substrate of longstanding persistent atrial fibrillation in patients with structural heart disease: epicardial breakthrough. Circulation. 2010;122(17):1674-82.

61. Verheule S, Eckstein J, Linz D, Maesen B, Bidar E, Gharaviri A, et al. Role of endo-epicardial dissociation of electrical activity and transmural conduction in the development of persistent atrial fibrillation. Prog Biophys Mol Biol. 2014;115(2-3):173-85.

62. de Groot N, van der Does L, Yaksh A, Lanters E, Teuwen C, Knops P, et al. Direct Proof of Endo-Epicardial Asynchrony of the Atrial Wall During Atrial Fibrillation in Humans. Circ Arrhythm Electrophysiol. 2016;9(5).

63. Scherf D, Terranova R. Mechanism of auricular flutter and fibrillation. Am J Physiol. 1949;159(1):137-42.

64. Jalife J. Deja vu in the theories of atrial fibrillation dynamics. Cardiovasc Res. 2011;89(4):766-75.

65. Mansour M, Mandapati R, Berenfeld O, Chen J, Samie FH, Jalife J. Left-to-right gradient of atrial frequencies during acute atrial fibrillation in the isolated sheep heart. Circulation. 2001;103(21):2631-6.

66. Mandapati R, Skanes A, Chen J, Berenfeld O, Jalife J. Stable microreentrant sources as a mechanism of atrial fibrillation in the isolated sheep heart. Circulation. 2000;101(2):194-9.

67. Jalife J, Berenfeld O, Mansour M. Mother rotors and fibrillatory conduction: a mechanism of atrial fibrillation. Cardiovasc Res. 2002;54(2):204-16.

68. Ehrlich JR, Cha TJ, Zhang L, Chartier D, Melnyk P, Hohnloser SH, et al. Cellular electrophysiology of canine pulmonary vein cardiomyocytes: action potential and ionic current properties. J Physiol. 2003;551(Pt 3):801-13.

69. Nattel S. Paroxysmal atrial fibrillation and pulmonary veins: relationships between clinical forms and automatic versus re-entrant mechanisms. Can J Cardiol. 2013;29(10):1147-9.

70. Hocini M, Ho SY, Kawara T, Linnenbank AC, Potse M, Shah D, et al. Electrical conduction in canine pulmonary veins: electrophysiological and anatomic correlation. Circulation. 2002;105(20):2442-8.

71. Verheule S, Wilson EE, Arora R, Engle SK, Scott LR, Olgin JE. Tissue structure and connexin expression of canine pulmonary veins. Cardiovasc Res. 2002;55(4):727-38.

72. Atienza F, Almendral J, Moreno J, Vaidyanathan R, Talkachou A, Kalifa J, et al. Activation of inward rectifier potassium channels accelerates atrial fibrillation in humans: evidence for a reentrant mechanism. Circulation. 2006;114(23):2434-42.

73. Kanj M, Wazni O, Natale A. Pulmonary vein antrum isolation. Heart Rhythm. 2007;4(3 Suppl):S73-9.

74. Atienza F, Jalife J. Reentry and atrial fibrillation. Heart Rhythm. 2007;4(3 Suppl):S13-6.

75. Oral H, Scharf C, Chugh A, Hall B, Cheung P, Good E, et al. Catheter ablation for paroxysmal atrial fibrillation: segmental pulmonary vein ostial ablation versus left atrial ablation. Circulation. 2003;108(19):2355-60.

76. Proietti R, Santangeli P, Di Biase L, Joza J, Bernier ML, Wang Y, et al. Comparative effectiveness of wide antral versus ostial pulmonary vein isolation: a systematic review and meta-analysis. Circ Arrhythm Electrophysiol. 2014;7(1):39-45.

77. Ganesan AN, Shipp NJ, Brooks AG, Kuklik P, Lau DH, Lim HS, et al. Long-term outcomes of catheter ablation of atrial fibrillation: a systematic review and meta-analysis. J Am Heart Assoc. 2013;2(2):e004549.

78. Knight BP, Novak PG, Sangrigoli R, Champagne J, Dubuc M, Adler SW, et al. Long-Term Outcomes After Ablation for Paroxysmal Atrial Fibrillation Using the Second-Generation Cryoballoon: Final Results From STOP AF Post-Approval Study. JACC Clin Electrophysiol. 2019;5(3):306-14.

79. Gökoğlan Y, Mohanty S, Güneş MF, Trivedi C, Santangeli P, Gianni C, et al. Pulmonary Vein Antrum Isolation in Patients With Paroxysmal Atrial Fibrillation: More Than a Decade of Follow-Up. Circ Arrhythm Electrophysiol. 2016;9(5).

80. Hoffmann E, Straube F, Wegscheider K, Kuniss M, Andresen D, Wu LQ, et al. Outcomes of cryoballoon or radiofrequency ablation in symptomatic paroxysmal or persistent atrial fibrillation. Europace. 2019;21(9):1313-24.

81. Usui E, Miyazaki S, Taniguchi H, Ichihara N, Kanaji Y, Takagi T, et al. Recurrence after "long-term success" in catheter ablation of paroxysmal atrial fibrillation. Heart Rhythm. 2015;12(5):893-8.

82. Rolf S, Hindricks G, Sommer P, Richter S, Arya A, Bollmann A, et al. Electroanatomical mapping of atrial fibrillation: Review of the current techniques and advances. J Atr Fibrillation. 2014;7(4):1140.

83. Verma A, Wazni OM, Marrouche NF, Martin DO, Kilicaslan F, Minor S, et al. Pre-existent left atrial scarring in patients undergoing pulmonary vein antrum isolation: an independent predictor of procedural failure. J Am Coll Cardiol. 2005;45(2):285-92.

84. Rolf S, Kircher S, Arya A, Eitel C, Sommer P, Richter S, et al. Tailored atrial substrate modification based on low-voltage areas in catheter ablation of atrial fibrillation. Circ Arrhythm Electrophysiol. 2014;7(5):825-33.

85. Williams SE, Linton N, O'Neill L, Harrison J, Whitaker J, Mukherjee R, et al. The effect of activation rate on left atrial bipolar voltage in patients with paroxysmal atrial fibrillation. J Cardiovasc Electrophysiol. 2017;28(9):1028-36.

86. Hwang M, Kim J, Lim B, Song JS, Joung B, Shim EB, et al. Multiple factors influence the morphology of the bipolar electrogram: An in silico modeling study. PLoS Comput Biol. 2019;15(4):e1006765.

87. Anter E, Josephson ME. Bipolar voltage amplitude: What does it really mean? Heart Rhythm. 2016;13(1):326-7.

88. Wong GR, Nalliah CJ, Lee G, Voskoboinik A, Prabhu S, Parameswaran R, et al. Dynamic Atrial Substrate During High-Density Mapping of Paroxysmal and Persistent AF: Implications for Substrate Ablation. JACC Clin Electrophysiol. 2019;5(11):1265-77.

89. Xintarakou A, Tzeis S, Psarras S, Asvestas D, Vardas P. Atrial fibrosis as a dominant factor for the development of atrial fibrillation: facts and gaps. Europace. 2020;22(3):342-51.

90. Hansen BJ, Zhao J, Fedorov VV. Fibrosis and Atrial Fibrillation: Computerized and Optical Mapping; A View into the Human Atria at Submillimeter Resolution. JACC Clin Electrophysiol. 2017;3(6):531-46.

91. Vasquez C, Mohandas P, Louie KL, Benamer N, Bapat AC, Morley GE. Enhanced fibroblast-myocyte interactions in response to cardiac injury. Circ Res. 2010;107(8):1011-20.

92. Lin Y, Yang B, Garcia FC, Ju W, Zhang F, Chen H, et al. Comparison of left atrial electrophysiologic abnormalities during sinus rhythm in patients with different type of atrial fibrillation. J Interv Card Electrophysiol. 2014;39(1):57-67.

93. Yagishita A, Sparano D, Cakulev I, Gimbel JR, Phelan T, Mustafa H, et al. Identification and electrophysiological characterization of early left atrial structural remodeling as a predictor for atrial fibrillation recurrence after pulmonary vein isolation. J Cardiovasc Electrophysiol. 2017;28(6):642-50.

94. Yang B, Jiang C, Lin Y, Yang G, Chu H, Cai H, et al. STABLE-SR (Electrophysiological Substrate Ablation in the Left Atrium During Sinus Rhythm) for the Treatment of Nonparoxysmal Atrial Fibrillation: A Prospective, Multicenter Randomized Clinical Trial. Circ Arrhythm Electrophysiol. 2017;10(11).

95. Oakes RS, Badger TJ, Kholmovski EG, Akoum N, Burgon NS, Fish EN, et al. Detection and quantification of left atrial structural remodeling with delayed-enhancement magnetic resonance imaging in patients with atrial fibrillation. Circulation. 2009;119(13):1758-67.

96. Zghaib T, Keramati A, Chrispin J, Huang D, Balouch MA, Ciuffo L, et al. Multimodal Examination of Atrial Fibrillation Substrate: Correlation of Left Atrial Bipolar Voltage Using Multi-Electrode Fast Automated Mapping, Point-by-Point Mapping, and Magnetic Resonance Image Intensity Ratio. JACC Clin Electrophysiol. 2018;4(1):59-68.

97. Marrouche NF, Wilber D, Hindricks G, Jais P, Akoum N, Marchlinski F, et al. Association of atrial tissue fibrosis identified by delayed enhancement MRI and atrial fibrillation catheter ablation: the DECAAF study. JAMA. 2014;311(5):498-506.

98. McGann C, Akoum N, Patel A, Kholmovski E, Revelo P, Damal K, et al. Atrial fibrillation ablation outcome is predicted by left atrial remodeling on MRI. Circ Arrhythm Electrophysiol. 2014;7(1):23-30.

99. Mahnkopf C, Badger TJ, Burgon NS, Daccarett M, Haslam TS, Badger CT, et al. Evaluation of the left atrial substrate in patients with lone atrial fibrillation using delayed-enhanced MRI: implications for disease progression and response to catheter ablation. Heart Rhythm. 2010;7(10):1475-81.

100. Wijffels MC, Kirchhof CJ, Dorland R, Allessie MA. Atrial fibrillation begets atrial fibrillation. A study in awake chronically instrumented goats. Circulation. 1995;92(7):1954-68.

101. Schotten U, Verheule S, Kirchhof P, Goette A. Pathophysiological mechanisms of atrial fibrillation: a translational appraisal. Physiol Rev. 2011;91(1):265-325.

102. Dharmaprani D, Schopp M, Kuklik P, Chapman D, Lahiri A, Dykes L, et al. Renewal Theory as a Universal Quantitative Framework to Characterize Phase Singularity Regeneration in Mammalian Cardiac Fibrillation. Circ Arrhythm Electrophysiol. 2019;12(12):e007569.

103. Schuessler RB, Grayson TM, Bromberg BI, Cox JL, Boineau JP. Cholinergically mediated tachyarrhythmias induced by a single extrastimulus in the isolated canine right atrium. Circ Res. 1992;71(5):1254-67.

104. Kim MY, Sandler BC, Sikkel MB, Cantwell CD, Leong KM, Luther V, et al. Anatomical Distribution of Ectopy-Triggering Plexuses in Patients With Atrial Fibrillation. Circ Arrhythm Electrophysiol. 2020;13(9):e008715.

105. Kim MY, Sandler B, Sikkel MB, Cantwell CD, Leong KM, Luther V, et al. The ectopy-triggering ganglionated plexuses in atrial fibrillation. Auton Neurosci. 2020;228:102699.

106. Stiles MK, Sanders P, Lau DH. Targeting the Substrate in Ablation of Persistent Atrial Fibrillation: Recent Lessons and Future Directions. Front Physiol. 2018;9:1158.

107. Severs NJ, Bruce AF, Dupont E, Rothery S. Remodelling of gap junctions and connexin expression in diseased myocardium. Cardiovasc Res. 2008;80(1):9-19.

108. Miyamoto K, Tsuchiya T, Narita S, Yamaguchi T, Nagamoto Y, Ando S, et al. Bipolar electrogram amplitudes in the left atrium are related to local conduction velocity in patients with atrial fibrillation. Europace. 2009;11(12):1597-605.

109. Honarbakhsh S, Schilling RJ, Orini M, Providencia R, Keating E, Finlay M, et al. Structural remodeling and conduction velocity dynamics in the human left atrium: Relationship with reentrant mechanisms sustaining atrial fibrillation. Heart Rhythm. 2018.

110. Hansen BJ, Zhao J, Csepe TA, Moore BT, Li N, Jayne LA, et al. Atrial fibrillation driven by micro-anatomic intramural re-entry revealed by simultaneous sub-epicardial and sub-endocardial optical mapping in explanted human hearts. Eur Heart J. 2015;36(35):2390-401.

111. Angel N, Li LI, Macleod RS, Marrouche N, Ranjan R, Dosdall DJ. Diverse Fibrosis Architecture and Premature Stimulation Facilitate Initiation of Reentrant Activity Following Chronic Atrial Fibrillation. J Cardiovasc Electrophysiol. 2015;26(12):1352-60.

112. Zhao J, Hansen BJ, Csepe TA, Lim P, Wang Y, Williams M, et al. Integration of High-Resolution Optical Mapping and 3-Dimensional Micro-Computed Tomographic

Imaging to Resolve the Structural Basis of Atrial Conduction in the Human Heart. Circ Arrhythm Electrophysiol. 2015;8(6):1514-7.

113. Wong CX, Stiles MK, John B, Brooks AG, Lau DH, Dimitri H, et al. Direction-dependent conduction in lone atrial fibrillation. Heart Rhythm. 2010;7(9):1192-9.

114. Haissaguerre M, Shah AJ, Cochet H, Hocini M, Dubois R, Efimov I, et al. Intermittent drivers anchoring to structural heterogeneities as a major pathophysiological mechanism of human persistent atrial fibrillation. J Physiol. 2016;594(9):2387-98.

115. Jadidi AS, Cochet H, Shah AJ, Kim SJ, Duncan E, Miyazaki S, et al. Inverse relationship between fractionated electrograms and atrial fibrosis in persistent atrial fibrillation: combined magnetic resonance imaging and high-density mapping. J Am Coll Cardiol. 2013;62(9):802-12.

116. Lazar S, Dixit S, Marchlinski FE, Callans DJ, Gerstenfeld EP. Presence of left-to-right atrial frequency gradient in paroxysmal but not persistent atrial fibrillation in humans. Circulation. 2004;110(20):3181-6.

117. Lazar S, Dixit S, Callans DJ, Lin D, Marchlinski FE, Gerstenfeld EP. Effect of pulmonary vein isolation on the left-to-right atrial dominant frequency gradient in human atrial fibrillation. Heart Rhythm. 2006;3(8):889-95.

118. Saksena S, Giorgberidze I, Mehra R, Hill M, Prakash A, Krol RB, et al. Electrophysiology and endocardial mapping of induced atrial fibrillation in patients with spontaneous atrial fibrillation. Am J Cardiol. 1999;83(2):187-93.

119. Saksena S, Skadsberg ND, Rao HB, Filipecki A. Biatrial and three-dimensional mapping of spontaneous atrial arrhythmias in patients with refractory atrial fibrillation. J Cardiovasc Electrophysiol. 2005;16(5):494-504.

120. Chang SL, Tai CT, Lin YJ, Wongcharoen W, Lo LW, Tuan TC, et al. Biatrial substrate properties in patients with atrial fibrillation. J Cardiovasc Electrophysiol. 2007;18(11):1134-9.

121. Calo L, Lamberti F, Loricchio ML, De Ruvo E, Colivicchi F, Bianconi L, et al. Left atrial ablation versus biatrial ablation for persistent and permanent atrial fibrillation: a prospective and randomized study. J Am Coll Cardiol. 2006;47(12):2504-12.

122. Nademanee K, McKenzie J, Kosar E, Schwab M, Sunsaneewitayakul B, Vasavakul T, et al. A new approach for catheter ablation of atrial fibrillation: mapping of the electrophysiologic substrate. J Am Coll Cardiol. 2004;43(11):2044-53.

123. Rostock T, Steven D, Hoffmann B, Servatius H, Drewitz I, Sydow K, et al. Chronic atrial fibrillation is a biatrial arrhythmia: data from catheter ablation of chronic atrial fibrillation aiming arrhythmia termination using a sequential ablation approach. Circ Arrhythm Electrophysiol. 2008;1(5):344-53.

124. Miller JM, Kowal RC, Swarup V, Daubert JP, Daoud EG, Day JD, et al. Initial independent outcomes from focal impulse and rotor modulation ablation for atrial fibrillation: multicenter FIRM registry. J Cardiovasc Electrophysiol. 2014;25(9):921-9.

125. Miller JM, Kalra V, Das MK, Jain R, Garlie JB, Brewster JA, et al. Clinical Benefit of Ablating Localized Sources for Human Atrial Fibrillation: The Indiana University FIRM Registry. J Am Coll Cardiol. 2017;69(10):1247-56.

126. Haissaguerre M, Hocini M, Denis A, Shah AJ, Komatsu Y, Yamashita S, et al. Driver domains in persistent atrial fibrillation. Circulation. 2014;130(7):530-8.

127. Knecht S, Sohal M, Deisenhofer I, Albenque JP, Arentz T, Neumann T, et al. Multicentre evaluation of non-invasive biatrial mapping for persistent atrial fibrillation ablation: the AFACART study. Europace. 2017;19(8):1302-9.

128. Agarwal YK, Aronow WS, Levy JA, Spodick DH. Association of interatrial block with development of atrial fibrillation. Am J Cardiol. 2003;91(7):882.

129. Ariyarajah V, Spodick DH. The Bachmann Bundle and interatrial conduction. Cardiol Rev. 2006;14(4):194-9.

130. Knol WG, Teuwen CP, Kleinrensink GJ, Bogers A, de Groot NMS, Taverne Y. The Bachmann bundle and interatrial conduction: comparing atrial morphology to electrical activity. Heart Rhythm. 2019;16(4):606-14.

131. Platonov PG, Mitrofanova L, Ivanov V, Ho SY. Substrates for intra-atrial and interatrial conduction in the atrial septum: anatomical study on 84 human hearts. Heart Rhythm. 2008;5(8):1189-95.

132. Wazni OM, Dandamudi G, Sood N, Hoyt R, Tyler J, Durrani S, et al. Cryoballoon Ablation as Initial Therapy for Atrial Fibrillation. N Engl J Med. 2021;384(4):316-24.

133. Andrade JG, Wells GA, Deyell MW, Bennett M, Essebag V, Champagne J, et al. Cryoablation or Drug Therapy for Initial Treatment of Atrial Fibrillation. N Engl J Med. 2020.

134. Wynn GJ, El-Kadri M, Haq I, Das M, Modi S, Snowdon R, et al. Long-term outcomes after ablation of persistent atrial fibrillation: an observational study over 6 years. Open Heart. 2016;3(2):e000394.

135. Verma A, Jiang CY, Betts TR, Chen J, Deisenhofer I, Mantovan R, et al. Approaches to catheter ablation for persistent atrial fibrillation. N Engl J Med. 2015;372(19):1812-22.

136. Weerasooriya R, Shah AJ, Hocini M, Jaïs P, Haïssaguerre M. Contemporary challenges of catheter ablation for atrial fibrillation. Clin Ther. 2014;36(9):1145-50.

137. Jais P, Hocini M, Hsu LF, Sanders P, Scavee C, Weerasooriya R, et al. Technique and results of linear ablation at the mitral isthmus. Circulation. 2004;110(19):2996-3002.

138. Fassini G, Riva S, Chiodelli R, Trevisi N, Berti M, Carbucicchio C, et al. Left mitral isthmus ablation associated with PV Isolation: long-term results of a prospective randomized study. J Cardiovasc Electrophysiol. 2005;16(11):1150-6.

139. Hocini M, Jais P, Sanders P, Takahashi Y, Rotter M, Rostock T, et al. Techniques, evaluation, and consequences of linear block at the left atrial roof in paroxysmal atrial fibrillation: a prospective randomized study. Circulation. 2005;112(24):3688-96.

140. Willems S, Klemm H, Rostock T, Brandstrup B, Ventura R, Steven D, et al. Substrate modification combined with pulmonary vein isolation improves outcome of catheter ablation in patients with persistent atrial fibrillation: a prospective randomized comparison. Eur Heart J. 2006;27(23):2871-8.

141. Gaita F, Caponi D, Scaglione M, Montefusco A, Corleto A, Di Monte F, et al. Long-term clinical results of 2 different ablation strategies in patients with paroxysmal and persistent atrial fibrillation. Circ Arrhythm Electrophysiol. 2008;1(4):269-75.

142. Sawhney N, Anousheh R, Chen W, Feld GK. Circumferential pulmonary vein ablation with additional linear ablation results in an increased incidence of left atrial flutter compared with segmental pulmonary vein isolation as an initial approach to ablation of paroxysmal atrial fibrillation. Circ Arrhythm Electrophysiol. 2010;3(3):243-8.

143. Haissaguerre M, Hocini M, Sanders P, Sacher F, Rotter M, Takahashi Y, et al. Catheter ablation of long-lasting persistent atrial fibrillation: clinical outcome and mechanisms of subsequent arrhythmias. J Cardiovasc Electrophysiol. 2005;16(11):1138-47.

144. Haissaguerre M, Sanders P, Hocini M, Takahashi Y, Rotter M, Sacher F, et al. Catheter ablation of long-lasting persistent atrial fibrillation: critical structures for termination. J Cardiovasc Electrophysiol. 2005;16(11):1125-37.

145. Wynn GJ, Das M, Bonnett LJ, Panikker S, Wong T, Gupta D. Efficacy of catheter ablation for persistent atrial fibrillation: a systematic review and meta-analysis of evidence from randomized and nonrandomized controlled trials. Circ Arrhythm Electrophysiol. 2014;7(5):841-52.

146. Wong KC, Betts TR. A review of mitral isthmus ablation. Indian Pacing Electrophysiol J. 2012;12(4):152-70.

147. Elbatran AI, Anderson RH, Mori S, Saba MM. The rationale for isolation of the left atrial pulmonary venous component to control atrial fibrillation: A review article. Heart Rhythm. 2019;16(9):1392-8.

148. Thiyagarajah A, Kadhim K, Lau DH, Emami M, Linz D, Khokhar K, et al. Feasibility, Safety, and Efficacy of Posterior Wall Isolation During Atrial Fibrillation Ablation: A Systematic Review and Meta-Analysis. Circ Arrhythm Electrophysiol. 2019;12(8):e007005.

149. Kim JS, Shin SY, Na JO, Choi CU, Kim SH, Kim JW, et al. Does isolation of the left atrial posterior wall improve clinical outcomes after radiofrequency catheter ablation for persistent atrial fibrillation?: A prospective randomized clinical trial. Int J Cardiol. 2015;181:277-83.

150. Bai R, Di Biase L, Mohanty P, Trivedi C, Dello Russo A, Themistoclakis S, et al. Proven isolation of the pulmonary vein antrum with or without left atrial posterior wall isolation in patients with persistent atrial fibrillation. Heart Rhythm. 2016;13(1):132-40.

151. Lee JM, Shim J, Park J, Yu HT, Kim TH, Park JK, et al. The Electrical Isolation of the Left Atrial Posterior Wall in Catheter Ablation of Persistent Atrial Fibrillation. JACC Clin Electrophysiol. 2019;5(11):1253-61.

152. Pak HN, Park J, Park JW, Yang SY, Yu HT, Kim TH, et al. Electrical Posterior Box Isolation in Persistent Atrial Fibrillation Changed to Paroxysmal Atrial Fibrillation: A Multicenter, Prospective, Randomized Study. Circ Arrhythm Electrophysiol. 2020;13(9):e008531.

153. Kim D, Yu HT, Kim T-H, Uhm J-S, Joung B, Lee M-H, et al. Electrical Posterior Box Isolation in Repeat Ablation for Atrial Fibrillation. JACC: Clinical Electrophysiology.0(0).

154. Aryana A, Allen SL, Pujara DK, Bowers MR, O'Neill PG, Yamauchi Y, et al. Concomitant Pulmonary Vein and Posterior Wall Isolation Using Cryoballoon With Adjunct Radiofrequency in Persistent Atrial Fibrillation. JACC Clin Electrophysiol. 2021;7(2):187-96.

155. Chieng D, Sugumar H, Ling LH, Segan L, Azzopardi S, Prabhu S, et al. Catheter ablation for persistent atrial fibrillation: A multicenter randomized trial of pulmonary vein isolation (PVI) versus PVI with posterior left atrial wall isolation (PWI) - The CAPLA study. Am Heart J. 2022;243:210-20.

156. Hocini M, Shah AJ, Nault I, Sanders P, Wright M, Narayan SM, et al. Localized reentry within the left atrial appendage: arrhythmogenic role in patients undergoing ablation of persistent atrial fibrillation. Heart Rhythm. 2011;8(12):1853-61.

157. Romero J, Michaud GF, Avendano R, Briceno DF, Kumar S, Carlos Diaz J, et al. Benefit of left atrial appendage electrical isolation for persistent and long-standing persistent atrial fibrillation: a systematic review and meta-analysis. Europace. 2018;20(8):1268-78.

158. Di Biase L, Burkhardt JD, Mohanty P, Mohanty S, Sanchez JE, Trivedi C, et al. Left Atrial Appendage Isolation in Patients With Longstanding Persistent AF Undergoing Catheter Ablation: BELIEF Trial. J Am Coll Cardiol. 2016;68(18):1929-40.

159. Heeger CH, Rillig A, Geisler D, Wohlmuth P, Fink T, Mathew S, et al. Left Atrial Appendage Isolation in Patients Not Responding to Pulmonary Vein Isolation. Circulation. 2019;139(5):712-5.

160. Valderrabano M, Chen HR, Sidhu J, Rao L, Ling Y, Khoury DS. Retrograde ethanol infusion in the vein of Marshall: regional left atrial ablation, vagal denervation and feasibility in humans. Circ Arrhythm Electrophysiol. 2009;2(1):50-6.

161. Valderrabano M, Liu X, Sasaridis C, Sidhu J, Little S, Khoury DS. Ethanol infusion in the vein of Marshall: Adjunctive effects during ablation of atrial fibrillation. Heart Rhythm. 2009;6(11):1552-8.

162. Pambrun T, Denis A, Duchateau J, Sacher F, Hocini M, Jais P, et al. MARSHALL bundles elimination, Pulmonary veins isolation and Lines completion for ANatomical ablation of persistent atrial fibrillation: MARSHALL-PLAN case series. J Cardiovasc Electrophysiol. 2019;30(1):7-15.

163. Derval N, Duchateau J, Denis A, Ramirez FD, Mahida S, Andre C, et al. Marshall bundle elimination, Pulmonary vein isolation, and Line completion for ANatomical ablation of persistent atrial fibrillation (Marshall-PLAN): Prospective, single-center study. Heart Rhythm. 2021;18(4):529-37.

164. Valderrabano M, Peterson LE, Swarup V, Schurmann PA, Makkar A, Doshi RN, et al. Effect of Catheter Ablation With Vein of Marshall Ethanol Infusion vs Catheter Ablation Alone on Persistent Atrial Fibrillation: The VENUS Randomized Clinical Trial. JAMA. 2020;324(16):1620-8.

165. Kim MY, Sikkel MB, Hunter RJ, Haywood GA, Tomlinson DR, Tayebjee MH, et al. A novel approach to mapping the atrial ganglionated plexus network by generating a distribution probability atlas. J Cardiovasc Electrophysiol. 2018;29(12):1624-34.

166. Kim MY, Coyle C, Tomlinson DR, Sikkel MB, Sohaib A, Luther V, et al. Ectopy-triggering ganglionated plexuses ablation to prevent atrial fibrillation: GANGLIA-AF study. Heart Rhythm. 2022;19(4):516-24.

167. Sun J, Chen M, Wang Q, Zhang PP, Li W, Zhang R, et al. Adding six short lines on pulmonary vein isolation circumferences reduces recurrence of paroxysmal atrial fibrillation: Results from a multicenter, single-blind, randomized trial. Heart Rhythm. 2022;19(3):344-51.

168. Skanes AC, Mandapati R, Berenfeld O, Davidenko JM, Jalife J. Spatiotemporal periodicity during atrial fibrillation in the isolated sheep heart. Circulation. 1998;98(12):1236-48.

169. Latchamsetty R, Kocheril AG. Review of Dominant Frequency Analysis in Atrial Fibrillation. J Atr Fibrillation. 2009;2(3):204.

170. Sanders P, Berenfeld O, Hocini M, Jais P, Vaidyanathan R, Hsu LF, et al. Spectral analysis identifies sites of high-frequency activity maintaining atrial fibrillation in humans. Circulation. 2005;112(6):789-97.

171. Atienza F, Almendral J, Jalife J, Zlochiver S, Ploutz-Snyder R, Torrecilla EG, et al. Real-time dominant frequency mapping and ablation of dominant frequency sites in atrial fibrillation with left-to-right frequency gradients predicts long-term maintenance of sinus rhythm. Heart Rhythm. 2009;6(1):33-40.

172. Atienza F, Almendral J, Ormaetxe JM, Moya A, Martinez-Alday JD, Hernandez-Madrid A, et al. Comparison of radiofrequency catheter ablation of drivers and circumferential pulmonary vein isolation in atrial fibrillation: a noninferiority randomized multicenter RADAR-AF trial. J Am Coll Cardiol. 2014;64(23):2455-67.

173. Gadenz L, Hashemi J, Shariat MH, Gula L, Redfearn DP. Clinical Role of Dominant Frequency Measurements in Atrial Fibrillation Ablation - A Systematic Review. J Atr Fibrillation. 2017;9(6):1548.

174. Umapathy K, Nair K, Masse S, Krishnan S, Rogers J, Nash MP, et al. Phase mapping of cardiac fibrillation. Circ Arrhythm Electrophysiol. 2010;3(1):105-14.

175. Handa BS, Roney CH, Houston C, Qureshi NA, Li X, Pitcher DS, et al. Analytical approaches for myocardial fibrillation signals. Comput Biol Med. 2018;102:315-26.

176. Aronis KN, Berger RD, Ashikaga H. Rotors: How Do We Know When They Are Real? Circ Arrhythm Electrophysiol. 2017;10(9).

177. Laughner J, Shome S, Child N, Shuros A, Neuzil P, Gill J, et al. Practical Considerations of Mapping Persistent Atrial Fibrillation With Whole-Chamber Basket Catheters. JACC Clin Electrophysiol. 2016;2(1):55-65.

178. Roney CH, Cantwell CD, Bayer JD, Qureshi NA, Lim PB, Tweedy JH, et al. Spatial Resolution Requirements for Accurate Identification of Drivers of Atrial Fibrillation. Circ Arrhythm Electrophysiol. 2017;10(5):e004899.

179. King B, Porta-Sánchez A, Massé S, Zamiri N, Balasundaram K, Kusha M, et al. Effect of spatial resolution and filtering on mapping cardiac fibrillation. Heart Rhythm. 2017;14(4):608-15.

180. Rodrigo M, Climent AM, Liberos A, Fernández-Avilés F, Berenfeld O, Atienza F, et al. Technical Considerations on Phase Mapping for Identification of Atrial Reentrant Activity in Direct- and Inverse-Computed Electrograms. Circ Arrhythm Electrophysiol. 2017;10(9).

181. Guillem MS, Climent AM, Rodrigo M, Fernández-Avilés F, Atienza F, Berenfeld O. Presence and stability of rotors in atrial fibrillation: evidence and therapeutic implications. Cardiovasc Res. 2016;109(4):480-92.

182. Schricker AA, Lalani GG, Krummen DE, Narayan SM. Rotors as drivers of atrial fibrillation and targets for ablation. Curr Cardiol Rep. 2014;16(8):509.

183. Narayan SM, Krummen DE, Rappel WJ. Clinical mapping approach to diagnose electrical rotors and focal impulse sources for human atrial fibrillation. J Cardiovasc Electrophysiol. 2012;23(5):447-54.

184. Narayan SM, Krummen DE, Shivkumar K, Clopton P, Rappel WJ, Miller JM. Treatment of atrial fibrillation by the ablation of localized sources: CONFIRM (Conventional Ablation for Atrial Fibrillation With or Without Focal Impulse and Rotor Modulation) trial. J Am Coll Cardiol. 2012;60(7):628-36.

185. Narayan SM, Baykaner T, Clopton P, Schricker A, Lalani GG, Krummen DE, et al. Ablation of rotor and focal sources reduces late recurrence of atrial fibrillation compared with trigger ablation alone: extended follow-up of the CONFIRM trial (Conventional Ablation for Atrial Fibrillation With or Without Focal Impulse and Rotor Modulation). J Am Coll Cardiol. 2014;63(17):1761-8.

186. Benharash P, Buch E, Frank P, Share M, Tung R, Shivkumar K, et al. Quantitative analysis of localized sources identified by focal impulse and rotor modulation mapping in atrial fibrillation. Circ Arrhythm Electrophysiol. 2015;8(3):554-61.

187. Child N, Clayton RH, Roney CR, Laughner JI, Shuros A, Neuzil P, et al. Unraveling the Underlying Arrhythmia Mechanism in Persistent Atrial Fibrillation: Results From the STARLIGHT Study. Circ Arrhythm Electrophysiol. 2018;11(6):e005897.

188. Parameswaran R, Voskoboinik A, Gorelik A, Lee G, Kistler PM, Sanders P, et al. Clinical impact of rotor ablation in atrial fibrillation: a systematic review. Europace. 2018;20(7):1099-106.

189. Brachmann J HJ, Wilber DJ, Sarver AE, Rapkin J, Shpun S, Szili-Torok T. Prospective randomized comparison of rotor ablation vs conventional ablation for threatment of persistent atrial fibrillation - The REAFFIRM rial. Heart Rhythm. 2019;16(5):963.

190. Mody BP, Raza A, Jacobson J, Iwai S, Frenkel D, Rojas R, et al. Ablation of long-standing persistent atrial fibrillation. Ann Transl Med. 2017;5(15):305.

191. Pathik B, Kalman JM, Walters T, Kuklik P, Zhao J, Madry A, et al. Absence of rotational activity detected using 2-dimensional phase mapping in the corresponding 3-dimensional phase maps in human persistent atrial fibrillation. Heart Rhythm. 2018;15(2):182-92.

192. Ramanathan C, Ghanem RN, Jia P, Ryu K, Rudy Y. Noninvasive electrocardiographic imaging for cardiac electrophysiology and arrhythmia. Nat Med. 2004;10(4):422-8.

193. Cuculich PS, Wang Y, Lindsay BD, Faddis MN, Schuessler RB, Damiano RJ, et al. Noninvasive characterization of epicardial activation in humans with diverse atrial fibrillation patterns. Circulation. 2010;122(14):1364-72.

194. Duchateau J, Sacher F, Pambrun T, Derval N, Chamorro-Servent J, Denis A, et al. Performance and limitations of noninvasive cardiac activation mapping. Heart Rhythm. 2019;16(3):435-42.

195. Grace A, Willems S, Meyer C, Verma A, Heck P, Zhu M, et al. High-resolution noncontact charge-density mapping of endocardial activation. JCI Insight. 2019;4(6).

196. Shi R, Norman M, Chen Z, Wong T. Individualized ablation strategy guided by live simultaneous global mapping to treat persistent atrial fibrillation. Future Cardiol. 2018;14(3):237-49.

197. Willems S, Verma A, Betts TR, Murray S, Neuzil P, Ince H, et al. Targeting Nonpulmonary Vein Sources in Persistent Atrial Fibrillation Identified by Noncontact Charge Density Mapping. Circ Arrhythm Electrophysiol. 2019;12(7):e007233.

198. Kuklik P, Zeemering S, Maesen B, Maessen J, Crijns HJ, Verheule S, et al. Reconstruction of instantaneous phase of unipolar atrial contact electrogram using a concept of sinusoidal recomposition and Hilbert transform. IEEE Trans Biomed Eng. 2015;62(1):296-302.

199. Kuklik P, Zeemering S, van Hunnik A, Maesen B, Pison L, Lau DH, et al. Identification of Rotors during Human Atrial Fibrillation Using Contact Mapping and Phase Singularity Detection: Technical Considerations. IEEE Trans Biomed Eng. 2017;64(2):310-8.

200. Earley MJ, Abrams DJ, Sporton SC, Schilling RJ. Validation of the noncontact mapping system in the left atrium during permanent atrial fibrillation and sinus rhythm. J Am Coll Cardiol. 2006;48(3):485-91.

201. Shi R, Parikh P, Chen Z, Angel N, Norman M, Hussain W, et al. Validation of Dipole Density Mapping During Atrial Fibrillation and Sinus Rhythm in Human Left Atrium. JACC Clin Electrophysiol. 2020;6(2):171-81.

202. Leo M, Pope M, Briosa EGA, Betts TR. Atypical congenital atrial flutter unmasked by noncontact mapping. HeartRhythm Case Rep. 2020;6(9):660-2.

203. Pope MTB, Leo M, Briosa e Gala A, Betts TR. Clinical utility of non-contact charge density 'SuperMap' algorithm for the mapping and ablation of organized atrial arrhythmias. EP Europace. 2021.

204. Belhassen B, Pelleg A, Shoshani D, Laniado S. Atrial fibrillation induced by adenosine triphosphate. Am J Cardiol. 1984;53(9):1405-6.

205. Nakai T, Watanabe I, Kunimoto S, Kojima T, Kondo K, Saito S, et al. Electrophysiological effect of adenosine triphosphate and adenosine on atrial and ventricular action potential duration in humans. Jpn Circ J. 2000;64(6):430-5.

206. Belardinelli L, Isenberg G. Isolated atrial myocytes: adenosine and acetylcholine increase potassium conductance. Am J Physiol. 1983;244(5):H734-7.

207. Drury AN, Szent-Györgyi A. The physiological activity of adenine compounds with especial reference to their action upon the mammalian heart. J Physiol. 1929;68(3):213-37.

208. Berenfeld O. Ionic and substrate mechanism of atrial fibrillation: rotors and the exitacion frequency approach. Arch Cardiol Mex. 2010;80(4):301-14.

209. Li N, Csepe TA, Hansen BJ, Sul LV, Kalyanasundaram A, Zakharkin SO, et al. Adenosine-Induced Atrial Fibrillation: Localized Reentrant Drivers in Lateral Right Atria due to Heterogeneous Expression of Adenosine A1 Receptors and GIRK4 Subunits in the Human Heart. Circulation. 2016;134(6):486-98.

210. Hansen BJ, Zhao J, Helfrich KM, Li N, Iancau A, Zolotarev AM, et al. Unmasking Arrhythmogenic Hubs of Reentry Driving Persistent Atrial Fibrillation for Patient-Specific Treatment. J Am Heart Assoc. 2020;9(19):e017789.

211. Jalife J, Berenfeld O, Skanes A, Mandapati R. Mechanisms of atrial fibrillation: mother rotors or multiple daughter wavelets, or both? J Cardiovasc Electrophysiol. 1998;9(8 Suppl):S2-12.

212. Jalife J. Rotors and spiral waves in atrial fibrillation. J Cardiovasc Electrophysiol. 2003;14(7):776-80.

213. Belardinelli L, Shryock JC, Song Y, Wang D, Srinivas M. Ionic basis of the electrophysiological actions of adenosine on cardiomyocytes. FASEB J. 1995;9(5):359-65.

214. Pope M, Kuklik P, Briosa e Gala A, Mahmoudi M, Paisey J, Betts TR. Periodicity and spatial stability of complex propagation patterns in atrial fibrillation. Europace. 2020;22.

215. Zaman JAB, Sauer WH, Alhusseini MI, Baykaner T, Borne RT, Kowalewski CAB, et al. Identification and Characterization of Sites Where Persistent Atrial Fibrillation Is Terminated by Localized Ablation. Circ Arrhythm Electrophysiol. 2018;11(1):e005258.

216. Lee S, Sahadevan J, Khrestian CM, Cakulev I, Markowitz A, Waldo AL. Simultaneous Biatrial High-Density (510-512 Electrodes) Epicardial Mapping of Persistent and Long-Standing Persistent Atrial Fibrillation in Patients: New Insights Into the Mechanism of Its Maintenance. Circulation. 2015;132(22):2108-17.

217. Ip JE, Cheung JW, Chung JH, Liu CF, Thomas G, Markowitz SM, et al. Adenosine-induced atrial fibrillation: insights into mechanism. Circ Arrhythm Electrophysiol. 2013;6(3):e34-7.

218. Cheung JW, Lin FS, Ip JE, Bender SR, Siddiqi FK, Liu CF, et al. Adenosine-induced pulmonary vein ectopy as a predictor of recurrent atrial fibrillation after pulmonary vein isolation. Circ Arrhythm Electrophysiol. 2013;6(6):1066-73.

219. Honarbakhsh S, Schilling RJ, Dhillon G, Ullah W, Keating E, Providencia R, et al. A Novel Mapping System for Panoramic Mapping of the Left Atrium: Application to Detect and Characterize Localized Sources Maintaining Atrial Fibrillation. JACC Clin Electrophysiol. 2018;4(1):124-34.

220. Honarbakhsh S, Hunter RJ, Ullah W, Keating E, Finlay M, Schilling RJ. Ablation in Persistent Atrial Fibrillation Using Stochastic Trajectory Analysis of Ranked Signals (STAR) Mapping Method. JACC Clin Electrophysiol. 2019;5(7):817-29.

221. Roberts-Thomson KC, Stevenson IH, Kistler PM, Haqqani HM, Goldblatt JC, Sanders P, et al. Anatomically determined functional conduction delay in the posterior left atrium relationship to structural heart disease. J Am Coll Cardiol. 2008;51(8):856-62.

222. Shi R, Chen Z, Butcher C, Zaman JA, Boyalla V, Wang YK, et al. Diverse activation patterns during persistent atrial fibrillation by noncontact charge-density mapping of human atrium. J Arrhythm. 2020;36(4):692-702.

223. Honarbakhsh S, Schilling RJ, Providencia R, Keating E, Sporton S, Lowe M, et al. Automated detection of repetitive focal activations in persistent atrial fibrillation: Validation of a novel detection algorithm and application through panoramic and sequential mapping. J Cardiovasc Electrophysiol. 2019;30(1):58-66.

224. Kowalewski CAB, Shenasa F, Rodrigo M, Clopton P, Meckler G, Alhusseini MI, et al. Interaction of Localized Drivers and Disorganized Activation in Persistent Atrial Fibrillation: Reconciling Putative Mechanisms Using Multiple Mapping Techniques. Circ Arrhythm Electrophysiol. 2018;11(6):e005846.

225. Honarbakhsh S, Schilling RJ, Finlay M, Keating E, Ullah W, Hunter RJ. STAR mapping method to identify driving sites in persistent atrial fibrillation: Application through sequential mapping. J Cardiovasc Electrophysiol. 2019.

226. Williams SE, Linton NWF, Harrison J, Chubb H, Whitaker J, Gill J, et al. Intra-Atrial Conduction Delay Revealed by Multisite Incremental Atrial Pacing is an Independent Marker of Remodeling in Human Atrial Fibrillation. JACC Clin Electrophysiol. 2017;3(9):1006-17.

227. Walters TE, Lee G, Morris G, Spence S, Larobina M, Atkinson V, et al. Temporal Stability of Rotors and Atrial Activation Patterns in Persistent Human Atrial Fibrillation: A High-Density Epicardial Mapping Study of Prolonged Recordings. JACC Clin Electrophysiol. 2015;1(1-2):14-24.

228. Weiss JN, Qu Z, Chen PS, Lin SF, Karagueuzian HS, Hayashi H, et al. The dynamics of cardiac fibrillation. Circulation. 2005;112(8):1232-40.

229. Shiroshita-Takeshita A, Brundel BJ, Nattel S. Atrial fibrillation: basic mechanisms, remodeling and triggers. J Interv Card Electrophysiol. 2005;13(3):181-93.

230. Rodrigo M, Climent AM, Hernandez-Romero I, Liberos A, Baykaner T, Rogers AJ, et al. Noninvasive Assessment of Complexity of Atrial Fibrillation: Correlation With Contact Mapping and Impact of Ablation. Circ Arrhythm Electrophysiol. 2020;13(3):e007700.

231. Shi R, Chen Z, Pope MTB, Zaman JAB, Debney M, Marinelli A, et al. Individualized ablation strategy to treat persistent atrial fibrillation: Core-to-boundary approach guided by charge-density mapping. Heart Rhythm. 2021.

232. Kuklik P, Bidar E, Gharaviri A, Maessen J, Schotten U. Application of phase coherence in assessment of spatial alignment of electrodes during simultaneous endocardial-epicardial direct contact mapping of atrial fibrillation. Europace. 2014;16 Suppl 4:iv135-iv40.

233. Andrade JG, Champagne J, Dubuc M, Deyell MW, Verma A, Macle L, et al. Cryoballoon or Radiofrequency Ablation for Atrial Fibrillation Assessed by Continuous Monitoring: A Randomized Clinical Trial. Circulation. 2019;140(22):1779-88.

234. Andrade JG, Deyell MW, Verma A, Macle L, Champagne J, Leong-Sit P, et al. Association of Atrial Fibrillation Episode Duration With Arrhythmia Recurrence Following Ablation: A Secondary Analysis of a Randomized Clinical Trial. JAMA Netw Open. 2020;3(7):e208748.

235. Kochhauser S, Jiang CY, Betts TR, Chen J, Deisenhofer I, Mantovan R, et al. Impact of acute atrial fibrillation termination and prolongation of atrial fibrillation cycle length on the outcome of ablation of persistent atrial fibrillation: A substudy of the STAR AF II trial. Heart Rhythm. 2017;14(4):476-83.

236. Yuen HC, Roh SY, Lee DI, Ahn J, Kim DH, Shim J, et al. Atrial fibrillation cycle length as a predictor for the extent of substrate ablation. Europace. 2015;17(9):1391-401.

237. Drewitz I, Willems S, Salukhe TV, Steven D, Hoffmann BA, Servatius H, et al. Atrial fibrillation cycle length is a sole independent predictor of a substrate for consecutive arrhythmias in patients with persistent atrial fibrillation. Circ Arrhythm Electrophysiol. 2010;3(4):351-60.

238. Vandersickel N, Watanabe M, Tao Q, Fostier J, Zeppenfeld K, Panfilov AV. Dynamical anchoring of distant arrhythmia sources by fibrotic regions via restructuring of the activation pattern. PLoS Comput Biol. 2018;14(12):e1006637.

239. Wazni OM, Dandamudi G, Sood N, Hoyt R, Tyler J, Durrani S, et al. Cryoballoon Ablation as Initial Therapy for Atrial Fibrillation. N Engl J Med. 2020.

240. Andrade JG, Aguilar M, Atzema C, Bell A, Cairns JA, Cheung CC, et al. The 2020 Canadian Cardiovascular Society/Canadian Heart Rhythm Society Comprehensive Guidelines for the Management of Atrial Fibrillation. Can J Cardiol. 2020;36(12):1847-948.

241. Mormann F, Lehnertz K, David P, Elger C. Mean phase coherence as a measure of phase synchronisation and its application to the EEG of epilepsy patients. . Physica D. 2000;144:358-69.

242. Marwan N, Romano M, Thiel M, Kurths J. Recurrence plots for the analysis of complex systems. Physics Reports. 2007;438(5-6):237-329.

243. Zeemering S, van Hunnik A, van Rosmalen F, Bonizzi P, Scaf B, Delhaas T, et al. A Novel Tool for the Identification and Characterization of Repetitive Patterns in High-Density Contact Mapping of Atrial Fibrillation. Front Physiol. 2020;11:570118.

244. Handa BS, Li X, Baxan N, Roney C, Shchendrygina A, Mansfield CA, et al. Ventricular fibrillation mechanism and global fibrillatory organisation are determined by gap junction coupling and fibrosis pattern. Cardiovasc Res. 2020.

245. Ng FS, Handa BS, Li X, Peters NS. Toward Mechanism-Directed Electrophenotype-Based Treatments for Atrial Fibrillation. Front Physiol. 2020;11:987.

246. Lee AM, Aziz A, Didesch J, Clark KL, Schuessler RB, Damiano RJ, Jr. Importance of atrial surface area and refractory period in sustaining atrial fibrillation: testing the critical mass hypothesis. J Thorac Cardiovasc Surg. 2013;146(3):593-8.

247. Zou R, Kneller J, Leon LJ, Nattel S. Substrate size as a determinant of fibrillatory activity maintenance in a mathematical model of canine atrium. Am J Physiol Heart Circ Physiol. 2005;289(3):H1002-12.

248. Hardy C, Rivarola E, Scanavacca M. Role of Ganglionated Plexus Ablation in Atrial Fibrillation on the Basis of Supporting Evidence. J Atr Fibrillation. 2020;13(1):2405.

249. Shi R, Chen Z, Pope MTB, Zaman JAB, Debney M, Marinelli A, et al. Individualized ablation strategy to treat persistent atrial fibrillation: Core-to-boundary approach guided by charge-density mapping. Heart Rhythm. 2021;18(6):862-70.

250. Pope MT, Kuklik P, Briosa EGA, Leo M, Mahmoudi M, Paisey J, et al. Spatial and temporal variability of rotational, focal, and irregular activity: Practical implications for mapping of atrial fibrillation. J Cardiovasc Electrophysiol. 2021;32(9):2393-403.

251. Gibson DN, Di Biase L, Mohanty P, Patel JD, Bai R, Sanchez J, et al. Stiff left atrial syndrome after catheter ablation for atrial fibrillation: clinical characterization, prevalence, and predictors. Heart Rhythm. 2011;8(9):1364-71.

252. Nery PB, Belliveau D, Nair GM, Bernick J, Redpath CJ, Szczotka A, et al. Relationship Between Pulmonary Vein Reconnection and Atrial Fibrillation Recurrence: A Systematic Review and Meta-Analysis. JACC Clin Electrophysiol. 2016;2(4):474-83.

253. Sorensen SK, Johannessen A, Worck R, Hansen ML, Hansen J. Radiofrequency Versus Cryoballoon Catheter Ablation for Paroxysmal Atrial Fibrillation: Durability of Pulmonary Vein Isolation and Effect on Atrial Fibrillation Burden: The RACE-AF Randomized Controlled Trial. Circ Arrhythm Electrophysiol. 2021;14(5):e009573.

254. Maeda M, Oba K, Yamaguchi S, Arasaki O, Sata M, Masuzaki H, et al. Usefulness of Epicardial Adipose Tissue Volume to Predict Recurrent Atrial Fibrillation After Radiofrequency Catheter Ablation. Am J Cardiol. 2018;122(10):1694-700.

255. Bisbal F, Benito E, Teis A, Alarcon F, Sarrias A, Caixal G, et al. Magnetic Resonance Imaging-Guided Fibrosis Ablation for the Treatment of Atrial Fibrillation: The ALICIA Trial. Circ Arrhythm Electrophysiol. 2020;13(11):e008707.

256. Pope MTB, Kuklik P, Briosa EGA, Leo M, Mahmoudi M, Paisey J, et al. Impact of Adenosine on Wavefront Propagation in Persistent Atrial Fibrillation: Insights From Global Noncontact Charge Density Mapping of the Left Atrium. J Am Heart Assoc. 2022;11(11):e021166.

257. Baykaner T, Fazal M, Patel S, Zaman J. Is there rule to the chaos: Defining stable patterns in atrial fibrillation. J Cardiovasc Electrophysiol. 2021;32(9):2404-7.